Volume 1, Number 2

July-August, 1960

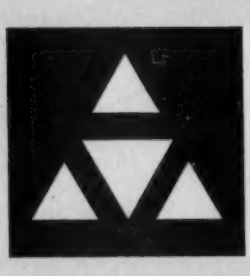

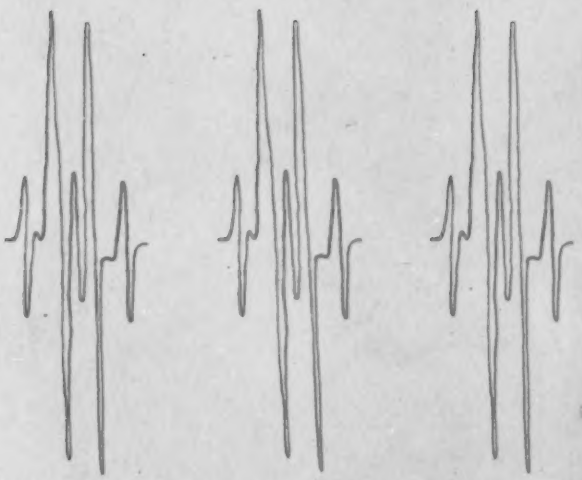

KINETICS AND CATALYSIS

КИНЕТИКА И КАТАЛИЗ

KINETIKA I KATALIZ

TRANSLATED FROM RUSSIAN

CONSULTANTS BUREAU

RESEARCH BY SOVIET EXPERTS

Translated by Western Scientists

BORATE GLASSES

by L. Ya. Mazelev

Boron as an element has been known for a long time, but the role of its oxide in glass has been studied little. This book is based mainly on the results of investigating silicate and borosilicate glasses. The purpose of the author's work was a systematic study of the technology of glass melting, the processes and reactions of glass formation, the crystallisation of glasses and the composition of the crystallisation products, the physicochemical properties and their relation to the composition and structure of glass and methods of calculating these properties. This book is important for all those interested in the problems of the structure of glass.

Cloth **176 pages** **$10.00**

SILICON AND ITS BINARY SYSTEMS

by A. S. Berezhnoi

Data accumulated on the physical chemistry of silicon and its binary systems are critically reviewed. The properties and descriptions of the crystal structures of silicon and all its binary compounds known at present are given in detail and the most important ways of using these substances in practical applications are indicated. Silicon carbide is treated in detail, as are silicon compounds of the transition metals. All sections have been provided with a historical outline and the basic literature is cited with each problem considered.

Cloth **265 pages** **$8.50**

CRYSTAL CHEMISTRY OF SIMPLE COMPOUNDS OF URANIUM, THORIUM, PLUTONIUM AND NEPTUNIUM

by E. S. Makarov

This book represents the first attempt to correlate crystal structure data on the simplest compounds of the most thoroughly studied actinide elements. No books dealing specifically with crystal chemistry of the actinides have been published hitherto either abroad or in the Soviet Union, although separate surveys by Zachariasen have appeared in various collective volumes.

The abundant factual data on crystal structures of actinide compounds are summarised in compact form. This work will enable research workers and engineers to make wider use of crystal structure data which, until now, have been scattered throughout numerous literature sources.

The author considers certain questions of general crystal chemistry, gives full details of the crystalline structures of the polymorphic modifications of the actinides and their simplest compounds, adopts Seaborg's cautious position regarding the parent of the "5f" family of elements, and advances an interesting theory concerning the dual chemical nature of the actinides.

Cloth **146 pages** **Illus.** **$5.25**

Payment may be made in sterling to Barclay's Bank in London, England.

Tables of contents upon request

CONSULTANTS BUREAU

227 W. 17th ST., NEW YORK 11, N. Y.

KINETIKA I KATALIZ
EDITORIAL BOARD:

A. A. Balandin
G. K. Boreskov *(Editor)*
V. T. Bykov
I. V. Kalechits
A. A. Koval'skii
V. N. Kondrat'ev
K. I. Matveev *(Secretary)*
S. Z. Roginskii
M. G. Slin'ko
V. V. Voevodskii *(Acting Editor)*
N. N. Vorozhtsov

KINETICS AND CATALYSIS

A translation of KINETIKA I KATALIZ,
a publication of the Academy of Sciences of the USSR

© 1961 CONSULTANTS BUREAU ENTERPRISES, INC.
227 West 17th Street, New York 11, N. Y.

Volume 1, Number 2 July-August, 1960

CONTENTS

	PAGE ENG.	PAGE RUSS.
Differential Methods for the Calculation of Rate Constants of Simple Chemical Reactions. E. S. Rudakov	163	177
Kinetics of Thermal Cracking of Hydrocarbons and Their Mixtures. G. M. Panchenkov and V. Ya. Baranov	172	188
Kinetics of Alkaline Hydrolysis of the Methyl Ester of Alanyl Glycyl Glycine in Aqueous Solution. D. G. Knorre, G. V. Kukushkina, and V. P. Mamaev	180	197
Influence of Defects in Crystals on the Rate of Thermal Decomposition of Solid Substances. V. V. Boldyrev	186	203
Adsorption, Ionization, and Catalytic Activation of Gases on Metals. A. I. Krasil'shchikov, L. G. Antonova, and F. P. Ivanovskii	193	212
Effect of Electronic Structure of Nickel Oxide on Oxygen Exchange. N. P. Keier	200	221
Mobility of Oxygen and Catalytic Activity of Vanadium Pentoxide Promoted by Potassium Sulfate. G. K. Boreskov, L. A. Kasatkina, V. V. Popovskii, and Yu. A. Balovnev	207	229
Kinetics of the Oxidation of Propylene to Acrolein on Copper Catalyst. O. V. Isaev and L. Ya. Margolis	214	237
The Distribution of Promoters on the Surface of Ammonia Synthesis Catalysts and the Activity of These Catalysts at High Pressure. V. N. Shishkova, S. S. Lachinov, and I. N. Konyukhova	219	242
The Composition, Methods of Preparation, and Nature of the Activity of Tricalcium Phosphate Catalysts. L. Kh. Freidlin and V. Z. Sharf	223	247
Application of the Method of Electron Paramagnetic Resonance to the Study of the Crystalline Properties of Chrome Catalyst. V. B. Kazanskii, Yu. I. Pecherskaya, and V. V. Voevodskii	232	257
A Study of the Activity of Nickel Catalysts. I. The Properties of Alloy Catalysts. G. D. Lyubarskii, L. I. Ivanovskaya, and G. G. Isaeva	235	260
Vapor-Phase Catalytic Oxidation of Butylenes to Maleic Anhydride. B. L. Moldavskii and Yu. D. Kernos	242	267
Reactions of Iron Carbides under the Conditions of the Fischer-Tropsch Synthesis. Yu. B. Kryukov, A. N. Bashkirov, L. G. Liberov, V. K. Butyugin, N. D. Stepanova, and Yu. B. Kagan	248	274
Study of the Electrical Conductivity of Catalysts Made of Zinc, Chromium, and Copper Oxides for the Conversion of Carbon Monoxide. T. A. Semenova, G. E. Braude, and F. P. Ivanovskii	255	282

Annual Subscription: $150 **Single Issue: $35** **Single Article: $12.50**

Note: The sale of photostatic copies of any portion of this copyright translation is expressly prohibited by the copyright owners.

CONTENTS (continued)

	PAGE	RUSS. PAGE
Chromatographic Analysis of Gas Adsorption Isotherms and the Specific Surface of Solids. S. Z. Roginskii, M. I. Yanovskii, Lu P'iei-chang, G. A. Gaziev, G. M. Zhabrova, B. M. Kadenatsi, V. V. Brazhnikov, I. E. Neimark, and M. A. Piontkovskaya	261	287
Aromatization of Narrow Hexane Fractions from Grozny Gasoline on a Chromium-Alumina Catalyst. B. A. Kazanskii, A. Z. Dorogochinskii, M. I. Rozengart, A. V. Lyuter, and M. G. Mitrofanov	268	294
Dehydrogenation of n-Decane on Oxide Catalysts. E. A. Timofeeva, V. S. Smirnov, and V. I. Zaeva	274	300
Investigation of Ortho-Para-Hydrogen Conversion on Solid Catalysts at 78-64°K. Communication I. R. A. Buyanov	280	306
Kinetics of First-Order Heterogeneous Reactions Retarded by Reaction Products and by Internal Diffusion. A. Ya. Rozovskii and V. V. Shchekin	286	313
Diffusion Kinetics for a Surface of Unequal Accessibility. O. M. Todes and A. P. Shapiro	296	324
LETTER TO THE EDITOR		
Detection of Hydrogen Atoms in a Low-Pressure Hydrogen Flame by the EPR Method. V. N. Panfilov, Yu. D. Tsvetkov, and V. V. Voevodskii	305	333
Boris Nikolaevich Dolgov	307	334

DIFFERENTIAL METHODS FOR THE CALCULATION OF RATE CONSTANTS OF SIMPLE CHEMICAL REACTIONS

E.S. Rudakov

Novosibirsk Institute of Organic Chemistry, Siberian Division,
Academy of Sciences of the USSR, All-Union Scientific
Research Institute of Petrochemical Processes
Translated from Kinetika i Kalaliz, Vol. 1, No. 2, pp.
177-187, July-August, 1960
Original article submitted January 4, 1960

New methods for the calculation of rate constants and the order of reactions are considered in this paper. The methods do not require a knowledge of initial or boundary conditions, are quite accurate, and permit determination of the rate constants from data obtained over only two experimental ranges.

Confirmation of the applicability of one kinetic equation or another to a given chemical reaction and calculation of the rate constant are usually carried out by methods originally proposed by van't Hoff [1]. However, a number of cases are known in which the classical method does not provide for sufficient reliability of the calculations,and the error in the rate constant is increased through incorrect treatment of the experimental results. On the other hand, the experimental procedure does have some connection with the method of calculation, and in some cases the procedure can be simplified and improved if the classical calculation procedure is abandoned and a change is made to the more flexible differential methods.

The present article considers questions associated with the application of the differential method, and reliable and rather simple methods are proposed for the treatment of experimental data from certain first and second order reactions. A knowledge of parameters, such as boundary conditions, is not required.

1. Kinetic Equations and Parameters

In addition to "concentration–time" data, calculation of the rate constant requires a knowledge of certain parameters, which, in a sense, are integration constants. The number of parameters and the selection of specific parameters depend on the methods used in the kinetic investigation and in the calculations. For example, in calculating a first order reaction which obeys the equation

$$\frac{d\varphi}{d\tau} = k(\varphi_\infty - \varphi), \tag{1}$$

where φ is the concentration of the reaction product or, in the general case, a physicochemical property of the system which is linearly connected with the concentration of reactant or product, the equation

$$k = -\frac{1}{\tau}\ln\frac{\varphi_\infty - \varphi}{\varphi_\infty - \varphi_0}, \tag{2}$$

is used if the parameters φ_∞ and φ_0 are known, and

$$k = -\frac{\Delta \ln (\varphi_\infty - \varphi)}{\Delta \tau}, \qquad (3)$$

is used if only one parameter, φ_∞, is known.*

In many cases, the parameters cannot be directly determined in a given experiment. There then arises the necessity for additional data (for example, under static conditions) or indirect calculations using other data. Moreover, the accuracy of parameters determined in such a manner is, as a rule, lower than the accuracy of ordinary experimental data. This circumstance is very significant.

It is usually assumed that fulfillment of one integral relationship or another or constancy of the calculated constants with time is a criterion of the reliability of the results. This point of view is generally incorrect. Analyzing the effect of an error in φ_∞ on the error in the rate constant for a reaction obeying Equation (1), Guggenheim [2] showed that strict fulfillment of a linear dependence between $\ln(\varphi_\alpha - \varphi)$ and time is not, by itself, a criterion of the accuracy of the values of φ_∞ used, nor is it a criterion of the reliability of the rate constants obtained by this route. We have established that an error in φ_∞ of 0.2 % causes a deviation in the rate constant of up to 2%. This means that if the accuracy of the measurement of φ_∞ is 0.5-1%, the deviation in the rate constant can attain significantly greater values.

Thus, the determination of rate constants through the use of parameters is characterized by an increase in the laboriousness, and an increase in the time between the kinetic measurements themselves and the time when the final result is obtained, and in addition it can lead to the development of a considerable and uncontrollable error in the rate constant. In this connection, it appeared to be of considerable interest to develop methods for kinetic calculations which would not require a knowledge of the parameters.

2. Methods of Calculation Without Parameters

In principle, such a possibility follows directly from (1):

$$-k \equiv \frac{\Delta}{\Delta \varphi}\left(\frac{d\varphi}{d\tau}\right). \qquad (4)$$

Consequently, the problem boils down to the calculation of the value of the derivative $\Delta / \Delta \varphi \, (d\varphi / d\tau)$ by an appropriate method.**

One such method has long been known. A graph of φ vs. τ is constructed from the experimental data; the tangents are determined either visually or by mechanical means, and the derivatives $\dot{\varphi}$ are calculated as functions of φ. A second graph is plotted in terms of $\dot{\varphi}_i$ and φ_i, a straight line is drawn through the points, and the slope of the line is equal to the rate constant, in accordance with Equation (1). This method is laborious (construction of two graphs); it contains arbitrary elements in the construction of the first curve and in the determination of the tangents, and therefore it cannot be recommended for accurate calculations.

The improved method of Guggenheim [2] included the construction of the kinetic curve $\varphi - \tau$, graphical determination at each point (φ_i, τ_i) of the value of φ'_i, which is shifted with respect to φ_i by a constant time interval θ, and calculation of the rate constant from the slope of the straight line on a second graph in which $\ln (\varphi - \varphi')$ is plotted against τ, the corresponding theoretical equation having the form

$$\ln (\varphi - \varphi') + k\tau = \ln [(\varphi_\infty - \varphi_0)(1 - e^{-k\theta})] = \text{const}. \qquad (5)$$

* The rate constant is equal to the slope of the straight line resulting from a plot of $\ln (\varphi_\infty - \varphi) - \tau$.

** It may be remarked that Equation (4) can be considered as the original kinetic equation. The initial integration of (4) yields an equation of the type of (1) and (3) which contains a single constant, φ_∞. A second integration of (4) gives Equation (2), which contains two constants, φ_∞ and φ_0. This can be used for classification of the methods of calculation.

Although the method of Guggenheim is widely used in precise investigations*, its disadvantages are obvious: It is laborious (construction of two graphs), and it has an arbitrary element in the construction of the first curve.

It is not difficult to see that this method, like the method of tangents, leads directly to an equation of the form of (4). According to (5).

$$-k = \frac{d \ln (\varphi - \varphi')}{d\tau} = \frac{d\,\Delta\varphi}{\Delta\varphi \cdot d\tau} = \frac{\Delta}{\Delta\varphi} \cdot \frac{d\varphi}{d\tau},$$

where $\Delta\varphi = \varphi - \varphi'$ corresponds to the time interval θ. This result shows that all methods of calculating rate constants without parameters come down, in the final analysis, to the differential form (4).

We shall consider below other methods of calculation without the use of parameters—methods based on the direct calculation of $d\varphi/d\tau$.

3. Calculation of $d\varphi/d\tau$

The calculation of rate constants by Equation (4) may be divided into two stages. The problem of the first stage is the determination of the derivative $d\varphi/d\tau$ from data on $\Delta\varphi_i$ and $\Delta\tau_i$. Further calculations do not cause any difficulty. In this connection, it seemed of interest to evaluate the deviations arising from replacement of average values of the rates $\Delta\varphi/\Delta\tau$ by their instantaneous values $d\varphi/d\tau$.

Such a substitution is not objectionable provided the intervals $\Delta\varphi$ and $\Delta\tau$ are sufficiently small; however, this is rarely encountered in actual practice. This is usually discussed in text-books, and, further, conclusions are reached as to the requirements for integrating kinetic equations. From this point of view, it would not be unexpected that for functions obeying (4), replacement of $\Delta\varphi/\Delta\tau$ by $d\varphi/d\tau$ could be carried out without the introduction of any appreciable error for $\Delta\varphi$ up to 10% of the total depth of conversion, $\varphi_\infty - \varphi$, if the value of $d\varphi/d\tau$ and the argument refer to the center of the interval $\Delta\varphi$ (index φ, for example, $\dot{\varphi}_\varphi$, τ_φ) or to the center of the interval $\Delta\tau$ (index τ, for example, $\dot{\varphi}_\tau$, τ_τ).

A simple calculation based on expansion of the functions $\varphi(\tau)$ and $\tau(\varphi)$ in a Taylor's series leads to the following results:

$$\frac{\Delta\varphi}{\Delta\tau} = \left(\frac{d\varphi}{d\tau}\right)_\varphi \cdot \left(1 - \frac{1}{3}\delta^2 - \frac{4}{45}\delta^4 - \ldots\right), \tag{6}$$

where $\delta = \frac{1}{2}\,\frac{k \cdot \Delta\varphi}{\dot{\varphi}_\varphi} \simeq \frac{1}{2} k\,\Delta\tau < 1$, and

$$\frac{\Delta\varphi}{\Delta\tau} = \left(\frac{\partial\varphi}{d\tau}\right)_\tau \cdot \left(1 + \frac{1}{6}\delta^2 + \frac{1}{120}\delta^4 + \cdots\right), \tag{7}$$

where $\delta = \frac{1}{2} k \cdot \Delta\tau < 1$.

The series in Equations (6) and (7) converges rapidly. For a numerical evaluation of the deviations, let us consider a reaction with a half-life of 60 minutes, $k = 0.0115$ min^{-1}, points being taken in the middle of each 12-minute interval during the investigation. We have $\delta = \frac{1}{2} \cdot 0.0115 \cdot 12 = 0.069$. In this case, the second term in the expansion is $1/3 \cdot \delta^2 \cdot 100 = 0.16\%$ in (6) and $1/6 \cdot \sigma^2 \cdot 100 = 0.08\%$ in (7). Such deviations are extremely small. Consequently, in a number of cases of practical importance, it is possible to disregard the second terms of the expansions in (6) and (7), which leads to:

$$\frac{\Delta\varphi}{\Delta\tau} = \left(\frac{d\varphi}{d\tau}\right)_\varphi = \left(\frac{d\varphi}{d\tau}\right)_\tau. \tag{8}$$

*See, for example, references [3, 4].

TABLE 1

Errors in Rate Constants for Different Experimental Regimes

Regime	Error in constant, ε	
	$\dot{\varphi}-\varphi$ method	$\ln \dot{\varphi}-\tau$ method
$\Delta\varphi \simeq$ const	$-\frac{1}{3}\delta^2_{av}$	$-\frac{1}{3}\delta^2_{av}$
$\Delta\varphi \cdot \Delta\tau \simeq$ const	0	$-\frac{1}{6}\delta^2_{av}$
$\Delta\tau \simeq$ const	$+\frac{1}{3}\delta^2_{av}$	0

In those cases where it is necessary (high accuracy of the measurements or greater experimental intervals $\Delta\varphi_i$ and $\Delta\tau_i$), it is possible to include the second series of the expansion. We now turn our attention to the case in which the deviation of $\Delta\varphi/\Delta\tau$ from $d\varphi/d\tau$ in (6) and (7) does not depend on the depth of conversion. This is possible only for functions obeying the differential form (4).

4. Calculation of the Rate Constant

There are two means of calculating rate constants corresponding to the two methods of determining the derivative.

The $\dot{\varphi}-\varphi$ method. The linear dependence of $\dot{\varphi}$ on φ is used in calculation. Using the experimental data (φ, τ) and Equation (6), secondary data ($\dot{\varphi}_\varphi, \varphi_\varphi$) are calculated, and these are plotted graphically using $\dot{\varphi}$ and φ as coordinates. A straight line is drawn through the points, and the slope of the line is -k.

The $\ln\dot{\varphi}-\tau$ method. The linear dependence of $\ln\dot{\varphi}$ on τ: $\ln\dot{\varphi} = -k\tau + \ln[(\varphi_\infty - \varphi_0)k]$, is used in the calculation. By means of the experimenta data (φ, τ) and Equation (7), secondary data ($\dot{\varphi}_\tau, \tau_\tau$) are calculated, and these are plotted on a graph of $\ln\dot{\varphi}-\tau$. A straight line is drawn through the points, and the slope of the line is $-k$.

TABLE 2

Illustrations of the $\dot{\varphi}-\varphi$ and $\ln\dot{\varphi}-\tau$ Methods Applied to an Ideal Experiment, k = 0.0100

Expt. data		Difference		$\dot{\varphi}-\varphi$ method		$\ln\dot{\varphi}-\tau$ method	
τ	φ	$\Delta\tau$	$\Delta\varphi$	$\dot{\varphi}_\varphi$	$\frac{\Delta\varphi}{\Delta\tau}\cdot 10^2$	τ_τ	$\ln\left(\frac{\Delta\varphi}{\Delta\tau}\cdot 10^2\right)$
50	3,9347	19	1,0495	4,4594	5,5231	59,5	1,7090
69	4,9842	8	0,3857	5,1770	4,8213	73,0	1,5730
77	5,3699	13	0,5644	6,6521	4,3385	83,5	1,4675
90	5,9343	20	0,7370	6,3028	3,6850	100,0	1,3043
110	6,6713						
k from average data				0,01001		0,010004	

TABLE 3

Calculation of Experimental Data by the $\dot{\varphi}-\varphi$ and $\ln\dot{\varphi}-\tau$ Methods

Experimental data		$\dot{\varphi}-\varphi$ method			$\ln\dot{\varphi}-\tau$ method		
φ, ml	$\Delta\tau$, sec	$\Delta\varphi$	$\frac{\Delta\varphi}{\Delta\tau}\cdot 10^2$	$\dot{\varphi}_\varphi$	$\Sigma\Delta\tau$	τ_τ	$\ln\left(\frac{\Delta\varphi}{\Delta\tau}\cdot 10^2\right)$
0,076					0		
0,166	535	0,090	167,1	0,121	535	267	5,119
0,263	611	0,097	158,7	0,214	1146	840	5,067
0,371	737	0,108	146,7	0,317	1883	1514	4,988
0,464	693	0,093	134,0	0,417	2576	2229	4,898
0,554	726	0,090	124,0	0,509	3302	2939	4,820
0,642	768	0,088	114,5	0,598	4070	3686	4,741
0,741	958	0,099	103,2	0,692	5028	4549	4,637
0,831	990	0,090	91,0	0,786	6018	5523	4,511
0,955	1562	0,124	79,3	0,893	7580	6799	4,373
1,036	1223	0,081	66,1	0,995	8803	8191	4,191

TABLE 4

Calculation of Rate Constants from Data for Two Intervals

$\Delta\varphi_i$	$\Delta\tau_i$	Zero approximation*			First approximation*		
		τ_τ	$\frac{\Delta\varphi}{\Delta\tau}\cdot 10^6$	$\ln\left(\frac{\Delta\varphi}{\Delta\tau}\cdot 10^6\right)$	δ	$\frac{1}{6}\delta^2$	$\ln\left(\frac{d\varphi}{d\tau}\cdot 10^6\right)$
0,478	3302	1651	144,8	4,975	0,19	0,006	4,975—0,006=4,969
0,482	5501	6052	87,6	4,473	0,31	0,017	4,473—0,017=4,456
$\Delta\tau_\tau$ =4401		$-\Delta\ln\left(\frac{\Delta\varphi}{\Delta\tau}\cdot 10^6\right)=0{,}502$			$-\Delta\ln\left(\frac{d\varphi}{d\tau}\cdot 10^6\right)=0{,}513$		
		$k_0=\frac{0{,}502}{4401}\ 114\cdot 10^{-6}\,\text{sec}^{-1}$			$k_1=\frac{0{,}513}{4401}=116{,}5\cdot 10^{-6}\,\text{sec}^{-1}$		

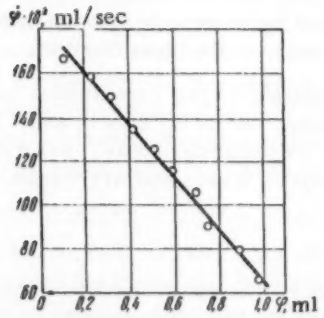

Fig. 1. Illustration of the $\dot\varphi-\varphi$ method of calculation.

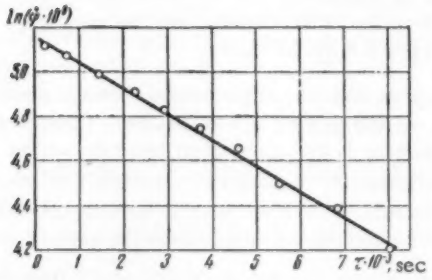

Fig. 2. Illustration of the $\ln\dot\varphi-\tau$ method of calculation.

The $\dot\varphi-\varphi$ method is more descriptive and clearly illustrates the law of mass action. The $\ln\varphi-\tau$ method is not so descriptive, and it includes an additional operation (taking the logarithm of $\dot\varphi$); however, it is more accurate. The difference in the methods, that in the first case the argument is φ and in the second case it is $-\tau$, can have a substantial effect on the excution of the experiment. Using the $\dot\varphi-\varphi$ method of calculation, the experimenter is not bound by the requirement of accounting for the absolute time, but can tolerate interruptions in the normal course of the reaction, for example, interruptions associated with temperature change. After restoration of normal conditions, the measurements can be continued, and the interruption is not reflected in the results of the calculations.

5. Experimental Regime and Evaluation of Rate Constant Deviations

We have considered above the errors arising during the calculation of the derivatives. However, the ultimate aim is the calculation of rate constants. It is an important fact that the errors introduced in the second stage of the calculation compensate the errors of the first stage.

The deviations arising in the second stage of the calculation depend not only on the values of the experimental intervals, $\Delta\varphi_i$ and $\Delta\tau_i$, but also on the experimental regime, which in turn is characterized by certain principles in the selection of the intervals. The most frequently used regimes are $\Delta\varphi_i\simeq$ const and $\Delta\tau_i\simeq$ const. The regime $\Delta\varphi_i\cdot\Delta\tau_i\simeq$ const is an intermediate case. Table 1 presents the results of a calculation of the error ϵ, arising when the rate constant is calculated by the $\dot\varphi-\varphi$ method

$$-\frac{\Delta}{\Delta\varphi_\varphi}\left(\frac{\Delta\varphi}{\Delta\tau}\right)=k(1+\varepsilon) \qquad (9)$$

and by the $\ln\dot\varphi-\tau$ method

$$-\frac{\Delta}{\Delta\tau_\tau}\left(\ln\frac{\Delta\varphi}{\Delta\tau}\right)=k(1+\varepsilon) \qquad (10)$$

for the different experimental regimes.

*"Zero approximation" denotes Eq. (6) or (7) with the second and subsequent terms of the expansion neglected [i.e., Eq. (8)]. "First approximation" denotes Eq. (6) or (7) with the second term of the expansion included – Publisher's note.

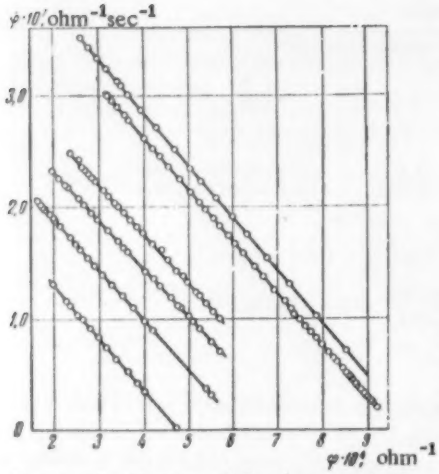

Fig. 3. Application of the $\dot{\varphi}-\varphi$ method to the calculation of reaction rate constants from conductometric data.

It may be seen from the data of the table that the errors in the rate constants obtained directly from the differences $\Delta\varphi_i$ and $\Delta\tau_i$ by means of the approximate Equation (8) lie within the limits

$$-\frac{1}{3}\delta_{av}^2 \leq \varepsilon \leq +\frac{1}{3}\delta_{av}^2.$$

for the regimes considered.

In the case of the reaction considered above ($k = 0.0115$ min $^{-1}$, $\Delta\tau_{av} = 12$ minutes, $\delta_{av} = 0.069$), this result means that the error is within the limits ± 0.16%. Considering that the error in the values of rate constants reaches ± 1-5% even when the most precise methods of investigation are used, it becomes clear that approximate Equation (8), which was obtained by dropping the second and subsequent terms of the series in Equations (6) and (7), is quite accurate enough for ordinary kinetic calculations.

The data of Table 1 indicate the best experimental regimes to be maintained if it is desired to avoid any error at all. These optimum regimes for kinetic investigations are $\Delta\varphi_i \cdot \Delta\tau_i \simeq$ const, if the $\dot{\varphi}-\varphi$ method of calculation is used, and $\Delta\tau_i \simeq$ const, if the ln $\dot{\varphi}-\tau$ method is used.

6. Illustration of the Calculation Methods

Table 2 shows calculations by the two methods as applied to an "ideal experiment": $d\varphi / d\tau = 0.0100(10.00-\varphi)$. The results of the calculations using averaged data are shown at the bottom of the table. As would be expected, the errors are within ± 0.1%.

Our data on the solvolysis of $(CH_3)_3Cl$ are shown in Table 3 and in Figs. 1 and 2; the data were obtained by titration, and the calculations were carried out by both methods. It is apparent that all of the points fall close to the straight lines, which indicates that this is a first order reaction. Calculations based on averaging the data gave the same rate constant in each of the two cases, $k = (117 \pm 0.5)\cdot 10^{-6}$ sec^{-1}.

Differential methods are convenient for calculating rate constants when the experimental data are somewhat inaccurate, i.e., when the scatter of the points on graphs of $\dot{\varphi}-\varphi$ and ln $\dot{\varphi}-\tau$ is considerable. Considerable scatter of the points about the kinetic straight line indicates imperfection in the experiment; however, within the normal error, the slope of the line gives the correct value of the constant. In contrast to integral methods of calculation, the differential methods do not obscure experimental errors, but on the contrary, they reveal them, and this certainly is useful as a criterion of the accuracy of the rate constants calculated from the data.

The $\dot{\varphi}-\varphi$ and ln $\dot{\varphi}-\tau$ differential methods also have two advantages over the previously used differential methods of calculation–the slope method and the method of Guggenheim. When used is made of the $\dot{\varphi}-\varphi$ and ln $\dot{\varphi}-\tau$ methods, there is no necessity of constructing accessory, so-called kinetic curves, and the experimental data are readily converted to the form required for plotting the final graphs.

The features of the $\dot{\varphi}-\varphi$ and ln $\dot{\varphi}-\tau$ methods indicated above permit a considerable reduction in the time between the kinetic measurements and the time at which the final result becomes available. As a rule we determined the constants during the course of the experiment.

We may remark here that the $\dot{\varphi}-\varphi$ and ln $\dot{\varphi}-\tau$ differential methods fail to have an advantage over integral methods in only a single special case–the case in which the value of parameters such as φ_∞ is known before hand (for example, the trivial case $\varphi_\infty = 0$).

7. Calculation of Rate Constants from Conductometric Data

When differential methods are used, it is expedient to measure not φ as a function of τ, but to measure $\Delta\varphi$ and $\Delta\tau$ directly as functions of φ (Table 3). In this connection, it is desirable to use those methods of investigation which are characterized by high accuracy in the determination of intervals.

One such method is the conductometric method. The sensitivity of the method can be increased considerably if an oscilloscope is used in conjunction with a special method of measurement, which includes the determination of $\Delta\tau$ between adjacent times at which the bridge is in balance, the position of which has previously been fixed. Such a method can increase the sensitivity to 0.005%. Moreover, in a number of cases it has been found possible to use a simple empirical relationship between the resistance of the solution, R, and the concentration of electrolyte, C.

$$C = \beta (R - R_c)^{-1}, \tag{11}$$

where β and R_C are calibration constants which do not vary greatly over a wide interval of C.

Using such a method, we investigated the solvolysis of $(CH_3)_3CCl$ in a series of water-containing media. We used the function $\varphi = (R - R_C)^{-1}$ as the parameter φ linearly connected with the concentration of reaction product, HCl. Calculations based on the experimental data (R, τ) were carried out by the $\dot{\varphi} - \varphi$ method. Figure 3 shows some of the kinetic lines for the reaction under different conditions.

Two stopwatches were used to measure the time intervals. These were mounted in the same housing, and were fitted with a device such that the stems actuating the mechanisms were depressed simultaneously. At the instant of measurement, one stopwatch was stopped and the other was simultaneously started. The time indicated on the first stopwatch was recorded. The apparatus was, of course, automatically ready for the next measurement. This device was very convenient in the work, and it guaranteed accuracy within the limits of ± 0.2 seconds during the continuous measurements of τ.

8. Calculation of Rate Constants with A Minimum Amount of Data

The possibility of calculating rate constants with only two experimental intervals $(\Delta\varphi_i, \Delta\tau_i)$ follows directly from Eq. (6) and (7). We shall consider an example of such a calculation by the $\ln \dot{\varphi} - \tau$ method using the data of Table 3. The upper and lower halves of the table were summed—so as to form two large intervals. The original data and the calculation of the constants are shown in Table 4.

The following will clarify the calculations. The values of τ_T were found in the following manner. For the first interval, $\tau_T = \frac{1}{2}\tau_1 = 1651$ seconds. For the second interval, $\tau_T = \Delta\tau_1 + \frac{1}{2}\Delta\tau_2 = 6052$ seconds. The constant in the zero approximation (8) was found by means of the formula $k_0 = -\Delta/\Delta\tau_T \ln \Delta\varphi/\Delta\tau$. The logarithms of $\Delta\varphi/\Delta\tau$ were taken from five-place tables of the function e^x [5]. Corrections of the first approximation were introduced in accordance with Eq. (7), which may be put in the form $\ln (d\varphi/d\tau)_T = \ln \Delta\varphi/\Delta\tau - \frac{1}{6}\delta^2$. Values of $\delta = \frac{1}{2} k_0 \Delta\tau_i$ were determined from data obtained from the zero approximation. This last approximation gave the value $k_2 = 116.7 \cdot 10^{-6}$ seconds^{-1}.

Corrections connected with the third member of the series, $1/120 \cdot \delta^4$ cannot be taken into account.

Thus, the first approximation gives a value of $k_1 = 116.5 \cdot 10^{-6}$ seconds^{-1}, which is in complete agreement with the value found above from these same data, $k = 117 (\pm 0.5) \cdot 10^{-6}$ seconds^{-1}. Hence, the following conclusions may be formed. If the order of the reaction is known beforehand, there is no necessity to carry out numerous measurements in the experiment. This method of calculating rate constants can by recommended for measurement of a low order of accuracy

9. CAlculation of Rate Constants for Second Order Reactions

In the preceding sections, we have considered the application of the $\dot{\varphi} - \varphi$ and $\ln \dot{\varphi} - \tau$ methods to the calculation of rate constants of first order reactions. However, these methods can also be used for second order reactions for which the kinetic equation has the form

$$\frac{dy}{d\tau} = ky (a \pm y). \tag{12}$$

As is well known, this equation describes reactions such as the saponification of esters, certain autocatalytic reactions, and many others.

That the methods can be used for second order reactions follows directly from the fact that the substitution $y = \varphi^{-1}$ in Eq. (12) leads to an equation which is linear in φ:

$$-\frac{d\varphi}{d\tau} = k(a\varphi \pm 1). \tag{13}$$

The differential form of this equation

$$-ka \equiv \frac{\Delta}{\Delta\varphi}\left(\frac{d\varphi}{d\tau}\right) \equiv \frac{\Delta}{\Delta\tau}\left(\ln\frac{d\varphi}{d\tau}\right)$$

differs from the form of (4) only in that the rate constant is multiplied by a constant factor. Consequently, the same methods of calculation and the same evaluations of accuracy described above for first order reactions are applicable to second order equations of the proper type.

When the $\dot{\varphi}-\varphi$ method is used, values of $\varphi = 1/y$, φ_φ, $\Delta\varphi/\Delta\tau$, and $d\varphi/d\tau$ are calculated, the last by means of Eq. (6). The slope of the line resulting from a plot of $\dot{\varphi}$ as a function of φ is equal to $-ka$; the intercept on the ordinate axis ($\varphi = 0$) is equal to $(d\varphi/d\tau)_{\varphi\to 0} = \pm k$. The equation of the line is Eq. (13).

When the $\ln\dot{\varphi}-\tau$ method is used, values of $\varphi = 1/y$, $\Delta\varphi/\varphi\tau$, τ_τ, and $\ln(-d\varphi/d\tau)_\tau$ are calculated, the last by means of Eq. (7). The slope of the line resulting from a plot of $\ln\dot{\varphi}$ as a function of τ is equal to $-k$; the intercept on the ordinate axis, $\tau = 0$, is equal to $\ln(-d\varphi/d\tau)_{\tau\to 0} = \ln(ak\varphi_0 \pm k)$. The equation of the line is:

$$\ln\left(-\frac{d\varphi}{d\tau}\right)_\tau = -k\tau_\tau + \ln(ak\varphi_0 \pm k).$$

It should be emphasized that in the $\ln\dot{\varphi}-\tau$ method the rate constant is equal to the slope of the kinetic line, as in the calculation of a first order rate constant by these two methods, while in the $\dot{\varphi}-\varphi$ method the rate constant is equal to the intercept on the ordinate axis. This must be taken into account in selecting the method of calculation.

10. Calculation of the Order of the Reaction

Sometimes difficulties arise in the determination of the order of the reaction, n

$$-\frac{dC}{d\tau} = kC^n \tag{14}$$

from the experimental data [6]. In this case, substitution of $\Delta C/d\tau$ for $dC/d\tau$ causes an error which depends both on the order of the reaction and on the depth of conversion:

$$\frac{\Delta C}{\Delta\tau} = \left(\frac{dC}{d\tau}\right)_c \cdot \left[1 - \frac{n(n+1)}{24}\cdot\left(\frac{\Delta C}{C_c}\right)^2 + \cdots\right], \tag{15}$$

where the subscript c indicates that the concentration C and its derivative are refered to the center of the interval ΔC.

With $\Delta C/C = 0.1$ and $n = 3$ (an unfavorable case), the error in the rate is only 0.5%. Taking the logarithms of (14) and (15) and simplifying, we have

$$\ln\left(-\frac{\Delta C}{\Delta\tau}\right) = \left[\ln k - \frac{n(n+1)}{24}\left(\frac{\Delta C}{C}\right)\right] + n\ln C_C. \tag{16}$$

If the experiment is carried out so that $\Delta C/C$ remains approximately constant, the slope of the line resulting from a plot of $\ln(-\Delta C/C)$ against $\ln C_c$ immediately gives the order of the reaction without any error; the rate constant is then easily calculated from the intercept on the ordinate axis.

Let us consider one other possible method for the calculation of the order of the reaction from the experimental data. The following expression may be obtained by integrating (14):

$$-\frac{d\tau}{d\ln C} = \frac{1}{C_0^{n-1} \cdot k} + (n-1)\cdot\tau, \qquad (17)$$

which is characterized by a somewhat unusual arrangement of the variables. This differential equation is linear with respect to time; therefore, calculation of the derivative $d\tau/d \ln C$ from data on $\Delta\tau_i$ and $\Delta \ln C_i$ can be carried out by the methods considered above (see sections 3, 5, 8). According to (17) the slope of the line representing a plot of $d\tau/d(\ln C)$ vs. τ gives the order of the reaction minus one. This method can be used if the concentration of the reactant or the property of the system which is proportional to concentration is controlled during the course of the reaction

SUMMARY

1. An analysis and classification of calculation methods for first order reactions have been proposed on the basis of the number of parameters applicable to the determination of the rate constant. It was shown that in many cases integral and well-known differential methods do not permit sufficiently rapid and accurate calculation of the rate constant.

2. In this connection, $\dot{\varphi}-\varphi$ and $\ln \dot{\varphi}-\tau$ methods were proposed for reactions for which the equation can be reduced to the form $-k \equiv (\Delta/\Delta\varphi)(d\varphi/d\tau) \equiv (\Delta/\Delta\tau)(\ln d\varphi/d\tau)$. At the base of these methods lie two methods for the direct calculation of the derivatives, from data for the intervals $\Delta\varphi_i$ and $\Delta\tau_i$:

$$\frac{\Delta\varphi}{\Delta\tau} = \left(\frac{d\varphi}{d\tau}\right)_\varphi \cdot \left(1 - \frac{1}{3}\delta^2\right) = \left(\frac{d\varphi}{d\tau}\right)_\tau \cdot \left(1 + \frac{1}{6}\delta^2\right).$$

In this case, there is no necessity of constructing so-called kinetic curves, and the experimental data are immediately convertable to the form required for construction of the straight lines. The proposed methods for calculating rate constants do not require a knowledge of the parameters.

3. If 8-10 intervals ($\Delta\varphi_i$, $\Delta\tau_i$) are fixed during the course of the experiment, calculation of the rate constant with an error not exceeding ± 0.2% is possible from the approximation $\Delta\varphi/\Delta\tau = (d\varphi/d\tau)_\varphi = (d\varphi/d\tau)_\tau$.

4. Evaluations are given of the error in the rate constant for different regimes of the kinetic investigation. Optimum regimes are proposed; these depend on the method of calculation, and are $\Delta\varphi_i \cdot \Delta\tau_i \simeq$ const ($\dot{\varphi}-\varphi$ method) and $\Delta\tau_i \simeq$ const ($\ln \dot{\varphi}-\tau$ method).

5. It was shown that first-approximation equations permit determination of the values of the rate constants from data obtained over two intervals.

6. The proposed methods can be used for calculation of the rate constants of second order reactions, and also for the determination of the order of the fraction from the data from one experiment.

We take this opportunity to express our deep appreciation to Corresponding Member AN SSSR V.V. Voevodskii for discussion of the work and critical comments.

LITERATURE CITED

1. J.H. van't Hoff, Outlines of Chemical Dynamics [Russian translation (IL, 1936).
2. E.A. Guggenheim, Philos. Mag 2, 538 (1926).
3. R.P. Bell and B.B. Darwent, Trans. Soc. 46, 34 (1950).
4. W.H. Cropper, F. Spieth and A.R. Olson, J. Am. Chem. Soc. 76, 6428 (1954).
5. B.I. Segal and K.A. Semendyaev, Five-Place Mathematical Tables [in Russian] (Moscow, 1959).
6. G.S. Berger, Zhur. Fiz. Khim. 31, 257 (1957).

KINETICS OF THERMAL CRACKING OF HYDROCARBONS AND THEIR MIXTURES

G.M. Panchenkov and V.Ya. Baranov

I.M. Gubkin Moscow Institute of the Petrochemical and Gas Industry
Translated from Kinetika i Kataliz, Vol. 1, No. 2, pp. 188-196,
July-August, 1960
Original article submitted December 21, 1959

An equation for the kinetics of thermal cracking has been obtained on the basis of a representation of a radical-chain mechanism for the cracking reaction. The derived equation has been shown applicable to the calculation of the kinetics of continuous-flow thermal cracking of either individual hydrocarbons (n-hexadecane) or petroleum products, at various temperatures and pressures. The values of thermal cracking rate constant upon changing pressure from atmospheric to 50 atm pass through a maximum at about 10 atm.

Thermal conversions of hydrocarbons occupy an important place in petroleum processing. Besides the production of cracked gasoline, additional possibilities have emerged for the use of thermal cracking for the light cracking of vacuum residua and the recracking of refractory catalytic distillates. The role of high-temperature cracking-pyrolysis has also increased. In this connection the task of investigating the kinetics and mechanism of thermal conversions of hydrocarbons and petroleum products is of great practical and theoretical interest. A solution of this problem is becoming especially urgent in connection with the rapid growth of the petrochemical synthesis industry, since raw material for this industry can be obtained as a result of thermal conversions of hydrocarbons.

Until recently it was considered that themal cracking is a homogeneous first-order reaction. The observed deviation from first order at increased depth of conversion was explained by A.V. Frost and A.I. Dintses [1] on the basis of chain-breaking by a substance forming in the same reaction. The empirical equation which they proposed for the kinetics of thermal decomposition was later derived by A.D. Stepukhovich [2] on the basis of a radical-chain scheme of hydrocarbon decomposition.

In our study of the kinetics of continuous-flow cracking of petroleum products we also found that the kinetics of thermal cracking are not always described by the first-order equation which one of us had derived for flow systems [3], written in the form:

$$n_0 x = \frac{\beta - 1}{\beta} n_0 \ln (1 - x) + K, \qquad (1)$$

where n_0 is the number of moles of initial substance fed to the reaction zone in unit time, x is the quantity of substance reacted (fraction of initial material reacted), $\beta = \nu_1 + \nu_2 + \ldots - 1$, $K = k/\beta$ is the apparent rate constant, k is the actual rate constant, and ν_1 represents the stoichiometric coefficients for the reaction products.

On coordinates of $n_0 x$ and $-n_0 \ln (1 - x)$ in the majority of the cases which we studied the slope of the straight lines varied with temperature and pressure; in some cases the values of β obtained from the slope were less than zero, which is impossible since the value of β is intrinsically positive. Such a phenomenon could not be observed if the thermal cracking reaction conformed strictly to a first-order equation.

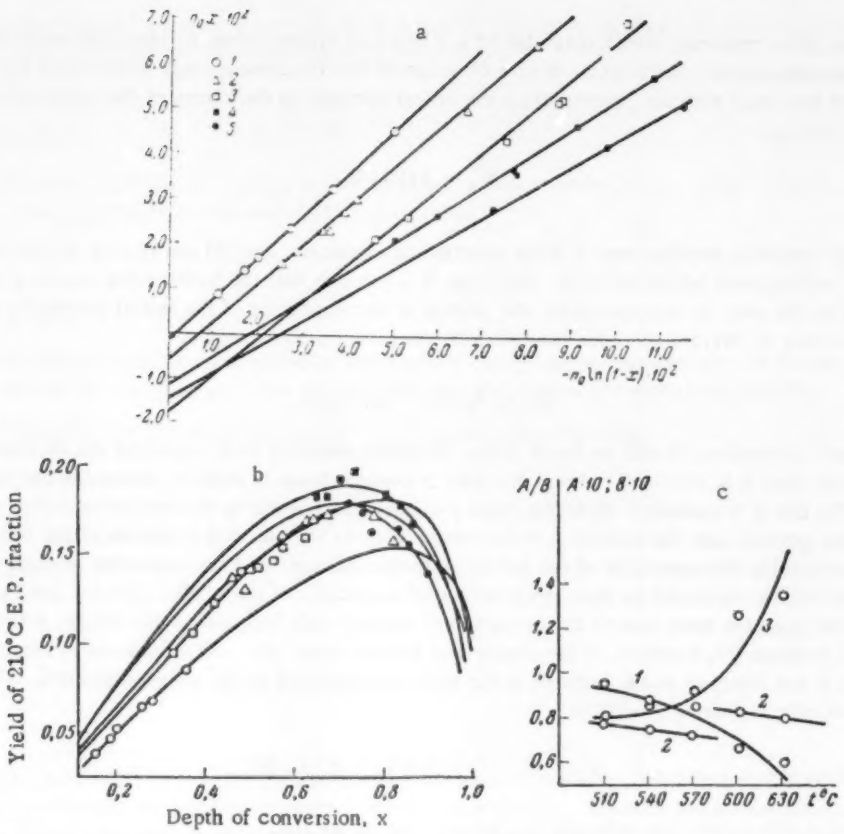

Fig. 1. a) Kinetics of thermal cracking of 310-410° fraction of Grozny paraffinic crude at atmospheric pressure; b) dependence of yield of 210° E.P. fraction upon depth of conversion. For Fig. a) and b): 1) 510°, 2) 540°, 3) 570°, 4) 600°, 5) 630°; c) temperature dependence curves for values of A/B, A, and B: 1) A/B= ϑ (t); 2) A= ψ (t); 3) B= ζ (t).

Such a relationship is presented in detail in Fig. 1a for the reaction of thermal cracking of a 310-410° fraction of Grozny paraffinic crude [4]. We obtained a similar relationship for a narrower fraction of Grozny paraffinic crude [5] and for a 320-450° fraction of Romashkino crude [6]. The slope of the straight line changes sharply above 580-590°. We have explained this phenomenon successfully, based on a radical-chain reaction mechanism for the thermal cracking of hydrocarbons.

Let us examine the derivation of the kinetic equation for thermal cracking which we obtained [6] based on the representation of thermal cracking as a radical-chain reaction. The derived equation will be used below for calculating the kinetics of the thermal cracking of various raw materials.

The kinetic equation for thermal cracking may be found either from a knowledge of the specific mechanism of each reaction (i.e., a knowledge of all the elemental reactions which constitute the process as a whole) or from certain over-all qualitative considerations which agree with the experiments. The first route is practically impossible, since the detailed mechanism of the overwhelming majority of chemical reactions is unknown to us. Therefore, only the second route is practicable

The thermal cracking reaction, if its kinetics are judged by the total conversion of the initial material, may be written:

$$A \rightarrow \nu_1 A_1 + \nu_2 A_2 + \ldots + \nu_n A_n, \qquad (a)$$

where A is the initial material, which may also be a mixture of hydrocarbons; A_i represents reaction products; ν_i represents stoichiometric coefficients. It may be assumed that the slowest stage of the cracking reaction is the reaction of low-mass radicals (forming from the initial material in the course of the reaction) with the initial molecules, i.e.

$$W_1 = k[R][A], \tag{2}$$

where W_1 is the cracking reaction rate, k is the reaction rate constant, and [R] and [A] are respectively the concentrations of radicals and initial material. However, it is possible that the hydrocarbon cracking reaction rate is determined by the rates of two processes: the process of decomposition of the initial molecules into free radicals and the process of interaction of the radicals with the initial molecules, i.e.

$$W_1 = k_1[A] + k_2[R][A]. \tag{3}$$

From both expressions, as will be shown below, formally identical final equations are obtained. From (2) and (3) it follows that it is necessary to know the radical concentration in order to determine the cracking reaction rate. For this it is necessary to define those processes which result in the formation and destruction of radicals. In the general case the radicals may be formed both by bimolecular collisions of the initial molecules and by monomolecular decomposition of the initial molecules because of a concentration of energy at a given bond. Radicals will be destroyed by their interaction with molecules of the initial material and by their recombination. The first reaction must lead to the formation of radicals with high molecular weight, which are converted to final products (for example, to isoalkanes and alkenes when the initial molecules are alkanes). The second process is not likely to occur, because of the high concentration of the initial materials. Therefore, the reaction rate of radical formation will be

$$W_2 = k_3[A]^2 + k_1[A] - k_4[A][R]. \tag{4}$$

Having applied to this process the principle of stationary states, we find

$$[R] = \frac{k_3}{k_4}[A] + \frac{k_1}{k_4}. \tag{5}$$

In this case cracking will proceed according to a radical mechanism.

In the third item of the expression (4), if the process takes place according to a radical-chain mechanism, it is also possible to take into account the process of regeneration of radicals as a result of their reaction with the initial molecules; then k_4 will no longer be equal to k or k_2, but will represent the difference between the rate constant of radical destruction k_4 and the rate constant of radical regeneration k_5. If the reaction of radical formation by bimolecular collisions of the initial molecules is unimportant, then from the expression (4) using the principle of stationary states we obtain $[R] = k_1/k_4$; for the case where the reaction of monomolecular decomposition of the initial molecules into radicals may be neglected, we obtain $[R] = k_3/k_4 [A]$.

Substituting (5) into (2) or (3), we obtain

$$W_1 = k'\{1 + k_3'[A]\}[A], \tag{6}$$

where in the case of substituting (5) into (2), $k' = k \cdot k_1/k_4$ and $k_3' = k_3/k_1$, and in the case of substituting (5) into (3), $k' = (k_1k_4 + k_1k_2)/k_4$ and $k_3' = k_2k_3/(k_1k_4 + k_2k_1)$.

Deciding the question of whether Equation (2) or (3) is to be given preference will be possible only after a detailed study of the mechanism of thermal cracking. For the solution of practical problems Equation (6) is entirely sufficient. From (6) it is seen that if bimolecular collisions are unimportant in radical formation, then (since in this case $[R] = k_1/k_4$) Equation (6) turns into an equation of a first-order reaction. This is possible if the cracking takes place at low pressures. But if the process of decomposition of the initial molecules into free radicals is unimportant, then the thermal cracking will proceed as a bimolecular process. Apparently we should encounter this situation at relatively low temperatures.

In case the thermal cracking is carried out in a flowing stream (as it always is in practice), the reaction rate equation based on Equation (6) according to [3], is written:

$$n_0 \frac{dx}{\rho dl} = k' \{1 + k_3' C_A\} C_A. \tag{7}$$

If the thermal cracking takes place in the gas phase at low pressures, then it may be assumed that the ideal gas laws are applicable to reactants and products; then

$$C_A = \frac{(1-x)P}{(1+\beta x)RT}, \tag{8}$$

where P is the total pressure, R is the universal gas constant, and T is the temperature. In the case of cracking under high pressure it is necessary to take into account the deviation of the gases from ideality.

Substituting (8) into (7), separating variables, and integrating, we obtain

$$n_0 x = -\frac{A}{B} n_0 \ln (1-x) - \frac{k' P V_r}{BR^2T^2}, \tag{9}$$

where

$$A = (1+\beta)^2/m + n;$$

$$B = \frac{\beta^2}{n} + \frac{\beta}{m}\left(2 + \beta - \frac{m}{n}\beta\right) - \frac{(1+\beta)^2 n}{m(m+n)};$$

$m = RT + k_3'P$, $n = \beta RT - k_3'P$, and V_r is the reaction volume; in addition, it is taken into consideration that for values of $\underline{x}$ which are not very large $\ln (m + nx) \approx \ln m + (n/m)x$. Equation (9) on coordinates n_0x and $-n_0 \ln (1-x)$ gives a straight line with slope equal to A/B and intercept equal to $k'PV_r/BR^2T^2 = K^*$ is the apparent rate constant. Both of these values depend upon both pressure and temperature.

In the cracking of petroleum products the yield of gasoline fraction usually passes through a maximum; therefore, strictly speaking, the thermal cracking reaction should be considered as a stepwise reaction of the following form:

$$A \rightarrow \nu_1 A_1 + \nu_2 A_2 + \nu_3 A_3 \rightarrow \nu_4 A_4 + \nu_5 A_5. \tag{b}$$

In this equation all products are formally considered as individual compounds with molecular weights equal to the average molecular weights of the corresponding fraction. In Equation (b) A is the initial material and A_1, A_2, and A_3 are respectively gas, coke, and gasoline. The second stage of the reaction is the decomposition of gasoline to coke and gas, i.e., to the products which are most stable thermodynamically.

The calculation of such a type of reaction presents significant difficulties, since the detailed mechanism of thermal cracking, as already stated, is unknown. It may be believed that the free radicals which lead to the process of cracking are formed both from the initial molecules of A and from molecules of the gasoline fraction. Such an approach leads to a very complex differential equation which requires a computer for solution.

It is also possible to proceed from cruder but simpler assumptions. It is known that the higher the molecular weight of the hydrocarbon, the less stable it is in the thermal cracking reaction. Therefore it may be supposed that the principal source of free radicals will be the initial molecules of A. These radicals will react both with the initial molecules of A and with molecules of the intermediate material A_3. Assuming that the rate of cracking is determined by Equation (2), the rate of thermal cracking of the initial molecules can be expressed by the equation

$$W_1 = k_1 [R][A]; \tag{10}$$

for the rate of thermal cracking of the intermediate product (gasoline)

$$W_2 = k_2 [A_3] [R]; \tag{11}$$

and for the rate of formation of free radicals

$$W_3 = k_3 [A]^2 + k_4 [A] - k_5 [A] [R], \tag{12}$$

neglecting the value $k_2 [A_3] [R]$, which characterizes the rate of radical destruction by reaction with the intermediate material, and which is small in comparison with $k_5 [A] [R]$. The constants of Equations (10), (11), and (12) differ from those of previous equations, although the same indexes [subscripts] are used for convenience only.

For a flow-type reaction Equations (10) and (11), according to [3], after substitution of (12) are written

$$n_0 \frac{dx}{\rho dl} = k' C_A (1 + k_3' C_A), \tag{13}$$

$$n_0 \frac{\nu_4}{\nu_3} \frac{dy}{\rho dl} = k'' C_{A_2} (1 + k_3' C_{A_2}). \tag{13a}$$

The remainder of the solution is similar to that given in [3] for successive reactions and makes it possible to obtain an equation defining the yield of intermediate (x_{A_2}) depending on the depth of conversion of the initial material,

$$x_{A_2} = \nu_3 x - y = \frac{\nu_3}{1 - K} [(1 - x)^K - (1 - x)], \tag{14}$$

where K is the ratio of the rate constants of the second and first stages of the reaction. Methods of finding K are known [4, 7]. Substituting (14) into (13) and integrating the obtained equation with certain simplifying assumptions, we obtain an expression which formally resembles (9) (the difference will reduce to the physical significance of the constants). Knowing the values of k' and K, it is easy to calculate the rate constant of the second stage of the cracking reaction. Equations formally resembling (13) and (13a) can be obtained by proceeding from equations of the type of (3) for the first and second stages.

We carried out the thermal cracking of n-hexadecane and various fractions of Grozny paraffinic crude in a flow unit. The unit for cracking at atmospheric pressure and the method of conducting the experiments was given in [8].

The experimental data were worked up according to Equation (9). The values obtained are brought together in the table.

An examination of the coefficient A/B of Equation (9) shows that the value of A decreases with increasing temperature, but B either increases somewhat or remains constant; consequently, the coefficient A/B must decrease with increasing temperature. The numerical values of A shown in the table were obtained by substituting the experimental data into the expression $A = \Sigma n_i / n_0 x RT$. The latter expression is obtained from the original $A = (1 + \beta)^2 / (m + n)$ upon introducing the values of m, n, and $\beta = \Sigma n_i / (n_0 x - 1)$ where Σn_i is the total of the moles of reaction products.

The rate constants k' in the table are calculated according to Equation (9).

The data presented in Fig. 1a on the kinetics of thermal cracking of Grozny paraffinic crude 310-410° fraction indicate that at 600 and 630° there is a sharp decrease of the slope of the straight line. This phenomenon may be explained on the basis that our assumption as to the temperature independence or near-independence of the value of B may well prove to be correct only up to 580-590°. A significant increase of B at 600 and 630° entails a sharp decrease both of the value of A/B and of the apparent rate constant. An increase of the value of A at these same temperatures can be explained by the intensive gas formation from the decomposition of both the initial raw material and the intermediate 210° E.P. fraction, which leads to a change of the value $\Sigma n_i / n_0 x$ from 5 at 510-570° to 6 at 600-630°. As stated above and as also shown in [3, 4, 6], the equations for the rate

Constants of Equation (9) for the Reaction of Thermal Cracking of Various Raw Materials

Raw material	Pressure, atm	Temp., °C	A/B	$\frac{\Sigma ni^*}{n_0 x}$	$A \cdot 10^2$	$B \cdot 10^2$	1st stage rate const., $k_1 \cdot 10^3$, sec^{-1}	1st stage activation energy, kcal/mole	$\frac{k_2}{k_1} = K$	2nd stage rate const., $k_2 \cdot 10^3$, sec^{-1}	2nd stage activation energy, kcal/mole
n-Hexadecane	1	520			6,50	5,08	8,06			8,06	—
		550	1,28	4,23	6,26	4,90	30,40	58,0	1,0	30,40	58,0
		580			6,04	4,72	111,0			111,0	—
310-410° fraction of Grozny paraffinic crude	1	510	0,95	—	7,79	8,15	2,64	—	0,30	0,79	—
		540	0,88	5,0	7,50	8,54	10,90	—	0,38	4,14	—
		570	0,85	—	7,23	8,50	34,40	56,4	0,49	16,80	67,0
		600	0,66	6,0	8,38	12,60	34,80	—	0,60	20,90	—
		630	0,60	—	8,10	13,50	49,70	—	0,72	35,80	—
300-360° fraction of Grozny paraffinic crude	1	510	0,95	—	7,79	8,20	1,73	—			
		530	0,91	—	7,59	8,34	4,64	—			
		550	0,87	—	7,40	8,51	10,28	—			
		570	0,81	5,0	7,23	8,98	22,70	56,0			
		590	0,75	—	7,06	9,47	49,60	—			
		610	0,56	—	6,92	12,30	27,50	—			
300-480° fraction of Grozny paraffinic crude	1	470	—	—	—	—	0,49 **	—		0,11 **	
		490	—	—	—	—	1,30 **	—		0,38 **	
		510	1,05	5,0	7,78	7,41	3,20	53,0	0,37	1,18	69,0
		540	1,03	—	7,50	7,28	10,40	—	0,53	5,50	
		570	0,96	—	7,23	7,50	37,50	—	0,73	27,40	
	10	470	1,18	—	7,06	6,00	0,79			0,37	
		490	1,15	4,3	6,88	5,98	2,06	53,6	0,47	1,15	66,0
		510	1,18	—	6,70	5,68	5,03		0,56	4,02	
									0,80		
	50	470	1,25	—	6,24	5,00	0,53	52,0	0,38	0,20	
		490	1,31	3,8	6,08	4,64	1,20		0,56	0,67	72,0
		510	1,30	—	5,92	4,55	3,17		0,76	2,41	

* Values cited are arithmetic averages for all experiments at given temperature.

** Values calculated on the basis of the Arrhenius equation.

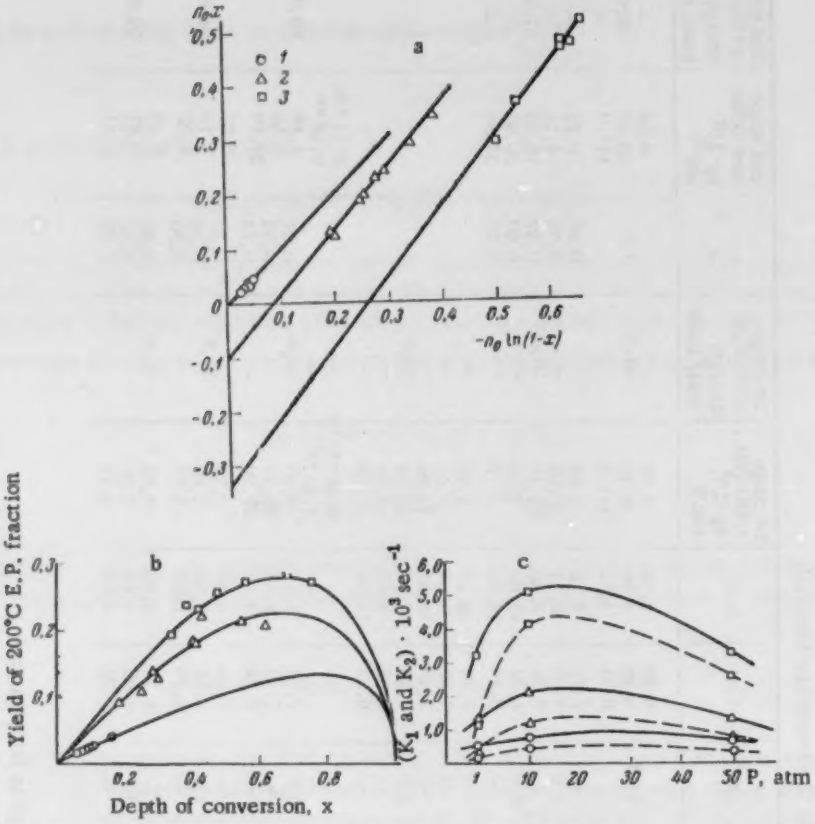

Fig. 2. a) Kinetics of thermal cracking of 300-480° fraction of Grozny paraffinic crude at temperature 510° and pressure 1, 10, and 50 atm; b) dependence of yield of 200° E.P. fraction on depth of conversion at 510° and various pressures. For Fig. a) and b); 1)1 atm, 2)10 atm, 3) 50 atm; c) pressure dependence of rate constant of first and second stages of cracking reaction: 1) 470°, 2) 490°, 3) 510° (k_1—solid line; k_2—broken line).

constant k' and the rate constant of the first stage of the cracking reaction k_1 are formally similar. Having assumed as a first approximation that k' is numerically equal to k_1, it is possible, knowing K, to find the value of the rate constant of the second stage of the cracking reaction k_2.

Figure 1b gives the dependence of the yield of intermediate fraction A_2 (210° E.P. fraction) upon depth of conversion. In the figure the experimental points are plotted on the theoretically calculated curves. Figure 1c shows the temperature dependence of A/B, A, and B.

The table also shows kinetic data calculated according to Equation (9) for the cracking of n-hexadecane. The values of rate constants and activation energy which are obtained are practically identical with the results obtained by calculation from Equation (1) [8], which makes it possible to consider (1) as a special case of the more general Equation (9).

In the case of cracking under pressure, an additional factor (pressure) influences the kinetics of thermal cracking. Cracking under pressure was carried out in a specially constructed flow unit. Figure 2a shows the kinetics of thermal cracking of a 300-480° fraction of Grozny paraffinic crude at 510° and at pressures of 1, 10, and 50 atm. We had obtained similar relationships for other temperatures also.

As is evident from Fig. 2a, the experimental points fall on the theoretically calculated straight lines with good agreement, which confirms the correctness of (9) for the case of cracking under pressure. Figure 2b also

shows the dependence of the yield of intermediate fraction (200° E.P.) on depth of conversion of the initial raw material. Here the experimental points are plotted on the theoretically calculated curves. As is evident from the graph, satisfactory agreement of theoretical and experimental results is observed. The values obtained by working up the experimental data are presented in the table. In the case of cracking at 50 atm we took into account the deviation of the properties of the hydrocarbon gases from those of an ideal gas.

From the table it is seen that for the case of cracking at atmospheric pressure the value of A/B is somewhat decreased upon increasing the temperature. At 10 and 50 atm the value of A/B for a given pressure remains practically constant, independent of temperature. However, an increase of pressure at constant temperature gives a marked increase of the value of A/B. This may be explained by the influence of pressure on the value of B. As is evident from the data of the table, increasing pressure at constant temperature lowers the value of B, which also leads to an increase of the value of A/B with increasing pressure. Figure 2c shows the pressure dependence of rate constants of the first and second stages of the cracking reaction. It is evident from the figure that upon increasing pressure from 1 to 50 atm the values of rate constant pass through a maximum at about 10 atm. A similar regularity was established by M.G. Gonikberg and V.V. Voevodskii [9] for the reaction of thermal cracking of alkane hydrocarbons. The relationship which we obtained, as is evident from Fig. 2c, becomes less marked at lower temperatures (within the limits of pressure studied).

This apparently explains the fact that in many studies on the cracking kinetics of petroleum products (studied in most of the known works at 425-470°) there has been noted an absence of any pressure effect on cracking rate.

SUMMARY

1. A kinetic equation for thermal cracking has been obtained on the basis of representations as to the radical-chain mechanism of the cracking reaction. The derived equation has been shown applicable to the calculation of the kinetics of thermal cracking both of individual hydrocarbons (n-hexadecane) and of petroleum products, at various temperatures and pressures.

2. It has been shown that the values of the rate constant for thermal cracking upon varying the pressure from atmospheric to 50 atm pass through a maximum at about 10 atm.

LITERATURE CITED

1. A.I. Dintses and A.V. Frost, Doklady Akad. Nauk SSSR 7, 510 (1934).
2. A.D. Stepukhovich, Zhur. Fiz. Khim. 28, 1882 (1954).
3. G.M. Panchenkov, Zhur. Fiz. Khim. 22, 203 (1948); 26, 454 (1952); Uch. Zap. Moskov. Gosudarst. Univ., No. 174, Neorg. i Fiz. Khim. 53 (1955); Heterogeneous Catalysis in the Chemical Industry [in Russian] (Goskhimizdat, Moscow, 1955) p. 292; Jour. Chim. Phys. 51, 740 (1954).
4. G.M. Panchenkov and V.Ya. Baranov, Izvest. Vyssh. Ucheb. Zaved., Neft' i Gaz [in press].
5. G.M. Panchenkov and V.Ya. Baranov, Collection: Kinetics and Catalysis [in Russian] (Izd. AN SSSR, Moscow, 1960) p. 251.
6. G.M. Panchenkov and V.Ya. Baranov, Doklady Akad. Nauk SSSR 126, 608 (1959).*
7. G.M. Panchenkov and V.Ya. Baranov, Khim. i Tekh. Topliva 9, 24 (1958).
8. G.M. Panchenkov and V.Ya. Baranov, Izvest. Vyssh. Ucheb. Zaved., Neft' i Gaz 1,103 (1958).
9. M.G. Gonikberg and V.V. Voevodskii, Izvest. Akad. Nauk SSSR, Otdel. Khim. Nauk 370 (1954).*

*Original Russian pagination. See C.B. translation

KINETICS OF ALKALINE HYDROLYSIS OF THE METHYL ESTER OF ALANYL GLYCYL GLYCINE IN AQUEOUS SOLUTION

D.G. Knorre, G.V. Kukushkina, and V.P. Mamaev

Institute of Chemical Physics, Academy of Sciences, USSR
Translated from Kinetika i Kataliz, Vol. 1, No. 2, pp. 197-202,
July-August, 1960
Original article submitted January 5, 1960

For in-process observation of the condensation of amino acids and peptides a semiquantitative method has been developed for determining non-N-terminal amino acids in peptides.

Bimolecular rate constants of the alkaline hydrolysis of the methyl ester of alanyl glycyl glycine have been determined. It was found that the activation energy is 10.5 kcal/mole and that the coefficient of the exponential function is $1.4 \cdot 10^8$ liter · mole^{-1} · sec^{-1}.

At 0 deg the rate constant of self-condensation of the methyl ester of alanyl glycyl glycine does not exceed $2 \cdot 10^{-7}$ liter · mole^{-1} · sec^{-1}, which is $4 \cdot 10^6$ times less than the rate constant of alkaline hydrolysis at the same temperature.

It is known that the formation of peptide bonds by means of direct interaction of carboxyl and amino groups is impossible, since the equilibrium of this reaction is strongly displaced in the direction of the initial substances [1].

Since the preparation of peptides from amino acids or from shorter peptides becomes in essence the acylation of an NH_2 group of an amino acid or peptide by an acyl group of another amino acid or another peptide, it is necessary in peptide syntheses to make use of derivatives of amino acids or peptides in which the carboxyl group is replaced by some other group which has a stronger acylating action. Recently it has been established that the synthesis of the polypeptide chains of protein in living cells goes by a similar route [2].

Before combining with each other, the amino acids are converted to derivatives in which their carboxyl group is connected by an ester bond to a molecule of the carbohydrate ribose, which enters into the composition of ribonucleic acid [3].

It is not difficult to demonstrate that any derivative of an amino acid or peptide which is capable of acylating the NH_2 groups of amino acids and peptides must be hydrolyzable in aqueous solution. Let us write the equations for the acylation and hydrolysis reactions in the form:

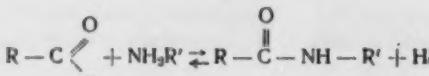

(1)

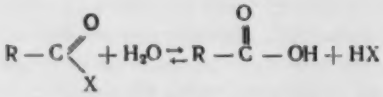

(2)

Let us also write the equation for the formation of the peptide bond directly, with participation of the free carboxyl group:

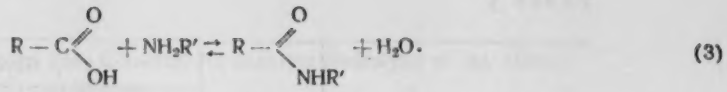

(3)

It is not difficult to be convinced that Reaction (2) can be accomplished by means of successively carrying out Reaction (1) and then Reaction (3) in the reverse direction. Therefore the free energy change for hydrolysis ΔG_2 must be equal to the difference of the values of ΔG for Reactions (1) and (3):

$$\Delta G_2 = \Delta G_1 - \Delta G_3.$$

Since we are assuming that the equilibrium of Reaction (1) is displaced to the right and the equilibrium of Reaction (3) (as already stated) is displaced to the left, then $\Delta G_1 < 0$, $\Delta G_3 > 0$, and consequently $\Delta G_2 < 0$, whereupon

$$\Delta G_2 < \Delta G_1.$$

Thus, if the compound RCOX possesses acylating activity, then its hydrolysis must be more favorable thermodynamically than the acylation of the NH_2 group of an amino acid or peptide. Consequently, any synthesis of the peptide bond in aqueous solution must inevitably be accompanied by hydrolysis of the acylating component. In this connection, for studying the mechanism of the biosynthesis of protein and also for studying the mechanism of the synthesis of peptides in aqueous or water-containing solutions, it is essential to know the ratio of the rates of amidation and hydrolysis of the acylating agent.

The objective of the present work was to establish the ratio of the rates of amidation and hydrolysis of one of the simplest classes of acylating agents, namely esters, in the example of the methyl ester of the tripeptide alanyl glycyl glycine.

EXPERIMENTAL METHOD

Synthesis of the ester of the tripeptide was carried out, starting from glycyl glycine and α-bromopropionyl chloride. The latter was obtained by the usual method from a mixture of 30 g of α-bromopropionic acid and 17 ml of $SOCl_2$, heating on a steam bath for two hours. The reaction product was distilled, collecting the 128-138° fraction. Glycyl glycine (7.9 g) was dissolved in 29 ml of 1.9 N NaOH, cooled to -1° and then stirred vigorously for two hours while adding by portions in turn 5.6 ml of α-bromopropionyl chloride in 40 ml of $CHCl_3$ and 44 ml of 1.9 N NaOH. Upon completing the addition of the solutions, mixing was continued for 15 minutes more; then the aqueous layer was separated and acidified with 70 ml of 1 N HCl. Next the aqueous solution was vacuum distilled at a temperature not exceeding 35°, to a volume of 30 ml. Upon cooling to 0°, a precipitate of α-bromopropionyl glycyl was formed. Yield 8 g, m.p. 155-156°.

Further, 1.52 g of α-bromopropionyl glycyl glycine was dissolved in 11.4 ml of 9 N solution of NH_3 and heated 4 hours at 50°. The solution was evaporated under vacuum at 50° and the oil which remained was mixed with 30 ml of absolute alcohol. Then the solution was decanted and the residue was dissolved in a minimum quantity of warm water and the tripeptide precipitated by absolute alcohol. Yield 1 g. Three recrystallizations give a product with m.p. 193°.

For preparing the ester of the tripeptide, 29 ml of absolute CH_3OH was saturated (with cooling) with dry HCl, and to the resulting solution there was added with cooling 2.9 g of alanyl glycyl glycine. The mixture was agitated until the tripeptide was completely dissolved and immediately boiled down under vacuum at 20-40°. The residue was dissolved in dry CH_3OH and the hydrochloride of the methyl ester of alanyl glycyl glycine was precipitated by the addition of absolute ether. After two hours the crystals were vacuum filtered. Yield 3.1 g. After an additional recrystallization, m.p. 145° [5].

For studying the kinetics of hydrolysis of the methyl ester of alanyl glycyl glycine, a weighed amount of the hydrochloride was dissolved in a solution buffered to the required pH and stirred in a thermostat. The concentration of unreacted ester was determined on samples withdrawn during the course of the reaction. For this purpose there was utilized a hydroxamic method [6]. To the sample there was added a mixture of 4 ml of 0.2M $(NH_2OH)_2 \cdot H_2SO_4$ and 2 ml of 1.0 N NaOH. After five minutes 2 ml of 0.1 M solution of $Fe_2(SO_4)_3$ in 2 N H_2SO_4 was added to the sample, and the density of the red color formed (complex of Fe^{3+} with the hydroxamate

TABLE 1

Compound analyzed	Alanine	Glycine		
		calc., mg	found	
			mg	%
Alanyl glycyl glycine	None	1.54	1.14	74
The same	None	2.23	1.55	69.5
Methyl ester of alanyl glycyl glycine	None	4.82	3.52	72.5
The same	None	3.42	2.53	74

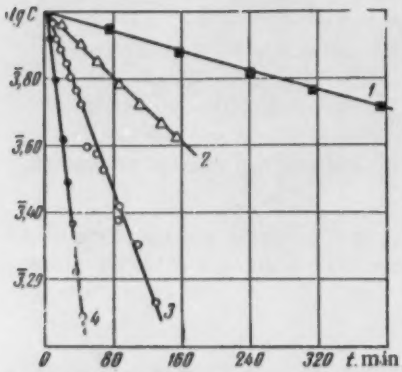

Fig. 1. Kinetic curves for consumption of methyl ester of alanyl glycyl glycine in 0.1 N $Na_2B_4O_7$ at various temperatures (°C): 1) 20.5; 2) 31.1; 3) 40.7; 4) 51.0.

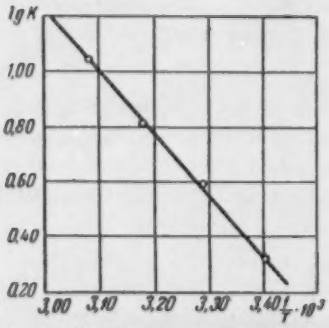

Fig. 2. Temperature dependence of rate constant for alkaline hydrolysis of methyl ester of alanyl glycyl glycine.

of the tripeptide) was determined in a FÉK-M photoelectric colorimeter with green filter, in 20-mm cells. In the experiments conducted with phosphate buffer, since the phosphate ions form complexes interfering with the formation of complexes with the hydroxamate, a 0.5 M solution of $Fe_2(SO_4)_3$ in 4 N H_2SO_4 was used. Under the indicated conditions of analysis, 1 ml of 0.01 M solution of the methyl ester of alanyl glycyl glycine gives a solution with optical density 0.69.

For determing the product of self-condensation of alanyl glycyl glycine (cyclic or linear hexapeptide) we decided to take advantage of the fact that the alanine moiety must appear in the hexapeptide without a free amino group. It was proposed to observe the appearance of such nonterminal alanine for the kinetics of self-condensation if such occurs. For the determination of nonterminal alanine we developed a special method. In principle this method consists of treating the solution with HNO_2, which destroys the terminal amino groups of the peptide. Then the mixture is hydrolyzed, and the remaining amino acids are determined chromatographically [7]. Alanine could appear on the chromatogram only in the case of hexapeptide formation, since all of the alanine in the tripeptide is N-terminal and is fully destroyed by the nitrous acid.

For this purpose a sample containing 3-4 mg of the tripeptide was treated for 20 minutes at 50° with vigorous agitation with 1 ml of 6 N HCl and 0.5 ml of 30% $NaNO_2$. Then the mixture was passed through a column with ÉDÉ-10 anion exchange resin in the OH^- form for eliminating NO_2^-, elutriated with 0.2 M CH_3COOH, and boiled to dryness; the residue was dissolved in a minimum quantity of water, and the solution was passed through a column with SDV-3 cation exchange resin in the H^+ form for eliminating Na^+ ions. Then elutriation was carried out with 0.2 N NH_3 and the elutriate was boiled to dryness. The residue was dissolved in 2-3 ml of 6N HCl; this was quantitatively transferred to an ampule, sealed, and heated for 16 hours at 105° (for acidic hydrolysis of the peptide). The hydrolyzate was freed from Cl^- by passing through a column with ÉDÉ-10 elutriated with 0.2 M CH_3COOH; the eluate was boiled to dryness and the residue was dissolved in 2 ml of water. Then an aliquot of the solution (usually 0.02 ml) was applied to a strip of chromatographic paper (Leningrad brand, slow) and chromatographed by a mixture of n-butanol–acetic acid–water, 5:1:4. The chromatogram was developed by 0.5% solution of ninhydrin in acetone. The spots were elutriated 4 hours by methanol containing $Cu(NO_3)_2$ (0.5 ml saturated solution in 0.5 liter). Color was determined in a FÉK-M photoelectric colorimeter with green filter and compared with the color given by a standard solution.

TABLE 2

Apparent and Actual Rate Constants for Alkaline Hydrolysis of the Methyl Ester of Alanyl Glycyl Glycine

Buffer	pH at 25°	T° C	at T°C [OH⁻]	k', sec^{-1}	k, $liter \cdot mole^{-1} \cdot sec^{-1}$
Borate	9,24	20,5	$1,34 \cdot 10^{-5}$	$2,8 \cdot 10^{-5}$	2,09
		31,1	$2,46 \cdot 10^{-5}$	$9,55 \cdot 10^{-5}$	3,9
		40,7	$4,18 \cdot 10^{-5}$	$2,7 \cdot 10^{-4}$	6,45
Phosphate	6,95	51,0	$6,90 \cdot 10^{-5}$	$7,65 \cdot 10^{-4}$	11,1
		51,0	$9,55 \cdot 10^{-7}$	$6,9 \cdot 10^{-6}$	7,2
		90,6	$7,9 \cdot 10^{-8}$	$3,8 \cdot 10^{-4}$	48

The method was proved out on alanyl glycyl glycine and its methyl ester. The results of determinations are shown in Table 1.

Thus, the N-terminal amino acid indeed disappears completely. The nonterminal amino acid is determined to the extent of 70%, which apparently is connected with losses in the repeated evaporations and the repeated passage through columns with ion exchange resins. The method, therefore, can be applied semiquantitatively.

Measurements of the pH of the buffers and determination of pK of the methyl ester of alanyl glycyl glycine were conducted with a glass electrode in a LP-57 electronic potentiometer.

EXPERIMENTAL RESULTS

Figure 1 is a semilogarithmic plot of the kinetic curves for hydrolysis of the methyl ester of alanyl glycyl glycine (0.01 M) in 0.1 N borate buffer with pH 9.24, at temperatures of 20.5, 31.1, 40.7, and 51.0°.

On coordinates of log C (concentration of unreacted ester) and t_{min} (time) the experimental points plot well as straight lines, which indicates a first-order reaction with respect to the ester. From the slope of these straight lines the first-order apparent rate constants (k', sec^{-1}) were determined; these represent the product of the actual rate constant and the OH^- concentration. The values of $[OH^-]$ were calculated, based on the values of the ion product of water and pK of the component of the buffer (in the given case, H_3BO_3), at the corresponding temperature [8]. For verifying the dependence of reaction rate on concentration $[OH^-]$, the first-order apparent rate constant k' was determined at 51.0° in phosphate buffer with pH 6.95. From the data presented in Table 2 it is seen that the actual rate constant in 0.2 M phosphate buffer differs from the value obtained in borate buffer by less than 1.5 times, although the corresponding values of k' differ by almost 100 times. Thus, the principal change of reaction rate upon changing from borate to phosphate buffer is caused by the change of solution pH.

Figure 2 shows the temperature dependence of $\underline{k}$ (coordinates log k and 1/T). The activation energy of the reaction, determined by the slope of the straight line obtained, proved to be equal to 10.5 kcal/mole. The Arrhenius equation for the rate constant $\underline{k}$ has the form

$$k = 1,4 \cdot 10^{8} e^{-\frac{10500}{RT}} \text{ liter} \cdot \text{mole}^{-1} \cdot \text{sec}^{-1} = 2,35 \cdot 10^{-15} e^{\frac{10500}{RT}} \text{ cm}^3 \cdot \text{molecule}^{-1} \cdot \text{sec}^{-1}. \quad (4)$$

Calculation of the value of $\underline{k}$ by this formula at 90.6° gives k= 63, in good agreement with the values obtained by measuring reaction kinetics at this temperature in phosphate buffer.

For selection of conditions for studying the self-condensation of the methyl ester of alanyl glycyl glycine we proceeded on the basis that the reactive form is the form with a free amino group, and therefore for maximum predominance of self-condensation over alkaline hydrolysis it is necessary to have a maximum ratio of the concentration of ester with free amino group NH_2R to the concentration of OH^-. It is not difficult to show that:

$$\frac{[NH_2R]}{[OH^-]} = \frac{[\text{ester}]}{K_w(10^{pH} + 10^{pK})}$$

where K_W is the ion product of water and pK is the logarithm of the ionization constant of the ammonium form of the ester.

For determining the value of pK we measured the pH of a 0.02 M solution of the hydrochloride of the ester in 0.01 N NaOH. Since in this case the concentrations of ester with the NH_2 group and with the NH_3^+ group were equal, then the pH of the solution was equal to pK of the NH_2 group of the ester. According to our measurements this value was equal to 7.78.

From the cited formula it is seen that the ratio $[NH_2R]/[OH^-]$ decreases sharply in the region pH > pK and is practically unchanged in the region pH < pK. Therefore, the optimum region of values of pH is the region near 7.78. In addition, it is desirable to have a maximum concentration of the ester of alanyl glycyl glycine in the solution.

It is also known that in the condensation of glycine esters to form diketopiperazine it is recommended that the reaction be conducted at the lowest possible temperature [9]. By analogy with this, in our case we attempted to detect condensation of the ester at 0°.

For this purpose there was prepared a 0.212 M solution of the hydrochloride of the ester of alanyl glycyl glycine in 0.106 N NaOH. In such a solution pH = pK, i.e., pH = 7.8 (if the temperature dependence of pK is neglected). The actual rate constant of alkaline hydrolysis of the ester of alanyl glycyl glycine at 0° according to Formula (4) is equal to 0.55 liter · $mole^{-1}$ · sec^{-1}, and the actual rate constant:

$$k' = k[OH^-] = k\frac{K_w}{[H^+]} = k \cdot 0{,}13 \cdot 10^{-14} \cdot 10^{7{,}8} = 4{,}5 \cdot 10^{-7} \text{ sec}^{-1},$$

which corresponds to a 50% conversion time of $1.53 \cdot 10^6$ seconds or 17.7 days.

Tests for the formation of condensation product (appearance of nonterminal alanine) were made on 0.1 ml samples withdrawn 36 and 42 days after beginning the experiment; these samples were analyzed for nonterminal alanine. The chromatogram showed an intense spot for nonterminal glycine, but only unmeasurably small traces of alanine were detected (less than 0.5γ). Since 1% of the sample taken is applied to the chromatogram, the content of alanine in the total sample does not exceed 50 γ, i.e., on the order of 0.5 μM.

The sample taken contains 21.2 μM of alanine. Thus, condensation occurred to not more than 3%. Hence the rate of condensation does not exceed:

$$w \leqslant \frac{0{,}212 \cdot 0{,}03}{3 \cdot 10^6} = 2 \cdot 10^{-9} \text{ mole/liter} \cdot \text{sec}$$

Assuming that the rate is proportional to the square of the concentration of free amino group, it is possible to estimate the upper limit of the condensation rate constant:

$$k \leqslant \frac{2 \cdot 10^{-9}}{(0{,}1)^2} = 2 \cdot 10^{-7} \text{ liter/mole} \cdot \text{sec}$$

Thus, the rate constant for alkaline hydrolysis of the methyl ester of alanyl glycyl glycine is at least $4 \cdot 10^6$ times larger than the rate constant of its self-condensation.

SUMMARY

1. A semiquantitative method has been developed for the determination of non-N-terminal amino acids in peptides, based on the destruction of the terminal amino groups by nitrous acid, with subsequent acidic hydrolysis of the peptides and chromatographic determination of the remaining amino acids. The method is applicable for following the course of the process of condensation of derivatives of amino acids and peptides by the appearance of a new nonterminal amino acid.

2. Bimolecular rate constants have been determined for the alkaline hydrolysis of the methyl ester of alanyl glycyl glycine in aqueous solution. It was found that the activation energy of the reaction is 10.5 kcal/ /mole and that the coefficient of the exponential function is $1.4 \cdot 10^8$ liter $\cdot$ mole$^{-1} \cdot$ sec^{-1}.

3. It was found that at 0° the rate constant for the self-condensation of the methyl ester of alanyl glycyl glycine does not exceed $2 \cdot 10^{-7}$ liter $\cdot$ mole$^{-1} \cdot$ sec^{-1}, which is $4 \cdot 10^6$ times less than the rate constant for alkaline hydrolysis at the same temperature.

LITERATURE CITED

1. R. Borsook, Advances in Protein Chemistry (Academic Press, Inc, New York, 1953) Vol. 8, p. 127.
2. M.B. Hoagland et al., J. Biol. Chem. 231, 241 (1958).
3. H.G. Zachan, G. Acs, and F. Lipmann, Proc. Nat. Acad. Sci. USA 44, 885 (1958).
4. E. Fischer, Ber. 36, 2986 (1903).
5. E. Wilson and E. Pascu, J. Org. Chem. 7, 126 (1942).
6. F. Lipmann and L. Tuttle, J. Biol. Chem. 159, 21 (1945).
7. R. Block, R. Lestrange, and G. Zweig, Paper Chromatography [Russian translation] (IL, Moscow, 1954).
8. G. Harned and B. Owen, Physical Chemistry of Electrolytic Solutions [Russian translation] (IL, Moscow, 1952).
9. E. Fischer and E. Fourneau, Ber. 34, 2868 (1901).

INFLUENCE OF DEFECTS IN CRYSTALS ON THE RATE OF THERMAL DECOMPOSITION OF SOLID SUBSTANCES*

V.V. Boldyrev

S.M. Kirov Tomsk Polytechnic Institute

Translated from Kinetika i Kataliz, Vol. 1, No. 2, pp. 203-211,
July-August, 1960
Original article submitted December 21, 1959

The influence of various defects in crystals on the rate of thermal decomposition of solid substances is discussed. It is shown that the character of the influence of various defects on the rate of decomposition depends on the reaction mechanism.

If decomposition proceeds through cleavage of the bonds within the anionic or cationic component lattice, the rate of thermal decomposition will be influenced by defects leading to an increase in the active surface of the crystal (change of habit, macrocracks, dislocations). Under conditions where the thermal decomposition process occurs as a result of transfer of an electron from anion to cation the rate also will be strongly affected by the number of ionic vacancies, the number of interstitial ions, and the free-electron concentration in the lattice.

A review of the main experimental works in this direction is given.

One of the main peculiarities of topochemical reactions lies in the fact that the reacting atoms, ions, or molecules forming the crystal are fixed at lattice points, and lack that mobility which these particles have in the gas or liquid phase. This peculiarity affects the course of topochemical reactions within the limits of the reaction zone.

Changes in the number of active positions in the crystal and their character can affect the rate of topochemical reactions. In connection with this, the rate of topochemical processes depends on the real structure of the solid substance, i.e., on the presence in the crystal of macro- and microdefects of different forms, which will influence the rate in the course of the reaction.

Despite the fact that the effect of the real structure has long been known and was noted in a number of works on the kinetics of thermal decomposition of solid substances [1-3], few systematic investigations in this direction have been conducted as yet.

Proceeding from this, and also taking into account the great possibilities for regulation of the rate of many practically important processes, which detailed study of a group of factors connected with the real structure of the solid substance may provide, we made a systematic study of the influence of various crystal defects on the rate of thermal decomposition of solid substances. Certain general conclusions which may be reached on the basis of our experimental data, as well as the data of other investigators, are discussed in the present article.

Before we discuss the influence of defects of various forms on the rate of thermal decomposition, we shall consider whether the ideal crystal, free of defects or faults but limited in space, will have the same reactivity at all its points. From the most elementary consideration it follows that the crystal surface will differ in its most im-

*Experimental data obtained by Yu.A. Zakharov, V.P. Dolgova, V.I. Eroshkin, A.V. Boldyreva, V.N. Manyakhina, A.V. Safiulina, É.G. Pinaevskaya, M.S. Sokolova, B.I. Treskova, V.A. Zhigareva, A.A. Shint, and L.K. Yakovlev together with the author or under his direction are used in the article.

portant physicochemical properties from the interior. This difference is, firstly, due to the presence of a large number of degrees of freedom of the surface particles in comparison with the interior particles; secondly, the surface layer of the crystal is acted on by an unsymmetrical electric field. This effect is considered in detail for the case of ionic crystals in works [4-14]. According to the results given in these works, ions on the surface are displaced from the normal lattice points under the action of the field, which in some cases may even lead to a change of coordination number. Under the influence of an unsymmetrical field, the polarization of ions in the surface layer is much increased. This effect is especially marked in the case of compounds with a large anion and a small cation. Finally, discrete electronic levels, lying within the forbidden zone, are formed in the surface layer of the crystal.

Speaking concretely of the properties determining the thermal stability of a solid substance, one may assume that it must be less on the crystal surface than in the interior. Hence reactions must begin at the surface, both in the case of dehydration of crystal hydrates (the main role in this case must be played by peculiarities in the positions of the surface particles, due to steric factors, change of distances between particles, and changes in the symmetry and stability of the cationic grouping under the influence of the field), and in the case of decomposition of ionic salts of the silver azide type (the main item in this case must be a decrease in the energy of transfer of an electron to the conductivity band in the surface layer, and also possible improvement of conditions for the movement of cations to interstitial positions, resulting from increased ion polarization). It must be taken into account that different crystal faces may differ in reactivity, since the density with which each face is covered by the reacting particles and the amount of displacement of the particles under the influence of an unsymmetrical field may vary, depending on its crystallographic orientation.

The crystal surface is heterogeneous. Every crystal has not only faces, but also edges and corners. In such places the surface effects must be especially intensified [8]. These specific points of the crystals must be especially favorable for thermal decomposition. These positions are of negligible importance only in the case where we have relatively large crystals, free of growth defects, mosaic structure, and dislocations. Real crystals, with which one usually must deal, have a developed internal surface formed by growth defects, mosaic-block boundaries, and dislocations, which is many times greater in area and far richer in points equivalent to edges and corners than the external geometrical surface of the crystal.

The necessity of calculating the energy of edges and corners in real-crystal thermodynamics is shown in works [15, 16]. According to calculations performed in [15], these positions are especially important in the case of very fine crystals (dimensions of the order of 10^{-5} cm), i.e., in those cases where, in general, it is worth while to take surface particles into account in crystal thermodynamics. In this case we note that the dimensions of microcrystalline blocks in the lattices of solid substances [17] are of just this order.

From the above, it follows that a change in the habit and dispersity of crystals, and the presence therein of macrocavities, cracks, boundaries between blocks, and dislocations,must affect the rate of thermal decomposition of solid substances. Besides these defects, which affect the rate mainly on account of surface effects, the thermal-decomposition process may be influenced by lattice defects—anionic and cationic vacancies, interstitial ions, and electronic defects (free electrons and positive holes). In many cases these defects determine the possibility of occurrence of the elementary steps in the thermal-decomposition process, and hence their concentration may be of substantial importance. It is very difficult to distinguish sharply between the effects of these two groups of defects on the rate. On the one hand, deformation of the lattice around anionic or cationic vacancies and interaction of electrons and positive holes with the lattice framework, leading to its polarization, to a certain extent have much in common with changes occuring in the surface layer under the action of an unsymmetrical electric field; on the other hand, dislocation lines, block boundaries, and the crystal surface are the places where the elementary stages of thermal decomposition,with participation of ionic and electronic defects, are localized.

It is to be expected that different defects will influence the rate in different ways, depending on the mechanism of thermal decomposition. Taking into account the peculiarities of the mechanism, all reactions of thermal decomposition of solid substances (mainly ionic salts) may be divided into two groups.

1. Reactions of thermal decomposition, proceeding through cleavage of bonds within an anionic or cationic lattice component (for instance, the thermal decomposition of potassium permanganate, lead oxalate, and calcium carbonate and the dehydration of crystal hydrates). This group, in turn, may be divided into two subgroups:

a and b. Subgroup a comprises reactions of thermal decomposition, in which the evolved gas may enter into reverse reaction with the solid product; these reactions usually go in one step. The phenomenon of "impedance," i.e., retardation of the reaction by a layer of formed product, is very important in these reactions. Such reactions are exemplified by the decomposition of crystal hydrates, alkali-metal carbonates, etc. Subgroup b comprises reactions of thermal decomposition which are practically irreversible either because the process goes through several consecutive steps, or on account of steric peculiarities. Such reactions are exemplified by the decomposition of potassium permanganate, nickel and lead oxalates, and ammonium bichromate.

2. The second group of reactions of thermal decomposition comprises those in which the decomposition process occurs as a result of transfer of an electron from anion to cation. Thus the decomposition proceeds through cleavage of the bond between the anionic and cationic lattice components. Such decomposition is exemplified by the decompositions of silver oxalate, silver azide, mercuric fulminate, and silver halides.

Let us consider the influence of various defects on the rate of thermal decomposition of solid substances.

Change of habit. According to the Gibbs-Curie-Wolf principle, a crystal with a ratio of face areas corresponding to minimum surface energy will be characterized by a minimum of free energy. Deviation of the crystal habit from equilibrium must lead to a change in its chemical activity. A change of habit must affect the rate of thermal decomposition owing to the change in the area occupied by more-reactive faces on the crystal surface, relative to that occupied by less-active ones. Moreover, when the habit changes, the over-all ratio of the number of ions at the surface of the crystal to that in its interior also changes.

The relation between the rate of thermal decomposition and the habit was studied by us in the case of dehydration of magnesium sulfate heptahydrate [18, 19]. By direct measurement of the growth rate of reaction-product nuclei under the microscope and comparison of the rates of dehydration of plates cut from a crystal, parallel to prism and tetrahedral faces, it was shown that the dehydration rate at a prism face is less than at a tetrahedral face. Study of the dehydration rate of crystals of the same weight but different habit showed that on change of habit the rate increases with the proportion of the total surface occupied by tetrahedral faces. The difference in the rates of thermal decomposition of iron formate crystals obtained by different routes, observed in work [20], is probably also due to a change of crystal habit. On the basis of these data, as well as data on the anisotropy of growth of product nuclei on thermal decomposition [21, 22], it may be assumed that a change of habit will have considerable influence either in the dehydration of crystal hydrates or in the thermal decomposition of substances of other types, only if the crystal does not contain other defects more strongly influencing the rate (or if the influence of these defects is suppressed for any reason, e.g., on account of impedance).

Growth figures, macrocracks in the crystal, may have a considerable effect on the rate. Thus, for instance, on dehydration of a cobaltous sulfate heptahydrate crystal the initial centers are located along the growth levels of the crystal. In the case of a substance decomposing according to the first group and subgroup a of our classification of decomposition reactions, the influence of these defects is felt mainly in the initial stage of the process and then gradually diminishes owing to impedance. These defects may strongly influence the rate of thermal decomposition of substances of other types throughout the reaction [23].

Dislocations and groupings thereof, formed in crystals during growth and also on deformation, may strongly affect the rate of thermal decomposition. It has been shown that many thermal-decomposition reactions of solid substances begin at the point of emersion of dislocations at the crystal surface and at the boundaries of their groupings [24-28]. We arrived at an explanation of the process of physical aging in crystals of solid substances, based on the concept of dislocations in the crystal. It is well known that the rate of thermal decomposition of some solid substances (on keeping after preparation) changes. In certain cases the rate of thermal decomposition may increase on keeping, owing to chemical changes in the solid substance. This phenomenon has acquired the name of chemical aging [28-30]. We observed chemical aging in a study of the thermal decomposition of ammonium permanganate [31]. In other cases the decomposition rate of the compound decreases on keeping [32, 33]. Chemical changes in the substance usually do not occur in this case, and the process is called physical aging [30-34]. We observed such aging in a study of the kinetics of thermal decomposition of lead oxalate [35, 36]. A detailed investigation of the process showed that as lead oxalate ages the decrease in its decomposition rate is accompanied by narrowing of the lines in the Debye patterns and a decrease in its heat of solution. It was found that the aging process may be induced artificially by irradiating the solution with uv light during preparation of the oxalate [37]. Annealing of the crystals at temperature below that of decomposition accelerates aging [36]. Study of the rate of the aging process [37] showed that it is described by a

unimolecular law and has a low activation energy, approximately one order less than the activation energies usually observed in ionic crystals for diffusion and self-diffusion processes. Changes in the form and size of the crystals do not occur on aging. The concept of dislocations makes it possible to explain the mechanism of the process of physical aging, which from this point of view may be represented as the formation of groupings of dislocations and the annihilation of part of them on keeping of the crystals. In this case, owing to the decrease in the total number of dislocations, which are the points in the solid substance where the thermal-decomposition process begins, the rate of thermal decomposition decreases.

From the point of view of the dislocation mechanism of aging it is understandable why the degree of dispersity affects the rate of thermal decomposition of freshly prepared and aged crystals differently [38]. In freshly prepared crystals the crystal interior is permeated by a network of dislocations; it differs little in activity from the outer surface. Aged crystals are characterized by lower density of dislocations, and hence the difference between their surface and interior is greater, as a result of which the dependence of the rate on the degree of dispersity is also greater.

Impurities in the crystal are another important type of crystal defect. Impurities either may form portions of a new phase in the crystal or may enter the lattice, replacing part of the atoms or ions of the main substance. If the impurity forms a new phase in the crystal, its effect on the rate may be due to deformation of a layer of the initial substance at its interface with portions of the impurity phase, on account of orientational noncorrespondence of their lattices [39]. With strong orientational tendencies at the interface, dislocations may arise, and thus the influence of the impurity phase may reach not only adjacent lattice layers, but also much deeper ones. Moreover, the presence of an interface between two solid phases must cause a change in the conditions for the occurrence of electronic and ionic processes at the initial substance–impurity interface. Owing to these factors, impurities may be expected to have a substantial effect on the rate of thermal decomposition of solid substances. We performed experiments in which part of the initial substance was partially converted to another by preliminary chemical treatment, and this new substance formed inclusions of the impurity phase in the initial substance. After such preliminary treatment the rate of thermal decomposition of the solid substance changes, especially in the initial stage. This occurs, for instance, in the deomposition of lead oxalate treated beforehand with hydrazine hydrate [35,-36]. On treatment part of the oxalate (about 0.5-1%) is reduced to metallic lead. As a result of this the subsequent thermal decomposition is accelerated. If the metallic lead is replaced by silver through cementation from solution, the decomposition rate of the oxalate changes. In exactly the same way preliminary treatment of potassium permanganate and lead formate with hydrogen sulfide, and silver permanganate with carbon monoxide, leads to an increase in the rate of subsequent thermal decomposition of these substances. The increase in the decomposition rate on chemical aging, which we considered above, probably also belongs to this class of phenomena. In the case of thermal-decomposition processes belonging to the second group of our classification, inclusions of impurities in the crystal may effect the ionic and electronic stages of thermal decomposition. Thus additions of metallic gold and silver to silver azide [40], and manganese dioxide to ammonium perchlorate [41], increase the rate of thermal decomposition of these substances by capturing electrons from the conductivity band and thereby decreasing the probability of their recombination with holes.

If the impurity does not form inclusions of a separate phase but enters the lattice of the initial substance its effect on the rate may be manifested, firstly, as a consequence of deformation and distortion of the lattice at the place of inclusion of the impurity, and also owing to the appearance of an additional number of dislocations on crystallization; secondly, the presence of an impurity may be reflected in the ionic and electronic processes, in which the elementary stages of thermal decomposition consist. The character of the influence of such impurities depends to a great extent on the mechanism of thermal decomposition of the solid substance.

If the decomposition corresponds to the first group of our classification, the entrance of an impurity into the crystal must in principle cause the lattice of the original substance to be deformed and distorted, and therefore must accelerate the subsequent thermal decomposition. This is exemplified by the decomposition of lead oxalate containing an admixture of cerium, which we studied. According to [42, 43] the primary stage of decomposition of lead oxalate consists in breaking of the bonds within the oxalate ion; hence the decomposition of this salt must be referred to the first group of our classification. A study of the kinetics showed that lead oxalate coprecipitated with cerium oxalate, which can form a solid solution with it [44], is decomposed at a higher rate than the pure compound.

In the case of decomposition of the second type, i.e., through transfer of an electron from anion to cation, the elementary stages of thermal decomposition consist in transfer of an electron from the valence zone to the conductivity zone and capture of it by anionic vacancies, impurities in the crystal, or cations located at special lattice points (e.g., at the thresholds of dislocations). Interstitial cations are drawn toward the electron traps thus formed if Frenkel defects predominate in the crystal, whereas anionic vacancies are so drawn if Schottky defects predominate. The initial centers of thermal decomposition grow by alternation of stages of electron capture and drift of anionic vacancies or interstitial cations toward the trap. From this highly simplified scheme of thermal decomposition of substances belonging to the second group, it is clear that if the thermal-decomposition process is to occur, the concentration of free electrons and interstitial ions or anionic vacancies must be sufficient, and the crystal must be free of positive holes—anionic groupings or atoms that have lost an electron (or the probability of recombination of an electron with a hole must be decreased in some other way).

On consideration of the effect of impurities on the rate of thermal decomposition it is important to know whether or not an impurity ion has the same charge as the main-lattice ion replaced by it. In the first case the effect of the impurity will amount mainly to lattice deformation, the degree of which must depend on the quantity of impurity introduced and the difference between the radii of impurity ions and lattice ions. The effect of such an impurity on electronic and ionic processes in the crystal will be slight, although it apparently cannot be entirely excluded. If the impurity has a charge different from that of the ion replaced by it, its introduction into the lattice must lead either to a change in the valence of the lattice ions or to the appearance of an additional number of cationic or anionic vacancies in the lattice. In the latter case introduction of an impurity into the lattice may strongly affect the rate of thermal decomposition. When an admixture of cadmium ions is introduced into silver oxalate, an additional number of cationic vacancies must be formed in the lattice; the latter entrap positive holes, which in the course of decomposition must be removed from the crystal, and decrease the concentration of interstitial ions [45]. Therefore the rate of thermal decomposition decreases [46]. In just this way the addition of cadmium diminishes the effect of preliminary irradiation with ultraviolet light, as well as gamma-radiation from Co^{60}, on the thermal decomposition of silver oxalate [47]. If mercurous or sodium ions are introduced into silver oxalate, vacancies are not formed, and the rate of thermal decomposition of the compound containing the impurity is higher than that of the pure salt [46, 48, 49]. When silver oxide containing an admixture of cadmium is decomposed, the effect of vacancy formation and the deforming action of the addition apparently are superposed [50]. If an impurity which generates an additional number of anionic vacancies in the crystal is introduced, such vacancies being effective electron traps in thermal decomposition, the rate must increase. This is confirmed by experimental data. The rate of thermal decomposition of silver azide containing an admixture of cyanamide ions, and thallium azide containing an admixture of sulfide ions, is far higher than for the pure compounds [51]. Apparently this is due to the formation of anionic vacancies on introduction of impurities into crystals of these substances.

Increased concentrations of ionic defects, leading to higher rates of thermal decomposition, also can be obtained in other ways. For instance, tempering of the crystals, irradiation of them with slow neutrons [52], etc., act in this direction.

From the scheme of the thermal decomposition mechanism for substances belonging to the second group, it follows that the rate of the process must depend not only on the concentration and form of the ionic defect, but also on the concentration of electrons in the conductivity zone. The electron concentration in the conductivity zone may be changed, for instance, as a result of adsorption on the surface of the solid substance of gas molecules which are electron donors or, contrariwise, acceptors. This must lead to a change in the rate of formation of initial reaction centers [53], as well as the rate of the thermal decomposition process at the original-substance–reaction-product interface [54]. The thermal decomposition of silver oxalate may be given as an example. According to [55, 56], the decomposition of silver oxalate in an atmosphere of hydrogen, usually an electron donor, is more rapid than in a vacuum, whereas in an atmosphere of oxygen, usually an electron acceptor, it is slower. Certain impurities apparently have a similar effect on the rate of thermal decomposition of silver oxalate [57-59].

The fact that different defects will influence the rate differently, depending on the thermal-decomposition mechanism, was mentioned above. In the table which we give at the conclusion of this article, it is shown how different defects influence the principal groups of thermal decomposition reactions.

Influence of Crystal Defects on the Rate of Thermal Decomposition of Solid Substances

Crystal defects influencing the rate	Decomposition occurs through		
	cleavage of bonds within the cationic or anionic lattice components		electron transfer from anion to anion
	reversible decomposition	irreversible decomposition	
Change of habit	Affect	Affect	Affect
Growth figures, vicinals, macrocracks			
Dislocations and groups thereof	Do not affect		
Inclusions of impurities in the lattice			
Ionic defects		Do not affect	
Electronic defects			

It is evident from the table that in the case of reactions belonging to the first group the presence of ionic and electronic defects in the crystal has negligible influence on the rate, since the primary elementary stages of decomposition occur within the anionic and cationic groupings, mainly through cleavage of coordinate and covalent bonds. In the case of reactions of this group, belonging to subgroup a, the role of dislocations and microcracks in the crystal is generally diminished owing to impedance. On decomposition of substances belonging to subgroup b these defects, on the contrary, become very important. In a thermal-decomposition reaction of the second group all forms of crystal defects considered by us may have influence. Ionic and electronic defects are especially important in this case. The density of dislocations in the crystal also may have a pronounced effect on the rate of these processes. If the concentration of these defects is decreased to a minimum, for instance, by choosing the appropriate conditions of preparing the crystals, the rate also will influenced by other defects: growth figures, change of habit, etc.

LITERATURE CITED

1. S.Z. Roginskii, Zhur. Fiz. Khim. 12, 427 (1938); 15, 708 (1941).
2. G.E. Huttig, Handbuch der Kathalyse 6 (1943).
3. V.V. Boldyrev, Methods of Study of the Kinetics of Thermal Decomposition of Solid Substances [in Russian] (Izd. Tomsk Gos. Univ. 1958).
4. B. Madelung, Z. Phys 20, 494 (1919).
5. J. Lennard-Jones and B. Dent, Proc. Roy. Soc. A121, 247 (1928).
6. B. Dent, Phil. Mag. 8, 530 (1929).
7. E. Verwey, Rec. trav. chim. 65, 521 (1946).
8. K. Moliere, W. Rathje, and I.N. Stranski, Disc. Faraday Soc. 5, 21 (1949).
9. A.A. Glauberman, Zhur. Fiz. Khim. 23, 124 (1949).
10. M. Nicolson, Proc. Roy. Soc. A228, 490 (1955).
11. V.F. Konusov, Zhur. Fiz. Khim. 31, 2469 (1957).
12. V.F. Konusov and A.A. Medvinskii, Izvest. Vyssh. Ucheb. Zavedenii, Fiz. 4, 19 (1958).
13. I.E. Tamm, Z. Phys. Sowjet. 1, 733 (1932); Z. Phys. 76, 849 (1932).
14. B.A. Lippmann, Ann. Phys. (USA) 2, 1, 16 (1926), Bull. Am. Phys. Soc. 2, 80 (1957).
15. O.K. Poltorak, Zhur. Fiz. Khim. 31, 2470 (1957).
16. E. Lange, Z. Elektochem. 58, 887 (1954).
17. C.G. Darwin, Phil. Mag. 27, 315 (1914); R.A. Hill and A.A. Wallace, Nature 178, 692 (1956); E. Cremer and F. Gatt, Radex Rundschau 7, 257 (1949).
18. V.V. Boldyrev, A.V. Safiulina, A.V. Boldyreva, and B.I. Treskova, Zhur. Fiz. Khim. [in press].
19. V.V. Boldyrev, Proceedings of the Seventh Sci. Conf. Tomsk State Univ. 4, 144 (1957).
20. V.P. Kornienko and M.S. Novakovskii, Nauch. Zapiski Khar'kov Gosudarst. Univ. 30, 278 (1950).
21. Solid State Chemistry (Ed. W.E. Garner) (Butterworths Sci. Publ., 1955).
22. B.E. Bartlett, F. Tompkins, and D. Young, Nature 179, 4555, 365 (1957).

23. F.P. Bowden and A.D. Yoffe, Fast Reaction in Solids (Butterworths, Sci. Publ., 1958).
24. J. Hedges and J. Mitchell, Phil. Mag. 44, 223 (1953).
25. F. C. Tompkins and D.A. Yong, Proc. Roy. Soc. A236, 10 (1956).
26. F.P. Bowden and J. MacAuslan, Nature 178, 408 (1956).
27. K. Singh, Trans. Faraday Soc. 52, 1623 (1956).
28. B. Bartlett, F. Tompkins and D. Young, J. Chem. Soc. 3323 (1956).
29. I. Simpson, D. Taylor, and D. Anderson, J. Chem. Soc. 2378 (1958).
30. F. Tompkins, Disc. Faraday Soc. 23, 20 (1957).
31. V.V. Boldyrev, Uchenye Zapiski Tomsk. Gosudarst. Univ. 29, 44 (1959).
32. J. Thomas and F. Tompkins, Proc. Roy. Soc. A210, 11 (1951).
33. B.V. Erofeev, P.I. Bel'kevich, and A.A. Volkova, Zhur. Fiz. Khim. 20, 1102 (1946).
34. G. Hüttig, Monatsh. Chem. 85, 369 (1954).
35. V.V. Boldyrev, L.K. Yakovlev, and V.N. Manyakhina, Uchenye Zapiski Tomsk. Gosudarst. Univ. 26, 44 (1955).
36. V.V. Boldyrev, Sbornik Nauch. Rabot Inst. Khim. Akad. Nauk Belorus SSR 5, 100 (1956).
37. V.V. Boldyrev, V.P. Dolgova, and A.A. Shint, Nauch. Doklady Vyssh. Shkol, Ser. Khim. i Khim. Tekhnol. 1, 26 (1959).
38. V.V. Boldyrev and V.P. Dolgova, Khim. Nauka i Prom. 4, 283 (1959).
39. G.V. Sakovich and V.V. Boldyrev, Zhur. Fiz. Khim. 32, 298 (1958).
40. J. MacAuslan, Proc. Roy. Soc. A246, 248 (1958).
41. A. Galwey and P. Jacobs, Trans. Faraday Soc. 55, 1165 (1959).
42. P. Yankowich and J. Coppeland, J. Am. Chem. Soc. 79, 2081 (1957).
43. R. David, Compt. rend 240, 782 (1955).
44. A.N. Kirgintsev. Zhur. Neorg. Khim. 2, 1672 (1957).
45. A.N. Murin and B.G. Lur'e, Zhur. Fiz. Khim. 32, 2575 (1958); A. Miller, and R. Maurer, Phys. Chem. Sol. 4, 196 (1958).
46. V.V. Boldyrev, V.I. Eroshkin, and Yu.A. Zakharov, Izvest. Vyssh. Ucheb. Zavedenii, Khim. i Khim. Tekhnol. 1, 63 (1960).
47. V.V. Boldyrev, Yu.A. Zakharov, V.I. Eroshkin, and M.S. Sokolova, Doklady Akad. Nauk SSSR 129, 365 (1959).*
48. D. Trandafelov. Zhur. Priklad. Khim. 31, 198 (1958).*
49. L. Suchow and S. Hersh, J. Phys. Chem. 57, 438 (1953).
50. V.V. Boldyrev and Yu.A. Zakharov. Khim. Nauka i Prom. 4, 287 (1959).
51. P. Gray and T. Waddington, Proc. Roy. Soc. A241, 110 (1957).
52. F. Bowden and K. Singh, Proc. Roy. Soc. A227, 30 (1954).
53. V.V. Boldyrev. Zhur. Fiz. Khim. 33, 11 (1959).
54. J. Mac Donald, Disc. Faraday Soc. 23, 230 (1957).
55. Z. Szabo and E. Biro-Sugar, Z. Elektrochem. 60, 871 (1956).
56. V.V. Sviridov and L.A. Makarevich. Doklady Akad. Nauk Belorus SSR 3, 208 (1959).
57. J. Mac Donald and C. Hinshelwood, J. Chem. Soc. 127, 2769 (1925).
58. J. Mac Donald, J. Chem. Soc. 832 (1936).
59. J. Mac Donald and R. Sandison, Trans. Faraday Soc. 34, 5 (1938).

*Original Russian pagination. See C.B. translation.

ADSORPTION, IONIZATION, AND CATALYTIC ACTIVATION OF GASES ON METALS

A.I. Krasil'shchikov, L.G. Antonova, and F. P. Ivanovskii

State Scientific Research Institute of the Nitrogen Industry
Translated from Kinetika i Kataliz, Vol. 1, No. 2, pp. 212-220,
July-August, 1960
Original article submitted December 22, 1959

We have investigated the electrochemical potential during the adsorption of hydrogen, carbon dioxide, ethylene, carbon monoxide, nitrogen, a mixture of ethylene and hydrogen, and a mixture of nitrogen and hydrogen on copper, cobalt, nickel, silver, and iron at temperatures from 250 to 425°C.

In all the cases investigated adsorption of gas on the metal was accompanied by a definite jump of the electrochemical potential. We believe this fact is related to the ionization of a part of the gas adsorbed on the surface of the metal.

The phenomena of adsorption and catalysis are coming to be understood in terms of a theory involving electron interaction [1-9], and this theory necessitates the development of new methods of investigation.

In our previous investigation [10-12] we attempted to develop and justify an electrochemical method of investigation based on the results of the classical experiments by Haber. These experiments were performed at high temperature [13]. In the present article we describe some basic results obtained with this method.

The diagram of the apparatus is shown in Fig. 1. The reaction tube was made of a special type of glass.* The tube was coated on the inside and outside with metal layers which served as electrodes. The inside layer served at the same time as gas adsorbent. The glass acquired electrical conductivity when heated, and played the role of solid electrolyte. The metal layer outside served as the reference electrode. This layer was made of silver and was in contact with air (air-silver reference electrode). The potential of the inside layer was measured with an electron voltmeter consisting of two balanced tubes which consumed very small amounts of current (of the order of $1 \cdot 10^{-10}$ amp). The precision of the calculation was approximately 1 mv, and the results were usually reproducible within a range of 20-30 mv.

EXPERIMENTAL RESULTS

In an atmosphere of pure hydrogen gas different metals acquire potentials close to the hydrogen equilibrium potential, i.e., about 1.2 v with respect to the air-silver reference electrode. The results of measurements in the temperature range of 250-425° are shown in Fig. 2.

The values of potential observed depend to a certain degree on the nature of the metal.** The most positive values of potential were for silver and iron, and the most negative for copper. The difference between the potentials of these metals is about 200-225 mv.

It should be noted that the potential of the hydrogen electrode on silver becomes stable only at 300° and higher. At 250° and lower the hydrogen electrode on silver is apparently poisoned by traces of oxygen. Active nickel layers could be prepared only from nickel nitrate. In the case of layers obtained from nickel chloride, the hydrogen electrode was apparently poisoned by traces of chloride.

---

* We used various types of conducting glass.

** In some cases (nickel and copper) the potential was partly dependent on temperature; the cause of this phenomenon is not quite clear.

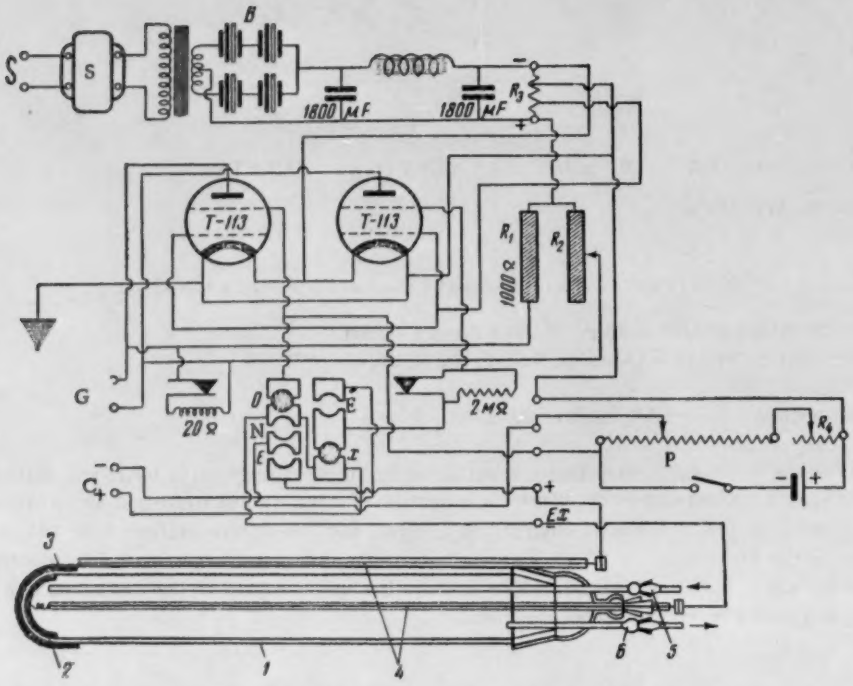

Fig. 1. Electrical diagram of the apparatus. 1) Reaction tube; 2) working electrode; 3) reference electrode; 4) platinum contacts; 5) gas inlet; 6) gas outlet, O, N, E, Ē, x) switch; E_x) difference of potential measured; C) normal cell. R_1, R_2, R_3, R_4) resistances; B) Selenium rectifier; S) stabilizer; G) zero galvanometer; P) potentiometer.

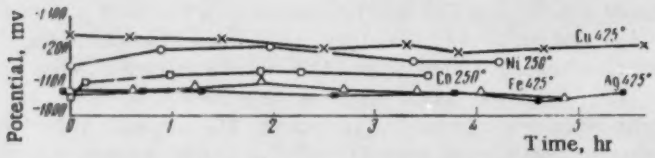

Fig. 2. Adsorption of hydrogen on different metals.

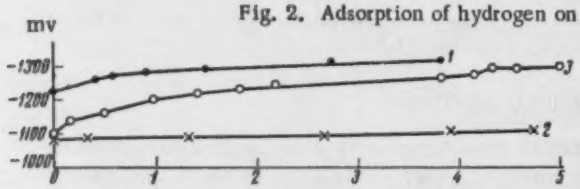

Fig. 3. Adsorption of hydrogen on copper at 300°. 1) Dry hydrogen; 2) hydrogen with an absolute humidity of 4.01%; 3) dry hydrogen (after the experiment with humid hydrogen).

In the case of a copper layer, when the hydrogen electrode was poisoned by water vapor, the potential was displaced toward more positive values. It must be noted, however, that at 300° and higher the poisoning of the hydrogen electrode on copper by water vapor is apparently reversible (Fig. 3). On the contrary, at lower temperatures (of the order of 250°) the poisoning is practically irreversible (Fig. 4). Stable values of hydrogen electrode potential are obtained on cobalt layers.

The values of the hydrogen electrode potential on the metals indicated, which are close to the equilibrium potential, lead to the conclusion that in this case there exists a direct equilibrium between the gaseous hydrogen adsorbed on the metal and hydrogen ions dissolved in the glass or adsorbed by it. In other words, one can assume that in these cases the situation is similar to that observed during the formation of a hydrogen electrode in liquid electrolyte at room temperature.

Other gases are also adsorbed with relative ease on these metals. For example, carbon dioxide is easily adsorbed on copper at 250° when the potential is about 500 mv with respect to the air-silver reference electrode

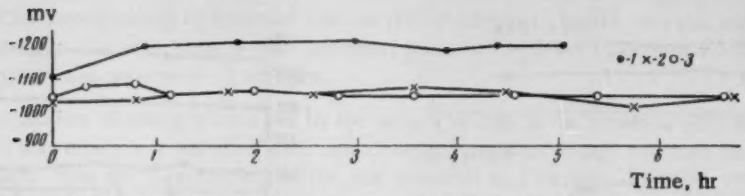

Fig. 4. Adsorption of hydrogen on copper at 250°. 1) Dry hydrogen; 2) hydrogen with an absolute humidity of 2.66%; 3) dry hydrogen (after the experiment with humid hydrogen).

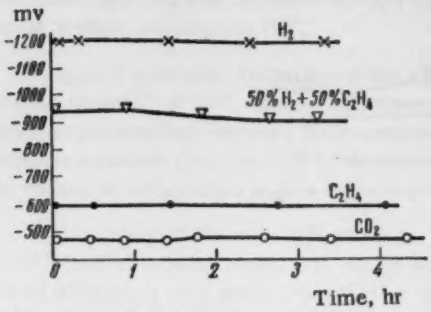

Fig. 5. Adsorption of various gases on copper at 250°.

(Fig. 5), and therfore carbon dioxide is easily separated from dry hydrogen circulating over the copper; under these conditions the potential of the copper layer becomes equal to the hydrogen electrode potential at this temperature. Carbon dioxide is as easily adsorbed on cobalt, and the potential shows the same value.

We also used this electrochemical method to investigate the adsorption phenomena occurring during the process of catalytic hydrogenation of ethylene. In the case of adsorption of ethylene on nickel the results were not sufficiently reproducible due to polymerization of ethylene, for which nickel is the recommended catalyst [14]. Therefore further experiments on the adsorption of ethylene were made with copper. The results on copper were reproducible when thoroughly purified ethylene was used. The results of the experiment at 250° are shown in Fig. 5.

Ethylene is adsorbed on copper at a potential of 600 mv with respect to the air-silver electrode, while hydrogen is adsorbed at a potential of 1200 mv. A stoichiometric mixture of both gases is adsorbed at an intermediate value of potential, about 900 mv. It is usually considered that one can neglect the adsorption of ethane formed under the condition of hydrogenation of ethylene [15]. According to the values of potential we obtained, hydrogen as well as ethylene is apparently adsorbed in considerable amounts by copper from the stoichiometric mixture.

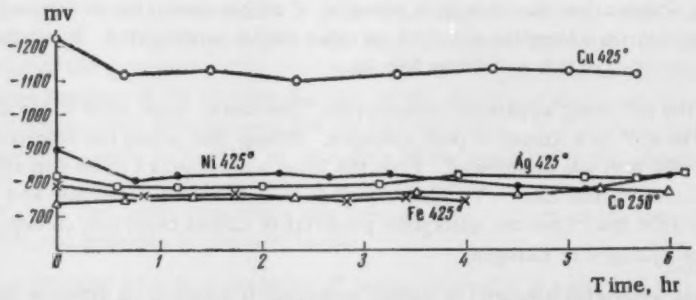

Fig. 6. Adsorption of carbon monoxide on different metals.

It is usually assumed that the adsorption of hydrogen is due to the detachment and passage of electrons from the gas to the metal. If the adsorption of ethylene were completely unconnected with electron transfer, or if the transfer were in the same direction in the case of hydrogen and ethylene, the adsorption potential of the mixture of these gases should be close to the adsorption potential of the more negative hydrogen. In reality, however, we obtain a very different picture (see Fig. 5). Therefore we must assume that the adsorption of hydrogen and ethylene on copper is due to the transfer of electrons in a reverse direction. Apparently under these conditions the electron from the metal passes to a molecule of ethylene, possibly at the place of the double bond. In fact it is known that in many cases the reaction mobility of an inert molecule is increased by the attachment of an electron [16]. For oxygen this has been shown experimentally [17, 18].

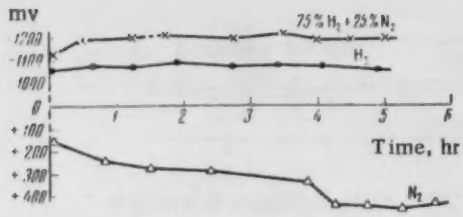

Fig. 7. Adsorption of nitrogen, hydrogen, and nitrogen-hydrogen mixture on iron at 425°

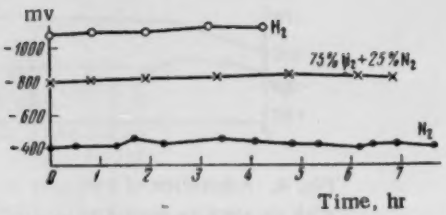

Fig. 8. Adsorption of nitrogen, hydrogen, and nitrogen-hydrogen mixture on cobalt at 250°

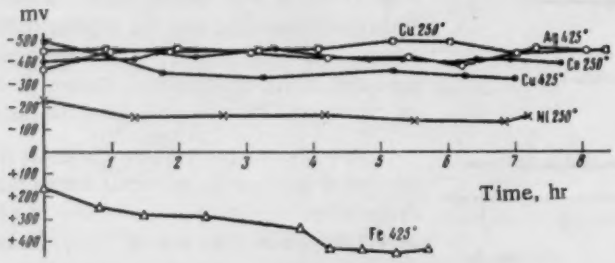

Fig. 9. Adsorption of nitrogen on different metals.

We also investigated the adsorption of carbon monoxide on different metals by this method. The results of these experiments are shown in Fig. 6.

Carbon monoxide is adsorbed on iron and cobalt at a potential of about 750 mv with respect to the air-silver reference electrode, and on nickel and silver at a potential of about 800 mv. It must be noted that these values are relatively close together and more negative than those obtained for all the other gases investigated except hydrogen. Thus, of all the gases investigated, carbon monoxide is the strongest reducing agent after hydrogen.

The results of experiments concerning the adsorption of carbon monoxide on copper are somewhat unexpected. Thus, Fig. 6 shows that the adsorption potential of carbon monoxide on copper (about 1100 mv) is considerably different from its adsorption potential on other metals investigated. It is relatively close to the hydrogen adsorption potential of this metal (see Fig. 2).

We performed the following additional experiments. The metal layer after being reduced in a stream of hydrogen was heated to 425° in a stream of pure hydrogen. During this period the adsorption potential of nitrogen on copper (about 400 mv) was established. Then the layer was subjected to an atmosphere of carbon monoxide at this temperature. In this case, as in other experiments with carbon monoxide and copper, the value of the potential reached 1100 mv. Thus the adsorption potential of carbon monoxide on copper is almost the same after the adsorption of hydrogen or nitrogen.

The fact that the adsorption potential of carbon monoxide is different on different metals (1100 mv on copper, about 800 mv on other metals) leads us to think that in this case the complex electronic structure of carbon monoxide plays an important role.

Experiments concerning adsorption of nitrogen and a nitrogen-hydrogen mixture (25% nitrogen, 75% hydrogen) were made with iron at 425°. The results of these experiments are shown in Fig. 7. It turns out that, contrary to all the other gases investigated, nitrogen is adsorbed on iron at potentials considerably more positive than the air-silver reference electrode, approximately +0.4 mv. However, the results of the experiment concerning the adsorption of nitrogen on iron gave much less reproducible values of potential than those relative to other gases. Thus, if in general we obtained a precision of ± 25 mv, this precision was only ± 150 mv in the case of adsorption of nitrogen on iron. The sign of the potential allows us to conclude that the adsorption of nitrogen on iron is due to electron transfer from iron to nitrogen. It is possible that in this case nitrogen is adsorbed not in the form of atoms but in the form of molecular ions, N_2^-.

Figure 7 shows that in the case of adsorption of a stoichiometric mixture of nitrogen and hydrogen on iron we obtain the potential corresponding to hydrogen and not that of nitrogen. In this case the stabilization of hydrogen potential is much easier even than in pure hydrogen, possibly dur to the additional activation of iron induced by the adsorption and desorption of nitrogen.

Apparently the amount of nitrogen adsorbed by the surface of iron in the presence of hydrogen is very small due,to the fact that nitrogen is adsorbed with considerable activation energy and then enters rapidly into reaction with hydrogen. Thus the measurement of the iron potential in a nitrogen-hydrogen mixture leads to results in good agreement with those predicted by the ordinary theory of ammonia synthesis, according to which the rate of formation of ammonia on iron is determined by the rate of activated adsorption of nitrogen, while the rate of decomposition of ammonia is determined by the rate of desorption of nitogen [19-22]. It could be considered that traces of ammonia on iron due to the interaction of the nitrogen-hydrogen mixture should be absent in these experiments [23].

Figure 8 represents the results of the experiment concerning the adsorption of nitrogen and hydrogen-nitrogen mixture on cobalt at 250°. As the results show, the hydrogen-nitrogen mixture is adsorbed on cobalt at values of potential intermediate between those corresponding to adsorption of nitrogen and adsorption of hydrogen. One can therefore conclude that, contrary to the case of iron, considerable amounts of hydrogen and nitrogen are present on the the surface of cobalt when it is in contact with the nitrogen-hydrogen mixture.

A summary of the most typical results concerning the adsorption of nitrogen on cobalt, nickel, and copper at 250° and on copper, silver, and iron at 425° is given in Fig. 9. These results show that the adsorption potential of nitrogen is very much dependent on the nature of the metal. The difference in the values of this potential on silver and iron reaches about 800 mv.

DISCUSSION OF RESULTS

In all the cases investigated,the adsorption of gases on metals at high temperature is accompanied by a definite jump of electrochemical potential. As a rule the value of such jumps corresponds approximately to the ordinarily observed values of the jump of electrode potential at the limit of separation between the metal and the solution. The reproducibility of the results indicates that when glass is used as a solid electrolyte the jumps of potential are equilibrium jumps.

It has been frequently stated that the catalytic activity of the metal can be reduced to its capacity to ionize the adsorbed gas. As a result of this assumption some attemps have been made to relate the catalytic activity directly to electronic structure of the metal [8]. However, it must be noted that the capacity of ionizing the adsorbed gas molecules is determined in general not only by the electronic structure of the metal but also by the nature of the gas and by the strength of the bond between the adsorbed gas and the surface of the metal. In fact the energy of the electron transfer from the metal to the gas, or in the reverse direction, depends not only on the work function of the electron but also on the affinity of the gas molecule for the electron and on the energy of the adsorptional bond between the gas and the metal. It is possible that carbon monoxide is an intermediate compound capable (according to the nature of the metal) of being adsorbed either by acquiring an electron or losing one. In fact carbon monoxide is on one hand a very strong reducing agent, for instance in the case of copper (Fig. 6), and enters very easily into reaction with oxygen; on the other hand the reaction between carbon monoxide and hydrogen is also well known.

It is very important that the adsorption potential of carbon monoxide is approximately 300-350 mv more electronegative on copper than on all the other metals investigated (iron, cobalt, nickel, silver).

Apparently the explanation of this fact must be sought in the complex electronic structure of carbon monoxide and in the selective character of the adsorptional affinity.

The existence of a definite jump of the electrochemical potential of the gas electrode at the interface between the metal and the solid electrolyte—glass—indicates that the gas adsorbed by the metal is in equilibrium with the ions of the gas dissolved in the glass or adsorbed at its surface.

The question arises as to the origin of these ions. In principle there are two possibilities. First it is possible that a certain portion of the adsorbed gas is ionized at the surface of the metal and the ions formed then migrate into the glass or on its surface; an equilibrium is then established between the adsorbed gas and its ions.

It is also possible that the ionization of gas molecules dissolved in glass or adsorbed on it form some kind of oxidation-reduction system under the effect of the glass itself.

If the ionization of the gas were due to the presence of glass then the nature of the metal should not affect the value of the adsorption potential to any considerable degree. However, our experiments showed that in many cases the gas adsorption potential depends greatly on the nature of the metal. These results indicate that the ionization of the gas adsorbed occurs on the metal itself.

It must be noted that measurement of the jumps of electrochemical potential is very fruitful for the study of the phenomena of adsorption and catalysis in liquid electrolytes [24, 25]. At the same time, the interpretation of the results obtained during the investigation of the phenomena of gas adsorption and catalysis by using the glass as a solid electrode is accompanied by some additional difficulties.

We have seen before that the degree and the character of the ionization of the gas depend to a great extent on the nature of the metal. On the basis of this result we have assumed that in general only a certain amount of the gas adsorbed on the metal is ionized.

The fact that the nature of the metal considerably affects the degree of ionization allows us to assume that ionization must take place not only at the limit of separation metal-glass but also at the limit of separation metal-gas (this is in agreement with the results of measurements of work function during adsorption of gases on metals).

The results of measurement of the adsorption potential of nitrogen (see Fig. 9) show that the negative nitrogen ion can be formed in very small amounts on copper, silver, or carbon, in some greater amount on nickel, and in much greater amount on iron. In fact it is only iron which can serve as catalyst for the synthesis of ammonia, i.e., for the hydrogenation of nitrogen. It is quite possible that for this reaction the splitting of the nitrogen molecule into atoms is not necessary; probably the molecular nitrogen ion has a sufficient reaction activity. In this case there is a definite analogy between the molecular nitrogen ion, N_2^-, and molecular oxygen ion, O_2^-, for which high reaction activity was demonstrated by electrochemical measurement [17, 18].

The results obtained lead to the conclusion that the adsorption of gas on metal cannot generally be identified with its ionization. Apparently in the majority of cases the catalytic process on a metal catalyst consists of the following basic stages: adsorption of the gas on the metal (1); ionization of part of the adsorbed gas (2); and interaction between the gas ions formed on the surface with other components of the reaction, and restitution of the initial charge on the surface of the metal (3).

As a rule the first stage must proceed very rapidly and stages 2 and 3 can be slow. If stage 2 is slow then the total reaction rate must depend greatly on the effect of the electric field on the surface of the catalyst and on the presence of impurities capable of modifying the work function of the electron of the metal catalyst. Then the stationary concentration of gas ions on the surface of the catalyst must be small. One can assume that the synthesis of ammonia isa reaction of just this type.

SUMMARY

1. We have described an electrochemical method of investigation of adsorption of gases on metals, using glass as the solid electrolyte.

2. We have investigated the adsorption of hydrogen, carbon dioxide, ethylene, a mixture of hydrogen and ethylene, carbon monoxide, nitrogen, and a mixture of nitrogen and hydrogen on copper, cobalt, nickel, silver, and iron in the temperature range of 250-425 °C.

3. It was shown that the electrochemical adsorption potential of a gas on a metal depends very much on the nature of the metal and that the maximum difference for the metals investigated is 200-225 mv for hydrogen, 300-350 mv for carbon monoxide, and 750-800 mv for nitrogen.

4. In the case of hydrogenation of ethylene on copper at 250°, hydrogen as well as ethylene is adsorbed in considerable amounts at the surface of the metal. It is assumed that the activation of ethylene is due to the attachment of an electron from the metal to the ethylene, possibly at the double bond.

5. In the case of adsorption of carbon monoxide the electrochemical potential on copper is 300-350 mv

more electronegative than on all the other metals investigated. The specific effect of the catalyst is due to the fact that carbon monoxide is a particularly strong reducing agent on copper.

6. In the case of adsorption of nitrogen the electrochemical potential on iron appears to be 800 mv more positive than on copper, cobalt, or silver. Nitrogen ions in any considerable amount can form only on iron, and only iron can serve as the catalyst for ammonia synthesis. It is assumed that the activation of nitrogen on iron consists of the formation of negative singly charged molecular nitrogen ions.

7. In all the cases investigated the adsorption of the gas on the metal at high temperature is accompanied by the appearance of a definite jump of the electrochemical potential. It is assumed that this fact is the result of the formation of gas ions on the surface of the metal.

8. Generally, the adsorption of a gas must not be identified with its ionization, since ionization can be a subsequent process, and furthermore it is possible that only a certain part of the adsorbed gas is ionized. The formation of molecular gas ions may lead in many cases to an increase of the reaction mobility of the adsorbed gas.

LITERATURE CITED

1. L.V. Pisarzhevskii, Selected Works [in Russian] (Izd. AN UkrSSR, Kiev, 1936).
2. V.A. Roiter, Zhur. Fiz. Khim. 4, 457 (1933).
3. G. Haber and J. Weiss, Proc. Roy. Soc. A147, 332 (1934); J. Weiss, Trans Faraday Soc. 31, 1947 (1935).
4. S.Z. Roginskii, Problems of Kinetics and Catalysis [in Russian] (Izd. AN SSSR, Moscow, 1955) p. 110.
5. F.F. Vol'kenshtein, Zhur. Fiz. Khim. 26, 1462 (1952); 27, 159, 167 (1953).
6. M.I. Temkin, Problems of Chemical Kinetics, Catalysis, and Reaction Capacity [in Russian] (Izd. AN SSSR, Moscow, 1955) p. 484.
7. G.K. Boreskov, Heterogeneous Catalysis in the Chemical Industry [in Russian] (Goskhimizdat, Moscow, 1955) p. 5; Problemy Fiz. Khim. 1, 101 (1958).
8. G.M. Schwab, Trans. Faraday Soc. 42, 689 (1946).
9. M. Boudart, J. Am. Chem. Soc. 74, 3556 (1952).
10. A.I. Krasil'shchikov and L.G. Antonova, Doklady Akad. Nauk SSSR 91, 291 (1953); Proceedings of the State Inst. on Nitrogen Production [in Russian] (Goskhimizdat, 1954) Vol. 4, p. 212.
11. L.G. Antonova and A.I. Krasil'shchikov, Proceedings of the State Inst. on Nitrogen Production [in Russian] (Goskhimizdat, 1957) Vol. 7, p. 292.
12. L.G. Antonova, F.P. Ivanovskii, T.G. Fil'chenkova, and A.I. Krasil'shchikov, Zhur. Fiz. Khim. 33, 416 (1959).
13. F. Haber, Z. anorg. Chem. 51, 245,289 (1906).
14. S.Ya. Pshezhetskii and A.T. Gladyshev, Zhur. Fiz. Khim. 15, 333 (1941).
15. E.K. Rideal, J. Chem. Soc. 309 (1922); C. Schuster, Z. Elektrochem. 38, 614 (1932).
16. C.A. Coulson, Ann. Rev. Phys. Chem. 3, No. 1 (1952).
17. A.I. Krasil'shchikov, Zhur. Fiz. Khim. 23, 332 (1949); 26, 216 (1952); Problems of Kinetics [in Russian] (Izd. AN SSSR, Moscow, 1955) Vol. 8, p. 146.
18. A.I. Krasil'shchikov, Transactions of the Conference on Electrochemistry [in Russian] (Izd. AN SSSR, Moscow, 1953) p. 71; Transactions of the Fourth Conference on Electrochemistry [in Russian] (Izd. AN SSSR, Moscow, 1959) p. 272.
19. M.I. Temkin and V.M. Pyzhev, Zhur. Fiz. Khim. 13, 851 (1939).
20. E. Winter, Z. phys. Chem. B13, 401 (1931).
21. P.H. Emmett and S. Brunauer, J. Am. Chem. Soc. 56, 35 (1934).
22. H.S. Taylor, J. Am. Chem. Soc. 53, 578 (1931).
23. I.A. Legenchenko, Zhur. Fiz. Khim. 24, 311 (1950).
24. A.I. Shlygin, Transactions of the Conference on Electrochemistry [in Russian] (Izd. AN SSSR, Moscow, 1953) p. 322.
25. D.V. Sokol'skii, Doklady Akad. Nauk SSSR 73, 949 (1950); 78, 721 (1951); Zhur. Fiz. Khim. 26, 364, 484 (1952).

EFFECT OF ELECTRONIC STRUCTURE OF NICKEL OXIDE ON OXYGEN EXCHANGE

N.P. Keier

Institute of Physical Chemistry, Academy of Sciences of the USSR
Translated from Kinetika i Kataliz, Vol. 1, No. 2, pp. 221-228,
July-August, 1960
Original article submitted March 3, 1960

We have investigated the exchange of oxygen between the surface layers (and also deeper layers) of nickel oxide and the surrounding medium. We also experimented with solid solutions of nickel oxide containing different amounts of dissolved lithium oxide, whose electrical conductivity differs from that of nickel oxide by several orders. It was shown that the presence of lithium cations in the lattice of nickel oxide considerably increases the rate of exchange of oxygen on the surface and in deeper layers of the oxide. The mechanism of the effect of the dissolved lithium oxide on the rate of exchange of oxygen in the surface layer and within the body of the oxide is discussed.

The electrical properties and the electronic structure of nickel oxide vary within wide limits as the result of formation of solid solutions with metal oxides whose cations have a charge different from that of the nickel cation regularly present in the lattice of nickel oxide [1-3]. The possibility of regulating the electrical properties of nickel oxide in this manner led to the possibility of transforming hole conductivity of this oxide into impurity conductivity, and as the result nickel oxide became one of the most widely used materials for study of the relationship between electrical properties and catalytic activity. Investigation of solid solutions of nickel oxide with oxides of lithium, sodium, magnesium, iron, and indium, whose electrical conductivities and activation energies are very different, showed that the electronic structure of nickel oxide has a strong effect on the chemical adsorption of gases, which is different for the molecules adsorbed in the form of electron donors or electron acceptors [4-6]. Catalytic activity, which is very often determined by the chemical adsorption of one of the components of the reacting gases, varies widely also when metal oxides affecting the electronic structure of nickel oxide are dissolved in it [7-10].

The results of our investigation of the electrical, chemisorptional, and catalytic properties of solid solutions of nickel oxide led us to the conclusion that it would be of interest to investigate the exchange of oxygen between the outside medium and the surface layer and deeper layers of the oxide. The capacity of the oxide for oxygen exchange is related to many factors, one of which is the strength of the bond of oxygen on the surface and within the oxide. The investigation of this exchange on nickel oxide and its solid solutions with other metal oxides which modify its electrical conductivity should give us indications of the change of electronic structure induced by different types of chemical defects in the lattice. This exchange was investigated in the case of nickel oxide and its solid solutions with lithium oxide, whose presence even in small amounts strongly affects the electrical conductivity.

METHOD OF INVESTIGATION

Nickel oxide was prepared by the decomposition of nickel carbonate obtained by precipitation from nickel sulfate solution with a sodium carbonate solution. The precipitate was washed to eliminate the sulfate ion. We used nickel sulfate marked "pure" and sodium carbonate marked "analytically pure." The decomposition of nickel carbonate was carried out at 900° in a stream of air for 2½ hours. Solid solutions of nickel oxide and lithium oxide were prepared by decomposing a mixture of nickel and lithium carbonates under similar

conditions. Samples of NiO containing 0.8 at. % Li were obtained from nickel carbonate impregnated with a solution of lithium carbonate. Samples of NiO containing 8 at.% Li were obtained by decomposing granules prepared by thorough mixing of finely pulverized nickel and lithium carbonates, pressing the powder into tablets under a pressure of 4000 atm, and then breaking them into granules (2-3 mm). The formation of the solid solution was verified by x-ray analysis. The lattice parameter of nickel oxide decreases when lithium oxide is dissolved in it (Table 1). The specific surface also changes. The values of the specific surface obtained by the BET method from equilibrium adsorption isotherms of nitrogen and krypton were quite close (Table 1). The values of specific electrical conductivity and activation energy are represented in the same table.

The electrical conductivity was measured on samples, degassed at 300° down to a residual pressure of 10^{-4} mm Hg, in special clamps with steel electrodes, using the bridge method.

The sample was degassed at 700° down to a pressure of 10^{-6} mm Hg when the exchange of O^{18} was studied. We used a reactor made of quartz glass with double walls, the space between the walls being degassed at 600° down to the pressure of 10^{-3} mm Hg so as to prevent the diffusion of air into the reactor. The exchange was studied under static conditions at a constant oxygen pressure, the initial concentration of O^{18} being 1.17%. In each experiment we used 4-6 g of catalyst. The amount of oxygen in the surface layer of the different samples varied from 0.6 to 0.18 cm^3, the oxygen containing the normal amount of O^{18}. The volume of oxygen in the gas phase over the catalyst during the exchange was 0.8-0.9 cm^3. The oxygen medium was maintained over the surface of the catalyst for a given period, during which the original concentration of O^{18} decreased 10-15% as a result of exchange. Then the gaseous medium was transferred with a Tepler mercury pump to special ampules for mass spectroscopic analysis and a new volume of oxygen containing 1.17% O^{18} was introduced into the reactor. The concentration of O^{18} in the oxygen over the catalyst decreased from 1.17 ± 0.02 to 0.90 ± 0.01% during the experiment.

The amount of oxygen exchanged on the surface was conveniently expressed as the percentage of the oxygen in the surface layer of the nickel oxide which was exchanged, while the oxygen exchanged in deeper layers of the oxide was expressed in arbitrary units: the number of layers in which oxygen was exchanged. If the (111), (100), and (110) faces are present in equal numbers on the surface of nickel oxide, the volume of oxygen per m^2 of the surface is 0.094 cm^3.

The portion of a single layer in which oxygen exchange occurs is calculated by the following formula:

$$n = \frac{V_g(1,17 - C_t)}{S_{sp}\,0,094\,(C_t - 0,2)\,g},$$

where V_g is the volume of oxygen over the catalyst; S_{sp} is the specific surface of the catalyst; g is the weight of the catalyst; C_t is the percentage of O^{18} in the gas exchanged during the period of time t; 0.2 is the percentage of O^{18} in the oxygen of the original nickel oxide; and 0.094 is the amount of oxygen per m^2 of the surface of the layer, in cm^3.

In these calculations we assume that the exchange proceeds by layers. As we shall show later, this assumption is confirmed by experimental data on nickel oxide. The value of the oxygen exchange expressed in fractions of a single layer easily allows us to pass to the value of exchange expressed in percentage of the oxygen in the surface layer of the nickel oxide, which is equal to 0.0368% in the case of NiO containing 0.08 at.% Li and 0.02% in NiO containing 8 at.% Li (considering that a single layer of NiO contains 0.0633% of the total oxygen).

EXPERIMENTAL RESULTS

The rate of exchange is significant only at about 400 °C. Preliminary results showed that the presence of dissolved lithium oxide in nickel oxide leads to a considerable increase of the rate of exchange.

Figure 1 represents kinetic isotherms of oxygen exchange determined at different temperatures on nickel oxide and its solid solutions with lithium oxide containing 0.8 and 8 at.% lithium.

Curves 1 and 2 represent the exchange of oxygen on nickel oxide at 450 and 650 °C. In the case of NiO

TABLE 1

Comparative Physical Constants and Specific Surfaces of the Samples

Sample	Lattice parameter, A	Specific electrical conductivity at 23°, ohm/cm^{-1}	Activation energy of electrical conductivity, kcal/mole	Specific surface, m^2/g
NiO	4.1833	10^{-6}	30.5	1 ± 0.1
NiO, 0.8 at.% Li	4.1829	10^{-1}	17.0	0.55 ± 0.05
NiO, 8 at. % Li	4.1698	1	10.5	0.3 ± 0.03

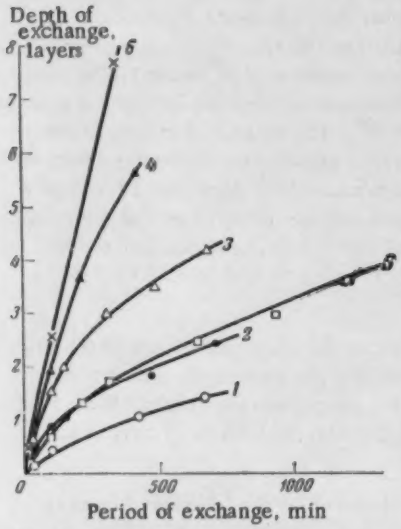

Fig. 1. Curves representing the variation of oxygen exchange, expressed in arbitrary units of the number of layers, as a function of time, in minutes. 1) NiO, 450°; 2) NiO, 650°; 3) NiO with 0.8 at.% Li, 450°; 4) NiO with 0.8 at.% Li, 500°; 5) NiO with 8 at.%, 400°; 6) NiO with 8 at.% Li, 435°; The pressure of oxygen, containing 1.17% O^{18}, was 3 mm Hg during exchange.

at 450°, the exchange reaches about 1½ layers after 700 min. Over the same period of time at 650°, the exchange reaches 2½ layers. On nickel oxide containing 0.8 at.% lithium, the exchange at 450° over the same period of time pentrates over 4 layers, and at 500° over a period of 400 min it reaches 5½ layers. When the concentration of lithium is increased to 8 at.% the rate of exchange becomes very high already at 400°, penetrating more than 2½ layers during 700 min, and reaching 3½ layers during 1100 min. At 435° the depth of exchange in this sample reaches 7½ layers over a period of 350 min.

Figure 2 and Table 2 represent the average rates of exchange expressed in percentage of the exchanged amount of oxygen of the surface and in the number of layers exchanged per hour for different degrees of exchange.

Table 2 shows that in the sample with lithium oxide the rate of exchange increases considerably in the surface as well as deeper layers. The amount of oxygen per gram of the catalyst investigated changes very little. Therefore the rate of exchange expressed in percentage of oxygen of the surface exchange per hour allows us to deduce the absolute rate of exchange of O^{18} in cm^3/g of sample. It can be seen that in spite of the considerable decrease of the specific surface of nickel oxide resulting from the dissolution of lithium oxide, the rate of exchange per gram of catalyst does not decrease but increases in the surface as well as deeper layers. When the concentration of lithium increases from 0.8 to 8 at.% the rate of exchange in the surface layer (number of exchange layers per hour) increases by a factor of two, while the rate of exchange expressed in percentage of the oxygen of the sample exchange per hour changes very little since it is compensated by the decrease of the specific surface. In any exchange mechanism the rate of exchange is proportional to the specific surface. The values of these rates represented in Table 2 show that the change of the exchange rate occurring as the result of the presence of lithium oxide in the sample is not due to the change of the specific surface and is of some other physical nature.

We have calculated the rate exchange constant in the surface layer and its variation with the rate of exchange. For a shallow exchange (up to 10-20% of a single layer) theate constants in some experiments exceeded by a factor of two the rate constant calculated for deeper exchange (20-80% of the surface layer). However, in the majority of cases the rate constants remained constant when the exchange in the surface layer varied from 0 to 70%. They had a tendency to increase for deeper exchange due to the fact that the rate of exchange of oxygen in the surface layer gradually approaches the rate of exchange in deeper layers. On the whole we did not succeed in obtaining a dependable value for the variation of the constant of rate exchange as a function of the degree of exchange in the surface layer either in the case of nickel oxide or its solid solutions with lithium oxide.

TABLE 2

Average Rates of Oxygen Exchange in the Surface Layer and Deeper Layers of Nickel Oxide and Its Solid Solutions with Lithium Oxide

Sample	t, °C	Rate of exchange in different layers					
		1		2		3	
		layer/hr	% O_2/hr	layer/hr	% O_2/hr	layer/hr	% O_2/hr
NiO	450	0.15	0.009	0.08	0.005	—	—
NiO, 0.8 at.% Li	450	1.00	0.036	0.67	0.024	0.40	0.014
NiO, 8 at. % Li	435	2.00	0.040	1.50	0.030	1.50	0.030

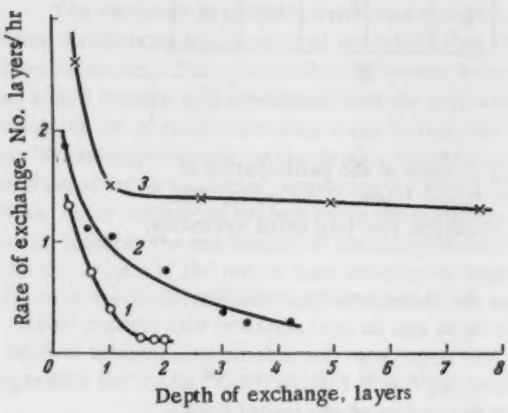

Fig. 2. Variation of the rate of oxygen exchange in the surface layer and deeper layers. 1) NiO, 565°; 2) NiO with 0.8 at.% Li, 450°; 3) NiO with 8 at.% Li, 435°

The variation of the rate of oxygen exchange in deeper layers, i.e., in the volume of the catalyst, occurring as the result of the presence of lithium oxide in nickel oxide is very interesting. Table 2 and Fig. 2 show that the rate of the "volume exchange" increases in the presence of lithium oxide. The curve representing the variation of the rate of exchange in depth as a function of the increase of the concentration of lithium in nickel oxide is quite indicative.

When the concentration of lithium is 0.8 at.% the rate of exchange at 450° decreases $2\frac{1}{2}$ times during the time that oxygen passes from the second to the fifth layer. When the concentration of lithium is 8 at.% the rate of exchange at 435° remains practically constant from the second to the eighth layer within the range investigated, which indicates that the rate of exchange of oxygen ions of the surface layer with the oxygen ions in the volume of the crystal is very high. At a higher temperature, 640°, the exchange reaches 60 layers over a period of 300 minutes. During the same period of time the exchange in nickel oxide, even at 710°, penetrates only 4 layers. The fact that the rate of exchange is so high means there must be an intense migration of the oxygen ion $(O^{18})^{2-}$ (exchanged at the surface) from the surface into deeper layers in the solid solution containing 8% lithium. In this case the concentration of the O^{18} oxygen isotope on the surface of the sample can differ greatly from its concentration in the oxygen undergoing exchange, even when the oxygen exchanged penetrates only a few layers according to the calculation. On the contrary, in the case of nickel oxide, due to the very low exchange rate between the surface oxygen and the oxygen in the deeper layers, one can expect that the concentration of O^{18} in the oxygen on the surface will correspond to that of the oxygen undergoing exchange. To check this assumption we measured the reverse exchange of O^{18} (already exchanged on nickel oxide and nickel oxide containing 8 at.% lithium) with the oxygen of the outside medium. In the case of nickel oxide such experiments were made at 450 and 565°. During direct exchange in the last case the exchange reached about 2 layers; the concentration of O^{18} at the surface was about 1%. The average rate of direct exchange was 0.8 layer/hour. In the case of reverse exchange at the same temperature, measured immediately after direct exchange, the rate was 0.77 layer/hour (we introduced a correction due to the change of the original concentration of O^{18} in the exchanging oxygen). The rates of direct and reverse exchange are almost identical.

In the case of a solid solution of NiO with 8 at.% lithium the rate of reverse exchange was measured at 555° after 960 minutes of exchange between the oxygen of the catalyst and the oxygen containing 1.17% O^{18}. The depth of the exchange during this period of time was calculated to be 7 layers. The rate of the reverse exchange at the same temperature, measured immediately after direct exchange as in the previous experiment, was approximately one-third of the direct exchange rate.

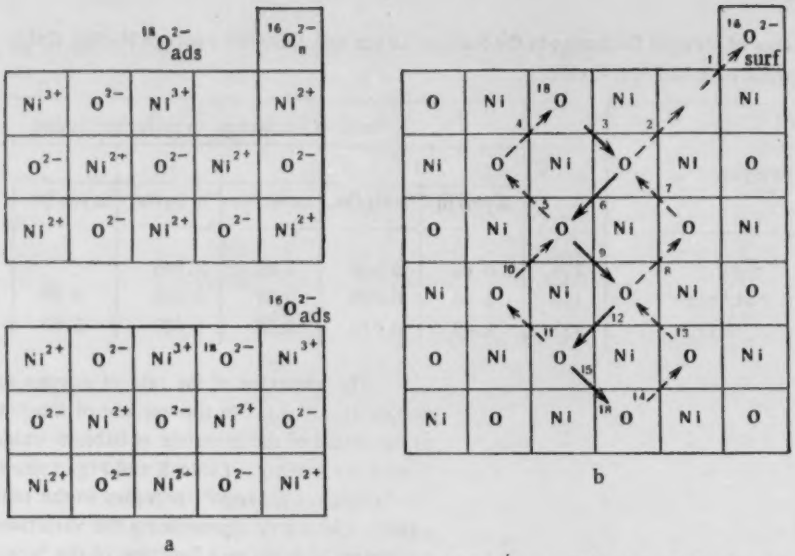

Fig. 3. Mechanism of oxygen exchange, taking account of the participation of anion vacancies. a) In the surface layer; b) in deeper layers of the oxide. The numbers indicate the consecutive movements of oxygen ions into anion vacancies.

These experiments confirm the conclusion resulting from the measurements of the kinetics of the exchange of oxygen on the surface and within the body of nickel oxide and its solid solutions with lithium oxide. These measurements showed that O^{18} which has exchanged in NiO remains on the surface, i.e., remains at those places where exchange occurred, while in the case of NiO containing 8 at.% lithium the O^{18} which has exchanged passes rapidly into the body of the catalyst and exchanges with the oxygen of the crystal lattice.

To determine the mechanism of the exchange between the oxygen of the catalyst and the O^{18} of the gaseous phase, it is of interest to measure also the rate of exchange of the adsorbed oxygen with the oxygen of the gaseous phase. For this purpose 0.1 cm^3 of oxygen containing 1.17% O^{18} was adsorbed on 7 g of nickel oxide at 247°. The oxygen was of the ordinary composition. When the exchange of the adsorbed oxygen was complete, the amount of O^{18} in the gaseous phase should have increased from 0.20 to 0.27%. Oxygen of the ordinary composition, containing 0.2% O^{18}, was maintained for different periods of time (up to 3 hours) at 247-380° over the nickel oxide containing adsorbed O^{18}. The concentration of O^{18} remained constant, equal to $0.2 \pm 0.1\%$. No exchange between the oxygen from the gaseous phase and the adsorbed oxygen occurred up to 400°. At this temperature the desorption of the adsorbed oxygen begins. At the same temperature the exchange of the oxygen with the oxide also begins. If the fact that no exchange of the adsorbed oxygen occurred in this experiment were due to the redistribution of O^{18} adsorbed on the surface layer and deeper layers, then the exchange should begin at lower temperatures, due to exchange of the adsorbed oxygen. Consequently the adsorbed oxygen does not exchange up to 400° either with the oxygen of the gaseous phase or with the oxygen of the oxide.

DISCUSSION OF RESULTS

Oxygen exchange proceeds through three consecutive stages: a) adsorption of oxygen, which occurs either with or without dissociation and, according to the variation of electrical conductivity, is accompanied by the passage of the electron from the nickel oxide to the adsorbing molecule [4]; b) exchange between the adsorbed oxygen and the oxygen of the lattice; c) desorption of the adsorbed oxygen which was exchanged.

In the case of nickel oxide and its solid solution with lithium oxide the oxygen is adsorbed at a much higher rate than the rate at which it is exchanged, and therefore there are no stages determining the rate of exchange. This conclusion is completely confirmed by the results of experiments on the exchange between adsorbed oxygen and the oxygen of the gaseous phase. The very small variation of the rate of exchange on nickel

oxide with increasing temperature excludes the possibility that the desorption of the adsorbed oxygen is the slowest stage in the exchange of oxygen. The increase of the rate of desorption with temperature is much more significant than the increase of the rate of exchange.

Apparently the slowest stage in the exchange of oxygen on nickel oxide is the exchange between the adsorbed oxygen and the oxygen ions of the lattice. The exchange between the oxygen ions on the surface and the oxygen ions in the deeper layers of the lattice is even slower. In the case of nickel oxide of approximately stoichiometric composition this process is extremely slow even at 710°. Over a period of 300 minutes the exchange of oxygen reaches less than 4 layers.

Comparison of rates of exchange of oxygen on nickel oxide and its solid solutions with lithium oxide indicates quite clearly that the presence of lithium cations in the lattice of nickel oxide increases considerably the rate of exchange on the surface, and that in the deeper layers even more. The increase of the rate of exchange of oxygen in the surface layer of nickel oxide due to the presence of dissolved lithium oxide was noted also by Winter [11].

The exchange in deep layers necessitates the presence of anion vacancies in the lattice of the oxide. Figure 3 represents the diagram of the mechanism of the exchange of oxygen in deep layers in the presence of anion vacancies. The considerable difference between the rates of direct and reverse exchange on NiO containing 8 at.% lithium is in agreement with the proposed mechanism of exchange in deep layers. The higher the concentration of anion vacancies in the lattice, the higher the rate of exchange in deep layers, and the less this rate of exchange depends on the depth. We may assume that the presence of lithium oxide in NiO favors the creation of anion vacancies, increasing the mobility of oxygen ions in the lattice. The fact that in the case of nickel oxide containing lithium oxide the variation of the surface and the volume exchange rates are parallel makes probable the mechanism of exchange in which the stage of the elementary exchange of adsorbed oxygen with the oxygen of the lattice may include the migration of the oxygen anion of the lattice to the surface of the crystal according to the following sequence:

1. $[^{16}O^{18}O]_{gas} \rightarrow [^{16}O^{18}O]^{-}_{ads} + Ni^{3+} \rightarrow {}^{16}O^{2-}_{ads} + {}^{18}O^{2-}_{ads} + 4Ni^{3+}$
2. ${}^{16}O^{2-}_{lat} \rightarrow {}^{16}O^{2-}_{surf} + A_v$
3. ${}^{18}O^{2-}_{ads} + A_v \rightarrow {}^{18}O^{2-}_{lat} - 2Ni^{3+}$
4. ${}^{16}O^{2-}_{surf} - A_v \rightarrow {}^{16}O^{2-}_{ads} + 2Ni^{3+}$

   Exchange between the adsorbed oxygen and the oxygen of the lattice.
5. ${}^{16}O^{2-}_{ads} + {}^{16}O^{2-}_{ads} \rightarrow [^{16}O_2]_{gas}$

where A_v is an anion vacancy.

The results of the experiment show that the stage most probably determining the rate of exchange must be the migration of the anion of the lattice to the surface (stage 2).

The kinetics of the exchange of oxygen in the surface layer indicates that there is very little difference in the capacity of oxygen for exchange in the surface layer. An analogous relationship was determined by Winter [12]. It follows then that we must exclude the mechanism leading to heterogeneity, in particular the predominant migration of anions toward any defects. The effect of the dissolved lithium oxide apparently spreads over the whole lattice, increasing the mobility of all the oxygen ions on the surface and within the lattice. The higher the concentration of lithium dissolved in the nickel oxide the stronger its effect on the mobility. The data obtained can be considered to result from the change of the energy state of the lattice as a whole in the presence of chemical defects in the lattice of nickel oxide. This is in agreement with the change of the lattice parameter occurring as the result of the presence of lithium oxide.

Local dislocations induced by the presence of defects have a great effect on the adsorptional and catalytic properties of nickel oxide. The result is that the capacity for chemical adsorption and catalysis varies along the surface of the catalyst. For oxygen exchange the variation of the strength of the bonds in the lattice as a whole is apparently much more significant.

The change of the energy state of the lattice of nickel oxide due to the presence of lithium oxide may

induce the displacement of the valence zone with respect to the free electron level in vacuum, which must lead to an anomalous change of the work function. In our samples of nickel oxide and its solid solutions with lithium oxide such a phenomenon was observed [13]. For example, in the case of NiO containing 0.8 at.% lithium the activation energy of the electrical conductivity is lower by 13 kcal/mole than in the case of NiO. As a result the Fermi level becomes lower and the work function should therefore increase by a corresponding amount. The work function measured on these samples was lower than in the case of NiO. This decrease is usually considered to be exclusively the result of the bending of zones in the presurface layer; however, it is possible that this is due to the shift of the valence zone induced by deep changes in the oxide as the result of introduced defects [14]. To observe a possible shift of the valence zone, one can measure the change of adsorption on these samples and the effect of field.

LITERATURE CITED

1. J.H. deBoer and E.J.W. Verwey, Proc. Phys. Soc. (Lond) 49, supplement, 597 (1937); E.J.W. Verwey, P.W. Haayman, F.C. Romeijn, and C.W. Oosterhout, Chem. Weekbl. 44, 705 (1948).
2. F.J. Morin, Phys. Rev. 93, 1199 (1954); Bell. System Techn. J. 5, 1047 (1958).
3. N.P. Keier, S.Z. Roginskii, and L.S. Sazonova, Izvest. Akad. Nauk SSSR, Ser. Fiz. 21, 183 (1957).
4. N.P. Keier and L.N. Kutseva, Doklady Akad. Nauk SSSR 177, 259 (1957).*
5. N.P. Keier and L.N. Kutseva, Izvest. Akad. Nauk SSSR, Otdel. Khim. Nauk 797 (1959).*
6. L.N. Kutseva and N.P. Keier, Problems of Kinetics and Catalysis (Izd. AN SSSR, Moscow, 1960) Vol. 10.
7. N.P. Keier, S.Z. Roginskii, and L.S. Sazonova, Doklady Akad. Nauk SSSR 111, 1274 (1956).*
8. G.M. Schwab and J. Block, Z. Electrochem 58, 576 (1954).
9. G. Parravano, J. Am. Chem. Soc. 75, 1448 (1953).
10. L.S. Sazonova, Dissertation [in Russian] (Inst. Fiz. Khim. AN SSSR, 1957).
11. E.R.S. Winter, Chemisorption (London, 1957) p. 189.
12. E.R.S. Winter, J. Chem. Soc. Lond. 2726 (1955).
13. É.Kh. Enikeev, L.Ya. Margolis, and S.Z. Roginskii, Doklady Akad. Nauk SSSR 130, 807 (1960).*
14. G.K. Boreskov, Problems of Physical Chemistry [in Russian] (Goskhimizat, Moscow, 1958) No. 1, p. 101.

*Original Russian pagination. See C.B. translation.

MOBILITY OF OXYGEN AND CATALYTIC ACTIVITY OF VANADIUM PENTOXIDE PROMOTED BY POTASSIUM SULFATE

G.K. Boreskov, L.A. Kasatkina, V.V. Popovskii, and Yu.A. Balovnev

L. Ya. Karpov Physicochemical Institute

Translated from Kinetika i Kataliz, Vol. 1, No. 2, pp. 229-236, July-August, 1960
Original article submitted March 23, 1960

The addition of small amounts of potassium sulfate to vanadium pentoxide induces a sharp increase in its conductivity, rate of oxygen isotope exchange, and catalytic activity in the reaction between hydrogen and oxygen. With increased amounts of potassium sulfate, all these properties vary in a similar way, passing through a maximum corresponding to the concentration of 0.1-0.3 mole of potassium sulfate per mole of vanadium pentoxide.

The limiting stage of oxygen isotope exchange is the displacement of the oxygen ions of the oxide by the ions of the oxygen adsorbed, and the reverse process. The rate of oxygen isotope exchange as well as the oxidation of hydrogen is determined by the amount of oxygen adsorbed, which increases with increasing conductivity of the sample.

The object of the experiments was to clarify the nature of the promoting effect of potassium sulfate on vanadium catalysts, which are widely used in industry for oxidation reactions. It has been shown previously [1] that the addition of potassium sulfate to vanadium pentoxide (0.5 and 1.0 mole/mole of V_2O_5) increases the mobility of oxygen of the vanadium pentoxide in terms of isotopic exchange with molecular oxygen, and also that not only the oxygen of V_2O_5 but also the oxygen of K_2SO_4 intervene in this exchange.

It appeared to be of interest to investigate the oxygen isotope exchange of samples of vanadium pentoxide to which potassium sulfate was added in quantities less than 0.5 mole/mole, and also to compare the rate of oxygen isotope exchange in these samples with their catalytic and semiconducting properties. We investigated samples of vanadium pentoxide containing different amounts of potassium sulfate; we studied the rate of oxidation of hydrogen and the rate of oxygen isotope exchange, and measured the electrical conductivity in vacuum, in an atmosphere of oxygen, and during oxidation of hydrogen.

We used vanadium pentoxide marked "analytically pure." The samples containing potassium sulfate were prepared by melting together the desired amounts of V_2O_5 and K_2SO_4. The specific surfaces of all samples were determined by the low temperature nitrogen adsorption method, and were of the order of 1-2 m^2/g.

Oxygen isotope exchange. The oxygen isotope exchange of vanadium samples with oxygen gas was investigated at 400-480° with a circulating apparatus similar to that described in a previous publication [2]. All samples were heated to 400° before the experiment to avoid the decrease of the surface of the sample during the exchange process.

As we have shown before [1], the kinetics of oxygen isotope exchange of vanadium samples with molecular oxygen can be well represented by the equation:

$$-\ln(1-F) = RS\frac{n_g + n_{sol}}{n_g \cdot n_{sol}}\tau, \qquad (1)$$

TABLE 1

The Rate and Activation Energy of the Process of Oxygen Isotope Exchange with Molecular Oxygen of Different Samples of Vanadium Pentoxide Containing Different Amounts of Potassium Sulfate

Sample	Temp., °C	P_{O_2}, mm	$R \cdot 10^6$, g/m²·hr	E, kcal/mole	Reaction order with respect to O
V_2O_5	440	40	0,032	44	0,5
	480	40	0,17		
	480	240	0,42		
	530	240	6,30 *		
	550	240	10,50 *		
$V_2O_5 \cdot 0,1\ K_2SO_4$	400	40	0,20	43	
	440	40	1,10		
	480	40	5,70		
$V_2O_5 \cdot 0,3\ K_2SO_4$	400	40	1,20	31	0,6
	440	10	2,10		
	440	40	4,70		
	440	120	8,50		
	480	40	14,0		
	480	148	29,5		
$V_2O_5 \cdot 0,5\ K_2SO_4$	440	40	2,40	35	0,7
	480	40	8,60		
	350	40	0,05 **		
	400	40	0,30 **		
	400	240	0,91 **		
	440	42	1,19 **		
	440	252	5,54 **		
	480	42	4,48 **		
	480	252	16,30 **		
$V_2O_5 \cdot K_2SO_4$	480	42	0,32**		

* The value of R is calculated on the basis of the results published earlier [3].

** The results were published in [1]. Here the values of R are somewhat lower since the decrease of the surface during the experiment was not taken into account.

where $F = \frac{C_0 - C}{C_0 - C_\infty}$ is the fraction of the oxygen exchanged; C_0 is the original concentration of O^{18} in the gas; C is the concentration of O^{18} in the circulating gas; $C_\infty = \frac{C_0 + 0.2\frac{n_{sol}}{n_g}}{1 + \frac{n_{sol}}{n_g}}$ is the equilibrium concentration of O^{18}; n_{sol} is the amount of oxygen in the solid; n_g is the amount of oxygen in the gas; S is the total surface of the solid; R is the rate of exchange independent of the concentration of oxygen isotope; and τ is the time.

The value of R, expressed in $g/m^2 \cdot hr$, was considered to be the measure of the sample's capacity for exchange.

The results of measurements of the rate of oxygen isotope exchange at different temperatures and pressure of oxygen are represented in Table 1.

These data show that at 440° the oxygen of the vanadium pentoxide begins to exchange with the molecular oxygen at a noticeable rate.

The pressure of 0.1-1 mole of K_2SO_4 per mole of V_2O_5 leads to an increase of the rate of exchange. Thus

TABLE 2

The Rate and Activation Energy of the Oxidation of Hydrogen on Different Vanadium Catalysts

Sample	Temp., °C	Oxidation rate		E, kcal/mole	n
		mole $H_2 \cdot 10^3$/ $m^2 \cdot$ hr.	g $O_2 \cdot 10^3$/ $m^2 \cdot$ hr.		
V_2O_5	400	0,0033	0,0529	21	0,8
	450	0,0098			
	500	0,020			
$V_2O_5 \cdot 0,1\ K_2SO_4$	350	0,55	11,50	5	0,9
	400	0,72			
$V_2O_5 \cdot 0,3\ K_2SO_4$	200	0,29	18,40	4	0,9
	350	0,98			
	400	1,15			
$V_2O_5 \cdot 0,5\ K_2SO_4$	300	0,0098	1,30	16	0,9
	350	0,028			
	400	0,081			
$V_2O_5 \cdot K_2SO_4$	375	0,0136	0,40	18	0,9
	400	0,025			

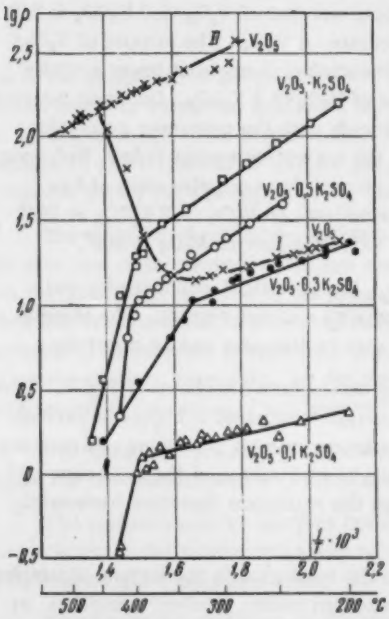

Fig. 1. Variation of the specific resistance in an atmosphere of oxygen at a pressure of 700 mm Hg as a function of temperature.

at 480° the rate of exchange of $V_2O_5 \cdot K_2SO_4$ is 1.9, that of $V_2O_5 \cdot 0.1\ K_2SO_4$ is 33.5, that of $V_2O_5 \cdot 0.5\ K_2SO_4$ is 50.5, and that of $V_2O_5 \cdot 0.3\ K_2SO_4$ is 82.3 times higher than the rate of exchange of pure vanadium pentoxide under the same conditions. The sample of $V_2O_5 \cdot 0.3\ K_2SO_4$ shows the maximum rate of exchange. At other temperatures the situation is analogous, but in some samples containing potassium sulfate the rate of oxygen exchange of the sample with the oxygen of the gas is higher at temperatures at which there is no exchange for pure V_2O_5.* The activation energy of the exchange process varies also with the composition of the sample, and the minimum activation energy corresponds to $V_2O_5 \cdot 0.3\ K_2SO_4$. The rate of exchange depends on the oxygen pressure. The order of the reaction with respect to oxygen is within the limits of 0.5-0.7.

Catalytic activity. The catalytic activity of the samples in the oxidation of hydrogen was investigated in a stationary-circulating apparatus [4]. The samples were first maintained in vacuum at 400° for 3 hours and then maintained at the same temperature for 2 hours in an oxygen atmosphere in order to make their composition approach their stationary composition under the conditions of the oxidation reaction.

Oxidation of hydrogen was studied at oxygen pressure of 720-760 mm Hg at different pressures of hydrogen (up to 20 mm Hg). We investigated the variation of the oxidation rate as a function of temperature, hydrogen concentration, and composition of the catalyst.

The reaction order with respect to hydrogen (n) is somewhat different for different samples, and therefore the catalytic activity of different samples was expressed in terms of the reaction rate at a hydrogen concentration of 0.1 mM/liter per unit surface of the catalyst. The rate of oxygen isotope exchange was expressed in g O_2 / $m^2 \cdot$ hr in order to compare it with the rate of oxidation.

*Potassium sulfate alone does not exchange its oxygen with oxygen gas even at 500°.

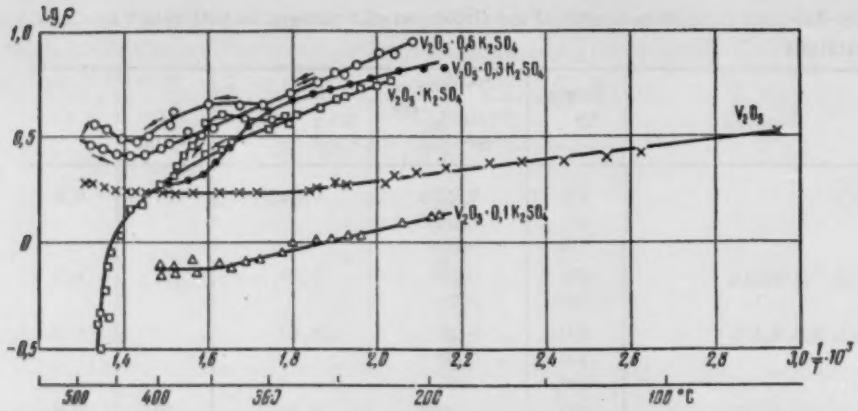

Fig. 2. Variation of the specific resistance in vacuum as a function of temperature.

TABLE 3

Electrical Resistance and Activation Energy of Conduction of Samples of Vanadium Pentoxide Containing Potassium Sulfate

Composition of sample	ρ_{350}, ohm · cm	Activation energy of conduction, kcal/mole
V_2O_5	230	4,6
$V_2O_5 \cdot 0{,}1\ K_2SO_4$	1,4	2,0
$V_2O_5 \cdot 0{,}3\ K_2SO_4$	10,0	3,3
$V_2O_5 \cdot 0{,}5\ K_2SO_4$	14,8	6,0
$V_2O_5 \cdot 1{,}0\ K_2SO_4$	32	6,3

The results of the investigation are represented in Table 2. These results show that all the samples containing potassium sulfate ensure a considerably higher oxidation rate of hydrogen as compared with pure vanadium pentoxide. Thus the reaction rate at 400° on $V_2O_5 \cdot K_2SO_4$ is 7.5 times, that of $V_2O_5 \cdot 0.5\ K_2SO_4$ is 24.5 times, that of $V_2O_5 \cdot 0.1\ K_2SO_4$ is 217 times, and that of $V_2O_5 \cdot 0.3\ K_2SO_4$ is 348 times higher than the reaction rate on V_2O_5. The sample of $V_2O_5 \cdot 0.3\ K_2SO_4$ had the maximum activity. Somewhat lower activity was manifested by the sample of $V_2O_5 \cdot 0.1\ K_2SO_4$. On these samples the oxidation of hydrogen proceeds with the minimum activation energy. Due to the fact that the activation energy is low, hydrogen is oxidized at a considerable rate on these samples even at low temperatures. Thus the oxidation rate on $V_2O_5 \cdot 0.3\ K_2SO_4$ at 200° is 14.5 times higher than the oxidation rate on V_2O_5 at 500°.

Electrical conductivity. The electrical conductivity was measured by the probe method with a direct current. The sample were pressed into cylinders 5 mm in diameter and 10 mm long.

The results of measurement of electrical conductivity in an oxygen atmosphere are shown in Fig. 1. Those made in vacuum are shown in Fig. 2. The electrical conductivity of vanadium pentoxide is higher in vacuum than in oxygen. Within the temperature range of 300-500° the resistance increases with increasing temperature (Fig. 2). The introduction of oxygen at low temperature (up to 350°) leads to an increase of the resistance and the activation energy of conduction. With further increase of temperature the resistance increases irreversibly (Fig. 1, passage from I to II).

The addition of potassium sulfate to vanadium pentoxide decreases the resistance in the oxygen atmosphere. The effect of temperature on the resistance of the samples containing potassium sulfate is rather complex: at temperatures above 350-400° the resistance decreases sharply and the straight lines representing the variation of the electrical conductivity as a function of temperature [$\lg\rho = f(1/T)$] have a break.

DISCUSSION

Vanadium pentoxide crystals belong to the rhombohedral system and are composed of tetrahedrons containing 1 vanadium atom and 4 oxygen atoms, three of which are common with the neighboring tetrahedrons.

According to its electrical properties vanadium pentoxide is an electronic semiconductor. The results of Fig. 1 show that in an oxygen atmosphere the specific resistance is relatively high, reaching 230 ohms at 350°; the activation energy of conduction is 4.6 kcal. The electrical conductivity of pure vanadium pentoxide is

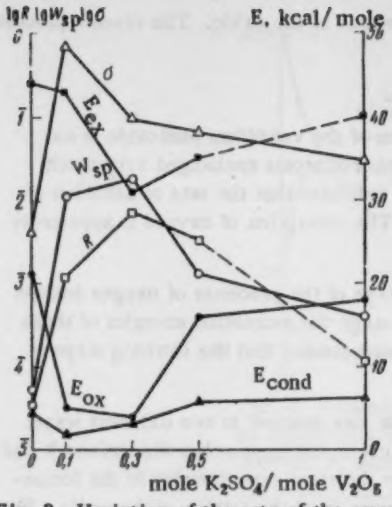

Fig. 3. Variation of the rate of the oxygen isotope exchange (R), the rate of oxidation of hydrogen (W_{sp}), their activation energies, and the electrical conductivity (δ) as a function of the composition of the catalyst.

apparently related to partial dissociation [5] leading to the formation of oxygen defects and V^{4+} ions, i.e., to the appearance of local donor levels. If the V^{4+} ions are located next to the anion defects, these local levels are occupied by electrons; the removal of the ion from the oxygen defect corresponds to the passage of the electron from the local level to the conduction zone.* This is confirmed by a sharp increase in conductivity when the degree of dissociation increases as the result of heating in vacuum. After heating in vacuum at 450°, the specific resistance, ρ_{350}, decreases to 1.7 ohm·cm. The activation energy of conduction below 300° is about 1 kcal, and it becomes negative at higher temperatures. The results obtained are in agreement with those published by Saimard, Arnotti, and Siegel [6], who observed a sharp increase in the conductivity of vanadium pentoxide during partial reduction.

The adsorption of oxygen in the form of negatively charged ions must lead to a decrease of the concentration of electrons in the pre-surface layer, and consequently to an increase of the resistance. In fact, the comparison of the results of measuring the resistance in vacuum and in an atmosphere of oxygen at temperature below 350° (Fig. 1 and 2) indicate that the resistance increases considerably as the result of adsorption of oxygen (ρ_{350} = 13.5 ohm·cm; E = 2.4 kcal). At higher temperatures the increase of resistance in an oxygen atmosphere is irreversible due to the absorption of oxygen. At 450° this processproceeds at a high rate and the resistance reaches values characteristic of vanadium pentoxide heated in oxygen. It is important to note that the temperature at which the hydrogen begins to be absorbed in vanadium pentoxide heated in vacuum is somewhat lower than the temperature at which the rate of oxygen isotope exchange becomes significant. This indicates that the exchange is limited not by the absorption but by the release of oxygen from vanadium pentoxide.

The addition of potassium sulfate to vanadium pentoxide leads to a sharp decrease of the resistance. In this case ions of tetravalent vanadium are formed even after the sample is heated in oxygen. Table 3 shows that the maximum decrease of the resistance occurs when the concentration of potassium sulfate is 0.1 mole. When the concentration of potassium sulfate is increased, the resistance and the activation energy of conduction increase. The decrease of resistance is apparently due to the formation of a solid solution of the potassium sulfate and vanadium pentoxide. As the concentration of potassium sulfate is increased, the resistance increases as the result of formation of new phases [7].

The resistance of samples containing potassium sulfate increases with the adsorption of oxygen, and the higher the concentration of potassium sulfate,the higher this increase.

The properties of the samples investigated are represented for comparison in Fig. 3. The data show that the variation of the conductivity, the rate of oxygen isotope exchange, and the catalytic activity in the oxidation of hydrogen follow the same trend.

The adsorption of oxygen is the stage common to both oxygen isotope exchange and hydrogen oxidation. The rate of these processes must increase with the amount of oxygen adsorbed. The mechanism of oxygen isotope exchange between the molecular oxygen and the oxygen of the oxide proceeds by the following stages:

1) Adsorption of oxygen, accompanied by dissociation into single atoms or ions. The effect of the adsorbed oxygen on the electrical conductivity of vanadium pentoxide indicates that negative oxygen ions, probably O^-, are formed in this case. Adsorptional equilibrium occurs under the conditions of oxygen isotope exchange.

*Here, as in later discussion, we shall consider as an approximation that vanadium pentoxide is an ionic crystal.

2) The exchange of the ions of adsorbed oxygen with ions of the oxygen of the oxide. The reverse process proceeds at the same rate.

3) Diffusion of oxygen ions into the lattice of vanadium pentoxide.

The kinetics of the exchange of the oxygen isotope with the oxygen of the vanadium pentoxide is expressed by equation (1) even at high rates of exchange, at which the number of atoms exchanged very much exceeds the number of atoms of oxygen on the surface of the oxide; this indicates that the rate of diffusion of oxygen into the oxide exceeds the rate of the exchange on the surface. The adsorption of oxygen is apparently not a limiting stage of the reaction.

As we have said before, the adsorption of oxygen is the common stage of the processes of oxygen isotope exchange and the oxidation of hydrogen. If this stage were the limiting stage the activation energies of these processes should coincide, which in fact is not the case. Therefore we must assume that the limiting stage of the exchange is the second stage.

The exchange of adsorbed oxygen with the oxygen ions of the oxide can proceed in two different ways: 1) With the participation of the anion defects of the oxide. When the anion defect approaches the surface it can be filled by the adsorbed oxygen. The reverse process, which proceeds at the same rate, consists in the formation of the anion defect on the surface as the result of the removal of oxygen from the lattice of the oxide. 2) As the result of electron transfer, leading to the exchange between the adsorbed oxygen ions and the anions of the oxide lattice, or the reverse. This exchange occurs without displacement of oxygen atoms, but it is possible that it is acompanied by a certain displacement of cations.

If the exchange occurs according to the first mechanism its rate is proportional to the concentration of the adsorbed oxygen atoms and the concentration of anion defects. In the case of vanadium pentoxide, the concentration of these is very small, and under the conditions in which the exchange occurs it is an equilibrium reaction with respect to the pressure of oxygen. Therefore the rate of exchange can be expressed by the following relationship:

$$R = k\Theta_0\Theta_d = k\frac{\sqrt{b_0 p_{O_2}}}{1+\sqrt{b_0 p_{O_2}}}\cdot\frac{1}{\sqrt{b_d p_{O_2}}}, \qquad (2)$$

where $\Theta_0 = \sqrt{b_0 p_{O_2}}/(1+\sqrt{b_0 p_{O_2}})$ is the fraction of the surface occupied by adsorbed oxygen atoms, and $\Theta_d = 1/\sqrt{b_d p_{O_2}}$ is the fraction of anion defects on the surface.

From equation (2) it follows that according to the fraction of the surface covered by the adsorbed oxygen, the rate of exchange is either independent of the oxygen pressure or is inversely proportional to the square root of the oxygen pressure. It was found, however, that the rate of exchange increases with the oxygen pressure, and is approximately proportional to the square root of the oxygen pressure. This would seem to favor the second mechanism, and we assume that the exchange occurs as the result of the transfer of electrons without the displacement of oxygen atoms. The new anion formed as the result of this transfer exchanges places very rapidly with other anions of the oxide, and the anions which were transformed into ions of the adsorbed oxygen rapidly enter into the exchange reaction with the oxygen of the gaseous phase.

In this case the rate of exchange is proportional to the number of oxygen atoms adsorbed:

$$R = k\Theta_0 = k\frac{\sqrt{b_0 p_{O_2}}}{1+\sqrt{b_0 p_{O_2}}} \qquad (3)$$

If the degree of adsorption is low, the value of R is

$$R \approx k\sqrt{b_0 p_{O_2}},$$

which is in good agreement with the experimental data.

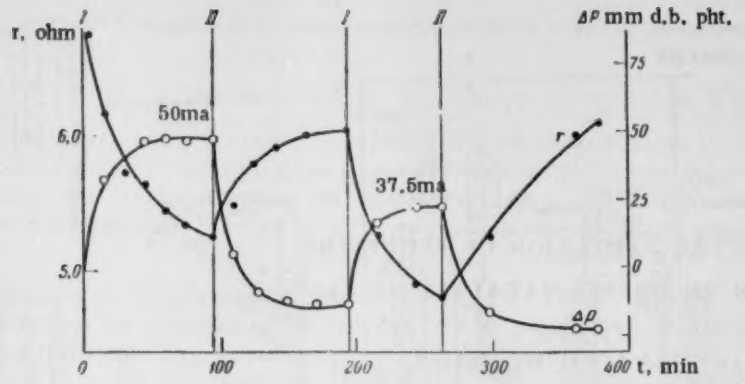

Fig. 4. Variation of the increase of pressure in the system (ΔP, mm of dibutylphtalate column) and the resistance of the $V_2O_5 \cdot 0.1\ K_2SO_4$ catalyst (r, ohm) during the oxidation of hydrogen. I) Electrolytic cell connected; II) electrolytic cell disconnected.

The oxidation of hydrogen occurs as the result of interaction between hydrogen and the oxygen adsorbed on the surface of the catalyst

$$W = k'\Theta_0 p_{H_2}. \qquad (4)$$

It was found experimentally that the order of the reaction with respect to hydrogen is somewhat lower than unity. This is apparently due to the decrease of the stationary concentration of adsorbed oxygen with increasing hydrogen pressure. This assumption is confirmed by measurements of the resistance of the tablet of catalyst during the oxidation of hydrogen. Figure 4 represents the results obtained for the sample of $V_2O_5 \cdot 0.1\ K_2SO_4$. When hydrogen is absent from the circulating gas, the resistance of the catalyst acquires a value characteristic of equilibrium in the filling of the surface by adsorbed oxygen. When oxyhydrogen is introduced into the system the pressure increases, due to the accumulation of hydrogen in the circulating mixture, and at the same time the resistance drops. This leads us to assume that the drop of resistance is due to the decrease in the concentration of oxygen on the surface of the catalyst as the result of its interaction with hydrogen. When the stationary state is reached, i.e., when all the added hydrogen enters the reaction and the pressure becomes constant, the resistance also acquires a constant value. This constant value of the resistance corresponds to the stationary concentration of the oxygen adsorbed on the surface of the catalyst during the process of the reaction at a given concentration of hydrogen in the reacting medium.

The concentration of hydrogen decreases, and simultaneously the resistance increases to its original value, when the cell is disconnected.

Analogous variations of the resistance during the reaction process were observed for other samples.

LITERATURE CITED

1. L.A. Kasatkina, G.K. Boreskov, and P.N. Sokolov, Zhur. Fiz. Khim. 34, 360 (1960).
2. L.A. Kasatkina and G.K. Boreskov, Zhur. Fiz. Khim. 29, 455 (1955).
3. L.A. Kasatkina, G.K. Boreskov, Z.L. Krylova, and V.V. Popovskii, Izv. Vyssh. Uchebn. Zav., Khimi. i Khimich. Tekh. 1. 12 (1958).
4. G.K. Boreskov and M.G. Slin'ko, Khim. Promyshlennost' 1, 19 (1955); G.K. Boreskov, M.G. Slin'ko, and A.G. Filippova, Doklady Akad. Nauk SSSR 92, 353 (1953).
5. B.V. Spitsyn and L.G. Maidanovskaya, Zhur. Fiz. Khim. 33, 180 (1959).
6. G. Saimard, D. Steiger, R. Arnott, and L. Siegel,* Collection: Chemistry and Chemical Technology [Russian translation] (IL, Moscow, 1956) No. 8, p. 3.
7. G.K. Boreskov, V.V. Illarionov, R.P. Ozerov, and E.V. Kil'disheva, Zhur. Obshch. Khim. 24, 23 (1954).**

*Names not verified.

**Original Russian pagination. See C. B. translation.

KINETICS OF THE OXIDATION OF PROPYLENE TO ACROLEIN ON COPPER CATALYST

O.V. Isaev and L.Ya. Margolis

Institute of Physical Chemistry, Academy of Sciences of the USSR
Translated from Kinetika i Kataliz, Vol. 1, No. 2, pp. 237-241,
July-August, 1960
Original article submitted December 19, 1959

A kinetic study has been made of atmospheric-pressure oxidation of propylene to acrolein and CO_2 on copper catalyst supported on Silit and pumice; it was shown that the propylene oxidation rate is proportional to oxygen concentration and is independent of propylene concentration. The activation energy for CO_2 formation on the catalyst supported on Silit (washed free of iron) is 28-30 kcal/mole, and on the catalyst supported on pumice, 23-25 kcal/mole.

The acrolein oxidation rate is proportional to oxygen concentration and is independent of acrolein concentration. The activation energy for CO_2 formation is 22-24 kcal/mole, and for CO, 38 kcal/mole. The acrolein oxidation rate is reduced considerably by the presence of propylene.

Acrolein has a high reactivity and serves as a valuable raw material for the synthesis of pharmaceuticals, plastics, and other synthetic materials. Despite the existence of foreign plant installations for the production of acrolein by propylene oxidation, no studies of the kinetics of this process appear in the literature.

The copper-catalyzed oxidation of propylene yields acrolein, carbon dioxide, and water. A small quantity of acetaldehyde is detected in the liquid products, and at higher process temperatures a significant quantity of carbon monoxide is observed in the gas. In addition, an organic coating is formed on the catalyst surface [1, 2], probably due to adsorption and polymerization of acrolein.

The aim of the present work is the determination of the process laws of the principal reactions of acrolein and carbon dioxide formation in the oxidation of propylene on copper catalyst.

Experiments were conducted in a dynamic unit at atmospheric pressure (Fig. 1). Oxygen and nitrogen were passed through purifying and drying columns filled with activated carbon and calcium chloride. Propylene was obtained in the same unit by dehydrating isopropanol at 400° on industrially prepared alumina. The catalyst was pretreated with 1 N sodium acetate solution for selective poisoning of polymerization and cracking reactions. The propylene was freed from ether, water, and unreacted alcohol by calcium chloride, activated carbon, and solid caustic. The gases were mixed in a mixing chamber (their feed rate and consequently the gas mixture composition were controlled by indicating rheometers) and fed to a quartz reactor charged with 2.5 ml of catalyst. The length of the catalyst bed was about 1 cm. A layer of quartz chips was placed on top of the catalyst for preheating the gas mixture. The temperature in the center of the catalyst bed was measured by a nichrome–constantan thermocouple. Another thermocouple, fastened to the electric heater sheath, was connected to a photoelectric thermoregulator made from a PP portable potentiometer. This system permitted temperature control of the catalyst with an accuracy of ± 0.5°. The temperature change from top to bottom of the catalyst bed did not exceed 2-3°. The gas from the reactor passed through a cooler and through an absorption column (externally water-cooled) which was washed with distilled water containing a small quantity of hydroquinone for stabilizing the acrolein. The gas after drying entered an automatic recording gas analyzer (infrared

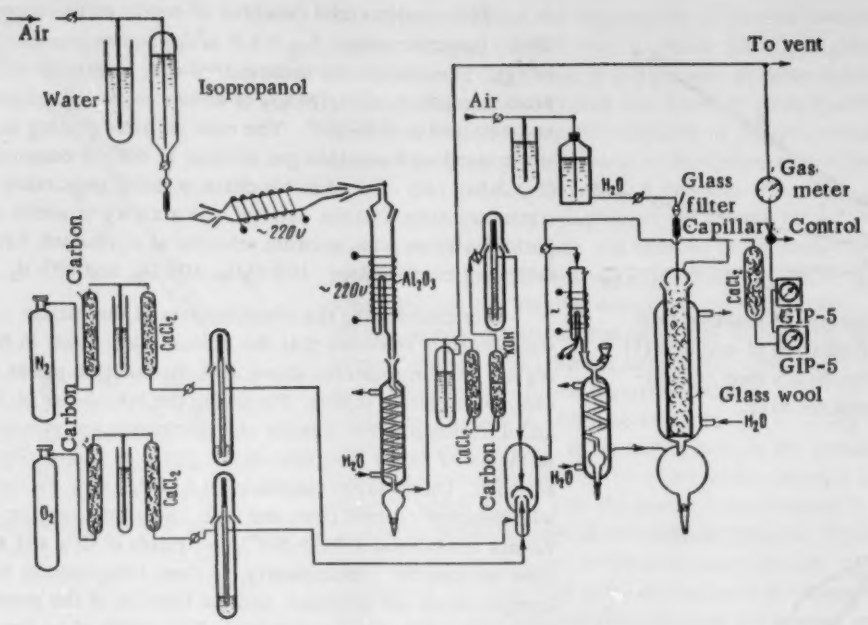

Fig. 1. Flow diagram of dynamic unit.

TABLE 1

Influence of Concentration of Components of Initial Gas Mixture upon Yield of Reaction Products

% Cu	Temperature, °C	Variation of propylene concentration					Variation of oxygen concentration					First-order constants,* sec^{-1}	
		Composition of initial mixture, %			Reaction products, %		Composition of initial mixture, %			Reaction products, %			
		C_3H_6	O_2	N_2	CO_2	Acrolein	O_2	C_3H_6	N_2	CO_2	Acrolein	k_{CO_2}	k_{acr}
0,5	373	15	10	75	1,2	0,26	3,0	30	67	0,55	0,077	0,62	0,052
		20	10	70	1,25	0,30	5,0	30	65	0,85	0,13	0,58	0,053
		30	10	60	1,1	0,31	10,0	30	60	1,8	0,27	0,61	0,054
		40	10	50	1,2	0,36	15,0	30	55	2,7	0,39	0,61	0,052
		60	10	30	1,2	0,25	—	—	—	—	Average	0,605	0,053
1,0	362	15	10	75	1,8	—	3,0	30	67	0,50	0,056	0,56	0,038
		20	10	70	1,6	0,30	5,0	30	65	0,75	0,11	0,50	0,045
		30	10	60	1,55	0,26	10,0	30	60	1,6	0,22	0,57	0,044
		40	10	50	1,6	0,29	15,0	30	55	2,4	0,32	0,57	0,042
		60	10	30	1,7	0,30	—	—	—	—	Average	0,54	0,0421

* Concentration of oxygen converted to acrolein and CO_2 was calculated taking into account stoichiometric reaction coefficients.

absorption, Type GIP-5), which permitted continuous determination of carbon monoxide and dioxide concentration during the process with ± 5% accuracy. The rate of the gas stream was checked by a gas meter with ± 1-2% accuracy. The concentration of acrolein in the water medium was determined by bromine-bromate, and the total aldehydes by the hydroxylamine method.

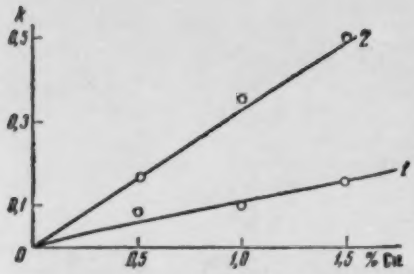

Fig. 2. Dependence of reaction rate constants for formation of acrolein (1) and carbon dioxide (2) upon concentration of copper on Silit.

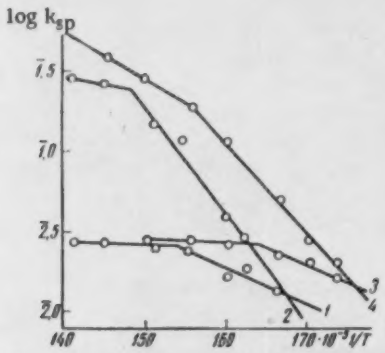

Fig. 3. Dependence of log k_{sp} upon 1/T for the reactions of formation of acrolein and carbon dioxide, for concentration of copper on Silit: 1% Cu: 1) acrolein; 2) CO_2; 1.5% Cu: 3) acrolein, 4) CO_2.

The catalysts used consisted of cupric oxide supported on Silit (specific surface S_{sp} = 1.2 m^2/g) and on pumice (S_{sp} = 6.5 m^2/g). The carrier was impregnated with a definite volume of an aqueous solution of Cu $(NO_3)_2$ of known copper concentration, dried and calcined at 600-700°. The catalyst after placing in the reactor was treated with reaction gas mixture at 400° to constant activity (1-1.5 hr). All of the kinetic characteristics were taken on the stationary surface of the catalyst, the activity of which was checked periodically on a gas mixture selected as a standard, having the following composition: 30% C_3H_6, 10% O_2, and 60% N_2.

For establishing the absolute rates of the various reactions it was necessary to ensure that the process takes place in the kinetic region. At temperatures above 400° the reaction passes into the external-diffusion region. For fixing the boundaries of the kinetic and diffusion regions, a series of experiments was conducted on the influence of linear flow rate on the yields of carbon dioxide and acrolein. On catalysts containing 0.5, 1.0, and 1.5% Cu on Silit, with constant contact time and with linear rate varying fourfold at various temperatures (350-380°), the yields of CO_2 and acrolein were unchanged. Consequently, at these temperatures no diffusion complications are observed, and the kinetics of the process may be studied under these conditions. The results of an investigation of the influence of reactant concentration upon the reaction rates of acrolein and CO_2 formation are presented in Table 1. These rates (W_{acr} and W_{CO_2}) are independent of propylene concentration and are proportional to oxygen concentration in the initial gas mixture.

The rate constants were calculated according to the first-order equation:

$$k = -\frac{\ln\left(1-\frac{C}{C_0}\right)}{\tau},$$

where C_0 is the initial concentration of oxygen, C is the concentration of oxygen converted to acrolein or CO_2, and τ is the contact time in seconds. At low degrees of conversion, where $C/C_0 < 1$, the logarithm of $(1 - C/C_0)$ can be expanded as a series which, taking only the first two terms, gives an equation for calculating rate constants:

$$k = \frac{\frac{C}{C_0}+\frac{1}{2}\left(\frac{C}{C_0}\right)^2}{\tau}.$$

On the basis of the data obtained the rate equations of these reactions may be written in the following manner:

$$W_{acr} = k_1[O_2]^1[C_3H_6]^0, \qquad W_{CO_2} = k_2[O_2]^1[C_3H_6]^0.$$

It is interesting to note that the form of the equations for these reactions is identical. Similar relationships were obtained by us previously [3] for the reactions of formation of aldehydes, CO, and CO_2 in the oxidation of propylene on vanadium pentoxide.

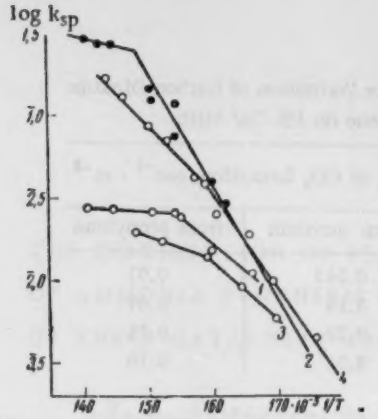

Fig. 4. Dependence of log k_{sp} upon 1/T for catalyst containing 1% Cu on different carriers: Acrolein (1) and CO_2 (2) on Celite; acrolein (3) and CO_2 (4) on pumice with grain size 5-7 mm.

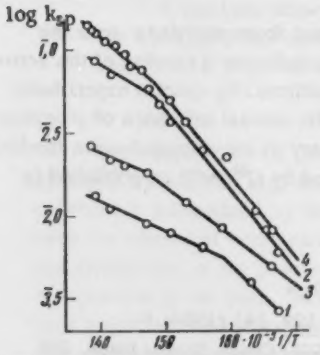

Fig. 5. Dependence of log k_{sp} upon 1/T for catalyst containing 0.25% Cu on pumice: Acrolein (1) and CO_2 (2) on catalyst with grain size 5-7 mm; acrolein (3) and CO_2 (4) on catalyst with grain size 2-3 mm.

Figure 2 shows the dependence of the rate constants upon the concentration of catalyst on the carrier (Silit), indicating the kinetic region of the course of the process. In order to eliminate completely any possible diffusion and thermal complications, experiments were conducted to study the influence of propylene and oxygen concentration on the reaction rates of formation of acrolein and CO_2 in a static unit at low pressures (0.5 mm Hg). The catalyst contained 1% Cu on Silit and was pumped out at 400° to a pressure of 10^{-6} mm Hg. The cupric oxide was reduced to the metal by propylene. After several experiments with a mixture of $C_3H_6 + O_2$ (30:10) diluted with nitrogen, the catalyst activity became constant. An increase of propylene concentration from 30 to 90% in mixtures with constant oxygen content (10%) did not change the concentration of acrolein and carbon dioxide in the reaction products. A change of oxygen concentration (from 9 to 40%) increased the yield of CO_2 and acrolein fourfold. Consequently, the reaction rates of the formation of acrolein and carbon dioxide conform to a first-order equation with respect to oxygen, which agrees with the conclusions obtained in studying the process in dynamic units at atmospheric pressure. Figure 3 shows the temperature dependence of specific rate constants $k_{sp} = k/S$ for samples of catalysts with different contents of copper supported on Silit, pretreated with hydrochloric acid and caustic, and washed with water for removal of iron contaminants. The activation energy for CO_2 formation for these samples is 28-30 kcal/mole and for acrolein formation 12-14 kcal/mole. It should be noted that the transition to the surface-diffusion region for the reaction of acrolein formation takes place at a lower temperature than for the reaction of CO_2 formation. The selectivity of the process of oxidizing propylene to acrolein is determined by the ratio of the rate constants of these reactions. In the temperature region below 320° the reaction rate constant for acrolein formation is greater than that for carbon dioxide formation; above 350°, on the other hand, the rate constant for CO_2 formation is greater than for acrolein. Therefore, it is desirable to carry out the oxidation of propylene to acrolein at low temperatures. It should be noted that the optimum temperature interval for conducting the process depends on the concentration of copper on the carrier. Figure 4 shows the dependence of log k_{sp} upon 1/T for two catalysts: 1% Cu on Silit (washed iron-free) and 1% Cu on pumice.

As seen from the figure, the activation energy for acrolein formation is the same on Silit and on pumice, 12-14 kcal/mole. The activation energy for CO_2 formation on Silit (washed iron-free) is 28-30 kcal/mole and on pumice 23-25 kcal/mole. It should be noted that on pumice, which has considerable porosity, a transition to the surface-diffusion region is observed, and the activation energy for CO_2 and acrolein formation is reduced to one-half its value. As seen from Fig. 5, crushing the pumice grains from 5-7 to 2-3 mm increases the temperature of transition to the surface-diffusion region.

We had established previously that propylene is oxidized to acrolein and carbon dioxide according to a parallel-successive scheme [2, 4]. The principal part of the CO_2 formed in this process is obtained as a result of the oxidation of acrolein [2]. Therefore, it was of definite interest to compare the kinetics of the oxidation of acrolein and propylene.

Experiments showed that the rate of acrolein oxidation is proportional to oxygen concentration and is independent of acrolein concentration. The rate constants for CO_2 and CO formation can be calculated by a first-order equation with respect to oxygen.

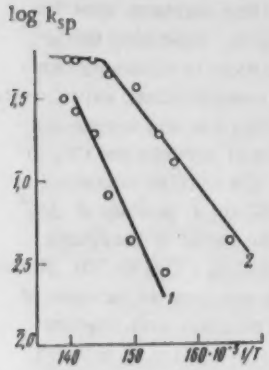

Fig. 6. Dependence of log k_{sp} upon 1/T for catalyst containing 1% Cu on Silit (washed free of iron) in the oxidation of acrolein to carbon monoxide (1) and carbon dioxide (2).

TABLE 2

Specific Rate Constants for Formation of Carbon Dioxide from Acrolein and Propylene on 1% Cu/ Silit

Temperature, °C	k_{sp} of CO_2 formation, $sec^{-1} \cdot m^{-2}$	
	from acrolein	from propylene
334	0.043	0.01
364	0.16	0.07
378	0.29	0.11
392	0.31	0.15

Figure 6 shows the temperature dependence of the specific rate constants of acrolein oxidation. The activation energy for the formation of carbon dioxide from acrolein is equal to 22-24 kcal/mole, and for carbon monoxide 38 kcal/mole. The formation of carbon monoxide from acrolein starts at a higher temperature than that for CO_2 formation. Specific reaction rate constants are presented in Table 2 for the formation of carbon dioxide from acrolein and propylene on a 1% Cu catalyst (on iron-free Silit) in the temperature region of 330-390°.

The reaction rate constants for formation of CO_2 from acrolein are greater than from propylene over the entire range of temperatures studied. This difference of the rate constants probably indicates a slowing of the acrolein oxidation reaction by the propylene present in the gas. This hypothesis was confirmed by special experiments on the oxidation of mixtures of propylene, acrolein, and oxygen. For establishing the mutual influence of propylene and acrolein on the reaction rate for the formation of carbon dioxide it was necessary to use a tagged-atom method. The results of a study of the oxidation of mixtures of propylene and acrolein, tagged by C^{14}, will be published in subsequent work.

LITERATURE CITED

1. O. V. Isaev and M. Ya. Kushnerev, Doklady Akad. Nauk SSSR 124, 858 (1959).*
2. O. V. Isaev, L. Ya. Margolis, and I. S. Sazonova, Doklady Akad. Nauk SSSR 129, 141 (1959).*
3. L. Ya. Margolis, E. P. Malyarova, and S. Z. Roginskii, Izvest. Akad. Nauk SSSR, Otdel. Khim. Nauk, 958 (1954).*
4. O. V. Isaev, L. Ya. Margolis, and S. Z. Roginskii, Zhur. Obshch. Khim. 29, 1522 (1959).*

* See C. B. translation.

THE DISTRIBUTION OF PROMOTERS ON THE SURFACE OF AMMONIA SYNTHESIS CATALYSTS AND THE ACTIVITY OF THESE CATALYSTS AT HIGH PRESSURE*

V. N. Shishkova, S. S. Lachinov, and I. N. Konyukhova

State Scientific Research Institute for the Nitrogen Industry
Translated from Kinetika i Kataliz, Vol. 1, No. 2, pp. 242-246, July-August
July-August, 1960
Original article submitted December 22, 1959; revised April 21, 1960

The free fraction of the surface, the fraction covered with alkalis, and the activity of iron catalysts for ammonia synthesis at high pressure have been determined.

It has been shown that there is no correspondence between the free iron surface area and the activity of the catalysts. The specific activity of doubly promoted catalysts is raised when the fraction of the surface covered with alkali increases.

Ammonia synthesis catalysts are the object of a great number of investigations. The raised interest in these catalysts reflects the high importance of ammonia synthesis in modern chemical technology. The activity of the catalysts is determined by the surface area and the specific catalytic activity. Both values are chiefly dependent upon the chemical composition of the catalysts. It is known from the studies of Emmett and Brunauer [1, 2] that the distribution of the promoters on the surface of iron catalysts for ammonia synthesis differs from the chemical composition of the bulk. Most of the authors [3, 4] adhere to the opinion that the catalytic action of iron catalysts originates from the presence of an active crystalline iron structure and that the promoters enable a highly dispersed and porous structure to be formed. Some investigators believe that α-Fe faces with increased parameters are the active parts [5]. Others suppose that promoters not only increase and stabilize the iron surface but also influence the kinetics of the process [6, 7]. Yet all these investigators start from the assumption that only metallic iron acts as a catalyst in ammonia synthesis.

In the study of O. F. Shcheglov, G. K. Boreskov and M. G. Slin'ko [8] the data obtained for the specific catalytic activity at atmospheric pressure of an unpromoted iron catalyst were nearly the same as those for a doubly promoted one. Nielsen and Bohlbro [7] did not find a correlation between the activity and the free iron surface area of two catalyst samples which contained different amounts of the same promoters. Using three catalyst samples Uchida and Todo [9, 10] were also unable to find a relation between the free iron surface and the catalytic activity of an iron catalyst at high pressure.

We have investigated the relation between the distribution of the promoters on the surface and the activity of iron-catalysts at high pressure.

EXPERIMENTAL

We have determined the total surface area of iron catalysts, the free fraction of the surface, that covered by alkalis and the activity at high pressure.

* The senior research workers G. M. Mironova and A. I. Ivanova took part in this investigation.

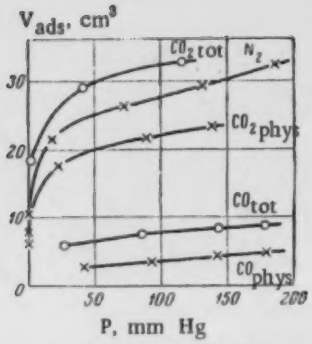

Fig. 1. CO, CO_2 and N_2 adsorption isotherms on catalyst 8b-58.

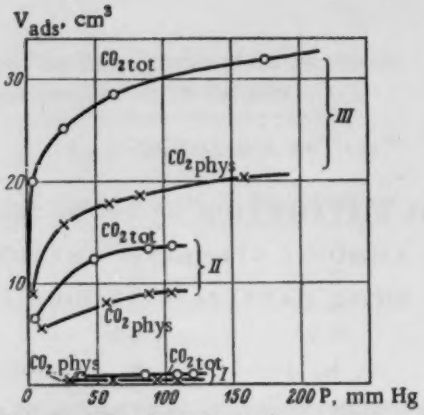

Fig. 2. CO_2 adsorption isotherms measured when catalyst K-55, which was promoted by 2.7% K_2O and 4.75% Al_2O_3, was being reduced: I) before reduction; II) after reducing during four hours; III) after reducing during eight hours.

The total surface area was determined by the BET method from nitrogen adsorption at low temperature; the free iron surface from carbon monoxide chemisorption [1, 2]; the surface area covered by alkalis from carbon dioxide chemisorption [1, 2].

All adsorption measurements were carried out volumetrically in a vacuum apparatus. Carbon dioxide was obtained by decomposing sodium bicarbonate and carbon monoxide by the action of concentrated sulfuric acid upon formic acid; nitrogen was prepared from sodium azide. Carbon dioxide was purified in columns with silica gel and in traps placed in dry ice. The gas obtained was frozen out in a trap by liquid nitrogen and the incondensable gases were pumped off to a pressure of 10^{-4} mm. The purification train for carbon monoxide consisted of a column with silica gel, fused caustic alkali, a tube with copper turnings (400°), and a trap cooled in liquid nitrogen. During chemisorption measurements the gas pressure in the apparatus was determined with an accuracy of 0.1 mm Hg.

The activity of the catalysts was determined in a high pressure apparatus.* The construction of the reactor allowed simultaneous investigation of four catalyst samples under equal conditions [11, 12]. Catalysts with 1-2 mm granules, prepared under technical conditions, were used in the experiments.

Most experiments were carried out in the following way: After the activity had been determined in the high pressure apparatus, the catalyst samples, which had been reduced at 500°, were passivated by nitrogen containing 0.2% oxygen and then transferred to the vacuum equipment where they were reduced by hydrogen at atmospheric pressure. This gas had before been freed of oxygen and moisture on a nickel-chromium catalyst, silica gel, fused caustic alkali and in traps cooled by liquid nitrogen. After reduction the catalyst was outgassed at 500° to a pressure of 10^{-5} mm Hg. Then the nitrogen, carbon monoxide and carbon dioxide adsorption isotherms were measured. The amount of chemisorbed carbon monoxide and dioxide was found in the following way: The isotherm was measured at −78°, where both physical adsorption and chemisorption takes place. Then the physically adsorbed gas was pumped off at room temperature, and the isotherm was again measured at −78°. In this case there is only physical adsorption of carbon monoxide or dioxide. The difference between these isotherms, which are parallel, gives the amount of chemisorbed gas. After the isotherms for a given gas had been determined, the catalyst was reduced and outgassed at 500° to a pressure of 10^{-5} mm Hg. The isotherms for combined physical and chemical adsorption and those for physical adsorption alone, as found on the catalyst 8b-58, are given in Fig. 1. Similar isotherms have been obtained for all catalysts investigated.

The fraction of the surface occupied by iron and alkali can be calculated as the ratio between carbon monoxide or dioxide, respectively, and the amount of nitrogen corresponding with a monlayer as the number of chemisorbed molecules on the area occupied by one nitrogen molecule.

Moreover, the fraction of the catalyst surface covered by alkali has been determined during the first

* The authors thank L. D. Kuznetsov, who has carried out the activity measurements.

TABLE 1

Catalyst Activity, Surface Area, Fraction Free Iron Surface and That Covered by Alkali *

Catalyst	Promoter content, %		S, m^2/g	θ_{Fe}	θ_{alk}	% NH_3	$k \cdot 10^{-3}$	$k/2S$	S_{Fe}, m^2/g	$k/2S_{Fe}$
1-55	Al_2O_3 —2,1	K_2O—0,3	10	0,30	0,08	5	0,2	8	3,0	30
2-55	Al_2O_3 —4,2	K_2O—0,07	13	0,20	0,11	4,0	0,1	4	3,0	20
3-55	Al_2O_3 —10,0	K_2O—0,04	17	0,23	0,09	4,3	0,1	3	4,0	10
4-55	Al_2O_3 —3,9	K_2O—2,1	11	0,18	0,50	13,7	2,2	100	2,0	550
5-55	Al_2O_3 —1,2	K_2O—2,6	3	0,27	0,78	13,6	2,1	350	1,0	1200
K-54	Al_2O_3 —3,9	K_2O—1,8	13	0,27	0,46	13,6	2,0	80	4,0	300
ÉA-58	K_2O —1,2 Al_2O_3 —4,0	SiO_2—1,2 CaO—3,5	15	0,06	0,18	14,6	2,5	90	1,0	1300
8b-58	K_2O —0,9 Al_2O_3 —3,2	SiO_2—0,9 CaO—4,0	13	0,08	0,21	21,2 **	3,6	140	1,0	1800
KS-1	K_2O —1,0 Al_2O_3 —2,9	SiO_2—0,9 CaO—2,8	11	0,19	0,32	16,6	3,2	150	2,0	800
ÉKG-59	K_2O —0,9 Al_2O_3 —3,8	SiO_2—1,0 CaO—3,4	13	0,19	0,38	16,7	3,2	120	2,5	600

* S is the surface area of the catalyst; k the reaction rate constant at 400°, 300 atm and space velocity 30,000 hr^{-1}, calculated from the relation of M. I. Temkin and V. M. Pyzhev [12] with $\alpha = 0.5$; S_{Fe} the free iron surface area; θ_{Fe} the former expressed as a fraction of the total surface area; S_{alk} the surface area covered by alkali; θ_{alk} the latter expressed as a fraction of the total surface area.

** At the space velocity 15,000 hr^{-1}.

TABLE 2

Total Surface Area and Fraction of the Surface Covered by Alkali During the Reduction of the Catalyst K-55

Reduction time, hr	S, m^2/g	θ_{alk}	S_{alk}, m^2/g
Before reduction	~0.3	0.20	~0.06
4	5	0.46	2
8	11	0.51	5
12	12	0.50	6

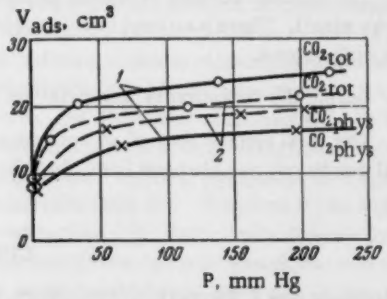

Fig. 3. CO_2 adsorption isotherms on catalyst K-55: 1) after the laboratory investigation ($\theta_{K_2O} = 0.45$); 2) taken from a technical column ($\theta_{K_2O} = 0.043$).

reduction. For this purpose the doubly promoted catalyst K-55 has been investigated. The reduction at 500° and space velocity 8000 hr^{-1} as well as the determination of the surface fraction covered by alkali were carried out in one and the same vacuum apparatus. This fraction has been measured for a catalyst of the same type after its activity had been determined during five days in a laboratory apparatus at high pressure, and also for a catalyst taken from a technical column, after this had worked more than two years without interruption.

The results of these experiments are shown in Tables 1 and 2.

From Table 1 it is obvious that in all catalysts investigated a great part of the surface is covered by the promoters, and that for doubly promoted catalysts the specific activity is found to be raised when a greater fraction of the surface is covered by alkali.

From the experiment with catalyst K-55 it follows that not only the total surface area, as was already known

[13], but also the fraction covered by alkali increases during the reduction of the catalyst (Table 2, Fig. 2). Consequently, during the reduction alkali oxides migrate to the surface. From Table 1 it follows also that the catalytic activity per unit of free iron surface area is not constant. So there is no relation between the free iron surface area and the activity of the catalysts. Consequently there is no similarity between the free iron surfaces of catalysts containing different amounts of different promoters. Obviously, the activity of iron catalysts does not originate from the free iron surface but from the chemical compounds which are formed on the catalyst surface during the reduction.

The results obtained when investigating the surface of the catalyst samples taken from an industrial column are shown in Fig. 3. We have measured the total surface area and the fraction of the surface covered by alkali for two samples of the catalyst K-55. For the catalyst which was taken from an industrial column the surface area covered by alkali was ten times smaller than for the catalyst investigated in the laboratory. The total surface had decreased little, from 12.9 to 12 m^2/g. The activity of the catalyst taken from an industrial column had decreased considerably [4]. Consequently, the decreased fraction of the surface covered by alkali is one of the reasons why in a technical column the activity of the catalyst is lowered, and this is confirmed by the data which show that the specific catalytic activity rises when a greater fraction of the surface is covered by alkali.

In a paper by Yu. S. Sinyak and others [15] it has been shown that in an iron catalyst potassium is present in two different forms. Uchida [9] has discovered that the activating action of potassium oxide is connected with its insoluble form.

It is not known why in the catalyst taken from a technical column the fraction of the surface covered by alkali has decreased; possibly it is connected with the carrying away of that part of the alkali which is soluble in water or with the formation potassium compounds which are unable to chemisorb carbon dioxide.

SUMMARY

1. For ammonia-synthesis catalysts of various compositions we have determined the distribution of the promoters on the surface and the activity at high pressure.

2. The specific activity of doubly promoted catalysts increases when a greater fraction of the surface is covered by alkali. There was found no relation between the activity of the ammonia-synthesis catalysts and the free iron surface area.

3. During the reduction of iron catalysts K_2O migrates to the surface.

4. The total surface area of an ammonia-synthesis catalyst which had worked more than two years under technical conditions had changed little, but the fraction of its surface covered by alkali had decreased several times.

LITERATURE CITED

1. S. Brunauer and P. Emmett, J. Am. Chem. Soc. 59, 310 (1937).
2. S. Brunauer and P. Emmett, J. Am. Chem. Soc. 62, 1732 (1940).
3. Mittasch and Kennecke, Z. Elektrochem. 38, 666 (1932).
4. Brill, Z. Elektrochem. 38, 669 (1932).
5. R. Westrik and P. Zwietering, Proc. Koninkl. nederl. akad. wet., Series B. 5, 492 (1953).
6. R. Love and P. Emmett, J. Am. Chem. Soc. 63, 3297 (1941).
7. A. Nielsen and H. Bohlbro J. Am. Chem. Soc. 74, 963 (1952).
8. O. F. Shcheglov, G. K. Boreskov, and M. G. Slin'ko, Doklady Akad. Nauk SSSR 105, 123 (1955).
9. H. Uchida and N. Todo, Bull. Chem. Soc. Japan 29, 762 (1956).
10. H. Uchida, Koro Kagaky gzassu Japan 60, 10, 25 (1957).
11. L. D. Kuznetsov and S. S. Lachinov, Zhur. Fiz. Khim. 33, 2542 (1959).
12. M. I. Temkin and V. M. Pyzhev, Zhur. Fiz. Khim. 13, 851 (1939).
13. W. K. Hall, W. H. Tarn, and R. B. Anderson, J. Am. Chem. Soc. 72, 5436 (1950).
14. S. S. Lachinov and V. A. Kurkovskii, Khim. Nauka i Prom. 1, 610 (1956).
15. Yu. E. Sinyak, S. Z. Roginskii, and M. I. Yanovskii, Doklady Akad. Nauk SSSR 118, 727 (1958).*

*Original Russian pagination. See C. B. translation.

THE COMPOSITION, METHODS OF PREPARATION, AND NATURE OF THE ACTIVITY OF TRICALCIUM PHOSPHATE CATALYSTS

L. Kh. Freidlin and V. Z. Sharf

The N. D. Zelinskii Institute of Organic Chemistry, Academy of Sciences of the USSR
Translated from Kinetika i Kataliz, Vol. 1, No. 2, pp. 247-256,
July-August, 1960
Original article submitted December 24, 1959

The tricalcium phosphate catalyst made by precipitation from dilute solution in an alkaline medium consists of a mixture of hydroxyapatite and tricalcium phosphate. Both salts show similar catalytic properties. The catalyst acidity is determined by an indicator method of titration. It has been found that both the acidity and catalytic activity of the phosphate vary in a similar way with the ignition temperature. The results obtained confirm the acid nature of the activity of the phosphate catalyst, which depends on the existence of chemically bound water.

Recent investigations have shown that calcium phosphate is a very active and selective catalyst for reactions of vapor phase hydrolysis, hydration, dehydration, alkylation, and condensation.

Calcium phosphate is one of the two known catalysts for the vapor phase hydrolysis of chlorobenzene to phenol [1]. Its activity for this reaction remains practically unaltered after 140 hr operation at 550° [2]. In the hydrolysis of 1,2,4-trichlorobenzene over this catalyst one of the chlorine atoms is replaced by hydrogen, and the product is m-chlorophenol [3]. Alkyl and aryl ethers and 4,5-dihydrosylvan are hydrolyzed nearly quantitatively, over phosphate even at 160° to the corresponding alcohols, phenols, and aldehydes or ketones [4]. Phosphate catalyzes the hydration of C=C in α,β-unsaturated aldehydes and the subsequent dealdolization of the ketols and aldols formed [5]. Tricalcium phosphate, particularly when associated with the phosphates of copper and cadmium, accelerates the vapor phase hydration of acetylene to acetaldehyde [6]. Phosphate shows high activity and a specific effect in the hydration of propene oxides and ethylene oxide [7]. High purity olefinic hydrocarbons (98-100%) are produced by the dehydration of alcohols and cyclohexanol over calcium phosphate, and the products do not crack or isomerize under the reaction conditions. Diethyl ether is dehydrated more slowly than ethyl alcohol, and diisopropyl ether more slowly than isopropyl alcohol [8].

Calcium phosphate is the most specific, productive, and stable of all the known catalysts for formic acid dehydration; the gas obtained contains 100% carbon monoxide [9]. Unlike alumina, phosphate catalyzes the alkylation of aromatic amines with alcohols, the alkyl groups going mainly to the ring [10]. Phosphate catalyzes the condensation of aldehydes, as, for example, in the process of acrolein production [11]:

$$CH_2O + CH_3CHO \xrightarrow{400^\circ} CH_2 = CHCHO + H_2O.$$

Calcium phosphate is recommended as a support for Ni catalysts for hydrocarbon dehydrogenation, as in the production of 1,3-butene from butene and butane, or of styrene from ethylbenzene [12], and also as a component of the mixed catalyst [Cr_2O_3–$Ca_3(PO_4)_2$–Ni_3PO_4] for purifying gases from acetylene [13]. It is used as a carrier for the Ni catalyst in the hydrogenation of fats [14].

It is evident from the above review that calcium phosphate is very widely used in catalytic processes.

TABLE 1

The Compositions of Tricalcium Phosphate Preparations Supplied by Different Firms, %

	CaO	P_2O_5	CaO : P_2O_5
Theoretical composition	54.21	45.79	3.0
Merck A.R.	52.83	46.85	2.86
De Hahn "Pure"	49.62	40.62	3.13
Pharmacopeia DAV	52.37	45.37	2.92

TABLE 2

The Water Contents of Precipitated Preparations of Tricalcium Phosphate and Hydroxyapatite

Salt	Total water content, %	Chemically bound water		Literature reference
		%	mole/mole phosphate	
Tricalcium phosphate	3.5-9.0	2.75	0.5	[19]
The same	6-10	2.75	0.5	[37]
The same	–	3.5	1.0	[24, 25]
Hydroxyapatite	5.5-6.0	2.11	–	[19]
The same	–	2.21 2.25	–	[24]

There was therefore a need to obtain information as to its composition, methods of preparation, and the nature of the active surface.

The Composition of and Methods of Preparing Tricalcium Phosphate

The production of tricalcium phosphate is a complex task, since mono- and di-substituted phosphates and the basic hydroxyapatite may be formed simultaneously.

It has been established that the composition of the precipitate depends on many factors – concentration, temperature, pH, and others. Precipitates of different composition are also obtained by changing the order of mixing solutions of equivalent quantities of disodium phosphate and calcium chloride [15].

Fabry [16] showed that, depending on the CaO concentration, temperature, and duration, tricalcium phosphate can react with different quantities of lime to form compounds with Ca/P ratios of 2.14, 2.26, or even 2.79, i.e., pseudoapatite $Ca_{10.5}(PO_4)_6(OH)_X$. Tricalcium phosphate and hydroxyapatite can form solid solutions [17]. These facts explain the large variation in the composition of the precipitates obtained by different investigators when the conditions are inadequately controlled [18].

It was shown by Kazakov [19] that precipitated calcium triphosphate can only be obtained under strictly controlled conditions: low concentrations of reacting ions Ca^{2+} and PO_4^{3-} (CaO 0.6 – 8 mg and P_2O_5 0.3 – 15 mg in 100 cm^3), a definite pH (6.4 – 7.0), and slow crystallization. Hydroxyapatite is obtained at concentrations of CaO 0.6 – 14 and P_2O_5 0.3 – 0.0011 mg in 100 cm^3, and with a pH between 7.0 and 9.2. Outside these conditions, the precipitate obtained is not of uniform composition. It will be seen that the conditions for obtaining tricalcium phosphate and hydroxyapatite are very similar. The precipitate obtained may therefore contain both salts.

It is interesting to note (Table 1) that the preparations from different firms have different compositions, and that not one of them corresponds to pure tricalcium phosphate [20]. The "National Formulary IV" (USA) and "Codex" (France) preparations of tricalcium phosphate actually have a composition corresponding to hydroxyapatite – $3Ca_3(PO_4)_2 \cdot Ca(OH)_2$ [21].

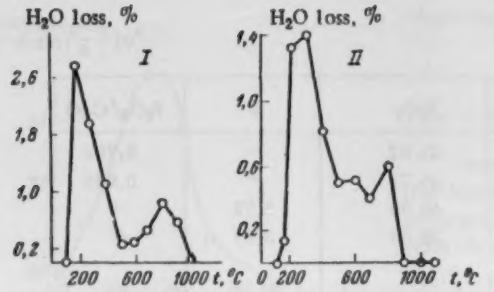

Fig. 1. Differential curves for the dehydration of tricalcium phosphate (I) and of hydroxyapatite (II). The heating time was 2 hr.

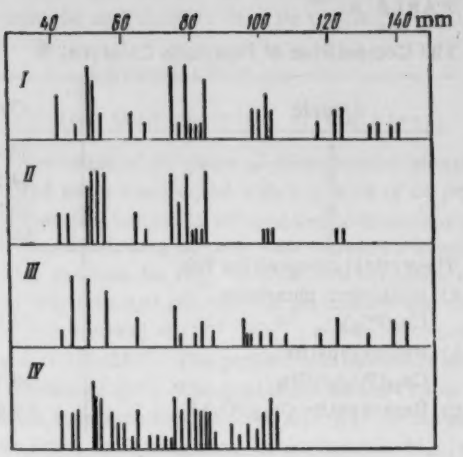

Fig. 2. X-ray patterns of phosphate catalysts: I) sample 1; II) sample 2; III) tricalcium phosphate (NIUIF data); IV) hydroxy apatite (NIUIF data).

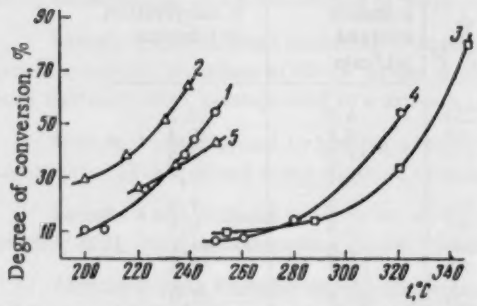

Fig. 3. Dehydration of tert-butyl alcohol over phosphate catalysts.

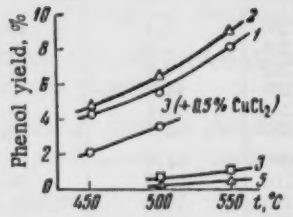

Fig. 4. Hydrolysis of chlorobenzene over phosphate catalysts.

(The numbers on the curves correspond to the numbers of the catalyst samples.)

Chemically Bound Water in Tricalcium Phosphate and Hydroxyapatite

An important feature of precipitated calcium phosphates, both tricalcium phosphate and hydroxyapatite, is that they are crystal hydrates. Freshly precipitated tricalcium phosphate retains up to 1000% of its dry weight of water [22]. Preparations dried at 100° contain 3.5-10% of water (Table 2). Dehydrations curves and thermograms show the dual nature of the bonding with water. Part of the water, 2.75-5.5% (0.5-1 mole), is chemically combined and firmly held in the phosphate molecule. Hydroyxapatite contains 2.11-2.25% of firmly held water. This matter has been investigated in considerable detail [19, 23].

Kazakov [19] found great similarities between the processes of dehydration of tricalcium phosphate and of hydroxyapatite. The first dehydration wave of tricalcium phosphate occurred between 100 and 400°, and 5.85% of water was evolved. This water loss did not affect the crystallo-optical properties of the material. Atmospheric moisture was reabsorbed by the heated product to a considerable extent. The bond between this water and the phosphate was of an adsorptive nature. The second, high temperature dehydration wave occurred over the range 400-900°, when 2.6% of water was evolved, corresponding to the hemihydrate $Ca_3(PO_4)_2 \cdot \frac{1}{2}H_2O$. This wave was irreversible, and produced a marked change in the phosphate structure (the material became cloudy and anisotropic), and the water was considered as chemically bound (Fig. 1).

There was a loss of 3.71% of water in the first dehydration wave of hydroxyapatite (100-400°). The crystalline structure was not affected by this dehydration or by subsequent rehydration. Only the water (2.11%) lost between 400 and 800° was water of constitution (Fig. 1). These conclusions have been confirmed in general by other investigators.

TABLE 3

The Composition of Phosphate Catalysts, %

Sample	CaO	P_2O_5	F	P_2O_5/CaO
1	56.30	42.87	–	0.762
3	54.20	45.71	–	0.845
4	55.90	40.00	3.72	–
5	54.20	39.50	3.20	–
Theoretical composition for:				
a) tricalcium phosphate $Ca_3(PO_4)_2$	54.21	45.79	–	0.845
b) hydroxyapatite $Ca_{10}(PO_4)_6(OH)_2$	55.78	42.44	–	0.761
c) fluoroapatite $Ca_{10}(PO_4)_6F_2$	55.60	42.22	3.77	0.761

TABLE 4

tert-Butyl Alcohol Dehydration over Phosphate Catalysts

Sample	Temp. °C	i-Butene evolved, ml/min	% dehydration to i-butene	Sample	Temp. °C	i-Butene evolved, ml/min	% dehydration to i-butene
1	200	4,1	10,2	3	254	4,0	10,2
	208	5,0	12,5		288	6,1	15,3
	223	10,8	27,0		320	14,2	35,5
	239	16,3	40,8		348	33,2	83,0
	242	18,1	45,2	4	250	3,0	7,5
	250	22,4	56,0		261	3,6	9,1
2	200	12,4	31,0		280	5,8	14,1
	216	15,8	39,5		322	22,7	56,6
	232	21,1	53,0	5	220	10,7	27,0
	240	26,5	66,2		235	14,5	36,2
					250	17,6	44,0

TABLE 5

Chlorobenzene Hydrolysis over Phosphate Catalysts.

Sample	Temp. °C	Yield, % phenol	Yield, % HCl	Sample	Temp. °C	Yield, % phenol	Yield, % HCl
1*	450	4,2	—	3	450	0,4	Traces
	500	5,6	0,9		550	0,7	
	550	8,1	6,4	3 (+0,5% $CuCl_2$)	450	2,1	0,3
2	450	4,6	2,3		500	3,6	0,5
	500	6,6	2,5	4	500	0,7	Traces
	550	9,5	9,0	5	500	0,8	—
					550	1,0	—

* According to [1].

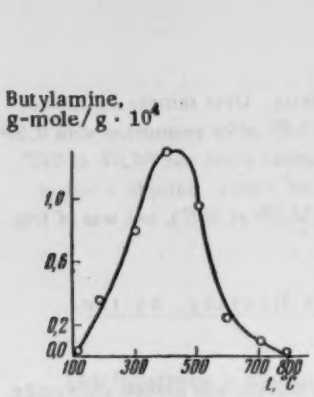

Fig. 5. The change in activity of phosphate catalyst 1 on ignition.

Basset [24] and Belopol'skii and his colleagues [25] attribute to tricalcium phosphate the monohydrate formula $Ca_3(PO_4)_2 \cdot H_2O$.

EXPERIMENTAL

The Production and Composition of Catalysts

Sample 1. A solution of 60 grams of diammonium phosphate in four liters of distilled water was treated with 1.2 liters of 25 percent ammonia, the mixture was heated to 40°, and then a 45 percent calcium chloride solution was added, drop by drop with vigorous stirring, until there was a negative reaction for PO_4^{3-} (tested with magnesia mixture). The mother liquor was decanted off, and the precipitate was washed throughly to complete removal of Ca^{2+}, PO_4^{3-}, and Cl^-, formed into granules, and dried at 100-110°. The product was heated to 900° and analyzed by the method of [26]. The analytical results (Table 3) showed that the composition corresponded to hydroxyapatite. X-ray patterns of material which had only been heated to 400° showed diffuse lines, indicating that the product was highly dispersed. X-ray patterns of the material heated to 900° corresponded to the hydroxyapatite structure (tricalcium phosphate lines were very weak) (Fig. 2). Two portions of the product were heated for 18 hr, one at 400° and one at 900°. Their specific surface areas, measured with nitrogen by the BET adsorption method, were found to be 51 and 7 m^2/g respectively. A similar method of preparing the catalyst has been used before [27 et al.].

Sample 2 was prepared according to Rathje's method [28] by mixing dilute solutions of calcium nitrate and monoammonium phosphate at 60-70° in the presence of ammonia. The x-ray patterns of material which had been heated to 900° corresponded to a mixture of hydroxyapatite and tricalcium phosphate (Fig. 2).

Sample 3 was obtained by heating a stoichiometric mixture of CaO and $Ca(H_2PO_4)_2$ to 1150° [29]. Both its composition (Table 3) and x-ray structure corresponded to tricalcium phosphate.

Sample 4 was prepared by sintering an equimolecular mixture of tricalcium phosphate and calcium fluoride at 1350° [29]. Both its composition (Table 3) and x-ray structure corresponded to fluoroapatite.

Sample 5 was a Khibinsk apatite concentrate, of similar composition to the synthetic fluoroapatite.

Dehydration of tert-Butyl Alcohol and the Hydrolysis of Chlorobenzene over Phosphate Catalysts

The catalytic activities of the above phosphates were investigated for the reactions of tert-butyl alcohol dehydration and chlorobenzene hydrolysis. These reactions were chosen because the first would show up low catalytic activity, and the second was of interest as occurring at high temperature. This made it possible to appraise thermal stability and specificity of catalyst action [1].

Both reactions were carried out with a dynamic type apparatus [1, 5]. The catalyst volume was 10 ml, the grain size 2 × 3 mm. tert-Butyl alcohol was passed at 10.2 ml/hr, and chlorobenzene and water at 3.5 ml/hr. The catalyst was regenerated after each experiment in a stream of air at 400-450°, and this completely restored its activity. The reaction velocity for tert-butyl alcohol dehydration was determined from the amount of isobutene evolved and dissolved in the catalyzate; dissolved isobutene was determined by the method of [30]. The phenol formed by chlorobenzene hydrolysis was determined bromometrically.

The experimental results (Table 4 and Fig. 3) showed that over sample 2 (mixture of tricalcium phosphate and hydroxyapatite) the isobutene yield was 31% at 200° and 66% at 240°. The same catalyst showed a high activity for chlorobenzene hydrolysis (Table 5 and Fig. 4); the phenol yield was 4.6% at 450° and 9.5% at 550°.

The catalytic activity of hydroxyapatite (sample 1) for tert-butyl alcohol dehydration was somewhat lower than that of sample 2. The isobutene yield was 10.2% at 200° and 40.8% at 239° (Table 4 and Fig. 3). For chlorobenzene hydrolysis, sample 1 had much the same activity as sample 2; the phenol yield was 4.2% at 450° and 8.1% at 550° (Table 5, Fig. 4).

Samples 3 and 4, obtained by sintering, and also sample 5, were of low activity. Over sample 3, the isobutene yield was 10.2% at 254°, and the phenol yield was less than 1% at 550°, or 3.6% after promotion with 0.5% of copper chloride. Over sample 4, the phenol yield was 1% at 550°, and the isobutene yield was 56.6% at 322°. Similar yields were obtained over precipitated phosphates at temperatures about 100° lower. Sample 5 was of relatively high activity for tert-butyl alcohol dehydration (the isobutene yield was 36.2% at 235°), but was of low activity for chlorobenzene hydrolysis (the phenol yield was less than 1% at 550°).

The Determination of Catalyst Acidity, and of Its Change on Heating, by the Indicator Method

Catalyst acidity was determined by the indicator method [31]. The catalyst sample was shaken vigorously with 5 ml of indicator solution (2 mg of p-dimethylaminoazobenzene in 100 ml of dry isooctane) in a mechanical shaker. The indicator was adsorbed in this process, and the white catalyst powder acquired a red color. The sample was then treated with 0.05-0.1 ml of 0.1 N n-butylamine in dry isooctane, and shaken again. More butylamine was added as the catalyst color weakened, and the sample was shaken until the red color vanished entirely. To complete the determination, the solid was allowed to settle, the liquid was decanted off, and the excess butylamine was titrated with 0.05 N trichloroacetic acid in isooctane.

None of the five phosphate samples affected the indicator color, after they had been carefully washed and dried at 100-110°. Samples 3, 4, 5, still did not alter the indicator color after they had been dried at 200 or 400°; but samples 1 and 2 did, giving a rose color after drying at 200°, and a red color after drying at 400°. This showed that the precipitated catalysts had acid properties.

The acidity of sample 1 was further investigated, after drying at temperatures in the range 200-800°. Figure 5 shows that the amine requirement of neutral phosphate increased with ignition temperature up to a maximum at 400°. The amine requirement for neutralization subsequently fell with increasing ignition temperature up to 500, 600, and 700°, and there was no change in indicator color after the sample had been heated to 800°.

DISCUSSION OF RESULTS

It is evident from the literature data that completely substituted calcium phosphate can only be obtained by precipitation from very dilute solutions at predetermined pH. When these conditions are not observed, the product is a complex mixture, containing an acid salt as well as neutral and basic phosphates. The catalyst composition is obviously of great importance; for example, dicalcium phosphate is inactive for the vapor phase hydrolysis of chlorobenzene [1], and its activity for formic acid dehydration falls continuously [9], since it is thermally unstable and is converted to the inactive pyrophosphate, even at 325-400° [32]. Thus, the conditions for phosphate preparation, which determine its composition, are of decisive importance in controlling the activity and stability of this catalyst.

The catalytic activity of calcium phosphate is usually attributed to the tricalcium salt. However, hydroxyapatite may also be formed under the conditions for obtaining tricalcium phosphate uncontaminated with acid salt. Probably, therefore, the phosphate catalysts used in different investigations were actually mixtures of tricalcium phosphate and hydroxyapatite in varying proportions. This was true in our work. According to its composition, our sample 1 was hydroxyapatite, but its x-ray diffraction pattern showed the presence of small amounts of tricalcium phosphate. The x-ray diffraction pattern of sample 2 showed that this was a mixture of tricalcium phosphate and hydroxyapatite. Both samples were active for tert-butyl alcohol dehydration and for chlorobenzene hydrolysis. Both showed high thermal stability, and both could be regenerated well. Our results led us to conclude that tricalcium phosphate and hydroxyapatite had similar catalytic properties.

It has been suggested previously that the activity of a phosphate catalyst is determined by its acid nature. With fully substituted calcium phosphates, the acidity is obviously associated with chemically bound water. Schematically, the crystalline hydrates $Ca_3(PO_4)_2 \cdot 0.5H_2O$ (I) and $Ca_3(PO_4)_2 \cdot H_2O$ (II) may be assigned the structures:

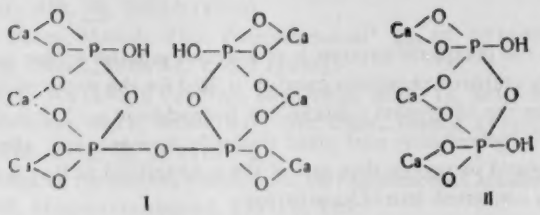

I II

This hypothesis is confirmed by the work of Semishin, who showed that solid crystalline hydrates – metal salts – are substances with more or less pronounced acidic properties [33]. Confirmation of the important role of chemically bound water in the activity of a phosphate catalyst is provided by the experiments on thermal deactivation. Thus, the activity of a phosphate catalyst was reduced by a factor of 4-5 after heating at 850° for 1 hour [1], by a factor of 5 after heating at 600-700° for 1 hour, and by a factor of 10 after heating at 800° for 5 hours [8].

A clear indication of the acid nature of the phosphate catalyst is that it is active for reactions accelerated by acids in the liquid phase, but not for those accelerated by bases, and that it is deactivated by caustic alkali and organic bases [4].

We have determined the acidity of phosphate catalysts directly, by the indicator method. Investigation of the change in acidity with heating temperature showed that there was an increase in acidity from 100-400° (Fig. 5). According to [19], adsorbed water is evolved from tricalcium phosphate and hydroxyapatite in this temperature region. The acid sites freed in this way become available for indicator, so that the amount of amine required for neutralization increases. Phosphate acidity decreased after heating at 500, 600, and 700°, and the indicator was not decolorized at all after heating the phosphate at 800°. It has been shown [19] that the crystal hydrate structure breaks down in this temperature region, and that loss of chemically bound water begins.

Thus the catalytic activity and the acidity of a phosphate vary in a similar way with temperature, and the content of chemically bound water must vary in the same way. From this view point, the activity of a tricalcium phosphate catalyst is determined by the content of available $\geqslant$P–OH groups. The very high stability of the bonds with water of constitution in a phosphate explains the stability of its catalytic action for the vapor phase hydrolysis of aryl halides at high temperature (> 400-450°). Thermal deactivation of the catalyst at 600-850° is accounted for by dehydration, which reduces the number of available $\geqslant$P–OH groups and the specific surface.

The existing kinetic data also confirms that the catalyst activity is due to acid $\geqslant$P–OH groups. Phosphate activity for ethanol dehydration was reduced by a factor of 5 after heating at 600-700° for 1 hour [8], and activity for formic acid decomposition nearly halved after heating at 800° for 5 hours [9]. However, the activation energy did not change for either process. Organic bases markedly reduced catalyst activity for alcohol dehydration by blocking acid sites, but the activation energy was unaltered. Reduction in phosphate activity for enthanol dehydration was found to be directly proportional to the amount of alkali added [34]. All these facts indicate that the nature of the active surface of the catalyst is not altered by thermal deactivation or by poisoning with caustic alkali or amines. In both cases, only the value of the factor before the exponential term is affected, indicating that there is a decrease in the number of active sites on the surface.

It is obvious that the thermal deactivation of a phosphate catalyst should be irreversible, and this is found to be so in practice. As shown above, all phosphate samples obtained by high temperature sintering were of very low catalytic activity and probably had very weak acid properties, indetectable by the indicator method. It is natural that hydroxyapatite, which contains chemically bound water equally difficult to remove, should have chemical properties similar to those of tricalcium phosphate. It may be assumed that there are two types of OH group in the hydroxyapatite molecule. One type is bonded to calcium atoms, the other to phosphorus atoms. Only the second type determines the catalytic properties of hydroxyapatite. It is obvious that Ca–OH groups are not catalytic centers. Support for this view is provided by the results of experiments on the thermal deactivation of hydroxyapatite. Deactivation was observed at 600-850°, whereas, according to Arnold [23], decomposition of Ca–OH groups, with evolution of water, is only observed at much higher temperatures (1200-1400°). In the vapor

phase hydrolysis of halogenobenzenes, Ca—OH groups must react with the hydrogen halide evolved to form nonhydrolyzable Ca—Cl groups. The OH groups are therefore destroyed during the reaction, and are not regenerated.

The establishment that the phosphate catalyst is of a hydroxyapatite nature makes it possible to explain the following. When a freshly prepared phosphate catalyst is used for the vapor phase hydrolysis of chlorobenzene, for the first few hours the catalyzate contains less hydrochloric acid than corresponds to the phenol yield [1, 35]. In subsequent tests, the hydrochloric acid yield gradually increases and, after some time reaches the stoichiometric value. It is natural to assume that part of the acid formed at first is absorbed by the catalyst, whereby the hydroxyapatite is converted into chloroapatite:

$$3\ Ca_3(PO_4)_2 \cdot Ca(OH)_2 + 2HCl \rightarrow 3\ Ca_3(PO_4)_2 \cdot CaCl_2 + 2H_2O.$$

In order to check this hypothesis, sample 2 was analyzed for its chlorine content after it had been used for a series of chlorobenzene hydrolysis tests (with subsequent air-steam regeneration). It was found to contain 4.65% of chlorine, corresponding to 68.5% of chloroapatite in the catalyst. Absorption of hydrogen chloride did not reduce its catalytic activity for chlorobenzene hydrolysis. This also confirmed that Ca—OH groups were not responsible for the catalytic activity of hydroxyapatite in the vapor phase hydrolysis of chlorobenzene.

SUMMARY

1. Existing data has been reviewed on the composition, methods of preparation, and catalytic activity of tricalcium phosphate.

2. The fully substituted phosphate can only be obtained under precise conditions of concentration, medium characteristics, etc., and the product is usually a mixture of tricalcium phosphate and hydroxyapatite.

3. Both salts show similar catalytic properties for the dehydration of tert-butyl alcohol and the vapor phase hydrolysis of chlorobenzene.

4. The acidity of the phosphate catalyst has been measured by the indicator method, and its change with ignition temperature has been investigated.

5. It has been found that the acidity and catalytic activity of a phosphate catalyst vary in a similar way with ignition temperature.

6. The results obtained provided an experimental confirmation for the acid nature of the activity of a phosphate catalyst, the acidity being due to the presence of chemically bound water.

The authors wish to thank V. V. Illarionov, their collaborator in the Samoilov NIUIF, for assistance in this work.

LITERATURE CITED

1. L. Kh. Freidlin, A. A. Balandin, and G. A. Fridman, Izvest. Akad. Nauk SSSR, Otdel. Khim. Nauk 1329 (1957)*; 145 (1958).*
2. Yoshimichi Chiba, J. Soc. Organ. Chem. Japan 13 (1955).
3. A. I. Naumov and Z. G. Lapteva, Zhur. Obshch. Khim. 6, 1647 (1956).*
4. L. Kh. Freidlin and V. Z. Sharf, Doklady Akad. Nauk SSSR 124, 849 (1959).*
5. L. Kh. Freidlin and V. Z. Sharf, Izvest. Akad. Nauk SSSR, Otdel. Khim. Nauk 1264 (1958)*; 512 (1957).*
6. Yu. A. Gorin, Khim. Promyshlennost' 3, 194 (1959).
7. L. Kh. Freidlin and V. Z. Sharf, Izvest. Akad. Nauk SSSR, Otdel. Khim. Nauk 182 (1960).*
8. Allardyce, Trans. Roy. Soc. Canada 21, 315 (1927); G. M. Schwab and E. Schwab-Agallidis, J. Am. Chem. Soc. 71, 1806 (1949); L. Kh. Freidlin, and A. M. Levit, Izvest. Akad. Nauk SSSR, Otdel. Khim. Nauk 163, 177 (1952).*
9. L. Kh. Freidlin and A. M. Levit, Izvest. Akad. Nauk SSSR, Otdel. Khim. Nauk 623 (1951).
10. A. G. Hill, J. H. Shipp, and A. J. Hill, Ind. Eng. Chem. 43, 1951 (1957).
11. R. Paul, Bull. Soc. Chim. France 5, 838 (1956); Collected Chemistry and Chemical Technology [Russian translation] (IL, Moscow, 1957).

*Original Russian pagination. See C. B. translation.

12. E. C. Britton, A. L. Dietzler, and C. R. Noddings, Ind. Eng. Chem. 43, 2871 (1951); Park M. Reilly, Chem. in Canada 5, 3, 25 (1953); Referat. Zhur. Khim. 11, 38.845 (1957).
13. US Patent 2 693 496; Chem. Abs. 49, 2723 h (1955).
14. B. N. Tiutinnikov and B. Fraev, Maslob. Zhir. Promyshlennost' 18, 10, 12 (1953).
15. H. W. E. Larson, Ind. Eng. Chem., Anal. Ed. 7, 401 (1935).
16. Cl. Fabry, J. Physiol. 46, 1, 361 (1954); Biochim. et Biophys. Acta, 14, 401 (1954).
17. M. I. Dallemaghe, H. Brasseaur, and J. Milon, Bull. Soc. Chim. France (1949), Mises au point D 138-45.
18. H. Brasseur, Bull. Soc. chim. Belg. 62, 383 (1953).
19. A. V. Kazakov, Proceedings of the Second Conference on Experimental Mineralogy and Petrography [in Russian] (Izd. AN USSR, Moscow-Leningrad, 1937) p. 129.
20. I. G. Lakomkin, Trudy Leningrad. Tekhnol. Inst. im Lensoveta 48, 143 (1958).
21. I. W. Millar, J. Am. Pharmacy Assoc. Pract. 30, 139 (1941).
22. N. N. Postnikov, Khim. Promyshlennost' 12, 373 (1951).
23. P. W. Arnold, Trans. Faraday Soc. 46, 1061 (1950).
24. H. Basset, Z. anorgan. Chem. 53, 34, 49 (1907).
25. A. P. Belopol'skii, A. A. Taperova, M. T. Serbrennikova, and M. N. Shul'gina, Khim. Promyshlennost' 14, 504 (1937).
26. S. N. Rozanov and S. S. Dragunov, The Chemical Analysis of Fertilizers [in Russian] (Khimtekhizdat, Moscow-Leningrad, 1933) p. 73, 127.
27. US Patent 2 770 656; Referat. Zhur. Khim. 16, 54 865 P (1958).
28. W. Rathje, Bodenkunde und Pflanzenernahr. 12, 121 (1939); E. P. Egan, Jr., Z. T. Wakefield, K. L. Elmore, J. Am. Chem. Soc. 72, 2419 (1950).
29. E. P. Egan, Jr., Z. T. Wakefield, and K. L. Elmore, J. Am. Chem. Soc. 73, 5579 (1951).
30. K. Bauer, Analysis of Organic Compounds [Russian translation] (IL, Moscow, 1953) p. 19.
31. O. Johnson, J. Phys. Chem. 59, 827 (1955).
32. A. Boulle, Compt. rend. Acad. Sci. 226, 1617 (1948).
33. V. I. Semishin, Zhur. Obshch. Khim. 10, 319, 382, 395 (1940).
34. L. Kh. Freidlinand V. Z. Sharf, Izvest. Akad. Nauk SSSR, Otdel. Khim. Nauk 2042 (1959).*
35. A. I. Naumov and E. I. Geidel'berg, Zhur. Obshch. Khim. 27, 2036 (1957).*

*Original Russian pagination. See C. B. translation.

APPLICATION OF THE METHOD OF ELECTRON PARAMAGNETIC RESONANCE TO THE STUDY OF THE CRYSTALLINE PROPERTIES OF CHROME CATALYST

V. B. Kazanskii, Yu. I. Pecherskaya, and V. V. Voevodskii

Institute of Chemical Physics, Academy of Sciences of the USSR
Translated from Kinetika i Kataliz, Vol. 1, No. 2, pp. 257-259,
July-August, 1960
Original article submitted December 26, 1959

A series of aluminochrome catalysts with different weight contents of chromic oxide were studied by the method of electron paramagnetic resonance. Conclusions of the geometrical dimensions and form of microcrystallites of the chromic oxide layer were reached on the basis of changes in the width and form of the resonance line in diluted samples.

Recently the method of electron paramagnetic resonance (EPR) has come to be widely used in the most diverse fields of physics, chemistry, and biology. Results obtained in a study by this method, of reduced chromic oxide on aluminum oxide, an industrial dehydration catalyst, are given below.

Eischens and Selwood [1-4] studied the crystalline properties of the system. They investigated the paramagnetic susceptibility and its temperature variation in the case of samples with different chromic acid contents and found that as the chromic oxide content decreases the paramagnetic susceptibility per gram of the substance increases, whereas the Curie point markedly falls, tending to zero on infinite dilution. In order to explain the results obtained, these authors assumed that when the chromic oxide content in the sample is less than 3-4% the Cr_2O_3 microcrystals consist of three to four atomic layers. In this case a considerable part of the Cr^{3+} ions are located in the surface layer of the microcrystallites, which also leads to lowering the Curie point.

No. of sample	Chromium content, %	Line width between points of maximum slope, oe	Asymmetry of line $l = m/n$
1	11.4	440	1.03
2	9.2	450	1.02
3	3.8	490	1.1
4	3.2	550	1.3
5	2.8	700	1.5
6	0.5	1050	2

Antiferromagnetic substances give an EPR signal only above the Curie point. Chromic oxide is an antiferromagnetic with a Curie point of +36° [5]; however, owing to the fact that its Curie point markedly falls when it is supported on an aluminum oxide surface, observation of resonance is possible even at room temperature in this case.

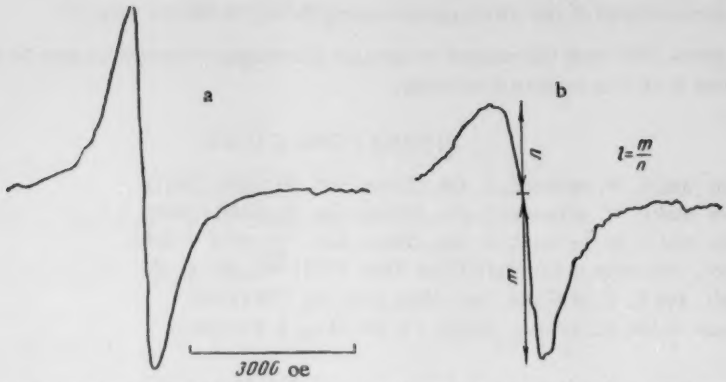

Fig. 1. a) Spectrum of Sample No. 2. Chromium content 9.2%; b) spectrum of Sample No. 5. Chromium content 2.8%.

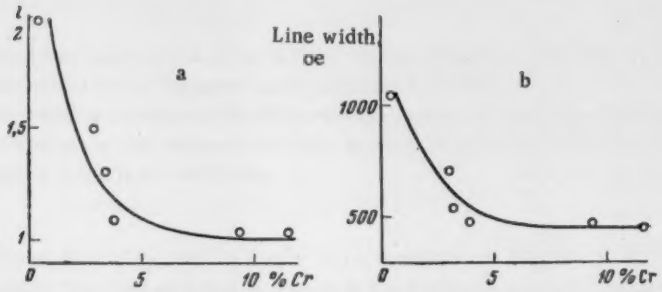

Fig. 2. a) Relation between the asymmetry of the line and the chromium content in the samples; b) relation between the line width and the chromium content in the samples.

Samples of the catalyst were prepared in the following manner: γ-aluminum oxide with a specific surface of about 180 m^2/g was impregnated with a chromic acid solution of variable concentration. Then the samples were dried in air at 350° and reduced with hydrogen at the same temperature. The chromium content in the samples was determined chemically. The EPR spectra were taken with an ÉPR-2 IKhF spectrometer [6]. On recording the spectrum the derivative of the absorption line with respect to the magnetic field was registered. Measurements were made at room temperature.

Data obtained for samples with varying chromium content are given in Figs. 1 and 2 and the table.

In samples with a high chromic oxide content a symmetrical line about 450 oe in width, having a g-factor of 1.95, was observed (Fig. 1a). A decrease in the chromic oxide content led to a change in the form of the line: it broadened and became asymmetric (Fig. 1b). This effect was especially pronounced with a chromic oxide content less than 5% (Fig. 2). Since the increase in width and the development of asymmetry of the line are observed in the same samples, naturally it must be assumed that line broadening is due to asymmetry of the g-factor.

If it is assumed, following Selwood, that in dilute samples of the catalyst the chromic oxide microcrystals have the form of lamellae a few atoms thick, attached to the base through a substratum, the results obtained by us becomes quite understandable. Actually, in this case the properties of the crystallites in the directions normal and parallel to the carrier surface must be different, which must lead to anisotropy of the g-factor and the change in line form, due to the latter. It is interesting that anisotropy of the g-factor was observed by us with the same chromic oxide content in the catalyst, as was the growth of paramagnetic susceptibility and the sharp fall of the Curie point in Selwood's experiments. Data obtained by the method of electron paramagnetic resonance confirm con-

clusions based on measurement of the paramagnetic susceptibility of chrome catalysts.

The results given, show that the method of electron paramagnetic resonance may be used to study the crystalline properties of certain supported catalysts.

LITERATURE CITED

1. R. P. Eischens and P. W. Selwood, J. Am. Chem. Soc. 69, 1950 (1947).
2. R. P. Eischens and P. W. Selwood, J. Am. Chem. Soc. 69, 2698 (1947).
3. R. P. Eischens and P. W. Selwood, J. Am. Chem. Soc. 70, 2271 (1948).
4. P. W. Selwood, Advances in Catalysis (New York, 1951) Vol. III, p. 28.
5. L. R. Maxwell and T. R. McGuire, Rev. Mod. phys. 25, 279 (1953).
6. A. G. Semenov and N. N. Bubnov, Pribor. i Tekh. Éksp. 1, 92 (1959).

A STUDY OF THE ACTIVITY OF NICKEL CATALYSTS

I. THE PROPERTIES OF ALLOY CATALYSTS

G. D. Lyubarskii, L. I. Ivanovskaya, and G. G. Isaeva

L. Ya. Karpov Physico-Chemical Institute
Translated from Kinetika i Kataliz, Vol. 1, No. 2, pp. 260-266,
July-August, 1960
Original article submitted December 28, 1959

The material which has been published on skeletal nickel catalysts is not definitive and does not permit comparison of activities obtained under different conditions.

The present paper is a study of the effect of such factors as alloy composition and technique of treatment and storage on the catalytic activity in the hydrogenation of benzene in a circulatory system under strictly isothermal conditions.

Various theories have been developed in recent years to relate the electronic structures and degree of catalytic activity of metals [1]. The alloying of metals is a convenient method of regulating the electronic structure. Thus a study of the catalytic activity of alloys of various compositions should bring out the relationship between these factors and aid in the discovery of rational procedures for selecting and preparing catalysts.

The Raney method of alloying nickel or some other metal with aluminum, which is subsequently dissolved out by treatment with an alkali to form the so-called skeletal nickel is one of the most convenient means for preparing active catalysts with highly developed surface areas. Such catalysts are known to have great scientific and industrial importance [2].

It is unfortunately true that the data on these catalysts have been obtained under non-uniform and frequently uncomparable conditions, and that the interpretations of this data have not always been consistent. There is, in addition, an almost complete absence of information on the effect of incorporating additives in nickel alloys. At the same time, the electronic structure of nickel can be altered markedly by addition of other metals to form solid solutions, and this should be reflected in the level of its catalytic activity.

A comparative study of the activity of alloy catalysts containing metallic additives is rendered quite complicated by the fact that the activity of the skeletal nickel is dependent on a number of factors such as the nickel-aluminum ratio in the original alloy, the conditions under which this alloy has been leached and stored, the test conditions, and the grain size and surface area. Unfortunately, these factors have not always been given sufficient attention in setting up experiments. Thus, a study of the effects of various additives on nickel alloys requires that an understanding of the effect of these secondary factors first be obtained, and the technique of preparation and testing of samples then be so standardized as to eliminate the possiblity of the distortion of results.

The hydrogenation of benzene to cyclohexane was used as a model reaction in studying catalytic activity. This reaction prossesses desirable features insofar as the equilibrium conditions are such that the reverse reaction is not pronounced at temperatures up to 200-220°, while the forward reaction proceeds without the formation of side products, thus markedly facilitating the determination of degree of reaction. On the other hand, the reaction $C_6H_6 + 3H_2 \rightleftharpoons C_6H_{12}$ is highly exothermic, with a heat of reaction of some 50 kcal/mole, and this makes

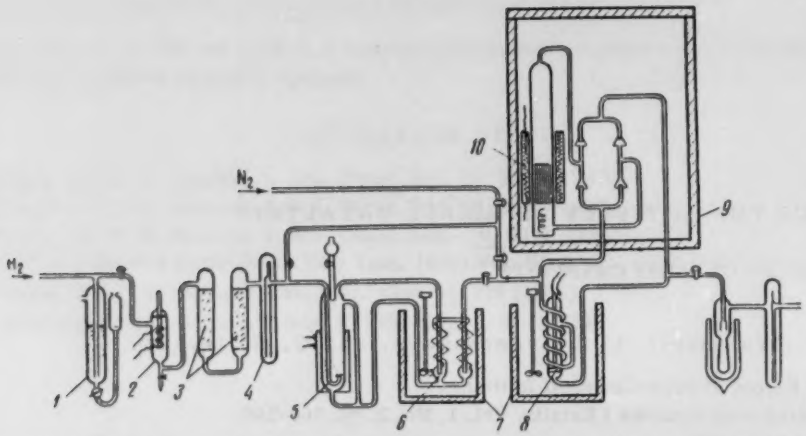

Fig. 1. Schematic representation of the circulation system: 1) Manostat; 2) nickel preliminary catalytic purifier; 3) drier; 4) flow meter; 5) vaporizer; 6) saturator; 7) thermostat; 8) reactor; 9) air thermostat; 10) circulating pump.

for difficulty in assuring isothermal reaction conditions. We have surmounted this difficulty by using a circulation method [3], which assured constancy of temperature, and at the same time made it possible to measure the reaction rate directly.

1. Technique of Determining Catalyst Activity

The apparatus is represented schematically in Fig. 1. Electrolytic hydrogen which had been further freed of oxygen over a Ni/Cr_2O_3 catalyst at 70-100° and dried was passed at a constant rate (as measured on a flow meter) through a glass filter into a benzene vaporizer whose temperature was maintained 7-10° higher than the saturation temperature. The hydrogen and benzene vapors then entered into a double saturator set in a precision thermostat and the excess of benzene condensed out. From here, a mixture of benzene vapors and hydrogen, of fixed composition, passed along a heater wound tube into a circulating system consisting of a reactor in a water bath and a glass circulating pump in an air bath, the temperature of the latter being held 10-15° higher than the temperature of saturation in order to avoid benzene condensation during circulation. The reacted gaseous mixture of stationary composition was continuously removed from the cycle at the same rate as material was introduced. The benzene and product cyclohexane were condensed in a trap and the condensate subjected to periodic refractometric analysis, the accuracy of determination being 0.1%. Each mixture contained an excess of hydrogen, the molar ratio hydrogen: benzene being 7 : 1 with a rate of hydrogen feed of approximately 7 liter/hour in most experiments. The usual charge of catalyst was 1 cm^3 (dry weight $\underline{d}$, 2 g/cm^3), while the rate of circulation was in excess of 500 liter/hour. The catalyst, in the form of chunks 0.25-0.5 mm in diameter, was washed with benzene in the reactor under a current of hydrogen after the system had been first carefully flushed out by circulating hydrogen through it. The layer of benzene under which the catalyst was loaded was blown away by room-temperature hydrogen, which was introduced through a side line bypassing the benzene vaporizer, and the reaction mixture then led into the reactor. A stationary state was generally reached after circulating the mixture for 1-2 hours.

The activity of each specimen of catalyst was determined from the degree of hydration of benzene per 1 g of catalyst under standard conditions. The specific activity is the activity per 1 m^2 of catalyst surface. The BET method of low temperature nitrogen adsorption was employed in surface areas.

Special experiments on the kinetics of this reaction had shown it to be of zero order with respect to benzene and of 0.5 order with respect to hydrogen.

The experiments were carried out with a considerable excess of hydrogen, and the alteration in the hydrogen concentration during reaction could therefore be neglected. On this basis the rate constant, $\underline{k}$, was calculated

TABLE 1

Effect of Dimensions of Catalyst Grains

Grain diameter, mm	Relative amount of gas in leaching	Specific surface area, S, m^2/g	Degree of conversion per 1 g catalyst, α, %, at			Specific activity at 38°		Energy of activation, E, kcal/mole
			38°	32°	27°	per 1 g, $k \cdot 10^2$, mole/g · hr	per 1 m^2, $k' \cdot 10^4$, $mole/m^2 \cdot hr$	
0.15-0.25	1.0	91.3	33.3	23.	15	1.47	1.61	13.5
0.25-0.50	1.0	85.9	31.5	21.7	15.1	1.40	1.65	12.4
0.50-1.0	0.96	83.5	32.8	22	16.5	1.45	1.73	11.6
1-2	0.78	79.1	29	20	14.5	1.29	1.63	11.8
2-3	0.62	72.7	23.8	17.3	12.3	1.07	1.43	11.4

TABLE 2

The Effect of the Conditions of Alloy Leaching

Alloy	Leaching temp.,°C	Leaching duration, min	Rel. amount of gas from leaching	S, m^2/g	α, %, at 38°	$k \cdot 10^2$, mole/g · hr
			Effect of Temperature			
Ni + Al + 1,5% Cr	100	15	0,93	84	37	1,65
	50	90	0,77	95	44	1,92
	19	240	0,72		35	1,58
Ni + Al (1 : 1)	100	15	0,91	81	27	1,20
	50	15	0,90	95	45	2,0
			Effect of Time			
Ni + Al + 5% Cr	100	15	0,81	86	26	1,14
	100	105	1,0		23	1,02
Ni + Al (1 : 1)	100	15	0,91		27	1,20
	100	60	0,95		20	0,90
			Effect of Nature of Alkali			
Ni + Al: a) KOH	100	15	0,91	80	27	1,20
b) NaOH	100	15	0,98	89	36	1,60

TABLE 3

The Dependence of Catalytic Activity on the Composition of the Original Alloy at 38°

Specimen No.	Alloy comp., %		S, m^2/g	Deg. of reaction, % per 1 g catalyst	$k \cdot 10^2$, mole/g · hr	$k' \cdot 10^2$, $mole/m^2 \cdot hr$	E*, kcal/mole
	Al	Ni					
1	70	30	97	13	0,58	0,60	12,4
2	58	42	93	20	0,91	0,97	12,9
3	50	50	80	27	1,27	1,50	11,5
4	50	50	91	26	1,16	1,27	12,4
5	48	52	90	31	1,4	1,55	12,4
6	44	56	80	32	1,42	1,75	12,5

* The energy of activation was usually determined from data at the three temperatures 27, 32, and 38°.

TABLE 4

The Aging of Catalysts in Various Media

Cr added to Ni (at. %)	Storage medium	Duration of storage, days	α at 39°	
			prior to storage	after storage
11	Alcohol	7	28	28
11	The same	13	28	30
7.2*	The same	21	28	26.5
4.5	The same	44	31	28.3
None	Water	4	32.5	27.0
11	The same	4	26.2	23.7
11	The same	32	26.2	22.5
4	Benzene	16.0	31.7	5.7
4	The same	43.0	31.7	2.5
4	The same	8	31.7	7.7 (50°)
4	The same	8	31.7	21.3 (70°)
4	The same	8	31.7	37.5 (85°)
4.5	Acetone	2	31	2.8
4.5	The same	7	31	1.8
None	The same	15	25	1.5 (50°)
3	10% acetone in alcohol	4	32	4.0
4	Ethyl cinnamate (4% solution in alcohol)	1	32	16.5
4	Ditto, 10% solution	4	32	1.0

* Added titanium.

TABLE 5

Aging and Surface Area

Storage medium	Duration of storage, days	S, m^2/g		Activity after storage (% of original value)
		prior to storage	after storage	
Benzene	8	86	71	12.0
	16	86	66	18.0
Acetone	2	86	92	9.0
	7	86	81	5.8
	15	81	81	4.0
10% solution of acetone in alcohol	4	84	89	12.5

from the equation $W = \alpha v = k$, α being the degree of conversion of the benzene and v the rate of feed of benzene in mole/hour per 1 g catalyst.

The specific rate constant k' is equal to k/S, where S is the specific surface area of the catalyst in m^2/g.

The effect of diffusional factors on the rate of hydrogenation of benzene was cleared up in a series of experiments using catalyst grains of various dimensions. Results from these experiments are presented in Table 1.

The data of this table make it apparent that the effect of the grain dimensions is felt only at diameters in excess of 1.5-2 mm, and our measurements were therefore carried out on chunks of 0.25-0.5 mm diameter.

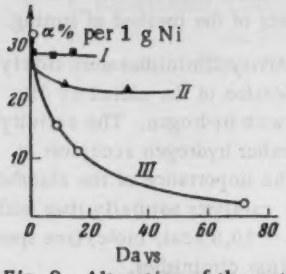

Fig. 2. Alteration of the activity of specimens during storage in various media: I) Ethyl alcohol; II) water; III) benzene.

2. The Effect of Composition and Method of Treatment of Alloys on Catalytic Activity

The alloys used in preparing the catalysts were obtained from pure (99.99%) metals. Alloying was carried out in graphite crucibles in a high-frequency electric furnace,* the alloys cast into molds, and the resulting slabs broken up and sieved. The 0.25-0.5 mm fraction was leached under fixed conditions by being treated with a 20% potassium hydroxide solution for 15 minutes at 100°, and the volume of evolved hydrogen measured to obtain a rough evaluation of the extent of extraction of aluminum from the alloy. The resulting catalyst was washed twice with cold alkali to remove the product aluminate and the alkali then removed by washing with distilled water, using phenophthalein as a control. This water was finally eliminated by a threefold washing in distilled alcohol and the catalyst stored under alcohol (usually for no more than two days) until the time of testing its activity.

The effect of the conditions of treatment of the alloy was brought out in a series of experiments involving variation of the temperature and time of leaching, the nature of the alkali, etc., the results of which are shown in Table 2.

The data of this table clearly support the results reported in the literature [2, 4] in showing a considerable increase in the activity to come from diminishing the time and temperature of leaching and employing sodium hydroxide in place of potassium hydroxide. An increase in the activity was also favored by washing with water which had been previously saturated with hydrogen.

The composition of the original alloy is of great importance (Table 3). An increase in the aluminum content of this alloy leads to an increase in the amount of aluminum extracted but diminishes considerably the actvity, mechanical strength, and thermal stability of the resulting catalyst. The specific activity per 1 m^2 of surface area also decreases.

The surface areas are in agreement with the results obtained by Watt [5] through nitrogen adsorption and are greater than those obtained by other authors and other methods [6].

In the thirties, A. Bag [7] proposed that skeletal nickel catalysts be obtained by the leaching of alloys containing 70% aluminum by weight.

In practice, such catalysts show low activity and poor stability in hydrogenation reactions. Our experiments proved that heating this catalyst in hydrogen for one hour at 200° reduced the degree of reaction of benzene at 38° from 9.6 to 3.2% and diminished the surface area from 97 to 63 m^2/g.

Catalysts obtained from alloys containing 50% aluminum were much more stable, and their activity was almost completely unaffected by heating in hydrogen to temperatures of 250-300°.

An analogous relation between catalytic activity and composition is observed in the case of nickel–magnesium alloys [8], the catalyst obtained by treating an alloy containing 50% magnesium with acetic acid being twice as active in the hydrogenation of styrene as one based on an alloy containing 70% magnesium.

Nickel–silicon alloys from which the silicon is leached can be used for obtaining skeletal nickel, just as can alloys of nickel and aluminum. Our data show that catalysts prepared in this manner have almost the same activity as those prepared from the nickel–aluminum and have high stability, also.

The leached catalyst specimens are very pyrophoric, so that they frequently heat to redness in air and lose their activity. The characteristic is clearly related to the surface oxidation of the highly dispersed metal and the adsorbed hydrogen, and is retained even after the alloys have been degassed at 150-200° for an extended period of time; it can be enhanced by incorporating such additives as vanadium and iron into the alloy. Because of their marked pyrophoric character, skeletal catalysts are usually stored under water, alcohol or some other liquid.

* The alloys were prepared by N. M. Kagan in the D. I. Lainer Laboratory of the Giprotsvetmetobrabotok Institute.

Specimens, especially those which have been freshly prepared, gradually age even when stored in this manner. Thus the establishment of standard indices necessitates an understanding of the effect of the method of storing.

The highest stability is observed for storage under alcohol (Table 4). The activity diminishes very slowly under water, possibly from surface interaction of the nickel and water, or from oxidation of the nickel by dissolved oxygen; the retention of activity is better in water which has been saturated with hydrogen. The activity of skeletal nickel falls rather rapidly to practically zero in benzene, acetone, and other hydrogen acceptors at room temperatures, a fact which is in line with the ideas of L. Kh. Freidlin [9] on the importance of the absorbed hydrogen for the Ni skeleton. The degree of reaction of benzene on the poisoned catalysts naturally rises with an increase in the temperature, but without alteration in the energy of activation ($E \sim 10.5$ kcal/mole) (see specimens stored in benzene, Table 4). Only the frequency factor in the Arrhenius equation diminishes.

The surface area and the loss of catalytic activity change but little during storage (Table 5), a fact which is in agreement with the data of Smith [10] on the parallel alteration in these factors. The value of the surface area is also only slightly altered by removal of the adsorbed hydrogen as the result of degassing the catalyst at 10^{-4} mm and 150°.

Figure 2 shows the change in activity of catalysts stored in various media. A diminution in the activity of skeletal nickel catalysts has been noted by a number of authors [7] and especial note has been made [9] of the great significance of atmospheric oxygen, which gradually reacts either with the nickel itself or with the adsorbed hydrogen. The activity remains constant in nitrogen or hydrogen.

The data presented above show the importance of correctly choosing and maintaining fixed conditions of treatment and testing in comparative studies of alloy catalysts.

The results obtained here have been employed in a study of the effect of addition of transition metals on the catalytic activity of nickel, a subject which will be treated in a later communication.

SUMMARY

1. A standard method of determining the activity of skeletal nickel catalysts in a circulating system has been developed and used for obtaining comparative data on the vapor phase hydrogenation of benzene in the neighborhood of room temperature.

2. The method of treating nickel–aluminum alloys with alkali has been shown to affect the activity of the resulting catalysts, the activity being increased by reducing the time and temperature of leaching and by using sodium hydroxide and water saturated with hydrogen.

3. The composition of the original alloy has a marked influence on the catalytic activity. The opimal activity is shown by specimens obtained through leaching an alloy containing ~45% aluminum.

4. The activity of the prepared catalyst is strongly affected by the method of storing and falls precipitately during storage in media which are hydrogen acceptors.

Neither the surface area nor the energy of activation for hydrogenation (~11 ± 1 kcal/mole) are appreciably altered by storage.

LITERATURE CITED

1. D. A. Dowden, J. Chem. Soc. Lond. 242 (1950); Ind. Eng. Chem. 44, 977 (1952); S. Z. Roginskii, Collection, Problems of Kinetics and Catalysis [in Russian] (Izd. AN SSSR, Moscow, 1955), Vol. 8; G. K. Boreskov, Collection, Problems of Physical Chemistry [in Russian] (Goskhimizdat, Moscow, 1958) Vol. 1, p. 101.
2. Collection, Catalysts for Organic Reactions [Russian translation] (IL, Moscow, 1955) p. 108; R. Shreter, Collection, New Methods of Organic Preparations [Russian translation] (IL, Moscow, 1950) p. 202.
3. M. I. Temkin, S. L. Kiperman, and L. I. Luk'yanova, Doklady Akad. Nauk SSSR 74, 763 (1950).
4. H. Adkins and Billica, J. Am. Chem. Soc. 70, 412, 695 (1948).
5. G. Watt and W. Roper, J. Am. Chem. Soc. 74, 1103 (1952).
6. H. A. Smith and Fuzek, J. Am. Chem. Soc. 68, 229 (1946); A. Eucken, Z. Elektrochem. 54, 108 (1951).
7. A. Bag, Soviet Patent 38127 (1933).
8. N. Pattison and E. Degering, J. Am. Chem. Soc. 72, 5756; 73, 486 (1951).

9. L. Kh. Freidlin, Collection, Problems of Chemical Kinetics, Catalysis, and Reactivity [in Russian] (Izd. AN SSSR, Moscow, 1955) p. 557.
10. H. Smith, J. Phys. Chem. 59, 820 (1955).

VAPOR-PHASE CATALYTIC OXIDATION OF BUYLENES TO MALEIC ANHYDRIDE*

B. L. Moldavskii and Yu. D. Kernos

All-Union Scientific Research Institute of Petrochemical Processes
Translated from Kinetika i Kataliz, Vol. 1, No. 2, pp. 267-273,
July-August, 1960
Original article submitted January 23, 1960

The vapor-phase oxidation of butylenes to maleic anhydride over molybdenum-cobalt, vanadium-phosphorus, molybdenum-vanadium and other catalysts was investigated. With the best catalysts (Mo–Co–P and V–P) the yield of maleic acid reached 85 g using 1 liter of catalyst per hour. Together with maleic acid, carbonyl compounds, volatile fatty acids and carbon dioxide were formed. Oxidation of divinyl gives a higher yield of maleic anhydride than the oxidation of butene-1 or butene-2.

The catalytic vapor-phase oxidation of butylenes to maleic anhydride is of both theoretical and practical interest. Like the oxidation of propylene to acrolein, this reaction makes it possible to oxidize an olefinic hydrocarbon without rupturing the double bond. The maleic anhydride obtained as a result of oxidation is a valuable intermediate for organic synthesis.

Maleic anhydride is produced industrially at present by the oxidation of benzene and is also obtained as a by-product from the oxidation of naphthalene to phthalic anhydride. In the literature there are reports that maleic anhydride can be obtained by the vapor-phase catalytic oxidation of various C_4 hydrocarbons [1], C_5–C_8 olefins [2], and also derivatives of cyclopentane and cyclohexane [3]. In addition, maleic anhydride can be obtained by the vapor-phase oxidation of various oxygenated compounds, such as furan and its derivatives [4, 5], crotonaldehyde [6, 7], and others.

There are few data on the catalytic oxidation of butylenes to maleic anhydride: the article of Bretton, Shen Wu Wan and B. F. Dodge [1], and several patents. The paper by these authors describes experiments on the vapor-phase catalytic oxidation of C_4 hydrocarbons over silver catalysts or vanadium pentoxide on α-alumina. With silver catalysts the oxidation of C_4 hydrocarbons led mainly to the formation of water and CO_2. For vanadium pentoxide in the case of the oxidation of butene-1 and butene-2 the yield of maleic acid relative to the reacted hydrocarbon did not exceed 12-14%. Together with maleic acid, considerable amounts of carbonyl compounds were obtained in the oxidation of butylenes. The authors obtained the maximum yield of maleic acid by the oxidation of divinyl: about 58% relative to the reacted hydrocarbon, and 34% relative to the divinyl converted.

Of the few patents available, mention should be made of the first patents on the oxidation of unsaturated C_4 hydrocarbons by Walters [8], Slotterbeck and Tribit [9], who used vanadium or molybdenum oxides for these purposes. In Beach's patent [10] it is indicated that in the case of the oxidation of cis-butene-2 over vanadium or molybdenum-vanadium oxide catalysts the yield of maleic anhydride is 40% higher than that for the oxidation of trans-butene-2. Reid and Sidobotham's patent [11], which recommends a V–P catalyst on α-alumina (25 : 75), gives interesting data showing the advantages of V–P over Mo–V catalysts. Hartig's patents [12] de-

*Report submitted to the Conference on Organic Catalysis, November 19, 1959.

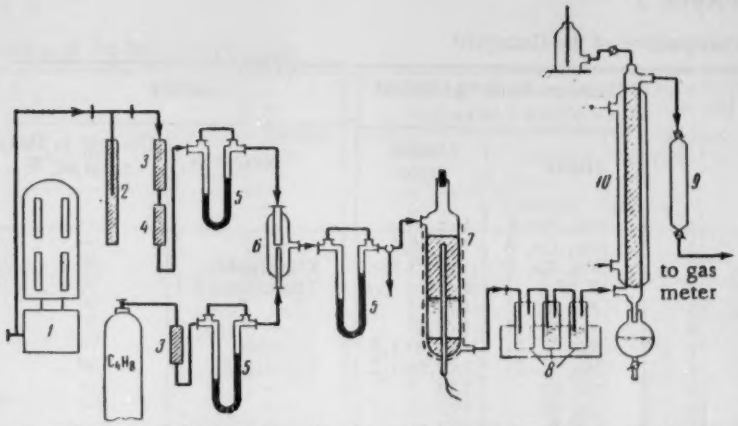

Fig. 1. Diagram of the apparatus for the oxidation of butylenes: 1) compressor; 2) pressure regulator; 3) ascarite; 4) drier; 5) flow meter; 6) mixer; 7) reactor; 8) absorbers; 9) gas buret; 9) scrubber.

scribe the preparation of Mo–Co catalysts, both in the pure form and with additions of H_3BO_3, H_3PO_4, and V_2O_5. The author recommends these catalysts mainly for the oxidation of n-butane to maleic anhydride.

The aim of the present investigation was the preliminary testing and the selection of catalysts with selective activity for the oxidation of butylenes to maleic anhydride. A number of catalysts recommended in the patent literature were tested, both in the pure form and diluted on carriers.

EXPERIMENTAL

The procedure, initial material and catalysts. The experiments for the investigation of the oxidation of butylenes were carried out in the apparatus shown in Fig. 1. The catalyst, with a particle size of 1-2 mm, was placed in the glass reactor 7 (diameter 20 mm), equipped with a pocket for thermocouple and electric heater. The gas mixture contained 1.5% butylenes, the remainder being air. This concentration was governed by the explosive limits of butylene-air mixtures (lower limit 1.8% butylenes, upper limit 8.5%). The butylenes were fed from a cylinder via the flow meter 5 to the mixer 6, to which air was also supplied from the compressor 1. The butylene-air mixture obtained was heated preliminarily in the reactor on a porcelain bed to the required temperature and was then passed over the catalyst. After oxidation the gas was separated from the maleic anhydride and the accompanying oxygenated compounds by washing with water in the absorbers 8 and scrubber 10.

The industrial fraction of butylenes, obtained after the first stage of dehydrogenation of n-butane, was used as raw material. Its composition was as follows: 25% butene-1; 54% butene-2; 3% isobutylene; 8% divinyl and 10% C_2 and C_3 hydrocarbons. For certain other experiments, mixtures enriched with butene-1 and butene-2 were used; these were prepared by dehydrogenation of primary and secondary n-butyl alcohols, respectively. The divinyl used was the technical product, of 90% purity. The compositions of the catalysts tested are given in Table 1.

The Mo–Co catalyst was made by mixing hot solutions of ammonium paramolybdate and $Co(NO_3)_2$. The cobalt molybdate precipitate was filtered, dried at 100°, crushed (the 1-2 mm fraction was selected) and baked at 450° for 3-4 hours. Mo–Co catalysts with additions of B or P were made by adding H_3BO_3 or H_3PO_4 to a solution of ammonium paramolybdate. Mo–Co–P catalyst was prepared on kieselguhr, the latter being added to a solution of ammonium paramolybdate and phosphoric acid before precipitation by cobalt nitrate.

V–P catalyst was obtained by mixing a solution of ammonium metavanadate with phosphoric acid and kieselguhr. The mixture was evaporated to dryness on a water bath.

Mo–V catalyst was prepared by impregnating kieselguhr with the ammonium salts of the appropriate acids. Mo–V–Ti catalyst was obtained in a similar manner but with the addition of metatitanic acid. Two Mo–V–Ti catalysts were made: on kieselguhr and on pumice.

TABLE 1

Composition of the Catalysts*

No. of catalyst	Elements forming catalyst		Carrier	
	Name	Atomic ratio	Name	Content in final catalyst, %
1	Mo, Co	1:1	—	—
2	Mo, Co, B	1:1:1,6	—	—
3	Mo, Co, P	1:1:0,5	Kieselguhr	50
4	V, P	1:1	The same	50
5	Mo, V	1:10	" "	50
6	Mo, V	1:0,3	" "	50
7	Mo, V, Ti	1:0,6:1,2	Pumice	70
8	Mo, V, Ti	1:0,6:1,2	Kieselguhr	50
9	Co, Cr	1:1	—	—
10	Co, W	1:1	—	—
11	Co, P	1:1	—	—

* The composition was calculated from the amounts taken.

TABLE 2

Oxidation of Butylenes Over Different Catalysts (C_4H_8 content in the gas mixture ~1.5%)

Catalyst	Volumetric v, hr^{-1}	Expt. temp. °C	Total conversion, C_4H_8, x, %	Yield of maleic acid		
				In mole %		In g/liter of catalyst per hr
				Relative to reacted C_4H_8	Relative to C_4H_8 fed	
Mo — Co, № 1	2000	400	56	34,0	19,8	28,6
	4000	450	59	33,4	20,0	57,7
Mo — Co — B, № 2	4000	450	84	15,0	12,6	36,5
Mo — Co — P, № 3	2000	400	—	—	16,4	23,7
	2000	450	76	37,2	28,3	41,0
	4000	450	45	35,0	16,6	48,0
	8000	500	47	32,2	15,1	87,0
V — P, № 4	2000	350	63	19,3	12,3	17,6
	2000	450	93	18,6	17,1	24,8
	4000	350	48	15,6	7,5	21,5
	4000	450	86	22,7	19,8	56,8
	8000	450	80	17,0	13,5	78,0
Mo — V, № 5	4000	450	52	8,8	2,5	6,4
Mo — V, № 6	4000	350	27	20,0	5,4	15,8
	4000	450	37	23,9	8,8	25,6
Mo — V — Ti, № 7	4000	400	18	47,7	8,7	25,2
	4000	450	23	52,0	11,8	34,4
	4000	500	31	45,8	13,9	40,3
Mo — V — Ti, № 8	4000	350	88	12,0	10,9	31,5
		450	93	19,6	18,3	53,0
Co — Cr, № 9	4000	450	100	—	—	None
Co — W, № 10	4000	450	100	—	—	None
Co — P, № 11	4000	450	8	—	—	Traces

Cobalt chromate, tungstate and phosphate were obtained by double decomposition reactions. All the catalysts were fired and baked in a way similar to the Mo—Co catalyst. The kieselguhr and pumice used as the carriers were first treated with nitric acid, washed with water, dried and ground. The 70-80 mesh fraction was selected and was then baked at 400°.

Before the beginning of the experiment the entire charge of fresh catalyst in the reactor was treated with

TABLE 3

Composition of the Reaction Products

Expt. No.	Catalyst	v, hr^{-1}	Temp., °C	x,%	Yield of reaction products relative to unreacted butylenes, %			
					$CO + CO_2$	carbonyl compounds (on C_3)	volatile acids (on C_2)	maleic acid
1	Mo — Co — P, № 3	2000	450	76	40,1	16,7	6,0	37,2
2*		2000	450	86	32,6	10,7	1,7	55,0
3		4000	450	45	45,3	12,6	7,1	35,0
4	V — P, № 4	2000	350	63	50,2	13,5	17,0	19,3
5		2000	450	93	67,0	12,5	1,9	18,6
6		4000	450	86	62,5	10,5	4,3	22,7
7	Mo — V — Ti, № 7	2000	450	41	40,5	10,5	3,7	45,3
8		4000	400	18	36,6	9,2	6,5	47,7
9		4000	450	23	35,0	10,1	2,9	52,0
10		4000	500	31	43,1	9,0	2,1	45,8
11	Mo — V — Ti, № 8	4000	350	88	74,9	8,9	4,2	12,0
12		4000	450	93	68,7	11,2	0,5	19,6

* The experiment was carried out in gas containing 90% divinyl, 5.9% butene-2 and 4.1% butene-1.

the reacting gas mixture under the experimental conditions for several hours until constant results were obtained.

Analytical method. The liquid and solid reaction products obtained by the oxidation of butylenes, trapped by the water in the absorbers and the scrubber, were analyzed as follows: The carbonyl compounds were determined by the hydroxylamine method, the total amount of acids was determined by titration of the solid residue obtained after evaporation of the aqueous solution from the absorber.* By special analyses it was found that the solid residue consists almost entirely of maleic acid. The volatile-acid content was calculated as the difference between the total acidity and the maleic acid content. The amounts of the carbonyl compounds and volatile fatty acids were calculated arbitrarily, on the basis of their containing two carbon atoms. The O_2, CO and CO_2 content in the gases was determined with the VTI apparatus. Both in the initial gas and in the reaction products the amount of butylenes was determined by the bromide-bromate method, and the composition of the butylene fraction by the gas-liquid chromatography method.

Experiments on oxidation and discussion of the results obtained. Table 2 gives the results of the testing of various catalysts. All three groups of catalysts, Mo—Co, V—P, and Mo—V, were tested. Under the experimental conditions the most active catalysts of the Mo—Co group were Mo—Co (No. 1). and Mo—Co—P (No. 3). With the latter, at 450° and a volumetric rate of 2000 $hour^{-1}$, the yield of maleic acid on the unreacted butylenes was 37%; calculated on the amount fed it was 28%. As regards the activity of the catalyst at high volumetric rates, V—P(No. 4) catalyst was hardly inferior to Mo—Co—P catalyst. At a volumetric rate of 8000 $hour^{-1}$ the yield of maleic acid was 78-87 g/liter of catalyst per hour. The activity of Mo—V catalyst depends on its Mo: V ratio. No. 6 catalyst, which contained 0.3 atoms of vanadium per atom of molybdenum, was more active than No. 5 catalyst, which contained 10 atoms of vanadium per atom of molybdenum. The addition of Ti increased the activity of Mo—V catalyst. 2 samples of Mo—V—Ti catalyst — on pumice (No. 7) and kieselguhr (No. 8) — were tested. The catalyst on kieselguhr gave higher yields of maleic acid, expressed in g/liter of catalyst per hour or as a % of the butylenes fed, while higher yields on the unreacted butylenes were obtained from the catalyst on pumice, which indicates the greater selectivity of this catalyst. With the Co—Cr and Co—W catalysts the butylenes were burned to CO_2. The Co—P catalyst had, in general, a low activity.

Table 3 gives data on the composition of the oxidation products obtained with several catalysts. According to the results in Table 3, an increase in the volumetric rate and temperature hardly influences the content of

* Subsequently, all the calculations were made with respect to maleic acid.

TABLE 4

Influence of the Composition and Structure of the Initial C_4 Hydrocarbons on the Maleic Acid Yield ($t = 450°$, $y = 2000$ hour^{-1}, C_4 content in the mixture with air ~1.5%)

Catalyst	Composition of the hydrocarbon part of the gas mixture, vol. %				Total conversion of C_4, %	Maleic acid yield		
						in mole %		in g/liter of catalyst per hour
	butene-1	butene-2	divinyl	C_2, C_3, etc., C_4.		relative to the reacted C_4H_8	relative to the C_4H_8 fed	
Mo–Co–P, No.3	25.3	53.5	8.1	14.9	76	37.2	28.3	41.0
	8.7	86.8	–	4.5	65	52.7	34.6	50.0
	4.1	5.9	90.0	–	92	55.0	50.8	73.3
Mo–V–Ti, No.8	78.8	17.8	–	3.4	91	14.5	13.6	19.7
	25.3	53.5	8.1	13.1	88	15.7	13.8	20.0
	42.8	52.0	–	5.2	90	13.9	12.4	18.0
	8.7	86.8	–	4.5	85	14.2	12.1	17.4
	4.1	5.9	90.0	–	92	25.3	23.9	34.7

TABLE 5

Isomerization of Butene-1 over Mo–V–Ti Catalyst ($t = 450°$)

v, hour^{-1}	Composition of the butylenes				
	before the experiment	after the experiment			
	butene-1 / butene-2	butene-1 / butene-2		cis-butene-2 / trans-butene-2	
		found	equilibrium composition	found	equilibrium composition
500	4.5	0.5	0.39	0.9	0.75
2000	4.5	1.0	0.39	1.0	0.75

carbonyl compounds in the reaction products. But the amount of volatile fatty acids is reduced with an increase in the reaction temperature. Similar results were obtained by Faith and Dendurent [2] by the vapor-phase oxidation of amylenes. The maleic acid content in the oxidation reaction products at different temperatures and volumetric rates was approximately constant for each catalyst, which made it possible to judge its selectivity. The most selective catalysts were Mo–Co–P (No. 3) and Mo–V–Ti (No. 7). The amount of CO and CO_2 in the reaction products obtained with these catalysts did not exceed 45%, whereas with other catalysts it reached 75%. It is of interest to note that, as may be seen from Table 3, the reduction of the CO and CO_2 content in the reaction products in the case of No. 3 and No. 7 catalysts is accompanied by an increase in the maleic acid content in the reaction products, but the amount of carbonyl compounds and volatile fatty acids remains unchanged. The composition of the carbonyl compounds in the reaction products of experiment No. 7 (Table 3) was determined. It was as follows: ketones (mainly methyl vinyl ketone) 23%, formaldehyde 63%, and acetaldehyde 14%.

To determine the influence of the structure of the initial C_4 olefin on the maleic acid yield, experiments were carried out on the oxidation of gaseous mixtures enriched with butene-1, butene-2 and divinyl. The results are given in Table 4. The experiments were carried out with two catalysts: No. 3 and No. 8 at 450° and a volumetric rate of 2000 hour^{-1}. It was found that as a result of the oxidation of divinyl a higher yield of maleic acid is obtained than by the oxidation of butylenes, which confirms the data of Bretton and others [1]. But variations in the composition of butylenes have little influence on the maleic acid yield.

The fact that butene-1 is oxidized to maleic acid at the same rate as butene-2 compelled us to assume that butene-1 is isomerized to butene-2 during the process of the reaction.

To check the correctness of this assumption, gas containing 80% butene-1 and 17% butene-2 was passed over Mo–V–Ti catalyst (No. 8) at 450° and two volumetric rates. The results of these experiments are given in Table 5.

The data obtained confirmed the possibility of the isomerization of butene-1 to butene-2 under the conditions of the previous experiments. At low volumetric rates the composition of butylenes approaches equilibrium. The fact that during the process of isomerization more cis-butene-2 is formed than is required for the equilibrium composition at the given temperature is also of interest [13]. As may be seen from the data of Table 5, with a reduction in the volumetric rate, i.e., with an increase in the contact time, the cis-butene-2/trans-butene-2 ratio decreases, approaching the equilibrium value. We noted a similar phenomenon when butene-1 was obtained by dehydrogenation of n-butanol at 350° over the γ-oxide of aluminum. In the mixture of butene-1 and butene-2 formed (as a result of isomerization) the cis-butene-2/trans-butene-2 ratio reached 1.8-2.0, whereas the equilibrium ratio at 350° must be about 0.7 [13]. This indicates that the isomerization of butene-1 to butene-2 evidently takes place via the cis form. Similar facts are given in the recent work of Lucchesi, Baeder and Langwell [14]. During the isomerization of butene-1 to butene-2 over aluminosilicate catalyst at 80° at brief contact times the authors observed the preferential formation of cis-butene-2, the amount of which decreased with an increase in the contact time as a result of the formation of the trans isomer.

A. Sh. Khabibulina, G. M. Borovaya and I. L. Belostotskaya took part in the work.

SUMMARY

1. A number of catalysts for the oxidation of butylenes to maleic anhydride were tested.

2. For all the catalysts, together with maleic anhydride the formation of considerable amounts of CO and CO_2, carbonyl compounds and volatile fatty acids was observed. With the best catalysts, the maleic anhydride content in the reaction products was 35-50 mole%.

3. The comparative oxidation of mixtures enriched with butene-1, butene-2 and divinyl was carried out. The highest yields were obtained by the oxidation of divinyl.

4. During the isomerization of butene-1 to butene-2 the cis-butene-2/trans-butene-2 ratio in the reaction products is more than the equilibrium ratio. This indicates that isomerization takes place via the cis form, and under the experimental conditions equilibrium is not attained.

LITERATURE CITED

1. R. H. Bretton, Shen Wu Wan, and B. F. Dodge, Ind. Eng. Chem. 44, 594 (1952).
2. W. L. Faith and M. S. Dendurent, Ref. 18, 393 (1939).
3. N. A. Milas and W. L. Walsh, J. Am. Chem. Soc. 61, 633 (1939).
4. N. A. Milas and W. L. Walsh, J. Am. Chem. Soc. 57, 1389 (1935).
5. E. R. Nielsen, Ind. Eng. Chem. 41, 365 (1949).
6. W. L. Faith and A. M. Schaible, J. Am. Chem. Soc. 60, 52 (1938).
7. S. K. Bhattacharyya and N. Venkataraman, J. Appl. Chem. 8, 737 (1958).
8. C. H. Walters, Amer. Patent 2097904 (1937).
9. O. C. Slotterbeck and S. W. Tribit, Amer. Patent 2260409 (1941).
10. L. K. Beach, Amer. Patent 2537568 (1949).
11. J. C. Reid and N. C. Sidebotham, Amer. Patent 2773838 (1951).
12. M. J. Hartig and G. Ridge, Amer. Patent 2625519 and 2691660 (1950).
13. H. H. Voge and N. C. May, J. Am. Chem. Soc. 68, 550 (1946).
14. P. Lucchesi, D. Baeder, and J. Langwell, J. Am. Chem. Soc. 81, 3235 (1959).

REACTIONS OF IRON CARBIDES UNDER THE CONDITIONS OF THE FISCHER-TROPSCH SYNTHESIS*

Yu. B. Kryukov, A. N. Bashkirov, L. G. Liberov, V. K. Butyugin, N. D. Stepanova, and Yu. B. Kagan

Institute of Petrochemical Synthesis, Academy of Sciences of the USSR
Translated from Kinetika i Kataliz, Vol. 1, No. 2, pp. 274-281,
July-August, 1960
Original article submitted January 23, 1960

By using radioactive carbon monoxide $C^{14}O$ we investigated the role of carbides in the high-yield synthesis of hydrocarbons on ferrous catalysts under high pressure. We have determined the principal reactions of carbides on catalytic surfaces and established that iron carbides do not act as intermediates in the formation of hydrocarbons.

On of the main mechanisms proposed for the conversion of carbon monoxide and hydrogen to hydrocarbons is based on the assumption that carbides actively participate in this reaction. The usual catalysts used for this synthesis (cobalt, nickel, and iron) can all react with carbon monoxide to yield the corresponding carbides. And therefore, this fact lead us to examine the latter ones as possible intermediates in the synthesis of hydrocarbons [1-3].

A great amount of research has been devoted to the verification of the carbide-methylene hypothesis and to the elucidation of the part played by carbides in the reaction [4-15]. The kinetic, physical, and other data seem to indicate that on nickel and cobalt catalysts, at least, the reaction proceeds without the formation of carbide intermediates.

However, some recent isotope exchange data [16] indicate that carbides might participate extensively in the formation of hydrocarbons from CO and H_2 on cobalt catalyts. As far as the participation of carbides in the same synthesis but over ferrous catalysts is concerned, the data are also conflicting. Thermodynamic calculations indicate that a direct reduction of Fe_2C or Fe_3C by hydrogen could not yield n-mono-olefins-1 and higher paraffins under the conditions of temperature and pressure normally used in this synthesis [9]. Yet certain workers have proposed, on the basis of kinetic data [5, 7], that the synthesis on ferrous catalysts may proceed through a reduced carbide stage. An attempt was made to determine the role of iron carbides by use of carbon-14 [14]. The catalysts were carbonized at first with ordinary carbon monoxide until the Fe_2C content was raised to 50-90%, and then with a small amount of radioactive carbon monoxide. After that the synthesis was carried out in the usual manner and the activity of the products was compared with the mean surface activity, which was determined by partially hydrogenating the carbide before and after the reaction. The resulting data led the workers to the conclusion that only about 10-20% of the products could have been formed through an intermediate reduced carbide stage.

If, however, we take into account the irregularity of the catalytic surface, then in the opinion of certain workers [12] the resulting data do not exclude the possibility that a large portion of the products might be formed by the hydrogenation of carbides.

* The paper was presented at the All-Union Conference on Organic Catalysis, November, 1959.

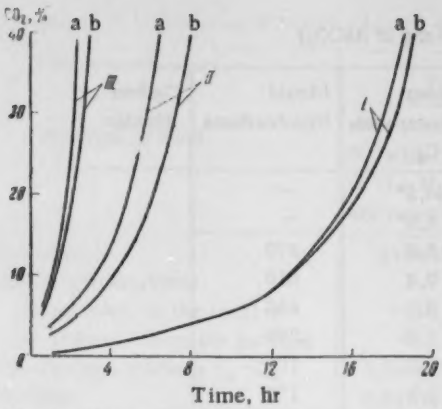

Fig. 1. The course of preliminary catalytic treatment with time. I) First; II) second; III) third treatment; a and b refer to concurrent experiments.

Though the literature data with regard to the synthetic role of carbides is inconclusive, most of the workers in the field consider the formation of carbide intermediates rather unlikely, even though carbides (particularly in the case of ferrous catalysts) have an important effect on the structure and the properties of catalytic surfaces.

Recently some experimental data have been reported which showed that fused ferrous catalysts remained completely inactive after being reduced at elevated temperatures, but regained their catalytic activity when subsequently exposed to the gaseous reaction mixture under the experimental conditions [17]. During this reactivation carbides gradually accumulated in the reaction vessel. It has also been established that the carbides thus formed (in the process of reactivation of the catalyst) were much more reactive than the carbides prepared by simply treating the original ferrous catalyst with carbon monoxide [18]. In tackling the problem of carbide participation in the synthesis of hydrocarbons it was important to keep the above-mentioned observations in mind and to design some experiments which would approximate as closely as possible the actual conditions used for the high-yield hydrocarbon synthesis on fused ferrous catalysts.

The present investigation, which was directed towards obtaining some new experimental data on the possible role of carbides as reaction intermediates, was based on the following preliminary treatment and assumptions.

The selected standard iron catalyst, which contained a trace of chromium [19, 20], was first reduced at 1000° in the usual manner and then worked up by being exposed to an inflowing gaseous mixture of $CO + H_2$ (1 : 1) containing some radioactive $C^{14}O$. The gradual activation of the catalyst is accompanied by the accumulation of radioactive iron carbide. Toward the end of this treatment, when the conversion rate of carbon monoxide to hydrocarbons becomes large, the catalytic surface has acquired the specific state that it has under normal synthetic conditions. If at any particular instant we should now replace the original gaseous mixture containing radioactive carbon monoxide with an ordinary mixture of the same composition the reactions taking place (formation of hydrocarbons, as well as the formation and elimination of carbides) will continue as before. These reactions should naturally follow the kinetics observed under normal synthetic conditions, with the sole difference that now nonradioactive carbides would be forming while carbides with carbon-14 would be consumed. One would expect that by determining the radioactive decay scheme in the synthetic products it should be possible to establish the principal routes by which iron carbides are used up under actual conditions of high-pressure synthesis and thus attempt an answer to the original question about the possible involvement of carbides in the formation of hydrocarbon chains.

EXPERIMENTAL

Condition selected for working up the catalyst. The work was done in a high-pressure laboratory apparatus [21].

A catalyst selected for the experiment was reduced at 1000°C, and then introduced into the reaction under normal working conditions (the initial gaseous 1 : 1 mixture of $CO + H_2$ was conveyed to the catalyst at the rate of 1500 liter/liter of catalyst per hour, at 300° under a pressure of 20 atm). The processing was complete after 18-20 hr, during which time the accumulated iron carbide content became 20-22% (estimated as Fe_2C). The carbide content of the metal was determined by burning a sample of the processed catalyst in a stream of oxygen. We also introduced a correction for the presence of hydrocarbons in the catalyst. Since during the processing period a very large amount of carbon monoxide (~350 liters) flows through the catalyst, a considerable quantity of liquid reaction products would accumulate on the catalytic surface, and hence it became necessary to reduce the duration of this processing. The problem presented by this requirement was solved in the following manner.

TABLE 1

The Specific Radioactivity of the Reaction Products (counts/min · mg of $BaCO_3$)

Sample No.	Sample removed after, min	Carbon monoxide	Methane	Gaseous hydrocarbons, C_2-C_4	Liquid hydrocarbons	Carbon dioxide
1	0-11	12.5*	37.5*	44.5*	–	
2	11-26	1.2	8.3	5.2*	–	
3	26-41	1.4	9.2	3.5	870	
4	41-56	1.7	9.1	2.4	610	
5	56-86	1.9	9.0	3.1	465	
6	86-116	2.3	9.0	2.6	250	
7	116-146	3.7*	9.3	3.2	180	
8	146-176	1.2	7.7	2.3	150	
9	176-206	2.1	8.8	2.6	44	
10	206-225	1.0	8.5	2.5	65	
Average		1.6	9	3	–	1.4

Note: 1) The carbide had an initial activity of 4700 counts/min · mg of $BaCO_3$. 2) The average values do not include the data marked by asterisks.

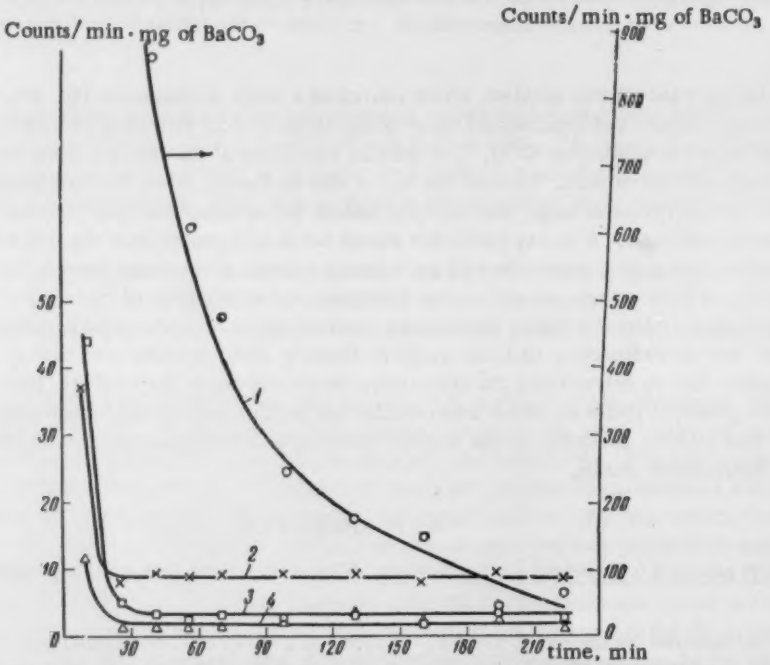

Fig. 2. The specific radioactivity of the reaction products as a function of time. 1) Liquid hydrocarbons; 2) methane; 3) gaseous hydrocarbons C_2-C_4; 4) carbon monoxide. The scale on the right is for curve 1.

After the normal preliminary processing the catalyst was hydrogenated in a stream of hydrogen at temperatures up to 450° and under 50 atm of pressure, and again worked up with the gaseous reaction mixture. Such a treatment increased the activity of the iron, and the second processing could be completed much faster (in 6-8 hours). At the same time after the second processing the carbide content was only 8-9%.

TABLE 2

The Over-All Distribution of Activity Among the Reaction Products (in counts/min · 10^5)

Reaction product	Total activity		Activity transferred from the carbide		
	after processing with $C^{14}O + H_2$ and pumping	after reaction between CO and H_2	total observed	total after discounting the activity due to CO	% of initial carbide
Iron carbide	173±4*	156±3*	–	–	–
Liquid hydrocarbons:					
a) retained on the catalyst	74±2	36±1	Traces	Traces	–
b) removed from the catalyst	–	40±1	1.6±0.2	0.8±0.1	0.5
Gaseous hydrocarbons C_2-C_4	0.53±0.05	3.3±0.3	2.8±0.3	1.3±0.1	0.8
Methane	0.29±0.02	9.3±0.5	9.1±0.5	7.5±0.4	4.4
Carbon monoxide	1.8 ±0.2	2.7±0.3	0.9±0.1	7 ±0.7	4
Carbon dioxide	0.5 ±0.05**	2.8±0.3	2.3±0.2	0	
Total	250	250	16.7	16.6	9.7

* After the preliminary processing 5.8% of carbide with a specific activity of 4700 counts/min · mg of $BaCO_3$ had accumulated on the catalyst; after the reaction between non-radioactive reactants we had 11.7% of carbide with an average activity of 2100 counts/min · mg of $BaCO_3$.

** From the reaction of CO with water vapor.

Similarly we found that after a third consequtive processing the activation took very little time (1.5-2 hr) and yielded only a 6% accumulation of iron carbide. In Fig. 1 we have reproduced some characteristic curves showing the course of catalytic processing in some typical experiments.* Samples of a catalyst were used repeatedly in our work. The reproducibility of our data was satisfactory. These preliminary experiments enabled us to proceed to experiments which involved the use of radioactive carbon monoxide.

Hydrocarbon synthesis over a catalyst containing radioactive iron carbide. The catalyst was first worked up in the prescribed manner. After the second processing and reduction the catalyst was allowed to come into contact with a reaction mixture consisting of $C^{14}O + H_2$ (1:1) at 300°C and under a pressure of 20 atm, with the gas flowing at the rate of 1500 liters/liter of catalyst per hour. Since the carbon monoxide in the synthetic mixture had a specific radioactivity of 4700 counts/min · mg of $BaCO_3$, the resulting iron carbide consequently exhibited the same specific radioactivity. The processing was continued for two hours until the rate of carbon monoxide conversion to hydrocarbons attained 95%. At the end of this period the pressure in the reactor was reduced, and for one hour the catalyst was degassed by pumping (to a pressure of 10^{-3} mm Hg) at 300°C. After that the catalyst was exposed to a non-radioactive gaseous reaction mixture under the normal working conditions and for 225 min the liquid reaction products and outflowing gases were collected. All of these materials were first collected in ten consecutive aliquots, then separated into methane, gaseous hydrocarbons C_2-C_4, liquid hydrocarbons, and unreacted carbon monoxide. Carbon dioxide was absorbed in a solution of sodium hydroxide.

The combined reaction products as well as the individual components after separation were analyzed radiometrically in the manner described before [22]. The resulting specific radioactivity data are presented in Table 1 and Fig. 2.

To interpret correctly the experimental data given in Table 1 it was esential to estimate the quantity of hydrocarbons which had formed while the catalyst was being worked up with the radioactive mixture, and which subsequently failed to be removed by the pumping to which the reactor was subjected before the introduction of the non-radioactive reaction mixture. We therefore took another sample of the same catalyst and subjected it to a similar treatment with the radioactive gaseous mixture, using the same reactor. After the usual treatment,

* The catalytic activity was measured by the % of CO_2 in the outflowing gases.

the second sample was degassed with pumping at 300° just like the first. Subsequently a stream of nitrogen under 20 atm pressure was passed through the hot (300°C) catalyst while non-radioactive liquid hydrocarbons (previously prepared over a similar catalyst) were introduced through a high-pressure burette. The liquid hydrocarbons were delivered to the catalytic surface at a rate equivalent to that at which they are formed from $CO + H_2$ on the same catalyst at 300°C under 20 atm. Under these conditions the active hydrocarbons still retained on the catalytic surface after the pumping were gradually leached out and replaced by the new non-radioactive hydrocarbons. This reproduced to a certain degree the processes taking place in the above-described main experiment. From the amount of leached radioactive hydrocarbons it was possible to estimate the amount of hydrocarbons normally retained on the catalyst after a two-hour processing and subsequent pumping.. It actually turned out that a very substantial amount of hydrocarbons remain adsorbed on the catalyst. The total amount of leached hydrocarbons corresponded to 1575 mg of $BaCO_3$ with the specific radioactivity of the initial carbon monoxide. Moreover, during the first four hours the amount of hydrocarbons leached out corresponds to 765 mg of $BaCO_3$ (which includes 30 mg of $BaCO_3$ on account of some adsorbed gaseous hydrocarbons C_2-C_4), which is very close to the figure obtained in the main experiment. Thus, in the course of the main experiment during the period when non-radioactive gaseous reactants were used (about four hours) we collected an amount of radioactive liquid hydrocarbons equivalent to 845 mg of $BaCO_3$ with the specific activity of the CO used initially in working up the catalyst. The activity obtained in the main experiment is slightly higher than the one leached out of the catalyst in the first four hours; this difference can be attributed to the fact that the conditions in the main experiment were somewhat more favorable to the desorption of radioactive products.

DISCUSSION OF RESULTS

From what has been said one has to conclude that the liquid hydrocarbons formed during the reaction period, when non-radioactive reactants were used, acquired their radioactivity entirely, or largely, through contamination by the adsorbed hydrocarbons which had formed during the initial processing of the catalyst and were not removed by subsequent degassing. The regular decline with time in the specific radioactivity of liquid hydrocarbons formed during the reaction between initially non-radioactive gases (see Table 1 and Fig. 2) can thus be attributed to a gradual leaching of radioactive hydrocarbons from the catalytic surface by the newly formed non-radioactive reaction products.

Things are somewhat different though in the case of methane and other gaseous products. The data in Table 1 and Fig. 2 indicate that after the eleventh minute the radioactivities of carbon monoxide, methane, and other gaseous hydrocarbons remain at a practically constant level until the end of the experiment. The slightly excessive specific radioactivity detected in the first sample can now, in view of the above-described results from the leaching experiment, be attributed to contamination with the corresponding radioactive products retained on the catalysts after the preliminary processing. This constancy indicates that some processes are going on which provide for an even level of specific radioactivity in the reaction products throughout the entire reaction. Except that it depends on the nature of these processes, the observed constant level of specific radioactivity can not be explained by the desorption of previously formed radioactive products. We are dealing in this case with a transfer of carbon-14 from the carbide to the carbon monoxide, methane, and gaseous hydrocarbons. It has earlier been established [22] that under the experimental conditions methane is completely inert; it is not involved in the formation of higher hydrocarbons and fails to undergo isotopic exchange reactions with carbon monoxide, hydrocarbons, or carbon dioxide. Hence, this excludes any possibility that these reaction products might have become contaminated with activity in the manner described in the preceding praragraph.

It is also possible that radioactive carbon is transferred from the carbide to the liquid hydrocarbons to the same extent as in the case of the gaseous hydrocarbons C_2-C_4. Assuming also that the CO, CH_4, and gas oil formed from carbide which were contained in the first aliquot had the same average specific radioactivity as they did in the remaining nine aliquot samples it is possible to determine the total amount of carbon-14 transferred during the experiment to CO and carbon-containing reaction products (see Table 2). The amount transferred would account for a radioactivity of 16.6×10^5 counts/min, which was distributed between:

liquid hydrocarbons	$1.6 \cdot 10^5$ counts/min
gaseous hydrocarbons C_2-C_4	$2.8 \cdot 10^5$
methane	$9.1 \cdot 10^5$
CO	$0.9 \cdot 10^5$
CO_2	$2.3 \cdot 10^5$

The activity retained on the catalyst after the experiment was determined by burning the catalyst in a stream of oxygen; it turned out to be $192 \cdot 10^5$ counts/min. If we subtract from this figure the activity of radioactive hydrocarbons which were not desorbed during the experiment ($36 \cdot 10^5$ counts/min)* and add the total activity transferred from the carbide to CO and to the reaction products we will get a number representing the quantity and activity of the carbide formed from $C^{14}O$ during the preliminary processing and present in the catalyst at the start of the synthesis involving non-radioactive gaseous reactants. The number is $173 \cdot 10^5$ counts/min. The data presented above permit a quantitative treatment of the various routes by which iron carbide is transformed into other products in the course of the synthesis of hydrocarbons from CO and H_2. Moreover one should take into account the fact that the specific radioactivity of carbon monoxide constitutes a part of the total specific radioactivity of the liquid and gaseous reaction products in the outflowing gases, while the specific radioactivity of carbon dioxide should be equal to that of carbon monoxide.

The data obtained in the above-described experiment are compiled in Table 2. They clearly demonstrate that only about 10% of the radioactive carbide initially formed during the preliminary processing was consumed during the regular reaction. At the same time it should be noted that there are essentially two ways in which the carbide reacts: It is either hydrogenated to methane or undergoes isotopic carbon exchange with carbon monoxide. Only a very insignificant portion of the radioactive carbon contained in the carbide was converted into higher hydrocarbons during the reaction. Comparing the specific radioactivity of the carbide with that of the reaction products and assuming that the activity of the latter ones remains constant with time (see Table 1 and Fig. 2) we can conclude that carbide intermediates could only account for less than 0.03% of the higher hydrocarbons formed in the reaction and about 0.16% of methane, while less than 0.03% of the carbon monoxide which had passed through the catalyst underwent isotopic exchange. These results demonstrate the low reactivity of iron carbide under the conditions of the Fischer-Tropsch hydrocarbon synthesis over fused ferrous catalysts and clearly contradict the hypothesis according to which carbides are involved as intermediates in the synthesis of hydrocarbons from CO and H_2. Moreover, it has been shown that the catalytic synthesis of hydrocarbons from CO and H_2 over fused ferrous catalysts is accompanied by the formation and hydrogenation of iron carbide. These observations at the same time fully conform with the hypothesis of combined catalytic action previously proposed for these catalysts [17, 18] and according to which the formation of hydrocarbons from CO and H_2 is first initiated by and then coupled with the competing reactions of carbide formation and hydrogenation.

We have also discovered in this work some previously unknown facts concerning the nature of the reaction between the ferrous catalyst and the reaction mixture components; these data are expressed in the observed activity distribution (with time) among the reaction products. This in turn makes it imperative to start an investigation of the mechanism involved in the formation of iron carbides and their subsequent reaction with hydrogen and carbon monoxide.

SUMMARY

1. By using carbon-14 we investigated the reactions of iron carbide under the conditions of high-yield Fischer-Tropsch hydrocarbon synthesis ($CO + H_2$, at 300°C and 20 atm); the carbide itself was formed by the reaction of the gaseous reaction mixture with the fused ferrous catalyst in the course of the synthesis.

2. We established the fact that under the normal conditions of the reaction most of this iron carbide (90%) is either hydrogenated to methane or undergoes isotopic carbon exchange with carbon monoxide. These two reactions are very slow in comparison with the rate of the main synthesis: Under the investigated conditions only one CO out of a thousand undergoes exchange, and 5 out of 3 methane atoms are formed by the hydrogenation of the carbide.

3. Of the higher hydrocarbons (over one carbon atom) only 0.03% could have been formed through a carbide intermediate. These data definitely contradict the hypothesis according to which carbides act as intermediates in the conversion of $CO + H_2$ to hydrocarbons.

*The determination was based on the experiment where the radioactive hydrocarbons retained on the catalyst after the processing were leached out with non-radioactive hydrocarbons.

LITERATURE CITED

1. F. Fischer and H. Tropsch, Brennstoff-Chemie 7, 97 (1926).
2. F. Fischer and H. Koch, Brennstoff-Chemie 13, 428 (1932).
3. S. Craxford and E. Rideal, J. Chem. Soc.,1604 (1939).
4. Ya. T. Éidus and N. D. Zelinskii, Izvest Akad. Nauk SSSR, Otdel Khim. Nauk 45 (1942).
5. Ya. T. Éidus, Izvest. Akad. Nauk SSSR, Otdel Khim. Nauk, 255 (1944).
6. Ya. T. Éidus, Izvest. Akad. Nauk SSSR, Otdel Khim. Nauk, 349 (1944).
7. Ya. T. Éidus, Izvest. Akad. Nauk SSSR, Otdel Khim. Nauk, 447 (1946).
8. G. E. Braude and B. P. Bruns, Zhur. Fiz. Khim. 22, 487 (1948).
9. J. Kummer, L. Browning, and D. Emmett, J. Chem. Phys. 16, 739 (1948).
10. J. Kummer, T. DeWitt and P. Emmett, J. Am. Chem. Soc. 70, 3632 (1948).
11. R. Griffith, Adv. in Catal. (Acad. Press, New York, 1948) Vol. 1, p. 97.
12. H. Pichler, "Twenty-five years of catalytic alkane synthesis from CO and H_2," Coll.: Catalysis and Catalysts in Organic Reactions [translated from English under the direction of A. A. Balandin and A. M. Rubinshtein] (IL, Moscow, 1955).
13. H. Pichler and H. Merkel, Brennstoff-Chemie 31, 1, 33 (1950).
14. S. Weller, J. Am. Chem. Soc. 69, 2432 (1947).
15. S. Weller, L. Hofer, and R. Anderson, J. Am. Chem. Soc. 70, 799 (1948).
16. O. A. Golovina, Dissertation [in Russian] (Inst. Fiz. Khim., AN SSSR, Moscow, 1958).
17. Yu. B. Kagan, A. N. Bashkirov, Yu. B. Kryukov, and S. M. Lokter, Khim. i Tekh. Topliva i Masel, 3, 14 (1958).
18. Yu. B. Kagan, A. N. Bashkirov, Yu. B. Kryukov, S. M. Lokter, and N. A. Orlova, Izvest. Akad. Nauk SSSR, Otdel. Khim. Nauk, 1274 (1958).*
19. A. N. Bashkirov, Yu. B. Kagan, Yu. B. Kryukov, and S. M. Lokter, Izvest. Akad. Nauk SSSR, Otdel Tekh. Nauk, 106 (1956).
20. Yu. B. Kagan, A. N. Bashkirov, S. M. Lokter, N. G. Morozov, and N. A. Orlova, Trudy Instituta Nefti, Akad. Nauk SSSR 12, 228 (1958).
21. A. N. Bashkirov, Yu. B. Kagan, S. M. Lokter, and N. G. Morozov, Trudy Instituta Nefti, Akad. Nauk SSSR 10, 236 (1957).
22. Yu. B. Kryukov et al., Khim. i Tekh. Topliva i Masel, 6, 26 (1957).

*Original Russian pagination. See C. B. translation.

STUDY OF THE ELECTRICAL CONDUCTIVITY OF CATALYSTS MADE OF ZINC, CHROMIUM, AND COPPER OXIDES FOR THE CONVERSION OF CARBON MONOXIDE

T. A. Semenova, G. E. Braude, and F. P. Ivanovskii

Scientific Research Institute of the Nitrogen Industry, Moscow
Translated from Kinetika i Kataliz, Vol. 1, No. 2, pp. 282-286,
July-August, 1960
Original article submitted December 14, 1959

The electrical conductivity of catalysts was studied by the probe method, both in vacuum and during the conversion of carbon monoxide with water vapor. The investigation showed that the activity and the electrical conductivity of the catalysts are inversely related.

It was shown previoulsy [1] that a three-component catalyst made of zinc, chromium, and copper oxides is an active catalyst for the low-temperature conversion of carbon monoxide with water vapor.

Investigation of the catalyst [2] showed that there exists a relationship between its activity and its chemical composition. The study of four samples of three-component catalysts – $ZnO \cdot Cr_2O_3 \cdot CuO$, $ZnO \cdot Cr_2O_3 \cdot 0.5CuO$, $ZnO \cdot Cr_2O_3 \cdot 0.14CuO$, $ZnO \cdot Cr_2O_3 \cdot 0.05CuO$, and also $ZnO \cdot Cr_2O_3$ – showed that with an increase in the concentration of copper in the catalyst the activity first increases and then decreases, the maximum activity corresponding to a composition of $ZnO \cdot Cr_2O_3 \cdot 0.5CuO$. For the activation energy the relationship is reversed, i.e., it is at the minimum value.

These catalysts are semiconductors, and therefore it appears to be of interest to determine their electrical conductivity. The electrical conductivity was studied by the probe method [3].

Measurements were made with catalysts formed by pressing powders into tablets 8 mm in diameter and 10-12 mm thick. To ensure good electrical contact copper plates were pressed into the edges of the tablets (the compression pressure being 2500 kg/cm^2).

The tablet of catalyst (Fig. 1) was introduced into a glass tube 3, between two spring-loaded molybdenum contacts with nickel edges (welded into the tube), which served simultaneously as contacts and terminals for the current. Spring-loaded molybdenum bars with nickel edges, also welded into the tube, served as probes. The electrical conductivity was measured in vacuum and also in the reacting medium. When the measurements were made in vacuum, the tube was connected to the apparatus serving to produce and measure the degree of vacuum. The electromagnetic break valve 4 disconnected the tube for the measurement of electrical conductivity from the reaction column 1, in which the activity of the catalyst was measured. The valve also served to supply the reaction mixture to the tablet. The tube in which the electrical conductivity was measured was placed in an electric furnace. The refrigerator-condenser 6 served to condense the water vapor left in the vapor-gas mixture in those cases when measurements were made in the reacting medium. The whole apparatus was sealed and the tube through which the gas and the vapor were introduced was heated with an electric coil.

The electrical circuit used for the measurement of electrical conductivity is represented in Fig. 2. Dry batteries were used as a source of direct current. The current intensity was measured with milli- and micro-

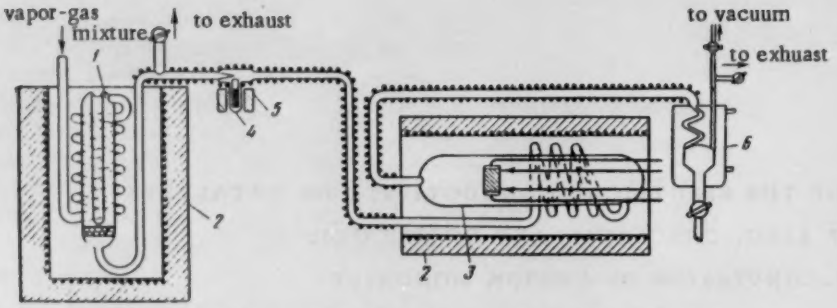

Fig. 1. Diagram of the apparatus used to measure electrical conductivity. 1) Reaction column; 2) electric furnace; 3) tube for measurement of electical conductivity; 4) electromagentic break valve; 5) electromagnetic coil; 6) refrigerator-condenser.

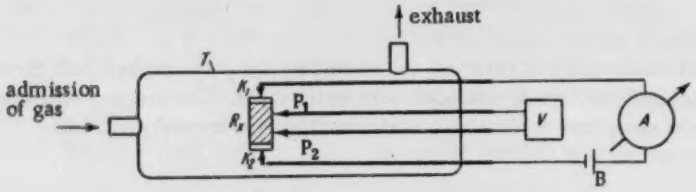

Fig. 2. Electrical diagram of the circuit used to measure electrical conductivity. T) Tube for the measurement of electrical conductivity; R_X) tablets; K_1 and K_2) contacts; P_1 and P_2) probes; A) milli- or microammeter; V) cathode voltmeter; B) current source.

ammeters. The difference of potential between the probes P_1 and P_2 was measured in a number of cases by a compensation method, using a high resistance potentiometer of the PPTV-1 type, which allowed us to measure the difference of potential up to 1.2 v. In most cases the difference of potential for the catalyst exceeded this value and was measured by using a cathode voltmeter of the ACh-M2 type. In these cases a current passes through the probes during measurements, which introduces an additional error. The amount of this error is determined by the resistance outside the apparatus (which was 11 meg in our case) and the resistance of the tablet itself. The calculations showed that the maximum error in this case did not exceed 7% of the minimum conductivity, of the order of 10^{-6} $ohm^{-1}cm^{-1}$.

The electrical conductivity σ was calculated by the formula

$$\sigma = \frac{IL}{v \cdot s \cdot \gamma} \ ohm^{-1} \cdot cm^{-1}$$

where I is the current intensity, v is the difference of potential between the probes, L is the distance between probes, s is the cross section of the tablet, and γ is the amount of catalyst in the tablet.

The results obtained with this apparatus can be reproduced satisfactorily. The deviation of the values of the electrical conductivity in parallel experiments did not exceed 15%.

Preliminary experiments showed that the composition of the reaction mixture does not affect the electrical conductivity of the catalyst. All the measurements were made with a constant concentration of the components of the reaction mixture.

The investigation of three-component catalysts showed that the necessary condition for their high activity

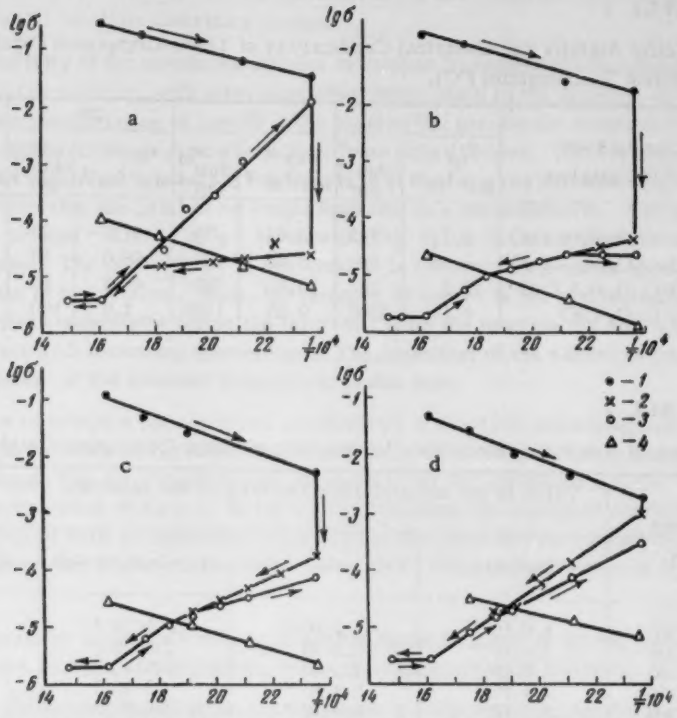

Fig. 3. Relationship between electrical conductivity and temperature for the following catalysts: a) $ZnO \cdot Cr_2O_3 \cdot CuO$; b) $ZnO \cdot Cr_2O_3 \cdot 0.5CuO$; c) $ZnO \cdot Cr_2O_3 \cdot 0.14CuO$; d) $ZnO \cdot Cr_2O_3 \cdot 0.05CuO$; 1) unreduced sample in vacuum; 2) reduction of the sample in the reaction mixture; 3) reduced sample in the reaction mixture; 4) reduced sample in vacuum. The arrows on the curves indicate the sequence of the experiments.

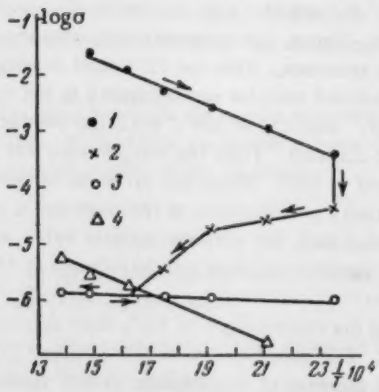

Fig. 4. Variation of the electrical conductivity as a function of temperature for $ZnO \cdot Cr_2O_3$ catalyst. (The symbols have the same meaning as those in Fig. 3.)

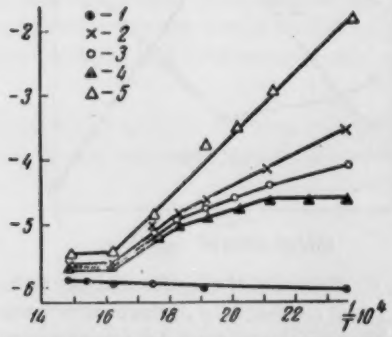

Fig. 5. Variation of the electrical conductivity as a function of temperature for different catalysts in the reaction medium. 1) $ZnO \cdot Cr_2O_3$; 2) $ZnO \cdot Cr_2O_3 \cdot 0.05CuO$; 3) $ZnO \cdot Cr_2O_3 \cdot 0.14CuO$; 4) $ZnO \cdot Cr_2O_3 \cdot 0.5\,CuO$; 5) $ZnO \cdot Cr_2O_3 \cdot CuO$.

TABLE 1

Specific Activity and Electrical Conductivity of Three-Component Catalysts at Different Temperatures (°C).

Composition of the catalyst	175		200		250		300	
	$k_{sp} \cdot 10^6$, $sec^{-1} m^{-1}$	$\sigma \cdot 10^6$, $ohm^{-1} \cdot cm^{-1}$	$k_{sp} \cdot 10^6$, $sec^{-1} m^{-1}$	$\sigma \cdot 10^6$, $ohm^{-1} \cdot cm^{-1}$	$k_{sp} \cdot 10^6$, $sec^{-1} m^{-1}$	$\sigma \cdot 10^6$, $ohm^{-1} \cdot cm^{-1}$	$k_{sp} \cdot 10^6$, $sec^{-1} m^{-1}$	$\sigma \cdot 10^6$, $ohm^{-1} \cdot cm^{-1}$
$ZnO \cdot Cr_2O_3 \cdot 0{,}05$ CuO	1,72	145	3,64	74	11,6	25	25,1	8,0
$ZnO \cdot Cr_2O_3 \cdot 0{,}14$ CuO	6,45	50	8,45	36	18,0	18	31,6	6,7
$ZnO \cdot Cr_2O_3 \cdot 0{,}5$ CuO	18,2	25	25,6	22	47,9	13	79,4	5,5
$ZnO \cdot Cr_2O_3 \cdot$ CuO	0,14	3200	0,35	1100	1,6	160	5,2	15,0

TABLE 2

Effect of Heating on Electrical Conductivity of Three-Component Catalysts

Temp., °C	Value of the electrical conductivity of the catalysts, $ohm^{-1} \cdot cm^{-1}$			
	$ZnO \cdot Cr_2O_3 \cdot 0{,}05$ CuO	$ZnO \cdot Cr_2O_3 \cdot 0{,}14$ CuO	$ZnO \cdot Cr_2O_3 \cdot 0{,}5$ CuO	$ZnO \cdot Cr_2O_3 \cdot$ CuO
300	$8{,}0 \cdot 10^{-6}$	$6{,}7 \cdot 10^{-6}$	$5{,}5 \cdot 10^{-6}$	$1{,}5 \cdot 10^{-5}$
350	$2{,}5 \cdot 10^{-6}$	$2{,}3 \cdot 10^{-6}$	$2{,}0 \cdot 10^{-6}$	$3{,}5 \cdot 10^{-6}$
400	$2{,}5 \cdot 10^{-6}$	$2{,}2 \cdot 10^{-6}$	$1{,}9 \cdot 10^{-6}$	$3{,}5 \cdot 10^{-6}$
350	$2{,}4 \cdot 10^{-6}$	$2{,}3 \cdot 10^{-6}$	$2{,}0 \cdot 10^{-6}$	$3{,}4 \cdot 10^{-6}$
300	$8{,}2 \cdot 10^{-6}$	$6{,}6 \cdot 10^{-6}$	$5{,}6 \cdot 10^{-6}$	$1{,}3 \cdot 10^{-5}$

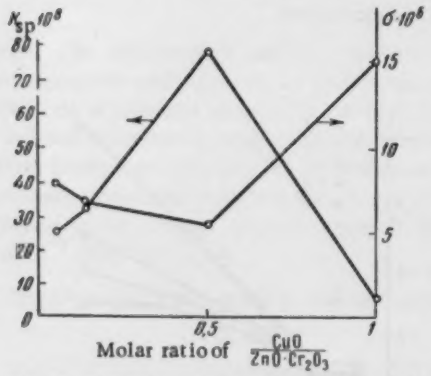

Fig. 6. Variation of specific activity and electrical conductivity of three-component catalysts as a function of the concentration of copper (at 300°C).

is the heating of the catalyst in the reaction medium up to 250-300°C. During this period the catalyst is reduced and an active zinc-chromium spinel is formed. Therefore the investigations were made in such a way that one could follow the variation of the electrical conductivity during the formation of the active component – the spinel – and also during the catalytic reaction. Hence, the measurements were made in a definite sequence. First the electrical conductivity of the unreduced samples was measured in the vacuum (10^{-5}-10^{-6} mm Hg) at 300°C until the conductivity became constant. Then the temperature was gradually decreased to 150°. When the variation of the electrical conductivity as a function of temperature in vacuum was determined, the electromagnetic valve was broken and the reaction mixture was introduced at 150°. Then the electrical conductivity was measured, first by increasing the temperature to 300°, then decreasing it to 150°. The investigation of the catalysts [2] showed that the increase of temperature to 400° leads to a decrease in the activity, but the activity can be completely restored by circulating the vapor-air mixture at 250-300°. After the electrical conductivity was measured the catalyst was kept at 400° for 10 hours and then measurements were made at 300°. When measurements in the reaction medium were made, the apparatus was evacuated after the completion of the reaction, and the electrical conductivity of the reduced catalyst was measured in vacuum at different temperatures.

The results of this investigation showed that the variation of the electrical conductivity as a function of time (Fig. 3) is the same for all catalysts containing copper.

The electrical conductivity of the unreduced samples in vacuum increases with increasing temperature. The introduction of the reaction mixture, with subsequent evacuation, leads to the decrease of electrical conductivity, and the higher the concentration of copper in the catalyst the greater the decrease of conductivity. For measurements made in the reaction medium the picture is entirely different. When the temperature is increased from 150 to 350° the electrical conductivity decreases, and then it remains constant for further increase of temperature. This indicates that the catalyst no longer functions as a semiconductor. The electrical conductivity of the unreduced catalyst – $ZnO \cdot Cr_2O_3$ – in vacuum (Fig. 4) has the same temperature dependence as the catalyst containing copper. The conductivity of this catalyst in the reaction medium increases almost imperceptibly with the increase of temperature. Thus, the presence of copper in the catalyst substantially changes the character of the electrical conductivity during the reaction. After the reaction the conductivity of all catalysts in vacuum increases with increasing temperature. The logarithm of the electrical conductivity is a linear function of the reciprocal of the absolute temperature in this case.

These results allow us to compare the electrical conductivity of catalysts containing different amounts of copper. For comparison, the variation of the conductivity as a function of temperature in the reaction medium is represented for all samples in Fig. 5. The electrical conductivity of the unreduced samples in vacuum increases with increasing concentration of copper. In the reacting medium the electrical conductivity of catalysts containing copper first decreases with an increasing concentration of copper and then increases. The $ZnO \cdot Cr_2O_3 \cdot 0.5CuO$ catalyst shows the minimum electrical conductivity. The reduced samples in vacuum give the same relationship.

The electrical conductivity of the $ZnO \cdot Cr_2O_3$ catalyst is lower than that of all the other catalysts, and the character of its variation as a function of temperature in the reaction medium is different.

Table 1 summarizes the results, which allow us to compare the electrical conductivity and the activity of the three-component catalysts investigated.

The catalytic activity was measured by the specific rate constant, which allowed us to eliminate the effect of the surface. The effect of copper on the electrical conductivity and activity of the catalyst is indicated particularly clearly in Fig. 6.

The results show that the higher the activity of the catalyst, the lower its electrical conductivity, and also the greater the difference between the value of the rate constant, the greater the difference between the values of the conductivity. Thus, there exists an inverse relationship between the activity and electrical conductivity of catalysts. We observed this relationship up to 350°C. As was indicated above, the activity of these three-component catalysts in the reaction medium decreases considerably when they are heated to 400°. The results concerning the measurement of the electrical conductivity during the heating of catalysts up to 400° are shown in Table 2.

The order in which the results appear in the table corresponds to the order in which the measurements were made. Thus, in the table we do not observe the inverse relationshp noted previously between the activity and electrical conductivity of the catalysts.

SUMMARY

1. We have investigated the electrical conductivity of zinc-chromium-copper oxide catalysts for the conversion of carbon monoxide.

2. We have shown that there exists an inverse relationship between the activity and electrical conductivity of the catalysts investigated.

LITERATURE CITED

1. F. P. Ivanovskii, G. E. Braude, and T. A. Semenova, Transactions of the State Scientific Research and Development Institute of the Nitrogen Industry [in Russian] (Goskhimizdat, 1957) No. 8.

2. F. P. Ivanovskii, G. E. Braude, T. A. Semenova, and B. G. Lyudkovskaya, Report on the Conference of the Physics and Physical Chemistry of Catalysts [in Russian] (Izd. AN SSSR, 1958).
3. A. F. Ioffe, Physics of Semiconductors [in Russian] (Izd. AN SSSR, 1957) p. 398.

CHROMATOGRAPHIC ANALYSIS OF GAS ADSORPTION ISOTHERMS AND THE SPECIFIC SURFACE OF SOLIDS

S. Z. Roginskii, M. I. Yanovskii, Lu P'iei-chang, G. A. Gaziev, G. M. Zhabrova, B. M. Kadenatsi, V. V. Brazhnikov, I. E. Neimark, and M. A. Piontkovskaya

Institute of Physical Chemistry, Academy of Sciences of the USSR
Translated from Kinetika i Kataliz, Vol. 1, No. 2, pp. 287-293, July-August, 1960
Original article submitted January 28, 1960

A chromatographic method of measuring adsorption isotherms of gases and vapors has been developed. Determination of the adsorption isotherm takes 15-25 minutes.

The investigation of the adsorption of normal heptane on a number of catalytic surfaces and adsorbents showed that there is satisfactory agreement between the adsorption isotherms determined by chromatographic methods and the isotherms determined under static conditions in vacuum.

The determination of adsorption isotherms and the specific surface of porous solids takes a considerable amount of time. For this reason it appears to us timely to develop rapid methods of determining these characteristics. Some progress in this direction has been made by A. M. Rubinshtein and V. A. Afanas'ev [1, 2], who proposed the use of a gravimetric method of measuring adsorption of vapor from a stream of an inert gas. However, this method is relatively complicated; several hours are necessary to obtain 10-12 points of the isotherm. Furthermore, the sensitivity of the method is not sufficiently high. With the filtration method used by B. V. Deryagin [3] it is not possible to measure blind pores, and the method requires some additional operations.

The chromatographic method seems to be more promising. Wilson [4], who has made a theoretical study of the relationship between chromatographic desorption curves and the shape of the adsorption isotherms of the substance, pointed out the possibility of using this method. The method was further developed in a number of investigations published in recent years [5-8]. However, the attampt to use the basic equation of the equilibrium theory of chromatography for determination of the adsorption isotherms from the chromatographic curves obtained with the use of liquid chromatography [9, 10] appeared not to be very successful because of the slowness with which the adsorption equilibrium is established in solutions and also the complication produced by the effect of the solvent on the adsorption of the dissolved substance. These complications are almost completely eliminated in gas adsorption chromatography when the gas carriers are helium, argon, H_2, N_2, etc., and in the case of adsorption of vapors of organic compounds (C_7H_{16}, CCl_4, C_2H_5OH, etc.) [7, 11, 12]. In the present article we describe the chromatographic apparatus we developed, which allowed us to measure very rapidly the adsorption isotherms for the determination of the surface of catalysts and adsorbents by two chromatographic methods. The results of these chromatographic methods are compared with those obtained with ordinary high vacuum methods under static conditions, and the effect of different parameters of the chromatographic process on the reproducibility of the results obtained is investigated.

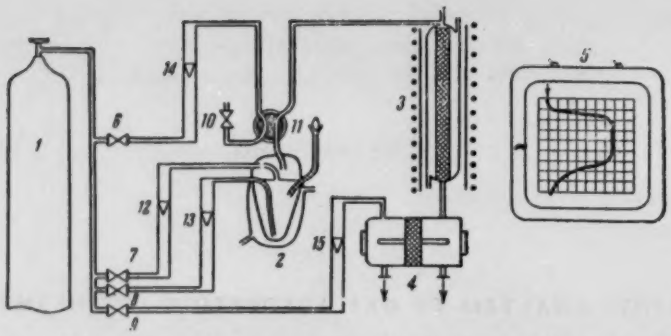

Fig. 1. Chromatographic arrangement. 1) Tank containing gas carrier; 2) bubbler containing material to be adsorbed; 3) chromatographic column; 4) ion detector; 5) ÉPP-09 potentiometer; 6, 7, 8, 9, 10) precision valves; 11) four-way valve; 12, 13, 14, 15) flowmeters.

EXPERIMENTAL

Method of Investigation

The diagram of the chromatographic apparatus is represented in Fig. 1. The essential part of the apparatus consists of a dynamic tube 3, filled with the adsorbent or catalyst, a thermostatic bubbler containing the adsorbent, 2, and a sensitive gas analyzer 4, whose indications are registered automatically by the potentiometer 5. An ion detector containing promethium-147 [13] was used as a gas analyzer. The advantage of an ion detector with respect to the detectors ordinarily used (based on the measurement of heat conductivity) consists in a much higher sensitivity and in the greater stability of indications during the variation of temperature and flow rate. Usually nitrogen was used as a gas carrier. In determining small surfaces, where higher sensitivity is needed, we used argon, which allowed us to increase the sensitivity of the detector by two orders. A definite ratio of gas flow, ensuring the necessary concentration of the adsorbing substance (determined by the ion detector 4), was achieved with precision valves 7 and 8. During the period of time spent on the preparation of the mixture of the required concentration the column and the whole circulation system were washed with inert gas passing through the valve 10 and the flowmeter 14. When stationary conditions were achieved, the flow of gas carrier containing the vapor of the adsorbing substance was directed to the column with the four-way valve 11. This moment was considered to be the beginning of the experiment. The automatically registered curve representing the variation of the indication of the gas analyzer as a function of time is called the "frontal diagram" (the right branch of this curve is represented in Fig. 2a). The height of the step of the frontal diagram corresponds to the original concentration of the adsorbent in the flow. At the end of this frontal experiment the valve 11 was again switched to its original position and the column was washed with pure gas carrier. To eliminate the possibility of the change of the flow rate during the momentary switching of the valve 11, pure gas carrier was blown through the precision valve 10 during the whole period necessary for obtaining the frontal diagram. The flow resistance of this precision valve 10 is made equal to the flow resistance of the dynamic tube. Under these conditions switching the flow

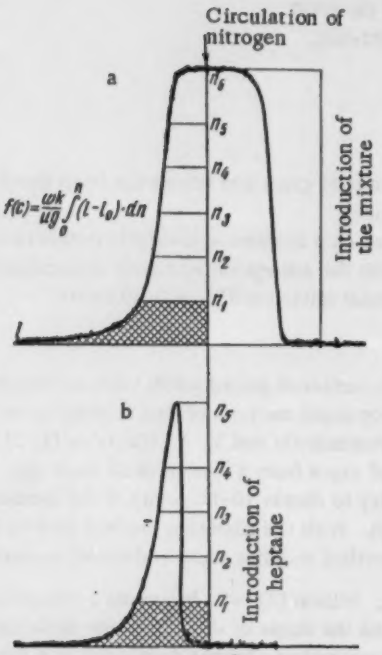

Fig. 2. Curve illustrating the method of calculation. a) Frontal variation; b) developmental variation.

TABLE 1

Determination of the Surface of Refractory Diatomaceous Brick by the Chromatographic Method

n, cm	S, cm^2	$P/P_s \cdot 10^2$	$f(c) \cdot 10^4$, mM/g	$P/P_s f(c)(1-P/P_s)$
2	8,2	2,3	189	1,25
4	13,5	4,6	310	1,55
6	18,2	6,9	418	1,77
8	22,4	9,2	515	1,97
10	25,8	11,5	593	2,19
12,4	29,3	14,25	673	2,47

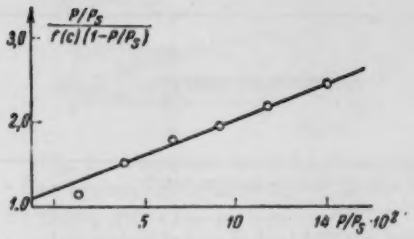

Fig. 3. Curve for the calculation of the surface according to the BET method.

does not induce any break in the curve. The moment at which a flow of pure gas carrier begins to be blown through the dynamic tube is marked on the chromatogram as the beginning of the "desorption curve" (the left branch of the curve in Fig. 2a). This curve makes it possible to determine the adsorption isotherm (see below).

The other method of chromatographic determination of the isotherm is even simpler. Instead of a preliminary saturation of the layer, the sample is periodically injected with a microsyringe through a rubber cap into the column, which is continuously washed by the gas carrier. The chromatographic curve is respresented in Fig. 2b.

Normal heptane was used as the adsorbing substance. The dimensions of the dynamic tube varied according to the amount of the specific surface of the catalyst or adsorbent investigated.

To calculate the isotherm from a curve of the type represented in Fig. 2a or 2b it is necessary to calibrate the indications of the detector. The calibration was made gravimetrically in the following way. After the desired ratio is achieved between the gas carrier passing through the bubbler and the diluting flow, and the indications of the detector become stable, one introduces two connected dynamic tubes filled with a weighed amount of active carbon. The concentration of adsorbing material is determined by the increase of weight of the carbon and by the volume of the gas carrier passing through, and from this it is possible to draw a calibration curve. Within the limits of our experiment, the detector has linear characteristics. When the gas carrier is nitrogen and the concentration of heptane is 4.6 mg/liter, one obtains a signal of 1 mv.

Treatment of Experimental Results

From the material balance of the chromatographic process [3-8] one can obtain the following basic equation:

$$\sigma q \left(\frac{\partial c}{\partial t}\right)_x + q(1-\sigma)\left(\frac{\partial a}{\partial t}\right)_x = -\omega \left(\frac{\partial c}{\partial x}\right)_t, \qquad (1)$$

where c is the concentration of the substance in the gas flow, in mg/cm^3; a is the amount of the adsorbed substance, in mg/cm^3 of the adsorbent; q is the cross section of the chromatographic column, in cm^2; σ is the fraction of the cross section not filled by the adsorbent; ω is the flow rate of the gas, in cm^3/min; t is time, in min, measured from the beginning of the experiment; and x is the distance, in cm, measured in the direction of the flow from the inlet into the column.

If we assume that the adsorption equilibrium is established instantaneously, and if we neglect the longitudinal diffusion, we can write:

$$da = \frac{-\omega - q\sigma\left(\frac{\partial x}{\partial t}\right)_c}{q(1-\sigma)\left(\frac{\partial x}{\partial t}\right)_c} dc. \qquad (2)$$

TABLE 2

Adsorbent or catalyst	Specific surface, m^2/g	
	obtained chromatographically	obtained under static conditions by gravimetric method
Refractory diatomaceous brick	34	41
Silica gel E	100	100
Silica gel 862 (gel of nickel hydroxide)	50	60
Nickel catalyst	16	20
Magnesium oxide	220	220
ZnO + 14.5% $ZnSO_4$	6	5
Lamp black	120	100
Iron powder	2.5	1.7*
Corundum	0.1	0.2**
Iron ammonia catalyst sample 11-58	17	14*
Iron ammonia catalyst sample 16-57	7	9*

* Adsorbing substance, nitrogen (volume method).
** Adsorbing substance, krypton (volume method).

The amount of substance adsorbed by 1 g of the adsorbent or catalyst is equal to

$$f(c) = \frac{Lq(1-\sigma)}{g}\int_0^a da, \tag{3}$$

where L is the length of the column, in cm; g is the weight of the adsorbent, in g.

From equations (2) and (3) we find

$$f(c) = -\frac{L}{g}\int_0^{c_*} \frac{\omega + q\sigma\left(\frac{\partial x}{\partial t}\right)_c}{\left(\frac{\partial x}{\partial t}\right)_c} dc \tag{4}$$

or

$$f(c) = \frac{1}{g}\int_0^c (v - v_0)\, dc, \tag{5}$$

where $v = L\omega \Big/ \left(\frac{\partial x}{\partial t}\right)_c$ is the volume of the gas carrier which has passed through the column of length L at the time of the appearance of the front with the concentration C at the outlet of the column; $v_0 = Lq\sigma$ is the free volume of the column.

Equation (5) shows that it is very easy to determine the adsorption isotherm from the experimentally obtained chromatographic desorption curve, v = v(c). The value of $\underline{v}$ can be expressed in terms of the indications of the detector according to the formula:

$$v = \frac{l}{u}\omega, \tag{6}$$

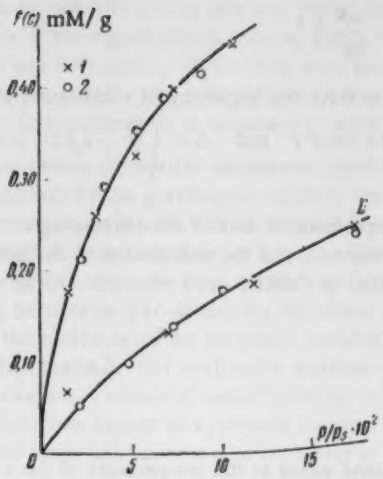

Fig. 4. Adsorption isotherm of heptane on MgO from $MgNO_3$ (I) and silica gel E (II). 1) Points obtained under static conditions by gravimetric method. 2) Points obtained by chromatographic method.

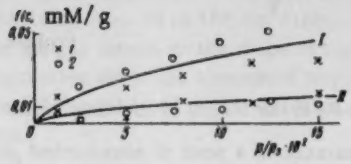

Fig. 6. Adsorption isotherm of heptane on a nickel catalyst (I) and ZnO + 14.5% $ZnSO_4$ (II). (The indications are the same as in Fig. 4.)

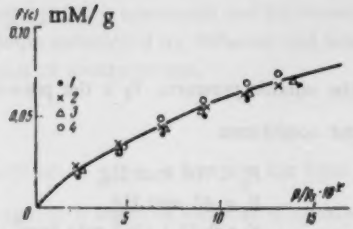

Fig. 7. Adsorption isotherm of heptane on heat resistant diatomaceous brick. Results from four parallel experiments.

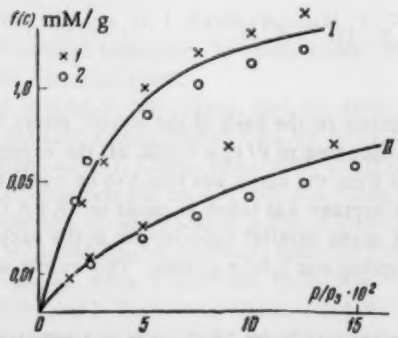

Fig. 5. Adsorption isotherm of heptane on silica gel 862 (I) and heat resistant diatomaceous brick (II). (The indications are the same as in Fig. 1.)

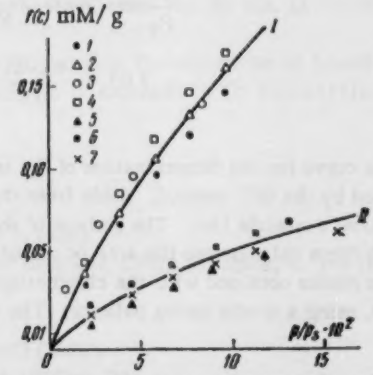

Fig. 8. Adsorption isotherm of heptane at different rates of flow (cm^3/min): On silica gel E (I): 1) 33; 2) 100; 3) 200; 4) 300. On brick (II): 5) 25; 6) 85; 7) 105.

$$c = K \cdot n, \tag{7}$$

where l is the length of the recorder chart from the beginning of the experiment, in cm; u is the chart speed, in cm/min; n is the deviation of the recording pen from the base line; and K is the constant of the detector, in mM/cm^3cm.

By substituting (6) and (7) into (5), we obtain

$$f(c) = \frac{\omega K}{ug} \int_0^n (l - l_0)\, dn = \frac{\omega K}{ug} S^*. \qquad (8)$$

Here l_0 is the length of the chart of the registering apparatus from the beginning of admittance of gas up to the appearance of a peak of nonadsorbed gas ($l_0/u = t_0$ is "dead time"; and $S = \int_0^n (l - l_0)\, dn$ is the area under the desorption curve (see Fig. 2a and 2b).

Equation (8) is the basic equation according to which the experimental data of the chromatogram are calculated. Results of the calculation of adsorption isotherms of heptane, and the calculation of the surface of the heat resistant diatomaceous brick calculated from it, are represented in Table 1 as an example. (The calculations refer to the chromatograph curve represented in Fig. 2a and 2b.)

$$\frac{P}{P_s} = \frac{K \cdot n\, 22{,}4\, P_0}{P_s}. \qquad (9)$$

Here P_0 is the outside pressure; P_s is the pressure of saturated heptane vapor at the temperature of the experiment.

For our conditions:

$P_0 = 750$ mm Hg — $\omega = 85$ cm³/mm
$P_s = 40$ mm Hg — $u = 0.3$ cm/min
$K = 2.75 \cdot 10^{-5}$ mM/cm³ · cm — $g = 3.390$ g

Temperature of the experiment, 23°.

If we substitute these values in (8) and (9) we obtain

$$\frac{P}{P_s} = \frac{2{,}75 \cdot 10^{-5} 22{,}4 \cdot 750}{40} \cdot n = 11{,}50 \cdot 10^{-3} \cdot n,$$

$$f(c) = \frac{85 \cdot 2{,}75 \cdot 10^{-5}}{0{,}3 \cdot 3{,}390} \cdot S = 2{,}3 \cdot 10^{-3} \cdot S.$$

The curve for the determination of the surface (Fig. 3) is drawn on the basis of the results, shown in Table 1, obtained by the BET method. Aside from the first point, corresponding to $P/P_s = 0.023$, all the experimental points follow a straight line. The surface of the brick calculated from the curve was found to be equal to 35 m²/g. In these calculations the area occupied by a molecule of heptane was taken as equal to 59.4 A [14]. To check the results obtained with the chromatographic method, we made parallel experiments in the vacuum apparatus, using a quartz spring balance. The sensitivity of the spring was 1.04 mg/mm. The weight was about 100 mg.

Before the experiments the sample was degassed up to constant weight for 1½-2 hours at a pressure of 10^{-5} mm Hg at 200°C. The adsorption isotherms were taken at 18°C.

Results Obtained

Figures 4, 5, and 6 represent the adsorption isotherms for heptane on samples of magnesium oxide and silica gel E, silica gel 862, brick, nickel catalyst, and ZnS + 14.5% $ZnSO_4$, obtained by the chromatographic method and under static conditions in vacuum.

Figure 7 shows that the results obtained in four parallel experiments by the chromatographic method are reproducible.

---

*Equation (8) leads to a simple method of calculating K from the area of the peak (Fig. 2b) on the curve. In the this case $K = (um)/(\omega S)$, where m represents the amount of material to be adsorbed introduced with the syringe (mM), $m = f(c) \cdot g$.

Figure 8 represents the isotherm of heptane on brick and silica gel at different rates of gas carrier flow; for silica gel the circulation rate was varied from 33 to 300, and for brick from 25 to 105 cm^3/min. Within the limits of the experimental error no effect of the rate of flow of the gas carrier on the shape of the adsorption isotherm was noticeable. This allows us to make a preliminary conclusion about the absence of any significant complication which could arise due to the kinetics of adsorption and the outer longitudinal diffusion. A further precision in measurement is necessary to make a definite statement.

The values of specific surface calculated from the adsorption isotherm, measured both chromatographically and in vacuum by the gravimetric method, are summarized in Table 2; the adsorbent was normal heptane. This table shows that within the limits of 250-0.2 m^2/g there is a satisfactory agreement between the results obtained chromatographically and those obtained under static conditions. However, the experiments described do not yet allow us to determine the limit within which the chromatographic method is applicable. First of all it would probably be necessary to determine the effect of the diameter of the pores of the adsorbent material, the dimensions of the molecule of the adsorbent material, the temperature, etc., on the precision and reproducibility of the results obtained. Our qualitative analysis of the effect of diffusional and kinetic factors showed that the agreement between the values of specific surface obtained by chromatographic measurement and by measurement under static conditions cannot be explained by mutual compensation effects introduced by diffusion and kinetics. To take these facts into account it is necessary to increase the precision of measurement.

SUMMARY

1. A chromatographic method for the measurement of adsorption of gases and vapors has been worked out.

2. It is shown that in the case of adsorption of normal heptane on a series of surfaces of catalysts and adsorbents there exists a satisfactory agreement between the adsorption isotherm obtained chromatographically and that determined in vacuum under static conditions.

LITERATURE CITED

1. V. A. Afanas'ev and A. M. Rubinshtein, Zavodskaya, Lab. 24, 830 (1958).
2. A. M. Rubinshtein and V. A. Afanas'ev, Peredovoi Nauch. Tekh. Opyt, tema No. 30, No. 11-57-98/8, 18 (1957).
3. B. V. Deryagin, N. I. Zakhavaeva, M. V. Talaev, and V. V. Filippovskii, Determination of Specific Surface of Powdered Substances by Measurement of Resistance to Filtration of Rarefied Air [in Russian] (Izd. AN SSSR, Moscow, 1957).
4. J. N. Wilson, J. Am. Chem. Soc. 62, 1583 (1940).
5. D. deVault, J. Am. Chem. Soc. 65, 532 (1943).
6. E. Glueckauf, J. Chem. Soc., 1302 (1947).
7. S. Z. Roginskii and M. I. Yanovskii, Zhur. Fiz. Khim. 24, 137 (1950).
8. E. Cremer, Z. anal. Chem. B 170, I, 219 (1959); F. Wolf and H. Beyer, Chem. Technik, 3, 143 (1959).
9. H. Weile-Molherbe, J. Chem. Soc., 303 (1953).
10. S. Classen, Arch. Kemi, Min. Geol. 23A, 1 (1946).
11. L. Graf and J. Toth, Acta Chim. Akad. Sci. Hung. 13, 3-4, 403 (1958).
12. S. J. Gregg and R. Stock, Das Chromatography (Amsterdam, 1958) p. 90.
13. S. N. Oziraner, G. A. Gaziev, M. I. Yanovskii, and V. S. Komyakov, Zavodskaya Lab. 25, 760 (1959).
14. H. K. Livingston, J. Colloid. Sci. 4, 447 (1949).

AROMATIZATION OF NARROW HEXANE FRACTIONS FROM GROZNY GASOLINE ON A CHROMIUM-ALUMINA CATALYST

B. A. Kazanskii, A. Z. Dorogochinskii, M. I. Rozengart,

A. V. Lyuter, and M. G. Mitrofanov

N. D. Zelinskii Institute of Organic Chemistry, Academy of Sciences of the USSR
Grozny Scientific Oil Research Institute
Translated from Kinetika i Kataliz, Vol. 1, No. 2, pp. 294-299,
July-August, 1960
Original article submitted February 13, 1960

Aromatization of n-hexane, n-heptane and narrow hexane fractions from Grozny gasolines has been carried out on chromium-alumina catalysts. It has been shown that in this way benzene can be obtained in considerable yields during working periods of more than 12 hours. Contamination by methylcyclopentane results in the deposition of coke, which poisons the catalyst; the same effect, but in a lesser degree, occurs with contamination by isohexanes. The catalysts isomerize n-hexane.

The large growth of petrochemical synthesis which will occur in our country in the next few years requires a great number of raw material resources. Benzene is one of the key points in the list of the various raw materials for synthesis. The benzene demand cannot be met by increasing its production from coal-tar or by an intensified extraction from straight run gasoline or from the products obtained by cracking.

The catalytic processes, for instance, platforming, now in use for the production of aromatic hydrocarbons and, in particular, benzene from oil, are mainly based on the aromatization of naphtenes containing six rings. Meanwhile the gasolines from the oils found in most of the eastern regions of the USSR have a preeminently paraffinic character and their naphtene content is very low. In this connection the dehydrocyclization of paraffinic hydrocarbons, and in particular, the conversion of n-hexane into benzene, becomes important again.

In this communication are reported the results obtained when aromatizing narrow hexane fractions from Grozny gasolines, n-hexane or n-heptane on a chromium-alumina catalyst KA.

As will be shown in the present investigation, during aromatization of n-hexane (550°) the catalyst is developed in the first three hours and the benzene yield increases; in the following six to seven hours it keeps a more or less constant level with an average of 69%, and after that it begins to fall, and at the end of a 24-hour working period it is about 50% (sampled in the last hour). Analogous results are obtained with heptane, as has been shown in the previous investigation [1] and follows from the experiments in the present study.

The aromatization of hexane fractions from straight run gasolines is complicated by the fact that they contain isohexanes and methylcyclopentanes. These impurities first of all lower the hexane content in the material to be aromatized, and in connection with this, the calculation based on the fraction fed gives a lower benzene yield. However, the decrease in benzene yield is not proportional to the lowering of the n-hexane concentration in the mixture to be aromatized, but is far more considerable, because methylcyclopentane and isohexanes not only dilute the n-hexane, but their presence also results in an increased deposition of coke on the catalyst and thereby poisons the latter. So the benzene yield from n-hexane in experiments lasting four hours was 65%, but the presence of 22% methylcyclopentane and 4% isohexanes in the mixture lowered the

TABLE 1

The Composition of the Gasoline Fractions (weight %)

Fraction	Boiling point	n-C_6H_{14}	2-Methyl-pentane	3-Methyl-pentane	Methylcyclo-pentane	C_6H_6
Hexane from Ozek-Suat oil	68	97.8	0.3	0.3	2.2	0
Fraction A	65-67	56.6	9.6	24.6	4.5	4.7
Fraction B	67-69	66.2	0.5	3.2	21.3	8.8
Fraction C	67-69	72.0	1.2	13.8	6.4	6.6

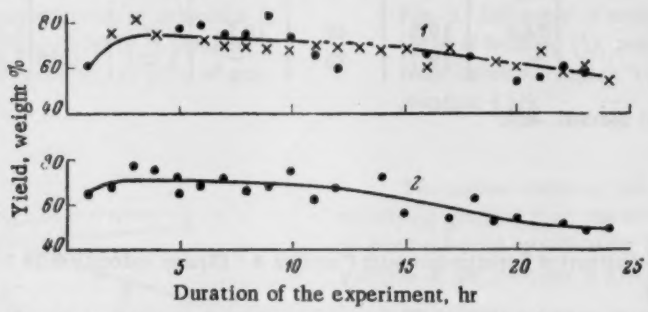

Fig. 1. Yield of aromatic hydrocarbons from n-heptane (1) at 550° (× is a parallel experiment) and from n-hexane (2) at 535° (space velocity 0.35 hr^{-1}).

benzene yield to 37%. At the same time the yield of gaseous products rose to 9% and coke to 10%, calculated on the feed; the yield of unsaturated compounds also increased from 4.5% to 10.9%.

During experiments lasting four hours at 550° and space velocity 0.37 hr^{-1} on one and the same catalyst sample the coke deposit when aromatizing n-hexane was 1.6%, when aromatizing a fraction containing 35% isohexanes it was 5%, and when aromatizing a fraction containing 22% methylcyclopentane it amounted to about 12%. Upon comparing these data it is obvious that methylcyclopentane poisons the catalyst more strongly than isohexanes do. This phenomenon obviously has to be explained by the fact that methylcyclopentanes and particularly methylcyclopentadienes polymerize more easily than isohexanes.

The negative role of methylcyclopentane and isohexanes is also apparent in the results of 12 hour experiments in a metallic apparatus containing 100 cc catalyst. When aromatizing n-hexane obtained from gasoline from Ozek-Suat oil and contaminated by 2.2% methylcyclopentane, the refractive index of the reaction product practically did not change during the whole experiment. For fractions containing 66% n-hexane and 21% methylcyclopentane the refractive index of the product decreased very considerably during the experiment. These results are also interesting because they show that from technical n-hexane nearly the same yield of benzene can be obtained as from pure n-hexane.

The aromatization of n-paraffins is more complicated than has been presumed formerly, and all its details are not clear as yet. In particular, the composition of the products obtained deserves a further investigation. By using gas-liquid chromatography (GLC) to analyze the reaction products we were able to detect the noticeable polymerizing action which the chromium-alumina catalyst exerts on paraffinic hydrocarbons: 2-methyl- and 3-methylpentanes were found to be present in the reaction products of the aromatization experiments with pure n-hexane.

The investigation has proved that it is certainly possible to obtain benzene in long working periods on a

TABLE 2

Results of the Aromatization Experiments (Temperature 550°, space velocity 0.37 hr^{-1}, duration 4 hr)

Expt. No.	Feed	Yield, in weight % on feed				$n^{20}D$ of the reaction product			Gas characteristics	
		gas	coke	benzene	unsaturated	first 2 hr	final 2 hr	for the entire expt.	spec. weight	H_2 content
1	n-Hexane	15.4	1.6	66	4.5	–	–	1.4670	0.193	96
2		13.9	1.9	64	–	–	–	1.4775	0.175	90
3	Mixture of n-hexane and dearomatized	22.0	8.1	44	–	–	–	1.4416	0.306	86
4	fraction B	20.0	6.2	49*	–	1.4538	1.4420	1.4480	0.263	85
5	Dearomatized	24.2	10.3	40	10.9	–	–	1.4429	0.330	86
6	fraction B	–	13.7	35	–	1.432	1.4210	1.4325	0.250	85

*Yield of benzene by GLC method, 46%.

TABLE 3

Results of Aromatization Experiments with Fraction A (Space velocity 0.36 hr^{-1}; duration 4 hr)

Experiment No.	Temperature, °C	Yield, in weight % on feed			
		gas	coke	benzene	hexenes
8	510	9.3	3.7	24	4.5
9	535	14	5.4	33	4.7
10	550	22	5.1	36	4.2

chromium-alumina catalyst not only from pure paraffins but also from hexane fractions with a high n-hexane content. The study has permitted evaluating the role played by the various components during the aromatization of narrow gasoline fractions. Moreover, it has been detected that isomerization of straight chain paraffinic hydrocarbons takes place during the aromatization of n-hexane on a chromium-alumina catalyst.

EXPERIMENTAL

The experiments were carried out in the flow system, the details of which have been described previously [1], with pyrex or quartz tubes containing 20 cc catalyst. We have also used an apparatus with an ÉYa-1T stainless steel reactor containing 100 cc catalyst. In the latter case the feed was supplied by a pump from a heated (300°) buret which was directly connected to the reactor. Leaving the latter, the reaction products entered a separator trap cooled by ammonia; the gases passed were collected in a gasometer.

The aromatic hydrocarbon content was determined from the refractive index of the reaction product, using calibrated graphs [1] or by the GLC method [2]. The deviation between these was generally 1-3 absolute % and did not exceed 5%. The unsaturated hydrocarbon content was determined bromometrically using the Kaufmann-Gal'pern method [3] or by conductometric titration [4]. Normal hexane and heptane were prepared from commercial samples by filtration through silica gel [15] and rectification. According to the GLC data n-hexane contained only 0.3% isohexanes, and n-heptane was free of contaminations. The hydrocarbons obtained had the following characteristic constants: n-hexane, b.p. 68.8°; $n^{20}D$ 1.3748; d^{20}_4 0.6592; n-heptane, b. p. 98.4°; $n^{20}D$ 1.3878, d^{20}_4 0.6836.

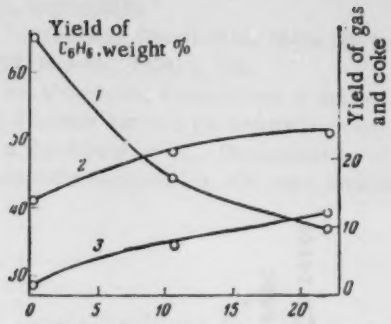

Fig. 2. Influence of the methylcyclpentane content on the aromatization of n-hexane at 550° (space velocity 0.37 hr^{-1}; duration 4 hr): 1) yield of benzene; 2) yield of gas; 3) yield of coke.

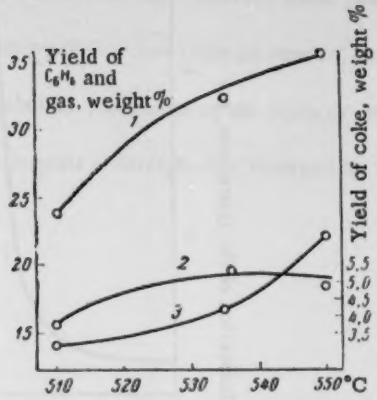

Fig. 3. Influence of temperature on the yield of benzene (1), coke (2) and gas (3) from fraction A (space velocity 0.37 hr^{-1}; duration 4 hr).

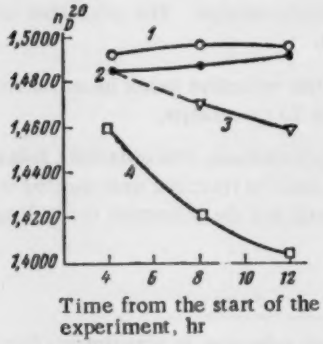

Fig. 4. Change in the refractive index of the reaction product when aromatizing various feeds: 1) hexane from Ozek-Suat gasoline; 2) n-heptane; 3) fraction C; 4) fraction B.

The narrow fractions to be fed were obtained by rectifying gasoline from the Grozny oil-distillation plant in semitechnical rectification columns. The composition of the fractions is given in Table 1.

The catalyst used contained 15 mole % Cr_2O_3, 82 mole % Al_2O_3 and 3 mole % K_2O. To characterize its aromatizing properties aromatization experiments were done with n-hexane at 550° and with n-heptane at 535° and space velocity 0.35 hr^{-1}, each experiment lasting 24 hr. After each experiment the catalyst was regenerated during 24 hr. As may be seen in Fig. 1, in both cases the yield of aromatic hydrocarbons changes with time in the same way.

The maximum yield of benzene was 69% that of toluene 75%; that is, the catalyst showed a high aptitude for aromatization. The yield of unsaturated compounds changed from 5.8% to 10.8% at the end of the experiment on hexane, and from 3 to 7.8% for heptane.

The influence of methylcyclopentane upon the aromatization of hexane was studied at 550° and space velocity 0.37 hr^{-1} during experiments lasting four hours. As feeds served: 1) n-hexane, 2) a mixture of n-hexane and the dearomatized fraction B (the mixture contained 11% methylcyclopentane), and 3) the dearomatized fraction B (73 weight % n-hexane, 23% methylcylopentane and 4% isohexanes). The results of the experiments are given in Table 2 and Fig. 2.

When the methylcyclopropane content in the feed is raised, the formation of coke increases almost linearly from 1.8% in experiments with pure hexane to 12% in experiments with the dearomatized fraction. This also resulted in a very diminished yield of benzene in the latter case: the yield of benzene dropped from 65 to 37%.

The influence of temperature upon the aromatization of a narrow hexane fraction was investigated at 510, 535, and 550° for fraction A containing 35% isohexanes as an example. The experimental conditions were the same as stated above. The results are given in Table 3 and Fig. 3. Raising the temperature from 510 to 550° results in increasing the yield of benzene from 24 to 36%, of gas from 9 to 22%, of coke from 3.7 to 5.1%. Cracking, which is accompanied by the formation of gas, is particularly intensified at the end of the temperature range investigated.

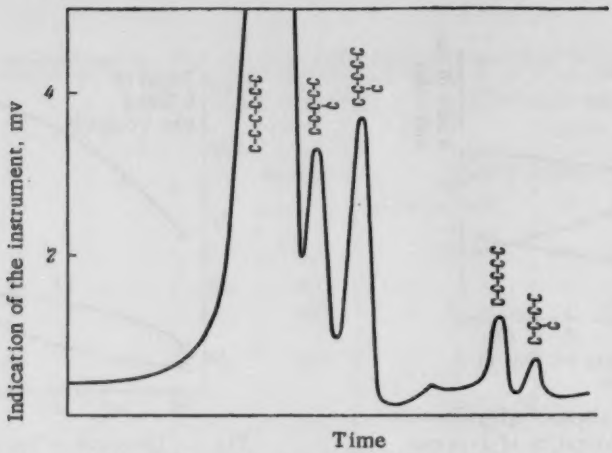

Fig. 5. Chromatogram for the paraffinic part of the reaction product from n-hexane.

Comparative experiments which lasted 12 hours, on the aromatization of n-paraffins and narrow fractions were carried out in a metallic apparatus with a reactor containing 100 cc catalyst. The refractive indices of the reaction product, collected at four-hour intervals, are given in Fig. 4.

When aromatizing a single n-paraffin, namely heptane (535°), the refractive index increases somewhat during the experiment, as was also the case in the glass apparatus with 20 cc catalyst.

When aromatizing Ozek-Suat hexane containing 2.2% methylcyclopentane, the refractive index practically does not change during the experiment (the experiments with hexane and the fractions were carried out at 550°). As the methylcyclopentane content is increased, the catalyst is poisoned and the refractive index drops (curves 3 and 4).

Investigation into the Composition of the Reaction Products

Upon investigating the composition of the products obtained from n-hexane in experiments Nos. 1 and 2 by means of the GLC method, we found peaks corresponding with 2-methylpentane and 3-methylpentane to be present. In the products of cracking appear branched hydrocarbons containing four and five carbon atoms. The paraffinic part of the reaction product from n-hexane was isolated by filtering through silica gel, and its chromatogram is shown in Fig. 5. According to the GLC data the reaction product of n-hexane contained about 3% isohexanes.

SUMMARY

1. Aromatization of n-hexane, n-heptane and narrow fractions from Grozny gasoline has been carried out on chromium-alumina catalysts. It has been proved that benzene can be obtained at atmospheric pressure from hexane fractions with a high n-hexane content during long working periods surpassing 12 hours.

2. It has been found that the poisoning action during hexane aromatization caused by deposition of coke on the catalyst is more profound for contamination by methylcyclopentane than for that by isohexanes.

3. It has been revealed that on chromium-alumina catalysts n-hexane is isomerized during the aromatization.

LITERATURE CITED

1. M. I. Rozengart and B. A. Kazanskii, Doklady Akad. Nauk SSSR 119, 716 (1958).*

*Original Russian pagination. See C. B. translation.

2. A. A. Zhukhovitskii, B. A. Kazanskii, O. D. Sterligov, and A. M. Turkel'taub, Doklady Akad. Nauk SSSR 123, 1037 (1958).*
3. G. D. Gal'pern, Transactions of the Oil Institute of the Academy of Sciences USSR [in Russian] (Izd. AN SSSR, Moscow, 1954) p. 140.
4. D. M. Musnikova, Transactions of the Second Scientific-Technical Conference at the Grozny Scientific Oil Research Institute [in Russian] (Grozny, 1957) p. 446.
5. G. S. Landsberg et al., Determination of the Separate Components of Straight Run Gasolines by a Combined Method [in Russian] (Izd. AN SSSR, Moscow, 1959).

*Original Russian pagination. See C. B. translation.

DEHYDROGENATION OF n-DECANE ON OXIDE CATALYSTS

E. A. Timofeeva, V. S. Smirnov and V. I. Zaeva

Institute of Organic Chemistry, Academy of Sciences of the USSR
Translated from Kinetika i Kataliz, Vol. 1, No. 2, pp. 300-305,
July-August, 1960
Original article submitted February 22, 1960

It has been proved that the dehydrogenation of n-decane on oxide catalysts can be carried out practically selectively with a 11% yield of alkenes, of which 76% are decenes. Meanwhile almost no aromatic hydrocarbons are formed.

As is well known [1], nowadays the main methods to obtain high-molecular olefins are: 1) thermal cracking of paraffins; 2) synthesis from CO and H_2 on iron or cobalt catalysts; 3) polymerization of olefins and 4) dehydration of higher alcohols. The products obtained by the first and the second (on iron catalysts) method consist mainly of a mixture of straight-chain α-olefins with different molecular weights. When the synthesis from CO and H_2 is carried out on cobalt catalysts, one obtains a considerably smaller amount of olefins than is found on iron; in these olefins the double bond is located in various positions. By the third method there are formed more or less branched hydrocarbons with the double bond in the center. Ziegler polymerization of ethylene results in the formation of straight-chain α-olefins with an even number of carbon atoms. Finally, the fourth way to obtain high-molecular olefins is applied only in special cases, since the alcohols are a relatively expensive basic material. In this way one obtains a mixture of straight-chain isomers.

High-molecular olefins have a extremely broad field of application. They are used, for instance, in oxosyntheses, in syntheses of lubricating greases, wetting agents, oil additions, corrosion inhibitors and so on.

The development of new methods to obtain olefins of the composition C_6 and higher, undoubtedly, is a pressing problem. In our studies we have found the conditions under which n-hexane [2] and n-nonane [3] are dehydrogenated selectively on a chromium-alumina catalyst. In the present study the dehydrogenation of n-decane has been investigated for the purpose of obtaining decenes. Meanwhile we also aimed at finding such conditions that the aromatization of n-decane would be reduced to a minimum. When n-decane is dehydrogenated on oxide catalysts, one should expect that there is formed a mixture of decenes having the double bond near to the middle of the molecule, since olefins with double bonds in the inner part of the molecule are the most stable. This has been proved, for instance, by calculations of the equilibrium concentrations of pentenes [4] and hexenes [5] and also by experimental data on the dehydrogenation of n-nonane [3].

In the literature there are no papers specially devoted to study of the dehydrogenation of n-decane, but there are investigations into its catalytic aromatization and cracking [6-8]. The aromatization of n-decane on a chromium-alumina catalyst has been investigated in most detail in the study by L. M. Rozenberg [8]. At 450, 470, and 500° and space velocity 0.25 hr^{-1} the yield of aromatic hydrocarbons was 31-60%. He also observed that olefins were formed, of which a great part (~10% of the product) seemed to be decenes, according to the boiling points of narrow fractions from the reaction product.

TABLE 1

The Influence of Temperature and Space Velocity upon the Formation of Olefins and Aromatic Hydrocarbons on a Chromium-Alumina Catalyst

Temperature, °C	Space velocity, hr^{-1}	Yield of reaction product, weight %	Amount of gas, liters (STP)	Product properties			
				$n^{20}D$	Iodine number	Provisory olefin content, %	Aromatic content, %
475	0.5	89.5	20.2	1.4404	28.1	15.5	24
475	2.1	93.8	10.1	1.4257	21.4	11.8	11
475	4.2	97.2	5.6	1.4195	17.4	9.6	6
500	2.1	90.4	13.5	1.4294	25.5	14.1	16
550	0.5	63.1	29.4	1.4485	54.6	30.1	38
550	2.1	77.6	20.3	1.4344	40.7	22.5	26

Note. The experiments of this series were carried out on a catalyst the activity of which had been lowered by irreversible poisoning with water.

TABLE 2

Conversion of n-Decane on the Catalysts, Chromium-Alumina and K-5, at the Space Velocity 2.1 hr^{-1}

Catalyst	Temperature, °C	Yield of product, %	Amount of gas, liters (STP)	Product properties			
				$n^{20}D$	Iodine number	Provisory olefin content, %	Aromatic content, %
Chromium-alumina	500	90.4	13.5	1.4294	25.5	14.1	16
K-5	500	98.5	7.2	1.4200	25.4	14.0	5
Chromium-alumina	550	77.6	20.3	1.4344	40.7	22.5	26
K-5	550	83.0	11.9	1.4199	43.6	24.0	10

TABLE 3

Influence of Temperature upon the Formation of Olefins and Aromatics on K-5 at the Space Velocity 2.1 hr^{-1}

Temperature, °C	Yield of product, %	Amount of gas, liters (STP)	Product properties			
			$n^{20}D$	Iodine number	Provisory olefin content, %	Aromatic content, %
450	98.9	2.0	1.4153	12.6	7.0	1.0
500	98.5	7.2	1.4200	25.4	14.0	5.6
550	83.0	11.0	1.4199	43.6	24.0	10.0
	(88.1)	(7.0)	(1.4136)	(35.5)	(19.6)	(2)

Note. The results of a second experiment carried out without regenerating the catalyst are given in parentheses.

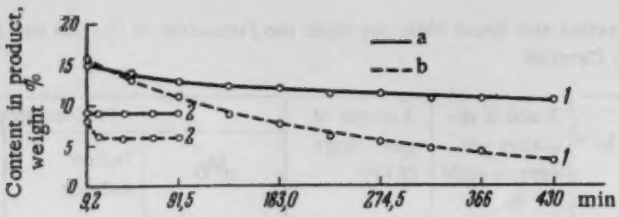

Fig. 1. Influence which the duration of the working period between the regenerations of a chromium-alumina catalyst has upon the formation of olefins (a) and aromatic hydrocarbons (b): 1) 475°, 2.1 hr^{-1}; 2) 475°, 4.2 hr^{-1}.

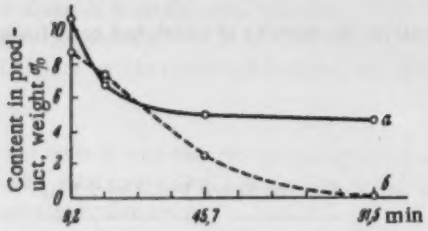

Fig. 2. Influence which poisoning of a chromium-alumina catalyst has upon the yield of olefins (a) and aromatic hydrocarbons (b) (475°; 2.1 hr^{-1}).

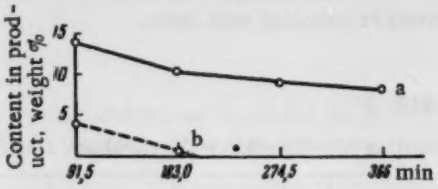

Fig. 3. Influence which the working period between regenerations of catalyst K-5 has upon the formation of olefins (a) and aromatic (b) hydrocarbons (500°; 2.1 hr^{-1}).

EXPERIMENTAL

The dehydrogenation of n-decane was carried out on two oxide catalysts: on chromium-alumina containing 94.2 mole% Al_2O_3 and 5.8 mole% Cr_2O_3 (the method of preparing the catalyst has been described previously [9]) and an industrial K-5 catalyst. It was investigated what influence temperature, space velocity and duration of the working period between catalyst regenerations have upon the yields of olefins and aromatic hydrocarbons. We have also carried out experiments on the dehydrogenation of n-decane on a chromium-alumina catalyst which had been poisoned by water, since there are indications in the literature [10] that water poisons a chromium-alumina catalyst more with respect to the dehydrocyclization of alkanes than with respect to the dehydrogenation. Styrene was also used as poison.

The method of carrying out the experiments and analyzing the products has been described in the paper [9]. The catalyst tube contained 30 cc catalyst; n-decane (b.p. 174°; $n^{20}D$ 1.4118; d^{20} 0.7293) was fed from a syringe (100 ml hydrocarbon was taken for each experiment), and as a rule, after this the catalyst was regenerated. Not only the reaction product obtained during the complete experiment but also samples for each 10 ml n-decane fed were analyzed. For a series of reaction products we took distillation curves in a column with 40 effective theoretical plates in order to determine the degree of cracking. The decenes were isolated by chromatography on silicagel treated with HCl and H_2O_2 according to the method of A. V. Topchiev and co-workers [11]. In the paraffinic part of the reaction product a qualitative estimation of tertiary carbon atoms was executed according to E. M. Terent'eva and L. M. Rozenberg [12].

Dehydrogenation of n-Decane on a Chromium-Alumina Catalyst

To examine the influence which temperature and space velocity has on the amount of paraffinic and aromatic hydrocarbons in the reaction product we have carried out experiments at 475, 500, and 550° and at space velocities 0.5, 2.1, and 4.2 hr^{-1}. The results obtained are given in Table 1.

It should be remarked that we used the molecular weight of decenes when deriving the olefin content from the iodine number. In reality the products contain a certain amount of alkenes which are formed by cracking and have a lower molecular weight than that of decenes. The higher the temperature of the experiment and the lower the space velocity at which the hydrocarbon is fed, the higher goes the degree of cracking, and consequently the more the data on the olefin content of the product, as they are given, differ from the actual ones. Therefore, in the tables the olefin content is given only with due reserve, and the iodine number is mentioned also.

When at the space velocity 2.1 hr^{-1} the temperature is raised from 475 to 550°, the olefin content in the product increases from 11.8 to 22.5% and the aromatic hydrocarbon content from 11.0 to 25.8%. Raising at 475° the space velocity from 0.5 to 4.2 hr^{-1} results in lowering the olefin content from 15.5 to 9.6% and the aromatic hydrocarbon percentage from 24.2 to 6.2% (see Table 1).

Upon distilling the reaction product obtained at 475° and 0.5 hr^{-1} from n-decane we isolated a decane-decene fraction (166-176°) in the amount of 74% of the entire product. This fraction contained 10.5% olefins (69% of all olefins formed) and 10.3% aromatic hydrocarbons.

Further, we have experimentally examined the influence which the duration of the working period between succesive regenerations of the catalyst has upon the formation of olefins and aromatic hydrocarbons. The temperature of the experiment was 475°, the space velocity 2.1 or 4.2 hr^{-1}. The results obtained are shown in Fig. 1. The olefin content in the reaction product obtained at a space velocity 2.1 hr^{-1} falls from 15% at the start of the experiment to 10% at the end, while the yield of aromatic hydrocarbons decreases by five times, from 16 to 3%. At the space velocity 4.2 hr^{-1} the yield of olefins stays at one level during the whole experiment; the aromatic hydrocarbon content in the reaction product is lowered from 8 to 6% in the first 18 minutes, but after that it remains constant.

Poisoning of the chromium-alumina catalyst by water was studied in the following way: n-decane was fed from a syringe at a space velocity 2.1 hr^{-1} and at temperature 475°, and simultaneously from another syringe water was admitted to give the ratio 0.38 mole water to 1 mole hydrocarbon. As a result of the poisoning by water, the olefin/aromatic ratio increased from 1.0 to 2.0. However, meanwhile the absolute olefin content was lowered from 12% before poisoning to 6% on the poisoned catalyst. The curves for dehydrogenation and aromatization of n-decane on a poisoned catalyst are shown in Fig. 2. It should be remarked that after this series of experiments had been carried out the activity of the catalyst was lowered irreversibly, though not very profoundly: the content of olefins and aromatics in the product had fallen by 2-3%.

Further, we have investigated the effect of styrene in lowering the aromatizing property of the catalyst. Styrene (5 ml) was fed into the system at a space velocity 2.1 hr^{-1} at 500°. The experiments were carried out after the decomposition products of styrene had been expelled by nitrogen. The poisoning of the catalyst by styrene resulted in lowering the yield of olefins by 3% and of aromatic hydrocarbons by 5.5%, and the ratio of these yields increased all in all only from 0.80 to 0.88.

Thus, we have not as yet obtained promising results from our experiments on poisoned catalysts.

Dehydrogenation of n-Decane on the Catalyst K-5

To compare the catalysts, the chromium-alumina and K-5, as to dehydrogenation and dehydrocyclization of n-decane, comparative data are assembled in Table 2.

It is striking that on K-5 the formation of aromatic hydrocarbons is considerably less than on the chromium-alumina catalyst (by 3 times at 500° and by 2.5 times at 550°) and that the yields of reaction product are higher (at 500° by 8%, at 550° by 5%). On both catalysts practically equal amounts of olefins are formed.

The results of experiments in which the influence of temperature upon the formation of olefins and aromatic hydrocarbons from n-decane on catalyst K-5 was investigated are given in Table 3.

On K-5, just as is the case on the chromium-alumina catalyst, raising the temperature from 450 to 550° is accompanied by an increased content of olefins (from 7.0 to 24%) and aromatic hydrocarbons (from 1 to 10%).

The product obtained from n-decane at 550° in the second experiment was rectified. In this, 80% was isolated as the decane-decene fraction boiling in the range 166-176°. In this fraction was detected not more than 6% olefins and 2% aromatic hydrocarbons. As the fraction boiling below 166°, 16% was isolated. Its iodine number

was 150, and the olefin content (from the average molecular weight) was 61%. So under these conditions a strong cracking takes place and the main part of the olefins formed appears as the mixture with the boiling point below that of the decenes.

In Fig. 3 is shown how the content of olefins and aromatic hydrocarbons in the product at 500° and space velocity 2.1 hr^{-1} depends upon the duration of the working period between regenerations of the catalyst. Altogether 400 ml n-decane was fed to the catalyst in four experiments (each lasting 91.5 min). The gas liberated in these experiments consisted of 89.2% hydrogen, 3.5% unsaturated hydrocarbons and 7.3% saturated ones. From the graph shown it is obvious that the olefin content falls from 14% in the product obtained from n-decane in the first experiment to 9% in that of the fourth experiment. From the start of the second experiment aromatic hydrocarbons are no longer formed.

The reaction product of n-decane assembled for these four experiments (yield 98.8%) had $n^{20}D$ equal to 1.4153 and contained 10.5% olefins and 1.3% aromatic hydrocarbons; 95.5% of this product could be distilled in the boiling range (166-176°) of n-decane and decenes. Here was concentrated about 76% of all olefins formed. Up to 166° no more than 2% of the product was boiled away; 80% of this came from olefins (estimated from the mean molecular weight).

The C_{10} fraction of this product underwent chromatographic separation on silica gel, and an olefin concentrate was obtained in the amount of 6.2 ml with $n^{20}D = 1.4224$ consisting, obviously, of 85% of decenes. Aromatic hydrocarbons were absent. In the same way pure (judging from the iodine number) olefins in the amount of 1.5 ml were isolated from the product obtained from n-decane at 450° and space velocity 2.1 hr^{-1} on K-5. The olefins had a refractive index $n^{20}D = 1.4272$, which is close to the value for decene-5. In reference [13] the following values are given for $n^{20}D$ of the individual decenes: decene-1) 1.4220; decene-2) 1.4217; decene-3) 1.4231; decene-4) 1.4253; and decene-5) 1.4260. When analyzing the fractions isolated from the product of n-decane conversion at 500° and space velocity 2.1 hr^{-1} on the catalyst K-5, by means of combined light scattering*, it was found that, most probably, they contain decene-4 or decene-5, while decene-1 is absent. The test for tertiary carbon atoms in the paraffinic part of the product gave a negative result. Its constants coincided with the values of the n-decane fed.

In conclusion we seize the opportunity to express our thanks to N. I. Shuikin for valuable advice and for giving permission to execute the study at the organic catalysis laboratory of the Institute of Organic Chemistry of the Academy of Sciences, USSR.

SUMMARY

1. The conversion of n-decane at various temperatures and space velocities has been investigated on two catalysts, a chromium-alumina and a technical one, K-5.

2. Conditions for the selective dehydrogenation of n-decane on the catalyst K-5 were found such that the reaction product was obtained with a yield of 98.8% and contained 11% alkenes; about 76% of the latter were decenes. Aromatic hydrocarbons were practically absent in the reaction product. The paraffinic part of the product appears to be mainly unchanged n-decane.

LITERATURE CITED

1. F. Asinger, Chemie und Technologie der Monoolefine (Akademie Verlag, Berlin, 1957).
2. E. A. Timofeeva et al., Doklady Akad. Nauk SSSR, 125, 1272 (1959).**
3. E. A. Timofeeva et al., Doklady Akad. Nauk SSSR 129, 128 (1959).**
4. E. A. Timofeeva and N. I. Shuikin, Izvest. Akad. Nauk SSSR, Otdel. Khim. Nauk 570 (1953).**
5. E. A. Timofeev, V. S. Smirnov and Yu. N. Plotnikov, Izvest. Akad. Nauk SSSR, Otdel. Khim. Nauk 1433 (1959).**
6. V. I. Karzhev, M. Sever'yanova and A. Siova, Khim. Tverd. Topliva 559 (1936).
7. V. I. Karzhev and P. Z. Sorokin, Zhur. Fiz. Khim. 12, 42 (1938).
8. L. M. Rozenberg, Doklady Akad. Nauk SSSR 73, 719 (1950).

*The analysis was carried out by N. S. Andreev, co-worker at the Institute of Organic Chemistry of the Academy of Sciences USSR, and we thank him for it.

**Original Russian pagination. See C. B. translation.

9. E. A. Timofeeva, N. I. Shuikin, T. P. Dobrynina, G. S. Petryaeva and Yu. N. Plotnikov, Izvest. Akad. Nauk SSSR, Otdel. Khim. Nauk 292 (1960).*
10. W. J. Mattox, J. Am. Chem. Soc. 66, 2059 (1944).
11. A. V. Topchiev, E. Kh. Iskhakova, I. A. Musaev and G. D. Gal'pern, Khim. i Tekhnol. Topliva 11, 26 (1957).
12. E. M. Terent'eva and L. M. Rozenberg, Izvest. Akad. Nauk SSSR, Otdel. Khim. Nauk 385 (1959).*
13. Faraday's Encyclopedia of Hydrocarbon Compounds (Manchester, 1949) Vol. 7, No. 2.

*Original Russian pagination. See C. B. translation.

INVESTIGATION OF ORTHO-PARA-HYDROGEN CONVERSION ON SOLID CATALYSTS AT 78-64°K. COMMUNICATION I

R. A. Buyanov

Dubna Joint Institute of Nuclear Investigations
Translated from Kinetika i Kataliz, Vol. 1, No. 2, pp. 306-312,
July-August, 1960
Original article submitted March 16, 1960

By analyzing the magnetic properties of ions, catalysts were selected for the ortho-para-hydrogen conversion in the temperature range 78-64°K and pressures from 60 mm Hg to 150 atm.

Characteristics of the catalysts, the method of preparation and activation, and also the working conditions are given. It has been determined how the rate constant for the reaction of these catalysts depends upon temperature and pressure.

The rapid development of low temperature technique has made the following problems quite immediate: how can liquid hydrogen be stored for a long time, what are the heat balances during its utilization and so on?

As is well known, hydrogen usually consists of a mixture of two modifications, which differ in nuclear spin: ortho- and para-hydrogen. These modifications can be converted into each other by reaction $p\text{-}H_2$ + 340 cal/mole $\rightleftharpoons o\text{-}H_2$. The equilibrium constant of this reaction changes with temperature from K = 3.0 at T > 300° to K = 0.00 at T < 20°K.

Therefore, when liquefying ordinary hydrogen, which at normal temperature contains about 75% ortho-hydrogen, one obtains liquid hydrogen which is not in equilibrium with respect to the ortho modification. Subsequently there takes place a slow spontaneous conversion into the para modification until the content of ~99.8% $p\text{-}H_2$ is attained. This process is accompanied by the evolution of a great amount of internal heat, which is the main obstacle to prolonged storing of liquid hydrogen and plays an essential role in the heat balances for many processes. Obviously it is advantageous to carry out the reaction before liquid hydrogen is drawn from the liquefier. In this paper the results of a search for the most active catalysts, which accelerate the reaction directly in liquefier, are communicated and the main characteristics of the catalysts are given.

Selection, preparation and characteristics of the catalysts. As is well known, the low temperature mechanism of ortho-para-hydrogen conversion does not proceed by splitting the hydrogen molecule into atoms but by the reorientation of the nuclear spins within one molecule [1]. This mechanism takes place in the strongly inhomogeneous magnetic field of the paramagnetic molecules in the catalyst. The rate of such a reorientation will be [2, 3] proportional to the square of the effective magnetic moment μ_{eff} of the catalyst molecule; when expressed in Bohr magnetons this moment is equal to

$$\mu_{eff} = 2\sqrt{S(S+1)} = \sqrt{n(n+2)}, \quad (1)$$

where S represents the resultant spin moment of the catalyzing ion; n the number of unpared electrons of that ion.

This relation does not take into account the orbital moment of the ion, since in polyatomic molecules, as a rule, this moment is "frozen in" and does not manifest itself [4].

TABLE 1

Dependence of the Rate Constant Upon the Granule Size of Chromium-Nickel Catalyst (T = 78°K)

d, cm	1/d, cm^{-1}	mole · g^{-1} · sec^{-1}
0,44	2,27	$3,6 \cdot 10^{-4}$
0,342	2,92	$4,35 \cdot 10^{-4}$
0,21	4,8	$8 \cdot 10^{-4}$
0,095	10,5	$2,00 \cdot 10^{-3}$

It is obvious that, starting from these considerations, the approach to solve the problem how to select catalysts for the said reaction will be a very rational one. From this point of view elements of the transition series with partly filled 3-d, 4-d, 5-d or 4-f electron shells are the most interesting. Certain rare earth elements have the highest effective magnetic moment. However, because of their high price they are more of theoretical than of practical interest for our purpose. An inspection of all other elements leads to the conclusion that catalysts in the form of the hydroxides with Cr^{3+}, Mn^{4+}, Fe^{3+}, Co^{3+}, and Ni^{2+} ions, which have partly filled 3-d shells, will be the very best ones.

These hydroxides have a highly developed surface area (100-300 m^2/g) and, as will turn out, they show in a high degree the properties of magnetically diluted compounds. The dilution of their magnetic ions by hydroxyl groups obviously will nearly or completely eliminate exchange effects and other phenomena, which generally are associated with antiferromagnetism [4]. We have tried to define more precisely the structure of the gels investigated. However, the x-ray and electron photographs of iron and chromium hydroxides, which were taken for this purpose, gave very diffuse lines corresponding to a finely dispersed crystalline structure, but it was impossible to interpret them.

The $Cr(OH)_3$, $Fe(OH)_3$ and $Ni(OH)_2$ gels were obtained by precipitation from the chloride or the nitrate of the corresponding metal in a dilute solution of a weak base; $Mn(OH)_4$ by the reduction of a permanganate solution with ethyl alcohol. $Co(OH)_3$ was obtained by precipitating the hydroxide of bivalent cobalt under simultaneous oxidation in a solution of calcium hypochlorite to the trivalent compound. By decantation they were freed of foreign ions, then filtered, rinsed and dried at a temperature of 40°C. The more dilute the solutions that were used for the precipitation, and the more slowly the latter was carried out, the better were the catalytic and mechanical properties of the products finally obtained. After drying, the $Fe(OH)_3$ gel was heated at 135°C and the other gels at 90-100°C during 24 hours. After the heating the lumps were broken to the sizes required.

Besides the gels indicated, chromium-nickel, palladium, and platinum catalysts [5] of industrial origin, activated charcoal (brand AG-4), and the oxides Cr_2O_3, NiO, and Fe_2O_3 have been tested. The oxides were obtained from the corresponding hydroxides by heating during 8 hours at 500-600°C. The platinum and the palladium catalyst were metallic blacks deposited on tablets pressed from active alumina and containing 4.9 and 4.7 g metal, respectively, per liter of catalyst.

All gels and active charcoal were activated by outgassing to the pressure of $1 \cdot 10^{-2}$ mm Hg with warming them up in 24 hours to just that temperature at which they had been heated during the preparation. After that the heating was stopped, and the reactor was filled with pure hydrogen.

As was found, this was the best method to activate the gels. So, the gels had a considerably lower activity when they were outgassed without warming up or when pure and dry hydrogen was simply passed through the gels, and this activity was the lower the more time had elapsed between the heating in the final stage of preparation and the filling in the reactor in order to start activation. Obviously, the activity of the gels is lowered considerably because moisture is taken up from air during storage. On the other hand, more rigorously heating the reactor during activation results in decomposing the gels and sharply lowering their activity.

In the flow system the chromium-nickel, platinum, and palladium catalysts were activated by passing hydrogen at 140°C during 24 hours at a space velocity of 4000 hr^{-1}, and in the static one, at 250°C during eight hours. For these catalysts activating in such a way turned out to be the best method. In the case of gels it gave no advantages. When air got into a reactor filled with the chromium-nickel catalyst, the latter lost irreversibly its activity by the oxidation of the nickel black. As depended upon the duration of the contact with air, the activity of all other catalysts was lowered by two or more times, but it was recovered when activating again.

For all catalysts (hydroxides, oxides, and chromium-nickel) studied in the circulating system we used granules with a diameter of 0.98-0.70 mm.

By the static method were studied a platinum catalyst in the form of tablets with d = 4.6 mm and l = 5.5-6 mm, a palladium catalyst with d = 5.6 mm and l = 7.6-8 mm, and an iron catalyst in the form of fragments with 3.5-5 mm edges. Moreover, granules of a chromium-nickel catalyst were investigated in various sizes (d = 1-4.4 mm) in order to determine the influence of transfer processes.

Experimental method and conditions of the investigation. In the present study are given the results obtained when investigating catalysts in the temperature range 78-64°K at pressures from 60 mm Hg to 150 atm. The experiments at absolute pressures from 60 to 600 mm Hg were carried out under static conditions while circulating the gas in the circuit by means of a glass pump driven magnetically.

The hydrogen for these experiments was obtained in a glass electrolyzer, and it was carefully purified. It was freed of oxygen on a palladium catalyst, from the main mass of moisture on silica gel, and from nitrogen and the other contaminations in a trap filled with activated charcoal and placed in liquid nitrogen. After this purification the hydrogen was passed through a separate reactor with palladium catalyst at 150°C where equilibrium corresponding to 75% o-H_2 was established. Samples to be analyzed were taken during the course of the reaction, and this analysis was carried out by means of heat conduction in a gas analyzer specially constructed for this purpose [1].

The experiments were conducted in a flow system, at pressures from 2 to 150 excess atmospheres. Hydrogen purified in a continuous liquefier and compressed into a cylinder was the source of pure gas. In order to establish equilibrium of the ortho and para modifications, the gas compressed into the cylinder was passed over palladium catalyst. In these experiments the gas was analyzed continously in a gas analyzer by means of heat conductivity [6].

In both cases the reactors were cryostatted in liquid nitrogen at normal pressure or in nitrogen at the triple point.

Relations used for calculation. The results were calculated by means of the equation for first order reaction. For the reaction under static conditions with circulation the rate equation has the form:

$$n_к \frac{dC}{dt} = kV_к (1 - C/C_e), \tag{2}$$

where k represents the rate constant, mole · cm^{-3} · sec^{-1}; n_K the number of moles in the system, mole; V_K the amount of catalyst in the reactor, cc; t time from the start of the experiment, sec; C_0, C_e, C the initial and equilibrium concentration of para-hydrogen (%) and that at the time t, respectively.

Integrating this equation and taking into account the boundary conditions gives the following relation for the rate constant:

$$k = \frac{n_к}{V_к t} \ln \frac{1 - C_0/C_e}{1 - C/C_e}. \tag{3}$$

In the flow system the concentration in each point in the catalyst bed remains constant but it changes along the bed. Therefore, in this case the differential equation for the reaction rate is of the form:

$$n_s \frac{dC}{dV_к} = k(1 - C/C_e), \tag{4}$$

where n_s is hydrogen input, mole · sec^{-1}.

By integrating (4) the following relation is obtained for the rate constant:

$$k = \frac{n_s}{V_к} \ln \frac{1 - C_0/C_e}{1 - C/C_e}. \tag{5}$$

TABLE 2

Dependence of the Rate Constant upon Pressure (T = 78°K)

Catalyst	$k \cdot 10^5$, mole · cm^{-3} · sec^{-1}, at pressure, mm Hg					n	$k_0(t) \cdot 10^5$
	60	100	200	400	500		
Chromium-nickel	6,18	9,12	16,3	26,1	28,7	0,76	2,78
Iron	3,12	3,77	5,41	6,5	7,88	0,40	6,10
Platinum	0,72	0,91	1,13	—	—	0,37	1,58
Palladium	0,20	0,23	0,25	—	—	0,16	1,03

TABLE 3

Rate Constants $\underline{k}$ (mole · cm^{-3} · sec^{-1}) for Various Catalysts at 78 and 64°K, as Found in the Flow System (P = 3-150 excess atm)

Catalysts	$k_{78°K}$	$k_{64°K}$	Catalysts	$k_{78°K}$	$k_{64°K}$
Chromium-nickel	$1,5 - 1,7 \cdot 10^{-5}$	$1,4 - 1,5 \cdot 10^{-5}$	Activated charcoal AG-4	$< 6 \cdot 10^{-6}$	$< 6 \cdot 10^{-6}$
$Cr(OH)_3$	$0,56 - 0,74 \cdot 10^{-5}$	$0,53 - 0,68 \cdot 10^{-5}$			
$Mn(OH)_4$	$0,73 - 1,2 \cdot 10^{-5}$	$0,60 - 1,15 \cdot 10^{-5}$			
$Fe(OH)_3$	$1,0 - 2,3 \cdot 10^{-5}$	$0,7 - 1,67 \cdot 10^{-5}$	Cr_2O_3	$< 1 \cdot 10^{-5}$	$< 1 \cdot 10^{-5}$
$Co(OH)_3$	$0,24 - 0,28 \cdot 10^{-3}$	$0,2 - 0,25 \cdot 10^{-5}$	NiO_3	$< 2 \cdot 10^{-8}$	$< 2 \cdot 10^{-8}$
$Ni(OH)_2$	$0,44 - 0,69 \cdot 10^{-5}$	$0,35 - 0,65 \cdot 10^{-5}$	Fe_2O	$1,0 - 1,1 \cdot 10^{-4}$	$0,7 - 1,0 \cdot 10^{-4}$

EXPERIMENTAL RESULTS

In order to examine the influence which transfer processes have upon the reaction rate we have determined how the rate constant of ortho-para conversion depends upon the circulation rate of the gas and the granule size of the catalyst. These experiments were carried out on a chromium-nickel catalyst under static conditions with gas circulating. Varying the circulation rate from 950 to 2300 liter/hr had no influence upon the rate constant. On the other hand, variation of granule size from tablets with d = 4.4 mm to d = 0.8-1.1 mm resulted in a continuous increase of activity (Table 1).

As is obvious from the table, the process proceeds in the region of internal diffusion. Plotting of $\underline{k}$ versus 1/d leads to the conclusion that at the granule size 0.1-1.0 mm the kinetic region still is not attained.

However, further crushing the catalyst granules will no longer give a great effect and is inexpedient. Therefore, the experiments in the flow system under conditions close to those in hydrogen liquefiers were carried out on catalyst with granules of the size 0.7-0.98 mm.

Examination of the catalyst under static conditions with circulation of gas pointed out that in the pressure range 60-500 mm Hg there is observed a certain dependence of the rate constant upon the gas pressure. The results of experiments for four catalysts are given in Table 2.

The relation found for the rate constant as a function of pressure can be described by the equation $k = k_0(t)P^n$. The values of $k_0(t)$ and $\underline{n}$ are also given in Table 2.

Obviously, the dependence of the exponent $\underline{n}$ upon the rate constant $\underline{k}$, as is observed, might be explained by the increased filling of the adsorbed layer on the catalyst at high pressures. Moreover, the adsorption and desorption rate must play a certain role. Therefore, on the more active catalysts, where the reaction rate may be limited partially by the adsorption rate, the rate constant increases more markedly with pressure than is the case on less active catalysts. As was established, above 3-6 excess atm the rate constant did not depend on pressure.

TABLE 4

Values of $\underline{k}$ and k/μ^2_{eff} for Several Ions with Partly Filled 3-d Electron Shells in Hydroxides

Ion	μ_{eff}	$k \cdot 10^3$ g · cm^{-2} · sec^{-1}		$k/\mu^2_{eff} \cdot 10^3$	
		78°K	64°K	78°K	64°K
Cr^{+++}	3,87	0,74	0,68	4,9	4,5
Mn^{++++}	3,87	1,2	1,15	8,0	7,5
Fe^{+++}	5,92	2,26	1,67	6,5	4,8
Co^{+++}	4,92	0,28	0,25	1,2	1,0
Ni^{++}	2,83	0,65	0,61	8,1	7,7

Therefore, the pressure range between 600 mm Hg and 3 excess atm might be called a "transition" region characterized by $\underline{n}$ falling to 0.

The rate constants for pressures between 3 and 150 atm were determined in the flow system at flow rates between 50 and 240 liter/hr (reduced to standard conditions). Depending upon the activity of the catalyst, the amount filled in the reactor was varied from 1 to 3 cc. The measurements were carried out at the temperatures 78 and 64°K (Table 3).

Several batches of each catalyst were examined in the flow system. It was found that measurements on different samples of one and the same batch reproduced well. However, the activity of various batches fluctuated somewhat, and this is the reason why the rate constants $\underline{k}$, as given in Table 3, vary.

In their properties the hydroxides of paramagnetic ions are strongly suggestive of magnetically diluted solid solutions, for instance, chromic oxide in alumina. This magnetic dilution considerably reduces magnetic interaction between ions, and blocks exchange effects and other phenomena which are generally associated with antiferromagnetism.

As the dehydration of the gels goes further, especially when the temperature of their exothermic conversion is passed by, of course, their specific magnetic susceptibility falls jointly with the specific surface area. So, when chromium hydroxide is converted into the oxide, its specific surface area falls from 300 to 10-20 m^2/g [4]. Simultaneously aggregation of the ions takes place and results in strongly concentrating their magnetism in the oxides. This process leads to a considerable increase in exchange effects and the magnetic interaction between the ions. The paramagnetism of the hydroxides changes into the antiferromagnetism of the corresponding oxides, and this change is accompanied by a sharp fall in the catalytic activity of the sample.

These considerations are illustratively confirmed by the data in Table 3.

The fact that activated charcoal shows some activity can be explained, in the opinion of Selwood [4], by the presence of unpaired electrons, which is confirmed by the fact that a strong absorption is found when the charcoal is investigated by the paramagnetic resonance method. The activity of a chromium-nickel catalyst obviously is determined by the presence of finely dispersed metallic nickel.

An analysis of the results obtained with hydroxides confirms in the main that the approach of selecting by magnetic properties the catalysts for the reaction in question is a proper one. In Table 4 are given the maximum values of the rate constants and their ratio to the square of the effective magnetic moment of the catalyst ion.

As is obvious from the table, the ratio k/μ^2_{eff} in fact varies little for various catalysts. The trivalent cobalt ion forms an exception. In this case an anomaly is not unexpected, since as yet it is quite unknown whether any magnetically diluted compound of this ion does exist. Meanwhile, though in a series of investigations it has been assumed too that the free trivalent cobalt ion has a moment corresponding to four unpaired electrons, it has been found [4], however, that in solutions this ion is generally diamagnetic, and that in a series of solid salts its magnetic moment varies considerably and is substantially lower than the theoretical value. In this case the apparent magnetic moment of the Co^{3+} ion does not exceed $\mu_{eff} = 2$. As regards the other ions in Table 4, here in the scattering of the ratio k/μ^2_{eff} a certain role is played by several factors not taken into account in this paper, as, for instance, some deviation between the μ_{eff} value used and the actual one, the value of the effective surface area, a possibly incomplete removal from the surface of adsorbed contaminations blocking it, a decreased distance between the molecules at their effective collisions, which results from a higher nuclear charge, and so on.

Meanwhile the fact that the ratio is comparatively constant indicates that these factors not allowed for here did not play an important role.

The values of the apparent activation energy E_{act} are certainly of interest as a characteristic for the

"low temperature mechanism" of the reaction considered. For all catalysts investigated the apparent activation energies in the temperature range 78-64°K turned out to be very low; they ranged from 0 to 250 cal/mole.

Catalysts	E_{act}, cal/mole
Chromium-nickel	45-110
$Cr(OH)_3$	50-130
$Mn(OH)_4$	120-140
$Fe(OH)_3$	200-250
$Ni(OH)_2$	70-170

The smallness of the activation energy makes the values found scatter considerably. Moreover, they also differ somewhat for various catalyst batches. This determines the bounds between which the values are found. Meanwhile it should be remarked that it turns out that here not only the reactivity of hydrogen but even the properties of the catalysts depend upon temperature. Indeed, the ratio between the energy of ion interaction in the crystal lattice and that of their thermal motion depends upon temperature, and this ratio for the greater part determines the magnetic properties of a substance. Therefore, the activation energies obtained from the Arrhenius equation express here an over-all change in reactivity resulting from the two factors: the state of the reacting molecules and the magnetic properties of the catalyst.

SUMMARY

1. For various ions with partly filled electron shells the magnetic properties and their connection with catalytic activity in ortho-para-hydrogen conversion have been analyzed.

It has been shown that the considerable magnetic dilution of paramagnetic transition metal ions in hydroxides is accompanied by a high catalytic activity. On the other hand, the magnetic concentration of these ions in oxides results in the appearance of antiferromagnetism and a sharply lowered catalytic activity. This was the starting point for selecting the most active catalysts. It has been shown that the ratio k/μ^2_{eff} for the hydroxides investigated is satisfactorily constant.

2. It has been determined which influence mass transfer processes have upon the reaction rate, and the optimum catalyst size for its use in hydrogen liquifiers has been found. The activity of the catalysts has been determined in the temperature range 78-64°K at pressures from 50 mm Hg to 150 atm, and it has been investigated how the reaction rate constant depends upon pressure. It has been shown that adsorption-desorption processes have a considerable influence upon the reaction rate.

The apparent activation energy has been evaluated.

3. The method of preparing and activating catalysts for the ortho-para conversion is given. When catalysts after their activation come in contact with air, they lose part of their activity, but this is restored when they are activated again (the activity of a chromium-nickel catalyst is lost irreversibly).

4. With the catalysts recommended, para-hydrogen may be produced in big amounts. The price of the catalysts is low; under working conditions they are stable.

In conclusion we express our sincere thanks to G. K. Boreskov, Corresponding Member, Acad. Sci. USSR, for supervision of the research and valuable advice.

LITERATURE CITED

1. A. Farkas, Ortho-Hydrogen, Para-Hydrogen and Heavy Hydrogen [Russian translation] (ONTI, Moscow, 1936).
2. E. Wigner, Z. Phys. Chem. B23, 28 (1933).
3. F. Kalckar and E. Teller, Proc. Roy. Soc. A150, 520 (1935).
4. P. Selwood, Magnetochemistry [Russian translation] (IL, Moscow, 1958).
5. G. K. Boreskov and M. G. Slin'ko, Khim. Prom. 2, 69 (1959).
6. D. I. Vasil'ev and A. I. Shal'nikov, Pribor. i Tekh. Eksp. 4, 106 (1958).

KINETICS OF FIRST-ORDER HETEROGENEOUS REACTIONS RETARDED BY REACTION PRODUCTS AND BY INTERNAL DIFFUSION

A. Ya. Rozovskii and V. V. Shchekin

Institute of Petroleum Chemicals, Academy of Sciences of the USSR
Translated from Kinetika i Kataliz, Vol. 1, No. 2, pp.313-323,
July-August, 1960
Original article submitted December 28, 1959

A study is made of the kinetics of heterogeneous reactions of first order in the surface concentrations of the reactants; allowance is made for internal-diffusion effects. A kinetic equation and calculation formulas are proposed for use in estimating the region over which the reaction occurs, in determining the internal-diffusion retardation factor (the efficiency factor), and in calculating the rate constants. It is found that the efficiency factor depends on the adsorption coefficients.

The kinetic parameters of reactions are of great importance to the design of reaction plantsand to the theory of similitude for catalysts. The kinetic equations for the various processes are an important feature of any given reaction.

Balandin [1], Frost [2], and Panchenkov [3] have considered the kinetics of first-order reactions, but they made no allowance for mass transfer. Their equations have been applied with success to catalytic cracking, hydrogenation and dehydrogenation, isomerization, and other important reactions.

There are many papers on the effects of mass transfer within granules of catalysts; Zel'dovich [4] and Thiele [5] have given general methods of solving the problem, which has been considered more recently by Frank-Kamenetskii [6], Pshezhetskii and Rubinshtein [7, 8], Boreskov [9], Roiter [10], Hougen and Watson [11], Weisz and Prater [12], Korrigan et al. [13], Wheeler [14], and so on. These treatments have revealed the main laws of internal diffusion for certain classes of reaction and have led to some practical suggestions on the best structure for the catalyst, etc. However, the classes listed in the previous paragraph have not been dealt with in this way; this paper deals with those classes.

Basic Definitions and Assumptions

The observed rate W_0 of a reaction occurring in the internal-diffusion or transition ranges is less than the rate of W that would be found in the absence of such retardation. The internal-diffusion factor (rate factor) f is defined as

$$f = \frac{W_0}{W} \qquad (1)$$

(this is also the efficiency factor, degree of conversion, etc).

Our assumptions are:

1. That the porous structure is uniform and continuous, i.e., that the structure is the same in all parts of a grain and that no pore is closed. Any difference between grains is negligible.

2. That the surface of the catalyst is uniform in first approximation; a Langmuir isotherm describes the

adsorption of reactants and products, and conditions deviate negligibly from equilibrium in adsorption.

Further, we assume that although one pore differs from another in radius, the system as a whole can be specified in terms of the weighted mean radius r̄ as determined from adsorption measurements (this is reasonable, because the mean is weighted).

Highly porous catalysts (alumina, aluminosilicates, etc) have very small pores (r < 100 A); then Knudsen's equation

$$\frac{dn}{dt} = \frac{8}{3}\frac{\pi r^3}{\sqrt{2\pi M_g RT}}\frac{\Delta p_1}{\Delta x} \tag{2}$$

describes the diffusion at medium pressures, in which dn/dt is the flux through a capillary (mole/sec), r is radius (cm), T is absolute temperature, M_g is the mass per mole (g/mole), R is the gas constant (g-cm²/sec²-mole-deg or erg/mole-deg), Δp_1 is the fall in the partial pressure of the diffusing compounds (g/cm-sec² or dyne/cm²) along the length x (cm) of a pore.

For convenience we replace p_1 by the dimensionless pressure P' (a fraction of the total pressure P), so

$$\frac{dn}{dt} = \pi r^2 D_k' \frac{\Delta P'}{\Delta x}, \tag{3}$$

in which D'_k (mole/cm-sec) is called the diffusion coefficient:

$$D_k' = \frac{8}{3}\frac{rP}{\sqrt{2\pi M_g RT}}. \tag{4}$$

The rate W (mole/cm²-sec) of a reaction of first order in the surface concentration is [15]

$$W = k\theta, \tag{5}$$

in which θ is the dimensionless surface concentration (the extent to which the surface is saturated), k is the effective rate constant (in mole/cm²-sec, being the product of the rate constant in sec^{-1} by the concentration of active centers in mole/cm²). Then the original assumptions give us that

$$\theta = \frac{b_1' p_1}{1 + \sum b'_i p_i}, \tag{6}$$

in which the b'_i are the adsorption coefficients for the reagents (atm^{-1}), the p_i are the partial pressures (atm), and the i are the numbers of the compounds, one representing the reactant.

Suppose that the mixture at some point has attained a degree of conversion y; then we have

$$p_1 = \frac{1-y}{1+ny+\delta}P;\quad p_i = \frac{\nu_i y}{1+ny+\delta}P;\quad \frac{p_1}{P} = P', \tag{7}$$

in which the ν_i are stoichiometric factors, n is the change in the number of moles occurring as a result of the reaction, and δ is the degree of dilution of the reactant. We combine (5), (6), and (7) to get

$$W = K\frac{P'}{1+BP'}, \tag{8}$$

in which $K = kb_1/(1+\bar{b}_i)$ is the observed rate constant for this class of reaction, $B = \frac{\bar{b}_1 - \bar{b}_i}{1+\bar{b}_i}(1+\delta)$ is a parameter that defines the observed order of the reaction, $b_i = b'_i P$ is the dimensionless adsorption coefficient for the reactant (i = 1) or for a product, $\bar{b}_1 = \frac{b_1 + \delta b_\delta}{1+\delta}$ is the mean adsorption coefficient for the initial mixture.

and $\overline{b}_i = \frac{\sum_2^n \nu_i b_i + \delta b_h}{\sum_2^n \nu_i + \delta}$ is the mean adsorption coefficient for the products (see [15] for details).

Derivation of the Rate Factor

The concentration of reactant decreases from the outside to the center of a granule when the internal-diffusion retardation occurs. Consider a model pore directed from the surface to the center (along the concentration gradient). Let us suppose that the rate is limited by diffusion of the reactant in the Knudsen mode within the pore.

The loss of reactant within an infinitely small element dx of the pore as a result of diffusion, $-dV$, is the difference between the diffusion fluxes entering and leaving that element [4, 14]:

$$-dV = \pi r^2 D_k' \frac{d^2P}{dx^2}\, dx. \tag{9}$$

The number (dW_s) of molecules reacting in the element is

$$dW_s = k\theta dS = K\ \frac{P'}{1 + BP'} 2\pi r dx. \tag{10}$$

If conditions are steady, $-dV = dW_s$; then we have

$$\frac{d^2P'}{dx^2} = \frac{2K}{rD_k'} \frac{P'}{1 + BP'}. \tag{11}$$

This equation gives us the concentration as a function of position in the pore for this class of reactions. The boundary conditions are $dP'/dx = 0$ at $x = L$ (condition of symmetry) and $P' = P_0$ at $x = 0$ (L is the length of the pore in cm and P_0 is the dimensionless partial pressure of the reactant at the entrance to the pore); (11) is correct for the kinetic, transition, and internal-diffusion ranges.

We have to solve (11) for the rate and integrate the latter with respect to the layers of granules in order to describe the kinetics for a bed of catalyst. This is not possible in general, because the exact solution to (11) cannot be expressed in terms of elementary functions, so we shall use an approximate solution. All the same, we can use (11) to deduce some general laws.

We introduce a dimensionless parameter h

$$h_x = x\sqrt{\frac{2K}{rD_k'}};\ h = L\sqrt{\frac{2K}{rD_k'}}. \tag{12}$$

Then (12), with (11), gives us that

$$\frac{d^2z}{dh_x^2} = 1 - \frac{1}{z}, \tag{13}$$

in which $z = 1 + BP'$.

The boundary conditions for (13) are $dz/dh_x = 0$ at $h_x = h$, and $z = 1 + BP_0$ at $h_x = 0$.

The solution to (13) is a function of h and also contains $f(1 + BP_0)$, which is a function of B. The form of the latter function is controlled by B, which defines the observed order of the reaction. This result shows that the adsorption coefficients affect the reaction kinetics for this class of reactions.

We turn now to the approximate solution.

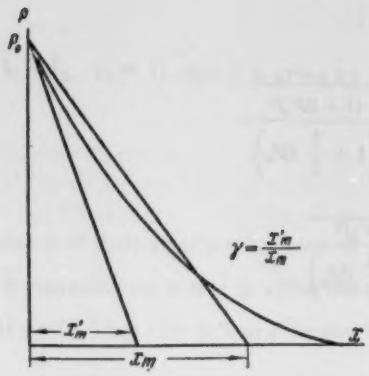

Variation in the dimensionless partial pressure of the reactant along a pore.

Internal-Diffusion Factor for Zero-Order and First-Order Reactions.

Order, n_p	Factor		γ
	from (20)	from literature	
0	$f = \frac{1}{L}\sqrt{\frac{rD_kC}{2\gamma k}}$	$f = \frac{1}{L}\sqrt{\frac{rD_kC}{k}}$	1/2
1	$f = \frac{1}{2L}\sqrt{\frac{rD_k}{k\gamma}}$	$f = \frac{1}{L}\sqrt{\frac{rD_k}{2k}}$	1/2

The reaction is limited as to rate by internal diffusion; we assume that the mean rate of reaction within a pore is a function of the mean concentration of the reactant at the working part of the surface of the pore:

$$W_0 = 2\pi r x_m \frac{K \frac{P_0}{2}^{n}}{1 + B\frac{P_0}{2}}, \tag{14}$$

in which x_m is the effective depth to which the reaction penetrates into the pore (see figure). We may select x_m to be such that (14) is exact.

The diffusion flux into the mouth of the pore is given by (3) taken with $x = 0$; we have to evaluate the gradient of the partial pressure at the mouth of the pore. The figure shows that the gradient is

$$\left|\frac{dP'}{dx}\right|_{x=0} = \frac{P_0}{x'_m}. \tag{15}$$

Let γ denote the ratio of the intercepts (figure):

$$\gamma = \frac{x'_m}{x_m}. \tag{16}$$

Then (3) becomes

$$V_0 = \pi r^2 D'_k \frac{P_0}{\gamma x_m}. \tag{17}$$

We find x_m from (14), (17), and the condition for the stationary state. We substitute for x_m in (14) to get

$$W_A = \pi r P_0 \sqrt{\frac{rD'_kK}{\gamma}} \sqrt{\frac{1}{1 + \frac{1}{2}BP_0}}. \tag{18}$$

The observed rate in the absence of retardation is

$$W = 2\pi r L K \frac{P_0}{1 + BP_0} \tag{19}$$

and the factor $\underline{f}$ is given* by

$$f = \frac{W_0}{W} = \frac{1}{2L}\sqrt{\frac{rD'_k}{K\gamma}\frac{(1+BP_0)^2}{\left(1+\frac{1}{2}BP_0\right)}}. \tag{20}$$

or

$$f = \frac{1}{h}\sqrt{\frac{(1+BP_0)^2}{2\gamma\left(1+\frac{1}{2}BP_0\right)}}. \tag{21}$$

This result is in agreement with the predictions made from (13).

To test this solution we will consider the $\underline{f}$ for zero-order and first-order reactions ($B \gg 1$ and $B \ll 1$ respectively) and will compare the results with ones given by others [5, 9, 14] for these cases, for which explicit solutions are available.

The $\underline{f}$ from these various sources are collected in the table.

We see that the expressions coincide, apart from the numerical factor γ, which in each case clearly takes the value $\frac{1}{2}$. Now the rate is a continuous function of the order, so the results indicate that the solution is applicable at least to the range $0 \leq n_p \leq 1$.

Now we turn to the conditions governing the transition to the internal-diffusion range. To this end we compare the equations for the transition range, for which the dimensionless partial pressure P_C of the reactant at the center of a grain (at the end of a pore) is $0 \leq P_C < P_0$. Then the condition $P_C = 0$ marks the boundary between these two ranges; this gives us $h = \sqrt{4 + 2BP_0}$ for the boundary or

$$h \geqslant \sqrt{4+2BP_0}. \tag{22}$$

for the internal-diffusion range itself. This result is sound, because the $\underline{h}$ given by (22) are precisely the same as the the values given by others for first-order reactions.

Strictly speaking, there is no corresponding condition for the boundary between the transition and kinetic regions, because $\underline{f}$ cannot be one in real cases, although it may come indefinitely close to that value. In practice we may say that an $\underline{h}$ comparable with one (with B not too large) gives an $\underline{f}$ of about 0.95 (i.e. close to 1), which corresponds to a close approximation to kinetic behavior.

Relation of the Internal-Diffusion Factor to the Adsorption Coefficients

We can simplify (10) in particular cases for certain values of the adsorption coefficients.

1. The reactant and the products are adsorbed very little; $\bar{b}_1, \bar{b}_i \ll 1$. Then, at the limit, we have

$$f = \frac{1}{h}. \tag{23}$$

Here $\underline{f}$ is virtually independent of the concentrations and so of the degree of reaction.

2. The mean adsorption coefficients are similar; $\bar{b}_1 \approx \bar{b}_i$. Here again $\underline{f}$ is given by (23).

3. The adsorption coefficients are large but not comparable:

a) zero-order reaction, $\bar{b}_1 \gg \bar{b}_i$, $b_1 \gg 1$; then $\underline{f}$ is proportional to $\sqrt{P_0}$.

* Previously [16] we have used the $\underline{f}$ found [5, 9, 14] for first-order reactions ($W = kC$). The more rigorous treatment has enabled us to revise the results given in [16].

$$f = \frac{1}{L}\sqrt{\frac{\overline{rD'k}}{k}}\sqrt{P_0}; \tag{24}$$

b) $\overline{b}_i \gg \overline{b}_1$, $b_1 \gg 1$; then $\underline{f}$ is given by

$$f = \frac{1}{h}\frac{1-P_0}{\sqrt{1-\frac{P_0}{2}}}. \tag{25}$$

The last case is of little significance, because the corresponding degree of reaction is very small.

4. A common case is that in which the reactant is supplied mixed with an inert diluent. It is easily shown that $\lim_{\delta\sim\infty} BP_0 = 0$. Then (23) defines $\underline{f}$ for any B if the dilution is great.

The internal-diffusion factor will be almost constant throughout the bed in cases 1, 2, and 4. In cases 3a and 3b, and in intermediate cases, $\underline{f}$ varies from point to point.

We differentiate (21) with respect to P_0 and get

$$\frac{df}{dP_0} = \frac{B}{4h}\frac{3+BP_0}{\left(1+\frac{1}{2}BP_0\right)^{3/2}}. \tag{26}$$

Now $h > 0$; $3 + BP_0 > 0$ and $1 + \frac{1}{2}BP_0 > 0$ for any $\overline{b}_1$ and $\overline{b}_i$ of physical significance, so the sign of B controls the sign of the first derivative. If $\overline{b}_1 > \overline{b}_i$, then $df/dP_0 > 0$, so the retardation is least at the first part of the bed and increases with the degree of reaction. If, on the other hand, the mean adsorption coefficient for the products is larger than the mean adsorption coefficient for the initial mixture, we have $df/dP_0 < 0$, so the retardation is largest at the first part of the bed and decreases as the reaction proceeds.*

The general conclusion to be drawn from this is that one part of the bed may differ from another as regards the effective kinetic conditions.

Kinetic Equation for a Reaction in a Bed of Catalyst

We shall deduce the final kinetic equation by means of the observed rate referred to unit surface area:

$$W_0 = \frac{V'dy}{\frac{dS}{dl}dl}, \tag{27}$$

in which V' is the rate at which the reactant is fed in (mole/sec) and l is the depth of the bed (cm). (Here $dS/dl = S_0$ is constant throughout the bed if the degree of filling is constant.)

We combine (27), (1), (8), and (21) to get

$$\frac{K\,S_0 dl}{V'h} = \frac{\sqrt{1+\frac{1}{2}BP_0}}{P_0}dy. \tag{28}$$

The equations derived by integrating (28) are complicated. A simpler solution may be obtained as follows.

We expand $\sqrt{1+\frac{1}{2}BP_0}$ in series form and reject all terms except the first two; we get

$$\sqrt{1+\frac{1}{2}BP_0} \approx 1+\frac{1}{4}BP_0. \tag{29}$$

*The last case is somewhat analogous to one considered by Pshezhetskii [8] (reaction rate inversely proportional to the concentration of a product), in which a similar result is reached by another method.

The error thereby introduced increases with BP_0 (we have $0 \leqslant P_0 \leqslant 1/(1+\delta)$; $-1 < B < \infty$).

If B < 0 (the products are adsorbed more strongly than the reactant), the maximum relative error (for B = = −1) for a mixture not containing a diluent is 6% for y = 0 and 0.4% for y = 0.5 (with n = 1). The error falls rapidly as the reactant is diluted; a 1 : 1 mixture gives a maximum error of 1.3% when y = 0. We conclude that (29) is a good approximation for all $B \leq 0$.

The error for B > 0 and in the range $0 < B \leq 2(1+\delta)$ does not exceed the error quoted above; further increase in B causes the error to increase. It is hardly likely in practical cases that the mean adsorption coefficient for the products will exceed the coefficient for the reactant by more than an order of magnitude, so (29) is a good approximation in almost every case.

We substitute (29) and (7) into (28) and get

$$\frac{K}{V'h}\frac{S_0 dl}{} = \frac{1+\delta+{}^1/_4 B+(n-{}^1/_4 B)y}{1-y}dy. \tag{30}$$

The integral of (30) gives us the kinetic equation in the form

$$\alpha_0 = v_0 \ln\frac{1}{1-y} - \beta v_0 y, \tag{31}$$

in which

$$\alpha_0 = \frac{K S_g}{h(1+n+\delta)} = \frac{S_g\sqrt{K\, rD_k'}}{L\sqrt{2}(1+n+\delta)}. \tag{32}$$

$$\beta = \frac{n-{}^1/_4 B}{1+n+\delta}, \tag{33}$$

in which v_0 is the specific rate of supply (mole/g-sec) and S_g is the specific surface of the catalyst, cm^2/g.

The relation of y to v_0 in (31) is the same as the relation appearing in Frost's equation for a reaction occurring in the kinetic range, but the constants have other physical meanings and depend on the parameters of the catalyst. Thus, the equations describing a first-order reaction in the kinetic range and in the internal-diffusion are formally the same. It is always necessary to look for internal-diffusion effects in any study of the kinetics of a reaction of this class.

The above relationships apply to cases in which internal diffusion of the reactant into the granules is the rate-limiting step; the same results are obtained if diffusion of the products from the granules is the rate-limiting step.

Activity of the Catalyst and Effective Range for the Reaction

We see from (8) that K defines the observed activity of the catalyst.

The K for the kinetic region can be determined from the constant α of Frost's equation:

$$K_n = \frac{\alpha(1+n+\delta)}{S_g}. \tag{34}$$

The K for the internal-diffusion range is given by (12) and (32) as

$$K = \frac{2\alpha_0^2(1+n+\delta)^2 L^2}{S_g^2 r D_k'}. \tag{35}$$

The parameter h is given by

$$h = \frac{2\alpha_0 L^2 (1 + n + \delta)}{S_g \bar{r} D'_k}. \tag{36}$$

The S_g and $\bar{r}$ of (35) and (36) are derived from adsorption measurements; α_0 is found from kinetic measurements; and D'_k may be calculated from (4). Then, if L is known, the effects of internal diffusion can be estimated without resort to special measurements.

The meaning of L is the shortest distance along a pore from the outside surface to the center; it depends on the shape of the grain. For example, for a parallel plate

$$L = \frac{a}{2}\sqrt{2}, \tag{37}$$

in which $\sqrt{2}$ is the factor that allows for the average deviations of the directions of a pore from a straight line (a being the thickness of the plate in cm); for irregular grains produced by crushing we have roughly that

$$L = \frac{a}{4}\sqrt{2}, \tag{38}$$

in which a is the smallest of the three linear dimensions of the grain.

The above method gives complicated expressions if the reaction occurs in the transition region. Now the error will be small on account of the fairly small fall in concentration occurring within a grain, so we can use Thiele's expression [5] $\eta = \frac{1}{h} th(h)$, if B is small, with h given the value found from (12). Further, we may determine the factor from the relation of the observed activity to the grain size by means of the formula [16]

$$\frac{h_1}{h_2} = \frac{L_1}{L_2}; \quad \frac{\text{th}(h_1)}{\text{th}(h_2)} = \frac{L_1 \alpha_1}{L_2 \alpha_2}. \tag{39}$$

Methods of Studying the Kinetics of Reactions Subject to Internal-Diffusion Retardation

We seem from (36) that h is determined by the grain size, by the activity, and by the porosity; correspondingly, these are various methods of examining the reaction kinetics.

1. Grain Size. The grain size is without effect on the rate if the reaction occurs in the kinetic range; the same is true for the extent of reaction. In the internal-diffusion range we have h and $1/\alpha_0$ as linear functions of grain size; $\alpha_0 a$ = constant (more exactly, $\alpha_0 L$ = constant) for variations in grain size.

2. Porosity. The porosity is without effect on the rate if the reaction occurs in the kinetic range; (32) defines the relation of activity to porosity for the internal-diffusion range. The results for specimens differing on only in V_g, S_g, and $\bar{r}$ must lie on a straight line when they are plotted in terms of α_0 against V_g (V_g is the specific pore volume, cm^3/g); the ratio α_0/V_g must be constant.

3. Activity. The range can be changed from the kinetic to the internal-diffusion and conversely by adjusting the activity; an experimental test for this transition is that the apparent activation energy changes by a factor two. The diffusion coefficient varies little with temperature, so these effects can be detected when kinetic studies are made over a wide range in temperature [17-19].

Let us suppose that α is a linear function of the amount G of some poison introduced into the catalyst; then α_0 will be a linear function of $G^{\frac{1}{2}}$ in the internal-diffusion range. More complex relations occur if the poison is adsorbed selectively near the mouths of the pores; a special examination is needed in such cases.

We have applied these methods to the production of ethylene from ethanol over alumina and to the hydrogenation of ethylene over Ni/Al_2O_3. The results have been published in part [20]; they show that our equation

does describe the kinetics for the internal-diffusion range. The above scheme has been found to be applicable to the production of ethylene from ethanol over γ-alumina (internal-diffusion range), to the production of ethylene from ethanol over α-alumina (kinetic range), and to the hydrogenation of ethylene over Ni/ Al_2O_3 (internal-diffusion range).

SUMMARY

1. A study has been made of the kinetics of heterogeneously catalyzed reactions of first order in the surface concentration of the reactant; allowance has been made for effects arising from transport processes within the grains.

2. An equation has been derived to describe such reactions for the internal-diffusion range.

3. Formulas are given for use in establishing the working range and in calculating the internal-diffusion factor for a heterogeneously catalyzed reaction occurring in the internal-diffusion range.

4. Some laws have been derived for the effects of internal diffusion on the kinetics, namely the relation of the internal-diffusion factor to the adsorption coefficients, the possible variation in the factor in a bed of catalyst, the sensitivity or otherwise of the kinetics to the rate-limiting step (diffusion of reactant into the grains or diffusion of the products from the grains), and so on.

5. Some methods of establishing the working range are given for use with reactions whose kinetics are influenced by internal diffusion.

LITERATURE CITED

1. A. A. Balandin, Zhur. Obshch. Khim. 15, 770 (1945); 12, 153 (1942).
2. A. V. Frost, Vestnik Mosk. Gos. Univ. No. 3-4, 111 (1946); T. V. Antipina and A. V. Frost, Uspekhi. Khim. 19, 342 (1950).
3. G. M. Panchenkov, Zhur. Fiz. Khim. 22, 209 (1948); 26, 453 (1952); Uch. Zap. Mosk. Gos. Univ. No. 174, 53 (1955); Heterogeneous Catalysis in the Chemical Industry [in Russian] (Goskhimizdat, Moscow, 1955).
4. Ya. B. Zel'dovich, Zhur. Fiz. Khim. 13, 163 (1939).
5. E. W. Thiele, Ind. Eng. Chem. 31, 916 (1939).
6. D. A. Frank-Kamenetskii, Diffusion and Heat Transfer in Chemical Kinetics [in Russian] (Moscow-Leningrad, 1947).
7. S. Ya. Pshezhetskii and A. T. Gladyshev, Zhur. Fiz. Khim. 15, 333 (1941); S. Ya. Pshezhetskii and R. N. Rubinshtein, Zhur. Fiz. Khim. 20, 1127 (1946); 20, 1421 (1946); Problems of Kinetics and Catalysis [in Russian] (Izd. AN SSSR, Moscow, 1949) Vol. 6, p. 426; S. Ya. Pshezhetskii, Zhur. Fiz. Khim. 21, 1019 (1947).
8. S. Ya. Pshezhetskii, Zhur. Fiz. Khim. 19, 376 (1945).
9. G. K. Boreskov, Khim. Prom. 8, 221 (1947); 9, 257 (1947); Problems of Kinetics and Catalysis [in Russian] (Izd. AN SSSR, Moscow, 1949) Vol. 6, p. 404; Catalysis in the Production of Sulfuric Acid [in Russian] (Goskhimizdat, Moscow-Leningrad, 1954); Heterogeneous Catalysis in the Chemical Industry [in Russian] (Goskhimizdat, Moscow, 1955) p. 22.
10. V. A. Roiter, Problems of Kinetics and Catalysis [in Russian] (Izd. AN SSSR, Moscow, 1949) Vol. 6, p. 357; Heterogeneous Catalysis in the Chemical Industry [in Russian] (Goskhimizdat, Moscow, 1955) p. 281; V. A. Roiter et al., Catalysis (Transactions of the All-Union Conference on Catalysis) [in Russian] (Izd. AN UkrSSR, Kiev, 1950) p. 143; V. A. Roiter, Izvest. Akad. Nauk SSSR, Otdel Khim. Nauk 576 (1950); V. A. Roiter and G. P. Korneichuk, Zhur. Fiz. Khim. 28, 1812 (1954).
11. O. A. Hougen and K. M. Watson, Ind. Eng. Chem. 35, 529 (1943); O. A. Uyechara and K. M. Watson, Ind. Eng. Chem. 35, 541 (1943); K. H. Jang and O. A. Hougen, Chem. Eng. Progr. 46, 146 (1950); O. A. Hougen, Z. Elektrochem. 57, 479 (1953); O. A. Hougen and K. M. Watson, Chem. Process Principles, III, Kinetics and Catalysis (New York, 1947).
12. P. B. Weisz and C. D. Prater, Adv. in Catal. 6, 142 (1954).
13. T. E. Korrigan et al., Chem. Eng. Progr. 49, 603 (1953).
14. A. Wheeler, Adv. in Catal. 3, 249 (1951); A. Wheeler, Catalysis, Problems of Theory and Methods of Investigation [Russian translation] (IL, Moscow, 1955) p. 479.
15. A. Ya. Rozovskii and V. V. Shchekin, Trudy Inst. Nefti Akad. Nauk SSSR 10, 275 (1957); A. Ya. Rozovskii,

Candidate's Dissertation, Inst. Neft. Khim. Sintez. Akad. Nauk SSSR (1959).
16. A. Ya. Rozovskii and V. V. Shchekin, Trudy Inst. Nefti Akad. Nauk SSSR 10, 286 (1957).
17. G. K. Boreskov and V. A. Dzis'ko, Zhur. Fiz. Khim. 24, 1135 (1950).
18. V. A. Roiter, G. P. Korneichuk, M. G. Lepersov, N. A. Stukanovskaya, and B. I. Tolchina, Zhur. Fiz. Khim. 24, 459 (1950).
19. V. A. Roiter and M. T. Rusov, Zhur. Fiz. Khim. 17, 87 (1943).
20. V. P. Prokof'eva, A. Ya. Rozovskii, and V. V. Shchekin, Trudy Inst. Nefti Akad. Nauk SSSR 12, 253 (1958).

DIFFUSION KINETICS FOR A SURFACE OF UNEQUAL ACCESSIBILITY

O. M. Todes and A. P. Shapiro

Yakut State University
Translated from Kinetika i Kataliz, Vol. 1, No. 2, pp. 324-332,
July-August, 1960
Original article submitted February 1, 1960

Limits are set to the applicability of equal-accessibility concepts by considering a schematic model. The law for an equally accessible surface, (3), can be applied if the dimensions of the regions of inhomogeneity are small compared to the thickness of the boundary layer, provided that inequality (31) is complied with, even though the active areas comprise only a very small portion of the total surface. The more general expression (30) applies to macroscopic inhomogeneities.

Diffusion to the surface of the catalyst is the rate-limiting step if the rate of a heterogeneous reaction is high, even though the concentrations of the reactants at the surface are small.

Figure 1 shows the concentration schematically for a reaction occurring in the diffusion range. Here C_0 is the concentration of reactant in the body of a flow moving along the surface, which is separated from that body by a boundary layer of thickness δ. The rate depends on C, the concentration at the surface. Consider a first-order reaction whose rate constant is k_1; in the steady state the diffusion flux in the layer is equal to the rate referred to unit area, i.e.

$$W = D\frac{C_0 - C'_n}{\delta} = k_1 C'. \tag{1}$$

For this equally accessible surface [1], for which the rate constant is much larger than the diffusion constant,

$$k_1 \gg \frac{D}{\delta}, \tag{2}$$

the entire process occurs in the diffusion range:

$$C'_n \ll C_0 \quad \text{and} \quad W \approx D\frac{C_0}{\delta}. \tag{3}$$

No real surface is equally accessible; in fact, it is often highly inhomogeneous, for k_1 may be very large for some areas (the active centers) and very small for others (inactive areas). The relative proportion of active surface, σ, may be very small, so we must examine the applicability of (1) and (3) to surfaces with $\sigma \ll 1$.

The applicability can be established as follows (Fig. 2). Let us suppose that the active areas occur as narrow parallel strips normal to the plane of the paper; the distance between the centers of adjacent strips is $2l$, so the width of each strip is $2\sigma l$. The thick lines of Fig. 2 represent the strips; the broken lines, the diffusion flows.

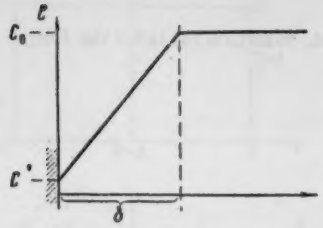

Fig. 1.

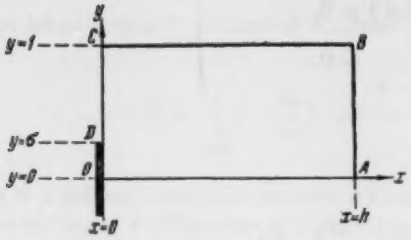

Fig. 3.

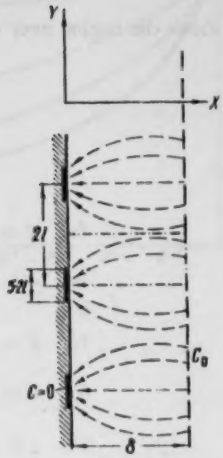

Fig. 2.

The X axis lies normal to the plane, the Y axis in the surface; then C does not depend on Z, so C = C(X, Y).

We assume that the rate constant is indefinitely larg so C' = 0.

The the entire boundary layer can be divided up into identical blocks each of height δ and length l; diffusion in each of these is independent of diffusion in all others. One such block is indicated in Fig. 2.

The problem to be solved is that of two-dimensional steady-state diffusion:

$$\frac{\partial^2 C}{\partial X^2} + \frac{\partial^2 C}{\partial^2 Y} = 0 \tag{4}$$

subject to the conditions

$$\left.\begin{aligned} &C = C_0 \text{ at the boundary;}\\ &C = 0 \text{ at the surface;}\\ &\partial C/\partial n = 0, \text{ i.e., there is no flux through the side faces of a block} \end{aligned}\right\} \tag{5}$$

We find the C(X, Y) satisfying (4) and (5), and then calculate the total diffusion flux j to the active surface as referred to unit area of the whole surface:

$$\frac{j}{l} = \frac{1}{l}\int_{Y_0}^{Y_{\sigma \cdot l}} \left(-D\frac{\partial C}{\partial X}\right)_{X=0} \cdot dY \tag{6}$$

and compare the result with (3) (i.e. with that for σ = 1).

First we introduce the dimensionless variables

$$x = \frac{X}{l},\quad y = \frac{Y}{l};\quad \varphi(x, y) = \frac{C}{C_0} \tag{7}$$

and the dimensionless parameter

$$h = \frac{\delta}{l}. \tag{8}$$

Figure 3 shows the region over which the integration is carried. Equation (4) takes the form

$$\frac{\partial^2 \varphi}{\partial x^2} + \frac{\partial^2 \varphi}{\partial y^2} = 0 \tag{9}$$

and (5) becomes

$$\left.\begin{array}{lll} \text{for } x = h & & \varphi(h, y) = 1, \\ \text{for } y = 0, \quad y = 1 & & \left.\frac{\partial \varphi}{\partial y}\right|_{y=0} = \left.\frac{\partial \varphi}{\partial y}\right|_{y=1} = 0, \\ \text{for } x = 0, & 0 \leqslant y \leqslant \sigma & \varphi(0, y) = 0, \\ \text{for } x = 0, & \sigma \leqslant y \leqslant 1 & \left.\frac{\partial \varphi}{\partial x}\right|_{x=0} = 0. \end{array}\right\} \tag{10}$$

We have to solve (9) with (10) to find the flux as

$$\frac{j}{l} = \frac{DC_0}{l} \int_{y=0}^{y=\sigma} \left(-\frac{\partial \varphi}{\partial x}\right)_{x=0} \cdot dy = \frac{DC_0}{\delta} \cdot h\Lambda, \tag{11}$$

in which

$$\Lambda = \int_{y=0}^{y=\sigma} \left(-\frac{\partial \varphi}{\partial x}\right)_{x=0} \cdot dy \tag{12}$$

must be calculated from the solution of (9) and (10)

This mathematical problem may be solved by means of the following method [2]. We consider the 0xy plane as the plane of the complex variable

$$z = x + iy$$

in which plane we introduce a regular function $f(z)$ such that its real part $\varphi(x, y)$ satisfies (9) and (10):

$$f(z) = f(x + iy) = \varphi(x, y) + i\Psi(x, y). \tag{13}$$

Then the imaginary part of $f(z)$, i.e., $\Psi(x, y)$, satisfies (9) and the Cauchy-Riemann conditions of $\varphi(x,y)$:

$$\frac{\partial \varphi}{\partial x} = \frac{\partial \Psi}{\partial y}; \quad \frac{\partial \varphi}{\partial y} = -\frac{\partial \Psi}{\partial x}. \tag{14}$$

Further, (10) and (14) imply that

$$-\frac{\partial \varphi}{\partial y} = \frac{\partial \Psi}{\partial x} = 0; \quad \Psi = \text{const} = \Psi_1.$$

on part OA of the rectangle ($y = 0$).

Again, on BC we must have Ψ also constant. On CD we have $\frac{\partial \Psi}{\partial x} = \frac{\partial \Psi}{\partial y}$, i.e., again Ψ = const., so along the whole of BCD we have

$$\Psi_{BCD} = \text{const} = \Psi_2.$$

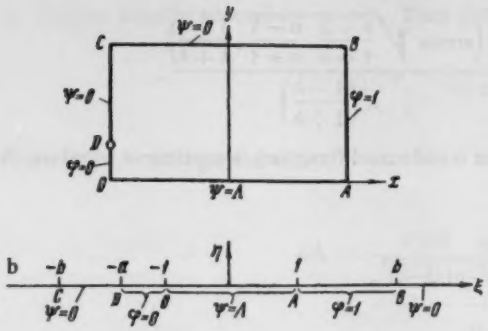

Fig. 4.

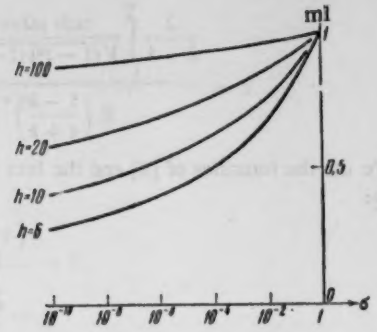

Fig. 5.

Now let us express Λ in terms of Ψ. From (12) and (14) we have

$$\Lambda = \int_{y=0}^{y=a} \left(-\frac{\partial \varphi}{\partial x}\right) \cdot dy = \int_{(OD)} \left(-\frac{\partial \Psi}{\partial y}\right) \cdot dy = \Psi_0 - \Psi_D = \Psi_1 - \Psi_2. \tag{15}$$

But Ψ is defined, apart from an arbitrary constant, so we can put $\Psi_2 = 0$. Then $\Psi_1 = \Lambda$, and the boundary conditions for φ and Ψ at the edge of OABCDO take the form shown in Fig. 4a. (Here the vertical axis has been moved to the middle of the rectangle.)

The Schwarz-Christofel formula

$$z = \int_0^{\zeta} \frac{dt}{\sqrt{(1-t^2)(1-k^2t^2)}} \tag{16}$$

is used to transform the rectangle in the plane $z = x + iy$ into the upper half-plane ($\eta > 0$) for the variable $\zeta = \xi + i\eta$. The points O, A, B, C, and D become the corresponding points on the straight line $\eta = 0$ of Fig. 4b.

Here b is related to the modulus of (16) by

$$b = \frac{1}{k} \tag{17}$$

The modulus is found from the relation for the sides of the rectangle

$$h = \frac{2K(k)}{\frac{2}{k+1} K\left(\frac{1-k}{1+k}\right)} = \frac{2K(k)}{K(k')}, \tag{18}$$

in which

$$k' = \sqrt{1-k^2}\ ; \quad K(k) = \int_0^1 \frac{dt}{\sqrt{(1-t^2)(1-k^2t^2)}} = F\left(\frac{\pi}{2}, k\right) \tag{19}$$

is a complete elliptic integral.

Here −a, the abscissa of D, is given by the incomplete elliptic integral

$$\sigma = \frac{\dfrac{2}{k+1}\displaystyle\int_1^a \frac{dt}{\sqrt{(1-t^2)(1-k^2t^2)}}}{K\left(\dfrac{1-k}{1+k}\right)} = \frac{F\left(\arcsin\sqrt{\dfrac{1+k}{1-k}\cdot\dfrac{a-1}{a+1}}, \dfrac{1-k}{1+k}\right)}{K\left(\dfrac{1-k}{1+k}\right)}. \tag{20}$$

We use the formulas of [2] and the fact that $\omega(\zeta)$ (the transformed function) is continuous to relate Λ to $\underline{a}$ and $\underline{b}$:

$$\Lambda = \frac{\displaystyle\int_0^b \frac{d\xi}{\sqrt{(\xi^2-1)(\xi+a)(b-\xi)}}}{\displaystyle\int_{-1}^{+1} \frac{d\xi}{\sqrt{(1-\xi^2)(\xi+a)(b-\xi)}}}. \tag{21}$$

We introduce trigonometric functions by means of the angles α and φ, which we use to express F and K above:

$$\left.\begin{aligned} F(\alpha, \varphi) &= \int_0^{\alpha} \frac{d\theta}{\sqrt{1-\sin^2\varphi\cdot\sin^2\theta}}; \\ K(\varphi) = F\left(\frac{\pi}{2}, \varphi\right) &= \int_0^{\frac{\pi}{2}} \frac{d\theta}{\sqrt{1-\sin^2\varphi\cdot\sin^2\theta}}. \end{aligned}\right\} \tag{22}$$

Here α and φ are related to $\underline{h}$ and σ by

$$\frac{1}{h} = \frac{K(\varphi)}{K\left(\dfrac{\pi}{2}-\varphi\right)}; \tag{23}$$

$$\sigma = \frac{F(\alpha, \varphi)}{F\left(\dfrac{\pi}{2}, \varphi\right)}. \tag{24}$$

Further, an angle ψ is given in terms of α and φ by

$$\sin\psi = \sin\alpha\cdot\sin\varphi, \tag{25}$$

so we have

$$\Lambda = \frac{K(\psi)}{K\left(\dfrac{\pi}{2}-\psi\right)}. \tag{26}$$

Equations (23)-(26) give Λ, and hence the correction factor $h\Lambda$ of (11), as functions of $\underline{h}$ and σ, i.e., they serve to solve the problems completely. If we could eliminate α, φ, and ψ from (23)-(26), we would have the result in explicit form. That form can be obtained only for limiting cases, though.

We will assume that l is small relative to the thickness of the boundary layer, i.e., that

$$h = \frac{\delta}{l} \gg 1, \tag{27}$$

which corresponds to φ small.

1. Surface equally accessible: $\sigma \to 1$. Then (24) and (25) give us that

$$\alpha \to \frac{\pi}{2}, \quad \sin\alpha \to 1; \quad \psi \to \varphi.$$

Then (23) and (26) give us that

$$h\Lambda = \frac{K(\psi)}{K\left(\frac{\pi}{2} - \psi\right)} \cdot \frac{K\left(\frac{\pi}{2} - \varphi\right)}{K(\varphi)} \to 1, \tag{28}$$

i.e., that the $h\Lambda$ of (11) tends to one, so (11) becomes (3).

2. The surface is highly inhomogeneous ($\sigma \ll 1$), so α is very small; we can use expansion for the elliptic integrals [3]:

$$\text{small } \alpha \quad F(\alpha, \varphi) \approx \alpha;$$

$$\text{small } \varphi \quad F\left(\frac{\pi}{2}, \varphi\right) = K(\varphi) \approx \frac{\pi}{2}.$$

Then (24) gives us that

$$\alpha \approx \frac{\pi}{2}\sigma.$$

Further, (25) implies that $\psi \approx \alpha\varphi$ and $K(\psi) \approx \frac{\pi}{2}$. For small angles

$$K\left(\frac{\pi}{2} - \varphi\right) \approx \ln\frac{4}{\sin\varphi} \approx \ln\frac{4}{\varphi}$$

and

$$K\left(\frac{\pi}{2} - \psi\right) \approx \ln\frac{4}{\psi} \approx \ln\frac{4}{\alpha\varphi} = \ln\frac{4}{\varphi} + \ln\frac{1}{\alpha}.$$

We insert these expansions into (23) and (26) to get

$$h \approx \frac{2}{\pi}\ln\frac{4}{\varphi}; \quad \Lambda \approx \frac{\frac{\pi}{2}}{\ln\frac{4}{\varphi} + \ln\frac{1}{\alpha}} = \frac{1}{h + \frac{2}{\pi}\ln\frac{2}{\pi\sigma}}.$$

Now $\frac{1}{\sigma} \gg 1$ here, so to a high degree of accuracy

$$\ln\frac{2}{\pi\sigma} = \ln\frac{1}{\sigma} + \ln\frac{2}{\pi} \approx \ln\frac{1}{\sigma}.$$

Thus the final form for $h\Lambda$ is in this case

$$h\Lambda \approx \frac{1}{1 + \frac{2}{\pi h}\ln\frac{1}{\sigma}}. \tag{29}$$

It is not possible for intermediate σ to obtain a simple explicit form for $h\Lambda$ as a function of σ and h, but

(29) itself is an adequate interpolation expression, because with $\sigma = 1$ ($\ln \frac{1}{\sigma} = \ln 1 = 0$) it becomes (28); so for $h \gg 1$ we can use (29) to obtain from (11) a convenient expression for the diffusion kinetics:

$$W \approx \frac{DC_0}{\delta} \cdot \frac{1}{1 + \frac{2}{\pi} \frac{l}{\delta} \ln \frac{1}{\sigma}} = \frac{DC_0}{\delta} \cdot \frac{1}{1 + \frac{4{,}6}{\pi} \cdot \frac{l}{\delta} \cdot \log \frac{1}{\sigma}}. \tag{30}$$

Of course, (30) is not of very high accuracy for intermediate values of σ, but it does enable us to estimate in a simple fashion the limits to the applicability of equal-accessibility concepts.

Now (29) and (30) show that the assumption of equal accessibility will give rise to large errors when $h\Lambda$ decreases from 1 to 0.5, i.e., when

$$\frac{2}{\pi h} \ln \frac{1}{\sigma} > 1 \quad \text{or} \quad \sigma < e^{-\frac{\pi h}{2}} = 10^{-\frac{\pi}{4{,}6} \frac{\delta}{l}}. \tag{31}$$

This shows that, for example, (3) can be used with $h \approx 6$ while σ remains larger than 10^{-4}. Figure 5 shows $h\Lambda$ as a function of σ for several values of h; we see that the surface may be considered as equally accessible even when the active areas constitute only a minute fraction of the total, provided that l remains small relative to the thickness of the boundary layer.

Mathematical Appendix

Formula (21) is deduced; the notation is

$$\omega(\zeta) = \Psi(\xi, \eta) - i\varphi(\xi, \eta) = -if(z), \tag{32}$$

in which $\omega(\zeta)$ is analytic. Figure 4b gives the boundary conditions for φ and Ψ.

The formula for calculating $\omega(\zeta)$ is [2]

$$\omega(\zeta) = \frac{C_0 + C_1\zeta + C_2\zeta^2}{\pi i \sqrt{(\zeta + a)(\zeta^2 - 1)(\zeta - b)}} + \frac{1}{\pi i \sqrt{(\zeta + a)(\zeta^2 - 1)(\zeta - b)}} \times$$

$$\times \left[\int_1^b \frac{\sqrt{(b - \xi)(\xi^2 - 1)(\xi + a)}}{\xi - \zeta} d\xi + \Lambda \int_{-1}^{+1} \frac{\sqrt{(\xi + a)(\xi^2 - 1)(\xi - b)}}{\xi - \zeta} d\xi \right], \tag{33}$$

in which C_0, C_1, and C_2 are real constants.

$$\omega(\zeta) = \frac{1}{\pi i \sqrt{(\zeta + a)(\zeta^2 - 1)(\zeta + b)}} [C_0 + C_1\zeta + C_2\zeta^2 + r(\zeta) + \Lambda S(\zeta)], \tag{34}$$

in which $r(\zeta)$, $S(\zeta)$ are integrals from (33); $\omega(\zeta)$ must be continuous, to which end the quantity in brackets in (34) becomes 0 when $\zeta = -a, 1, -1, b$.

Inserting these values for ζ and equating the bracket to zero, we get four linear equations for the unknowns, C_0, C_1, C_2, Λ.

We get (21) by using Kramer's formula

$$A = \frac{\begin{vmatrix} 1 & 1 & 1 & -r(1) \\ 1 & -1 & 1 & -r(-1) \\ 1 & -a & a^2 & -r(-a) \\ 1 & b & b^2 & -r(b) \end{vmatrix}}{\begin{vmatrix} 1 & 1 & 1 & S(1) \\ 1 & -1 & 1 & S(-1) \\ 1 & -a & a^2 & S(-a) \\ 1 & -b & b^2 & S(b) \end{vmatrix}} =$$

$$[(a-1)(b+1)(a+b)r(1)-(a+1)(b-1)(a+b)r(-1)+2(b^2-1)r(-a)-2(a^2-1)r(b)]/$$
$$/[(a-1)(b+1)(a+b)S(1)-(a+1)(b-1)(a+b)S(-1)+2(b^2-1)S(-a)-2(a^2-1)S(b)] \tag{35}$$

and substituting in (35) the $r(\zeta)$ and $S(\zeta)$, after which the integrals in the numerator and denominator are transformed.

Then (16) and (17) give us that

$$h = \frac{2\int_0^1 \frac{dt}{\sqrt{(1-t^2)(1-k^2t^2)}}}{\int_1^{\frac{1}{k}} \frac{dt}{\sqrt{(t^2-1)(1-k^2t^2)}}}. \tag{36}$$

In the first integral we make the substitution

$$\sin\theta = t, \tag{37}$$

and in the second

$$\sin\theta = \sqrt{\frac{1+k}{1-k}\cdot\frac{t-1}{t+1}}, \tag{38}$$

further, we introduce φ from

$$\sin\varphi = \frac{1-k}{1+k} = r, \tag{39}$$

and then

$$\frac{1}{h} = \frac{\frac{2}{k+1}K\left(\frac{1-k}{1+k}\right)}{2K(k)} = \frac{\frac{2}{k+1}K(r)}{2K\left(\frac{1-r}{1+r}\right)} = \frac{K(r)}{k(r')} = \frac{K(\varphi)}{K\left(\frac{\pi}{2}-\varphi\right)}, \tag{23}$$

in which $r' = \sqrt{1-r^2} = \cos\varphi = \sin\left(\frac{\pi}{2}-\varphi\right)$.

We can use the formula [3]

$$K\left(\frac{1-r}{1+r}\right) = \frac{1+r}{2}K(r'); \tag{40}$$

if we introduce the parameter

$$\alpha = \arcsin \sqrt{\frac{1+k}{1-k} \cdot \frac{a-1}{a+1}}. \qquad (41)$$

thereupon (20) becomes (24).

Finally, (26) may be derived from (21) by means of the parameter ψ introduced by (25).

LITERATURE CITED

1. D. A. Frank-Kamenetskii, Diffusion and Heat Transfer in Chemical Kinetics [in Russian] (Izd. AN SSSR, Moscow-Leningrad, 1947).
2. M. V. Keldysh and L. I. Sedov, Doklady Akad. Nauk SSSR 16, No. 7 (1937).
3. E. Yanke and F. Emde, Tables of Functions [Russian translation] (GTTI, Moscow-Leningrad, 1948).

LETTER TO THE EDITOR

DETECTION OF HYDROGEN ATOMS IN A LOW-PRESSURE HYDROGEN FLAME BY THE EPR METHOD

V. N. Panfilov, Yu. D. Tsvetkov, and V. V. Voevodskii

Institute of Chemical Physics, Academy of Sciences of the USSR
Translated from Kinetika i Kataliz, Vol. 1, No. 2, p. 333,
July-August, 1960
Original article submitted May 23, 1960

In the reaction zone of hydrogen oxidation according to the customary reaction scheme [1], atoms and free radicals are present in concentrations several orders greater than the equilibrium values. Experimental proof of the presence of superequilibrium concentrations of hydrogen atoms in the zone of the low-pressure flame was provided by data obtained by V. N. Kondrat'ev and E. I. Kondrat'eva [2] using a calorimetric method. The most direct method of detecting hydrogen atoms in the gas phase is the method of electron paramagnetic resonance, by means of which hydrogen atoms were detected in the discharge [3]. Preliminary data on the detection of hydrogen atoms in the zone of the low-pressure hydrogen flame by this method are set forth below.

The combustion of a hydrogen-oxygen mixture was investigated in the region slightly above the lower ignition limit. The experiments were performed in a stream in a silica tube of inner diameter 6 mm, placed in the resonator of an EPR spectrometer with high-frequency modulation of the magnetic field [4]. To diminish the probability of recombination of hydrogen atoms at the wall, the tube was treated beforehand with $K_2B_4O_7$ solution. The part of the tube directly before the resonator was heated to 550-600°. The total pressure of the mixture varied from 3 to 20 mm, the rate of consumption of the mixture was 1-3 ml/sec, and the stream velocity was 10-20 m/sec.

Under these conditions a hydrogen-atom EPR signal was recorded, consisting of a doublet with a g-factor of about 2 and a separation of about 500 oe. The signal intensity corresponded to 10^{15}-10^{16} hydrogen atoms in the resonator. The component width of the hydrogen doublet increased with the high-frequency modulation amplitude. Extrapolation to zero modulation amplitude gives a value of about 0.7 oe for the component width. Saturation of the signal was not observed at klystron power levels up to 3 mw.

The signal intensity was found to depend strongly on the total pressure of the mixture (as the pressure in a stoichiometric mixture decreased from 16 to 8 mm, the intensity increased tenfold), which apparently was due to a change in the stream velocity. Investigation of the relation between the signal amplitude and the hydrogen content in the mixture showed that at 8 mm pressure the signal amplitude increases with the hydrogen concentration.

At present, quantitative investigations of the relation between the concentration of hydrogen atoms and the temperature, pressure, and composition of the mixture are being conducted, and experiments for the purpose of detecting other atoms and radicals which might be expected in this reaction are being continued.

LITERATURE CITED

1. A. B. Nalbandyan and V. V. Voevodskii, Mechanism of Oxidation and Combustion of Hydrogen [in Russian] (Moscow, Izd. AN SSSR, 1949).
2. E. I. Kondrat'eva and V. N. Kondrat'ev, Zhur. Fiz. Khim. 20, 1239 (1946).
3. R. Beringer, Phys. Rev. 95, 1474 (1954).
4. A. G. Semenov and N. N. Bubnov, Pribor. i Tekh. Éksp., 1, 92 (1959).

BORIS NIKOLAEVICH DOLGOV

Translated from Kinetika i Kataliz, Vol. 1, No. 2, pp. 334-335,
July-August, 1960

The outstanding organic chemist, Professor Boris Nikolaevich Dolgov, died December 6, 1959 at the age of 65 after a long illness.

With the death of Boris Nikolaevich Dolgov we lost a remarkable man, a widely known scientist, and an excellent teacher, who devoted many years of his working life to investigations in the field of catalysis.

Dolgov was born August 14, 1894, in St. Petersburg, into the family of an artist-teacher. In 1912 he was admitted to the philology department of St. Petersburg University, and in 1914 he transferred to the chemistry division of the physics-mathematics department, where he graduated in 1925, defending his thesis on the theme: "Isomerization of Six-Membered Rings to Seven-Membered Ones." During the next three years Dolgov worked as a scientific co-worker at the Chemistry Institute of the Academy of Sciences. From 1928, for 11 years, he headed the Gaseous Reactions Laboratory of the newly established State High-Pressure Institute. In 1938 Dolgov defended his doctoral dissertation and received the title of Professor. In the same year he was appointed Head of the Organic Chemistry Department, Leningrad State University. From this time, on, Dolgov's scientific and pedagogical activity was continuously connected with Leningrad University.

Simultaneously with his work in the university, Dolgov rendered great assistance to branch chemistry institutes (GIVD, GIPKh, Khimgaz, Wood Technology Institute, etc.), taking part in their scientific work and the training of cadres of young scientists. In 1953 Dolgov was appointed Head of the Laboratory of Organosilicon Compounds, Institute of Silicate Chemistry, Academy of Sciences, USSR, which he directed until the end of his life.

Dolgov was a scientist of exceptional range and depth; his scientific activity was extensive and many-sided, and included investigations of great importance in organic catalysis, various fields of organic chemistry, and especially organosilicon chemistry.

From 1928 Dolgov was engaged in the development of catalytic hydrogenation of organic compounds under pressure at the State High-Pressure Institute, and directed studies of the synthesis of organic compounds from a base of carbon oxides. As a result of these investigations active catalysts were found, and the conditions for the preparation of hydrocarbons, alcohols, and other oxygen-containing organic compounds were studied.

The industrial catalyst for methanol synthesis developed by Dolgov was used in starting up the first domestic synthetic methanol plant.

Dolgov's work of many years in the field of catalytic syntheses on the basis of carbon oxides is creatively reflected in his important monograph "Chemical Utilization of Carbon Oxides."

Dolgov's investigations of catalytic conversions of aliphatic oxygen-containing compounds are of considerable theoretical and practical interest. In the study of catalytic conversions of primary alcohols and aldehydes he discovered a new reaction – etherification of alcohols without acid.

Dolgov showed that the dehydrocyclization reaction, studied earlier in the case of paraffin hydrocarbons, may be carried out with oxygen-containing aliphatic compounds. He discovered a new route of formation of phenols from alcohols, aldehydes, and ketones, and established the probable mechanisms of these complex conversions.

Dolgov's investigations in the field of organosilicon chemistry are of exceptional importance. His work, which he began in 1928 and continued until his last days, opened the first page of the domestic chemistry of organosilicon compounds and was a great contribution to this field of science. Among works published since 1925, his investigations on the replacement of a hydrogen atom bound to silicon, by alkoxy, aryloxy, amino, and other groups, are of great theoretical and practical interest. These works showed that organosilicon hydrides are convenient for introducing various substituents on a silicon atom.

Dolgov was an outstanding propagandist and popularizer of organosilicon chemistry. He was the first to evaluate the growing practical importance of organosilicon compounds and to indicate the prospects of their use in the national economy. Dolgov wrote many review articles on this subject, as well as the monograph "Chemistry of Organosilicon Compounds," published in 1933.

Throughout the period of Dolgov's scientific activity more than 200 scientific articles and author's certificates on inventions devised by him personally and together with his students were published.

In 1949 Dolgov wrote the textbook "Catalysis in Organic Chemistry," and a second, revised and considerably expanded, edition was published in 1959. This textbook deservedly enjoys great popularity in the Soviet Union and a number of countries of the People's Democracy.

Dolgov was a remarkable teacher. Young people always worked with him; he transmitted his knowledge to them, and educated specialists in organic catalysis and organosilicon compounds, who now are working in factories, scientific research institutes, and higher schools.

Dolgov received government awards many times.

The bright memory of Boris Nikolaevich Dolgov – a remarkable scientist-teacher and an interesting and fascinating conversationalist – will remain forever in the hearts of those who knew him, studied with him, and worked with him.

SIGNIFICANCE OF ABBREVIATIONS MOST FREQUENTLY ENCOUNTERED IN SOVIET PERIODICALS

FIAN	Phys. Inst. Acad. Sci. USSR.
GDI	Water Power Inst.
GITI	State Sci.-Tech. Press
GITTL	State Tech. and Theor. Lit. Press
GONTI	State United Sci.-Tech. Press
Gosenergoizdat	State Power Press
Goskhimizdat	State Chem. Press
GOST	All-Union State Standard
GTTI	State Tech. and Theor. Lit. Press
IL	Foreign Lit. Press
ISN (Izd. Sov. Nauk)	Soviet Science Press
Izd. AN SSSR	Acad. Sci. USSR Press
Izd. MGU	Moscow State Univ. Press
LEIIZhT	Leningrad Power Inst. of Railroad Engineering
LET	Leningrad Elec. Engr. School
LETI	Leningrad Electrotechnical Inst.
LETIIZhT	Leningrad Electrical Engineering Research Inst. of Railroad Engr.
Mashgiz	State Sci.-Tech. Press for Machine Construction Lit.
MEP	Ministry of Electrical Industry
MES	Ministry of Electrical Power Plants
MESEP	Ministry of Electrical Power Plants and the Electrical Industry
MGU	Moscow State Univ.
MKhTI	Moscow Inst. Chem. Tech.
MOPI	Moscow Regional Pedagogical Inst.
MSP	Ministry of Industrial Construction
NII ZVUKSZAPIOI	Scientific Research Inst. of Sound Recording
NIKFI	Sci. Inst. of Modern Motion Picture Photography
ONTI	United Sci.-Tech. Press
OTI	Division of Technical Information
OTN	Div. Tech. Sci.
Stroiizdat	Construction Press
TOE	Association of Power Engineers
TsKTI	Central Research Inst. for Boilers and Turbines
TsNIEL	Central Scientific Research Elec. Engr. Lab.
TsNIEL-MES	Central Scientific Research Elec. Engr. Lab.–Ministry of Electric Power Plants
TsVTI	Central Office of Economic Information
UF	Ural Branch
VIESKh	All-Union Inst. of Rural Elec. Power Stations
VNIIM	All-Union Scientific Research Inst. of Metrology
VNIIZhDT	All-Union Scientific Research Inst. of Railroad Engineering
VTI	All-Union Thermotech. Inst.
VZEI	All-Union Power Correspondence Inst.

Note: Abbreviations not on this list and not explained in the translation have been transliterated, no further information about their significance being available to us. – Publisher.

Now available . . . an insight into the Soviet problems and achievements in . . .

PRODUCTION of ISOTOPES

The eighteen papers which comprise this volume were originally read at the All-Union Scientific and Technical Conference on the Application of Radioactive Isotopes, Moscow, 1957. The reports consider the problems and achievements of Soviet scientists in the production of radioactive isotopes by irradiation of targets in Soviet reactors and cyclotrons. Not only is this work of significance to producers of isotopes, but many of the papers will prove useful to isotope users as well.

The Development of Isotope Production in the USSR.
Certain Aspects of the Production of Radioactive Isotopes in a Nuclear Reactor.
Production of Radioactive Isotopes in a 10-Mev Deuteron Cyclotron.
Determination of Product Yields in Nuclear Reactions.
Spectrochemical Methods of Analyzing High-Purity Materials Used in Reactor Construction and for the Production of Radioisotopes.
Quantitative Spectral Determination of Impurities in Radioactive Preparations.
The Production of Alpha-, Beta-, and Gamma-Sources Using Oxide Films on Aluminum and Its Alloys.
Stable Isotopes Enriched by the Electromagnetic Method.
Ultrahigh-Temperature Ion Source for Electromagnetic Separation of Isotopes of Elements in the Platinum Group.
Inhomogeneous-Field Mass-Spectrometer for Analysis of Light-Element Isotopes.
The Relative Abundance of Palladium and Germanium Isotopes.
Some Problems in the Theory of Isotope Separation.
Separation of Isotopes of Light Elements by Diffusion in Vapors.
A Diffusion Column for the Separation of Isotopes.
A Fractionating Column for Preparing BF_3 Enriched in the Isotope B^{10}.
An Investigation of the Separation of the Stable Isotopes of Light Elements.
The Separation of Carbon Isotopes.
Low-Temperature Methods for Separating Helium Isotopes ($He^3 - He^4$).

1959 durable paper covers 136 pp. $50.00

CONSULTANTS BUREAU
227 WEST 17th STREET NEW YORK 11 N. Y.

THE STRUCTURE OF GLASS

Volume 2

Proceedings of the Third All-Union Conference on the Glassy State, held in Leningrad, November 16-20, 1959.

This notable volume contains papers presented at the conference convened by the Institute of Silicate Chemistry of the Academy of Sciences, USSR, the D. I. Mendeleev All-Union Chemical Society, and the S. I. Vavilov (Order of Lenin) State Optical Institute for discussion of recent experimental studies of various properties of glass, the principal methods for investigating glass structure, and the problem of glass formation.

A complete account is given of research work on the glassy state since the previous conference. The most modern optical, spectroscopic, and electrical techniques were used in studying the structure of glass in all its aspects, and the results are interpreted in the light of contemporary physical theories of the solid state.

Volume 2: $25.00

CONTENTS include

Investigation of Glass Structures by the Methods of Optical Spectroscopy. *A. A. Lebedev*
Diffraction Methods for the Study of Glassy Substances. *E. A. Porai-Koshits*
The Cellular Structure of Glass. *W. Vogel*
Characteristic Vibrations of the Glass Network and Glass Structure. *A. G. Vlasov*
General Problems of the Structure and Properties of Glasses. *K. S. Evstrop'ev*
Additivity of the Properties of Silicate Glasses in Relation to their Structure. *L. I. Demkina*
Glassy Systems and the Problem of Glass Structure. *M. A. Bezborodov*
Chemical Characteristics of Polymeric Glass-Forming Substances and the Nature of Glass Formation. *R. L. Myuller*
Characteristics of Glass Formation in Chalcogenide Glasses *N. A. Goryunova and B. T. Kolomiets*
Glass as a Polymer. *V. V. Tarasov*
Formation of a Crystalline Phase from a Silicate Melt. *A. I. Avgustinik*
The Vitrification Process and Structure of Glass. *O. K. Botvinkin*
Formation of Glass Structure during the Melting Process. *L. G. Mel'nichenko*
The Structure of Glass in the Light of the Crystal Chemistry of Silicates. *N. V. Belov*

492 pages **illustrated**

Volume 1

Proceedings of the Second All-Union Conference on the Glassy State.

". . . The Glass Division of the American Ceramic Society and the National Science Foundation are to be congratulated for making this inspiring collection available . . ." — *Journal of Chemical Education*

"The book should be of great interest to scientific and technical personnel interested in glass technology, ceramics, the states of matter, and any work involving the vitreous state. They should all have the experience of reading this book." — *Chemistry in Canada*

". . . a stimulating experience . . ." — *Trans. British Ceramic Society*

". . . lively discussions which show the diversity of opinions on every experimental report." — *The Glass Industry*

". . . the volume is excellent . . . the translation was well worth while . . ." — *R. W. Douglas, Nature*

Volume 1: $20.00

Volumes 1 and 2: $40.00 per set

CONTENTS include

The Crystallite Theory of Glass Structure. *K. S. Evstropyev*
Structure and Properties of Organic Glasses. *P. P. Kobeko*
The Structure of Glass. *O. K. Botvinkin*
The Possibilities and Results of X-Ray Methods for Investigation of Glassy Substances. *E. A. Porai-Koshits*
Structural Peculiarities of Vitreous and Liquid Silicates. *O. A. Esin and P. V. Geld*
Raman Spectra and Structure of Glassy Substances. *E. F. Gross and V. A. Kolesova*
The Quantum Theory of Heat Capacity and the Structure of Silicate Glasses. *V. V. Tarasov*
The Infrared Spectra of Simple Glasses and Their Relationship to Glass Structure. *V. A. Florinskaya and R. S. Pechenkina*
The Coordination Principle of Ion Distribution in Silicate Glasses. *A. A. Appen*
Concepts of the Internal Structure of Silicate Glasses Which Follow from the Results of Studies of the Properties of Glasses in Certain Simple Systems. *L. I. Demkina*
Measurement of the Expansion of Glass as a Method for Investigating its Structure. *A. I. Stozharov*
The Theoretical Views of D. I. Mendeleev on the Structure of Silicates and Glasses, and Their Significance for Modern Science. *L. G. Melnichenko*
The Views of D. I. Mendeleev on the Chemical Nature of Silicates. *V. P. Barzakovsky*

296 pages **illustrated**

Complete contents available upon request

CONSULTANTS BUREAU
227 W. 17 ST., NEW YORK 11, N. Y.